Contributions to Improve Cognitive Strategies with Respect to Wireless Coexistence

Von der Fakultät für Ingenieurwissenschaften

Abteilung Elektrotechnik und Informationstechnik

der Universität Duisburg-Essen

zur Erlangung des akademischen Grades

Doktor der Ingenieurwissenschaften (Dr.-Ing.)

genehmigte Dissertation

von

Kaleem Ahmad

aus

Faisalabad, Pakistan

Gutachter: Prof. Dr. Ing. Thomas Kaiser

Gutachter: Prof. Dr. Ing. Uwe Meier

Tag der mündlichen Prüfung: 23-05-2013

To my parents and brother Azeem Ahmad.

Acknowledgements

Table of Contents

List of Figures

List of Tables

List of Abbreviation

AoA:	Angle-of-Arrival
AP:	Access Point
AR:	Autoregressive
ARQ:	Automatic Repeat Request
AUC:	Area Under the Curve
AWGN:	Additive White Gaussian Noise
BER:	Bit Error Rate
BT:	Bluetooth
BW:	Bandwidth
CA:	Collision Avoidance
CDMA:	Code Division Multiple Access
CE:	Cognitive Engine
CFD:	Cyclostationary Feature Detection
COCE:	Coexistence Optimized Cognitive Engine
CR:	Cognitive Radio
CRC:	Cyclic Redundancy Check
CREAM-MAC:	Cognitive Radio-EnAbled Multi-channel MAC
CSS:	Chirp Spread Spectrum
CT:	Central Tendency
CTMC:	Continues Time Markov Chain
CW:	Contention Window
DECT:	Digital Enhanced Cordless Telecommunication
DHD:	Dumb Hole Detection
DoM:	Degree of Membership
DSA:	Dynamic Spectrum Access
ED:	Energy Detection
EKBR:	Extended Knowledge Base Reasoning
EM:	Electromagnetic
EM:	Expectation Maximization
FEC:	Forward Error Correction
FF:	First Free

FFT:	Fast Fourier Transform
FIML:	Full Information Maximum Likelihood
FL:	Fuzzy Logic
FPS:	Fuzzy Power Spectrum
FSS:	Filter Swept Spectrogram
GA:	Genetic Algorithms
HB:	Hop Behavior
HDR:	Hardware Defined Radio
HMM:	Hidden Markov Model
IHD:	Intelligent Hole Detection
ISM:	Industrial Scientific Medical
ITU:	International Telecommunication Union
LBT:	Listen Before Talk
MAC:	Media Access Control
MBWA:	Mobile Broadband Wireless Access
MF:	Membership Function
MFD:	Matched Filter Detection
MIMO:	Multiple Input Multiple Output
ML:	Machine Learning
MLE:	Maximum Likelihood Estimator
MLPN :	Multilayer Linear Perceptron Network
MLPN:	Multilayer Linear Perceptron Network
MM:	Markov Model
MSK:	Minimum Shift Keying
NF:	Neuro Fuzzy
NFSC:	Neuro Fuzzy Signal Classifier
NLOS:	Non-Line-of-Sight
NN:	Neural Network
NPN:	Nonlinear Perceptron Network
OSA:	Opportunistic Spectrum Access
$\mathbf{P_d}$:	Probability of Detection
PDF:	Probability Density Function
PE:	Processing Element
$\mathbf{P_{FA}}$:	Probability of False Alarm

PFSS: Projected FSS

PHY: Physical Layer

PLR: Packet Loss Rate

POMDP: Partially Observable Markov Decision Process

PSD: Power Spectral Density

PSS: Projected SS

PU: Primary User

QoS: Quality-of-Service

RBF : Radial Basis Function

RBFN: Radial Basis Function Network

REM: Radio Environment Map

RFID: Radio Frequency Identification

RKB: Radio Knowledge Base

ROC: Receiver Operating Characteristics

RSA: Real-time Spectral Analyzer

RSSI: Received Signal Strength Indicator

SCF: Spectral Correlation Function

SD: Statistical Dispersion

SDR: Software Defined Radio

SIFS: Short Inter Frame Space

SM: Similarity Measure

SNR: Signal-to-Noise Ratio

SS: Swept Spectrogram

SU: Secondary User

SVM: Support Vector Machine

SVMFM: Support Vector Machine and Feature Matching

SWWVD : Smooth-Windowed Wigner-Ville Distribution

TB: Time Behavior

TDMA: Time Division Multiple Access

TN: True Negative

TNR: True Negative Rate

TP: True Positive

TPC: Transmit Power Control

TPR: True Positive Rate

TSCH: Time Slotted Channel Hopping

TW: Temporal Width

USRP: Universal Software Radio Peripheral

Wi-Fi: Wireless Fidelity

WiMAN: Wireless Metropolitan Area Network

WiMAX: Worldwide Interoperability for Microwave Access

WISA: Wireless Interface for Sensors and Actuators

WLAN: Wireless Local Area Network

WPAN: Wireless Personal Area Network

WSAN: Wireless Sensor Actuator Network

WSVM :   Wavelet SVM

Abstract

Cognitive radio (CR) can identify temporarily available opportunities in a shared radio environment to improve spectral efficiency and coexistence behavior of radio systems. It operates as a secondary user (SU) and accommodates itself in detected opportunities with an intention to avoid harmful collisions with coexisting primary user (PU) systems. Such opportunistic operation of a CR system requires efficient situational awareness and reliable decision making for radio resource allocation.

Situational awareness includes sensing the environment followed by a hypothesis testing for detection of available opportunities in the coexisting environment. This process is often known as spectral hole detection. Situational knowledge can be further enriched by forecasting the primary activities in the radio environment using predictive modeling based approaches. Improved knowledge about the coexisting environment essentially means better decision making for secondary resource allocation. This dissertation identifies limitations of existing predictive modeling and spectral hole detection based resource allocation strategies and suggest improvements.

Firstly, accurate and efficient estimation of statistical parameters of the radio environment is identified as a fundamental challenge to realize predictive modeling based cognitive approaches. Lots of useful training data which are essential to learn the system parameters are not available either because of environmental effects such as noise, interference and fading or because of limited system resources particularly sensor bandwidth. While handling environmental effects to improve signal reception in radio systems has already gained much attention, this dissertation addresses the problem of data losses caused by limited sensor bandwidth as it is totally ignored so far and presents bandwidth independent parameter estimation methods. Where, bandwidth independent means achieving the same level of estimation accuracy for any sensor bandwidth.

Secondly, this dissertation argues that the existing hole detection strategies are dumb because they provide very little information about the coexisting environment. Decision making for resource allocation based on this dumb hole detection approach cannot optimally exploit the opportunities available in the coexisting environment. As a solution, an intelligent hole detection scheme is proposed which suggests classifying the primary systems and using the documented knowledge of identified radio technologies to fully understand their coexistence behavior.

Finally, this dissertation presents a neuro-fuzzy signal classifier (NFSC) that uses bandwidth, operating frequency, pulse shape, hopping behavior and time behavior of signals as distinct features in order to

identify the PU signals in coexisting environments. This classifier provides the foundation for bandwidth independent parameter estimation and intelligent hole detection. MATLAB/Simulink based simulations are used to support the arguments throughout in this dissertation. A proof-of-concept demonstrator using microcontroller and hardware defined radio (HDR) based transceiver is also presented at the end.

Chapter 1

Introduction

Communication technologies ranging from internet to mobile phone have become very popular in different fields of life. More and more investment and efforts have been launched to design safer, cheaper and easy-to-use communication technologies. Wireless technologies, in particular, have become very successful due to their inherent support for mobility and have started replacing their wired counterparts in nearly every field of life. Presently, more and more new wireless technologies are being introduced and further research is being done to make the existing ones more reliable and useable.

Meanwhile, wireless technologies could also find remarkable places in industrial automation systems as they offer very flexible installation and mobile operation and avoid cable 'wear and tear' problems. However, despite their success and popularity, wireless technologies are still far behind their wired counterparts in terms of reliability. Since the transmission medium has to be shared, wireless technologies face a unique threat of *interference* from themselves which is growing with the popularity of wireless technologies. Harmful interference can be caused by either parasitic machine emissions, or by intentional or unintentional wireless systems as illustrated in Fig. 1.1.
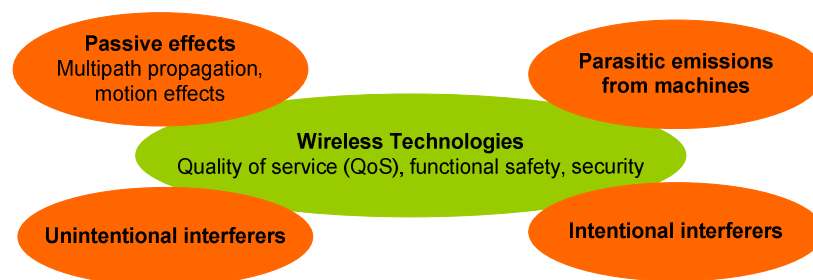
Figure 1.1: *Environmental effects cause impairments to wireless technologies*

Meanwhile, harmful interference, i.e. the level of interference where the performance degradation is felt, is a very broad concept. Different involved stakeholders may have diverse viewpoints about it because of their differing circumstances and priorities regarding their goals for QoS [STD28]. A robust communication system may tolerate high interference because error handling methods employed across

different layers of its protocol stack are able to handle the influence of interference. Those interference handling techniques can be divided into SUPRESS, REPAIR and AVOID type approaches. The transmission methods that attempt to restrain the influence of interference such as spreading, multi-carrier modulations, interleaving etc. can be categorized as SUPRESS type mechanisms. While, methods that can fix the damage caused by the interference such as forward error correction (FEC) and automatic repeat request (ARQ) can be considered as REPAIR type mechanisms. Finally, AVOID type interference handling methods like listen before talk (LBT) attempt to avoid the interference. This thesis work contributes to the last type; making use of cognitive strategies to avoid interfering effects.

1.1 Motivation

Currently, there are many state-of-the-art wireless technologies (see Fig 1.2) for specialized communication tasks and due to diverse application areas it is often required to run several wireless technologies simultaneously. For example, in their daily life most individuals are using IEEE 802.11 based WLAN for internet access and IEEE 802.15.1 based Bluetooth for short range communication such as connecting headsets or mobile phones to a laptop. Multiple wireless technologies, with common spectrum assignments, running simultaneously in partially or fully overlapping geographical regions are known as *coexisting* radio[1] systems. Where, *coexistence* is the ability of one system to perform a task in a given shared environment where other systems have an ability to perform their tasks and may or may not be using the same set of rules [STD23].

Meanwhile, the current frequency allocation paradigm is static and interference free operation of radio systems is enabled through either spatial or spectral guard bands in it. However, the increasing demand for spectrum utilization and frequency allocation information issued by corresponding regulatory authorities in US [NTIAC] and EU [EUROP], indicates that we are running short of spectral space since most of the spectrum is already assigned. On the other hand, spectrum usage surveys show that this spectrum scarcity is artificial and in fact the spectrum is critically underutilized [MIT99, YOU09, CAB08, JUN09] since legacy users do not need to transmit most of the time. This situation has led to the idea of open spectrum [ROB03, LLE08], which calls for opening up most of the spectrum for unlicensed users in ways that they can coexist with legacy spectrum users, creating huge new capacity with existing spectral resources. However, as an alternative to spatial and spectral guard bands there must be strategies to prevent coexisting radio systems interfering with each other destructively. Meanwhile, industrial, scientific, and medical (ISM) bands, such as the 2.4 GHz or 5.8 GHz bands, already offer an open spectral access. Therefore, more and more new radio technologies are choosing to operate in these bands.

---

[1] The terms 'radio' and 'wireless' are used interchangeably throughout in this document.

However, existing wireless technologies are designed and standardized without putting much thought into coexistence with other technologies (Appendix A1). Consequently, there is an urgent need to solve the coexistence problem in these bands.
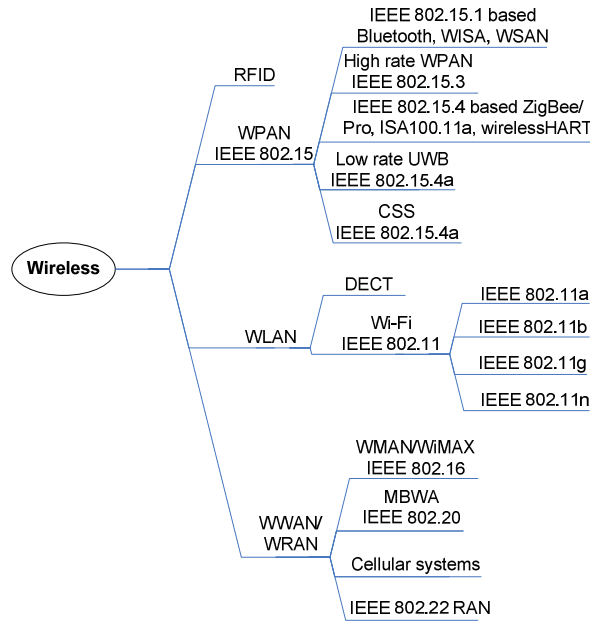
Figure 1.2: *Wireless technologies taxonomy*

Fortunately, the industry has already realized the necessity of a systematic approach in incorporating coexistence methodologies in designing future wireless devices and technologies. Several physical layer methods to solve the coexistence problem have been researched in recent years and a few of them are implemented in real-time systems. Adaptive hopping algorithms employed in Bluetooth [BTS01] are probably one of the most notable efforts because of its ability to blacklist channels with unacceptable level of interference. However, studies such as [QIX07] show that when the environment is fairly crowded there may not be enough interference free channels to exploit the strength of frequency hopping. Another worth mentioning example is time slotted channel hopping (TSCH) [TSC04] which is proposed for implementation in ISA100.11a and wirelessHART technologies [CHR10]. But it is expected to have a similar fate in overcrowded coexisting environments. Further discussion on state-of-the-art methods to solve the coexistence problem is included in Appendix A1.

Several standardization initiatives taken recently have also highlighted the significance of the coexistence problem. Notable of these are:

- IEEE 802.15.2 [STD23] recommended practice for coexistence between IEEE 802.11 and IEEE 802.15.1 based devices.
- IEEE 802.19 task group [PRA08] which is developing standards for coexistence between wireless standards (mainly IEEE 802 networks) of unlicensed devices.
- IEEE 1900.2 [STD28] recommended practice for the analysis of in-band and adjacent-band interference and coexistence between radio systems.

Appendix A2 includes detailed description of related existing standards.

Apart from these standardization efforts which are still in their infancy, the existing solutions are inadequate to tackle the coexistence of rapidly increasing wireless technologies because of some common limitations. The most prominent limitation is the lack of generality in these solutions since these are devised to solve the coexistence of a specific technology in the coexistence of some particular interfering radio technology. However, the pervasive use of wireless communication in everyday life makes it insensible to design technology specific solutions due to two reasons: firstly, it is difficult, if not impossible, to predict which technologies can be expected as coexisting or interfering systems. Secondly, designing technology specific coexistence solutions means that any new technology will have to find a unique solution for its coexistence with each existing technology, which is an impossible task. Furthermore, rigidness of conventional hardware defined radios (HDR) also hinders the efforts to solve the coexistence problem. Due to these reasons, more generic and flexible methods to solve the coexistence problem are needed.

Fortunately, the induction of cognitive radio (CR), "*a radio that is aware of its surroundings and adapts intelligently*" [MIT99], has created new opportunities to design generic strategies that can drive radio systems safely in dynamic, time-varying coexisting environments as illustrated in Fig. 1.3. Analogous to sand and pebbles poured into the gaps between larger rocks, a CR can fit itself *opportunistically* into temporarily available spectral gaps with an objective to keep the harmful interference to/from coexisting wireless systems below a threshold level.

Initial research to use CR for opportunistic spectrum access (see section 2.1 and Appendix A1) has shown satisfactory and encouraging results and provides motivation for this research work. However, the CR systems are yet in a research phase and a lot of work still needs to be done before they can be practically deployed. Most important research areas in the field of CR are design and development of hardware platforms, protocol architecture, standardization, and cognitive strategies for optimal resource allocation. This thesis work presents new contributions to cognitive strategies for resource allocation in coexisting environments.
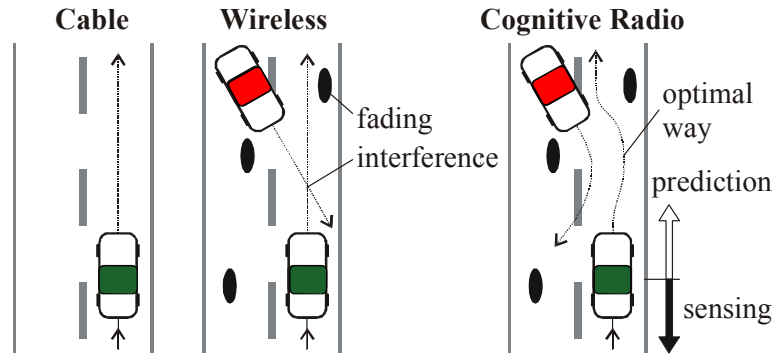
Figure 1.3: *Communication technology evolution*

The coexistence management perspective of existing cognitive strategies is often oriented around either of the following concepts:

- Switching to another 'free' frequency channel opportunistically.
- Transmitting using the same frequency channel by utilizing temporal gaps.

The first one can be seen as a frequency dimension solution and the second one as a time dimension solution. Collectively these two concepts are referred as opportunistic or dynamic spectrum access (OSA or DSA). Another approach for spectrum sharing is transmit power control (TPC) which allows transmission in an already occupied band given that the resulting interference is not harmful to the legacy users. Additionally, it may require the CR nodes to operate over ultra wide bandwidths to employ the TPC based approach. Nevertheless, all these cognitive solutions are limited to a single dimension and are vulnerable to failures in case of congestion in that particular dimension.

However, the electromagnetic (EM) resource space[2] is multidimensional [DRO05], where frequency, time, power and space are the primary features of radio signals. Each of which define an orthogonal dimension which can be used to separate transmissions of coexisting radio systems. There are several other orthogonal features, some of these, listed in IEEE 1900.2, are polarization, diversity, CDMA techniques, MIMO, dynamic routing behaviors, adaptive network management algorithms and adaptive error correction (a more comprehensive list can be found in Table 4, page. 36 of [STD28]). These variables are less subtle but getting more attention as experience and technology are developing. The idea of multidimensional EM resource space extends the size of shareable space beyond the conventional frequency, time or power based 'one-dimensional opportunity space' and offers 'multidimensional opportunity space' to achieve coexistence optimized operation of wireless systems. Hence, a good

---

[2] EM resource space, hyperspace, or electrospace are all used as synonyms in this document

cognitive strategy shall be able to optimize the transmission of underlying radio systems across multiple hyperspace dimensions.

Last but not least is the need for cognitive strategies that can not only be used to design new wireless technologies but can also be added to existing radio systems, either merely as 'add-on' or with least amendments in the existing technology in order to improve their coexistence capabilities. Unfortunately, existing cognitive strategies often only target modern software defined radios (SDR) based platforms.

With an aim to address these shortcomings and requirements this thesis presents a coexistence optimized cognitive engine (COCE). It employs generic cognitive strategies to find coexisting opportunities on multiple dimensions of the hyperspace. It can be deployed on top of a software defined radio based platform or as add-on for any of the existing radio technologies (Fig. 1.4).
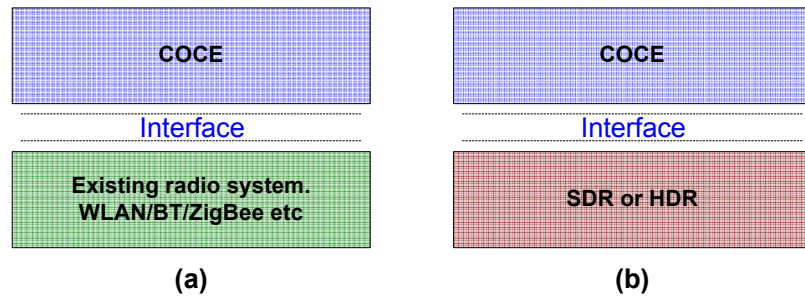
Figure 1.4: *COCE can be either* **(a)** *implemented on the top of an existing technology or* **(b)** *implemented using an SDR/HDR as underlying platform to realize a new radio system.*

1.2 Scope and Contributions

The overall scope of this thesis is to improve predictive modeling and spectral hole detection based resource allocation approaches with respect to coexistence. Detection and classification of radio system is an essential prerequisite. Furthermore, since narrowband data acquisition is common for industrial systems but causes considerable loss of valuable spectral and temporal information of radio signals, the treatment of lost data caused by narrowband sensing platforms is also included in this scope. The objective is to put the modeling capabilities of a narrowband CR system to the same accuracy level as a CR system equipped with a wideband sensing platform.

Briefly, this dissertation presents the following contributions to the subject:

1. *State-of-the-art*: A detailed analysis of the coexistence problem, including existing cognitive and non-cognitive solutions and related standards. It also includes:

      a. A description of distinct PHY/MAC level features of prominent industrial wireless technologies.

      b. Comparative analysis of traditional and probabilistic opportunistic spectrum access strategies.

      c. Parameter estimation methods for missing data with main focus on Markov model and renewal theory.

2. *Signal classification*: A neuro-fuzzy signal classifier which can identify standard wireless technologies and extract them from coexisting environments. It uses bandwidth, channel frequency, pulse shape, hopping behavior and temporal behavior of radio systems as distinct features.

3. *Predictive modeling*: It includes:

      a. Comparison of Markov model based opportunistic access with traditional opportunistic spectrum access approaches.

      b. Analysis of detection probability of narrowband sensors using a swept sensing method.

      c. A selective spectral projection method is presented that improves the acquisition and classification of signals which are wider than the sensor bandwidth without losing time related information of the signal.

      d. Renewal theory and hidden Markov model based bandwidth independent parameter estimation methods to incorporate missing data caused by limited sensor bandwidth.

4. *Real-time cognitive test-bed*: It demonstrates:

      a. Real-time operation of the neuro-fuzzy signal classifier.

      b. Comparison of Markov modeling based opportunistic spectrum access with traditional reactive opportunistic spectrum access in real-time environments.

      c. Comparison of intelligent hole detection with conventional dumb hole detection methods.

1.3 Thesis Structure

This thesis addresses the coexistence problem of wireless systems with a particular focus on industrial applications. This section walks through the rest of this document to provide a glimpse of its organization.

Chapter 2: Theoretical Foundation

An overview of theoretical concepts used in this thesis is presented in this chapter. A literature survey of related state-of-the-art work is mostly covered in this chapter. It starts with a brief introduction of cognitive radios and presents different technologies involved in different areas of cognitive radio

research. Then it presents a short introduction of machine learning fundamentals which are important to understand the work presented in this thesis.

Chapter 3: Problem Definition and Proposed Solution

This chapter formulates the problem and suggests cognitive strategies to improve wireless coexistence. Dumb hole detection, reactive/proactive sensing, and swept sensing are identified as key problems in existing cognitive solutions. In contrast to these approaches intelligent hole detection and bandwidth independent parameter estimation are proposed as appropriate new solutions to these problems. The modeling of complex coexisting environments, which are comprised of many unknown radio systems with diverse statistical behavior, is suggested using classification and extraction of individual radio systems.

Chapter 4: Classification and Extraction of Primary User Systems

A neuro-fuzzy signal classifier (NFSC) is presented in this chapter which decomposes the coexisting environment without any loss of temporal-spectral details of its constituent radio systems. This classifier uses bandwidth, channel frequency, hop behavior and temporal behavior of radio systems as distinct features and uses fuzzy logic based rules to classify the coexisting signals

Chapter 5: Bandwidth Independent Parameter Estimation

This chapter derives a formula for the detection probability of narrowband sensors using swept sensing. It later combines the results of this formula with the information provided by the NFSC to generate accurate estimations of parameters for Markov model based opportunistic spectrum access.

Chapter 6: Implementation and Results

Instead of using a wide-band SDR technology, a MSP430 microcontroller and a simple CC2500 narrow-band transceiver are used as a real-time demonstrator to implement selected features as proof-of-concept.

Chapter 7: Conclusion and Future Work

Based on simulations and real-time results it is concluded that predictive approaches perform better than the conventional non-predictive approaches. However, multidimensional opportunities of the hyperspace can only be optimally exploited using classification based intelligent hole detection.

Chapter 2

Theoretical Foundation

2.1 Cognitive Radio Fundamentals

In order to understand the concept and functions of cognitive radio it is important to understand the idea of cognition[3]. According to encyclopedia of computer science [RAL00] cognition includes mental states and processes such as thinking, reasoning, remembering, language understanding and generation, visual and auditory perception, learning, consciousness, and emotions. Cognitive science[4] is the interdisciplinary study of cognition. It can be defined as, roughly, the intersection of the disciplines of computer science, linguistics, philosophy, psychology, cognitive anthropology, and the cognitive neurosciences.

Thus, according to the computational view [RAL00] of cognitive science,

1. There are mental states and processes intervening between input stimuli and output responses.

2. These mental states and processes either are computations or else are computable. And hence,

3. mental states and processes are capable of being investigated scientifically.

Cognitive radio (CR), an application of computational cognitive science, is defined by Simon Haykin in [HAY05] as following:

"Cognitive radio is an intelligent wireless communication system that is aware of its surrounding environment (i.e., outside world), and uses the methodology of understanding-by-building to learn from the environment and adapt its internal states to statistical variations in the incoming RF stimuli by making corresponding changes in certain operating parameters (e.g., transmit power, carrier frequency, and modulation strategy) in real-time, with two primary objectives in mind:

---

[3] **Cognition:** "(1) of, relating to, being, or involving conscious intellectual activity (as thinking, reasoning, or remembering) (2) based on or capable of being reduced to empirical factual knowledge [MW]"

[4] **Cognitive Science:** "An interdisciplinary science that draws on many fields (as psychology, artificial intelligence, linguistics, and philosophy) in developing theories about human perception, thinking, and learning [MW]"

- *Highly reliable communications whenever and wherever needed.*

- *Efficient utilization of the radio spectrum."*

This is not the only definition of cognitive radio as there are many researchers and organizations that have their own opinion about *'what should be called a cognitive radio'.* Table 2.1 provides a comparison of some well-known opinions.

Table 2.1: *Criteria to be called a cognitive radio: well-known opinions [from YOU09]*

Defined by	Adapts (intelligently)	Autonomous	Can sense environment	Adaptive transmitter	Adaptive receiver	Environment aware	Goal driven	Learn the environment	Capabilities aware	Negotiate waveforms	No harmful interference
FCC	✓	✓	✓	✓							
S. Haykin	✓	✓	✓	✓	✓	✓	✓	✓			
IEEE P1900	✓	✓	✓	✓	✓						
IEEE USA	✓	✓	✓	✓	✓	✓					✓
ITU-R	✓	✓	✓	✓	✓	✓					
J. Mitola	✓	✓	✓	✓	✓	✓	✓	✓	✓	✓	
NTIA	✓	✓	✓	✓	✓	✓	✓				
SDRF CRWG	✓	✓	✓	✓	✓	✓	✓		✓		
VT CRWG	✓	✓	✓	✓	✓	✓	✓	✓	✓		

A CR employs *cognition* in the form of a *cognitive engine (CE),* added at the top of a radio platform (see Fig. 2.1) as mentioned in IEEE 1900.1 [STD18] by the following footnote to the definition of CR:

"Generally the cognitive functionality may be outside the boundary normally associated with a radio (e.g., environment sensing is a cognitive function that is not normally part of a radio)".
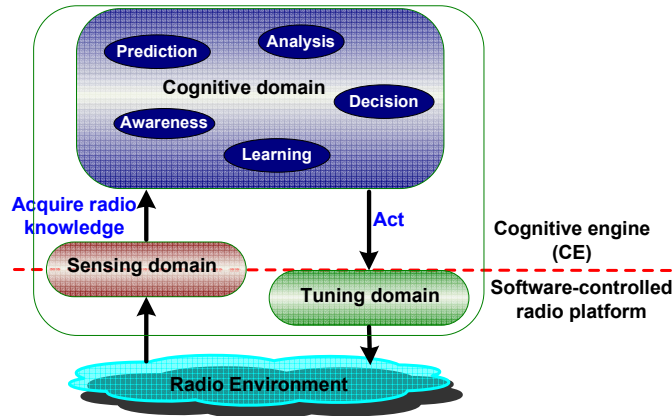
Figure 2.1: *A simplified block view of CR*

In order to exploit cognition the host radio platform has to be reconfigurable software-controlled. The degree of reconfigurability of the underlying radio architecture decides about the extent of cognition. Where software-controlled means *the use of software processing within the radio system or device to select the parameters of operation* [STD18]. Moreover, a software-controlled radio can be either a hardware defined radio (HDR) or a software defined radio (SDR). Where, HDR and SDR are defined as follows [STD18]:

HDR: *A type of radio that implements communication functions entirely through hardware such that changes in communications capabilities can only be achieved through hardware changes.*

SDR: *Uses software processing within the radio system or device to implement operating functions.*

Although, it is possible for an *intelligent radio* to use software-control to adapt the decision-making process even when a fixed set of hardware-defined physical layer implementations (HDR) is used. However, a software-defined, software-controlled intelligent radio can offer much more flexibility to change the physical layer parameters. Meanwhile, an intelligent radio is a subset of software-controlled radio and is defined as [STD18]:

A type of cognitive radio that is capable of machine learning.

Where, machine learning (ML) is defined in the following and further discussed in section 2.2.:

The capability to use experience and reasoning to adapt the decision-making process to improve subsequent performance relative to predefined objectives [STD18].

A CR can operate as a secondary user (SU) in a coexisting environment where several primary users (PU) are already operating. Conventionally, a user which has the license to use a frequency band is called a PU, while an un-licensed radio system which wants to use that frequency band opportunistically is called a

SU. Since an open access to the spectrum is assumed in this thesis work, this definition is simplified as follows:

Radio systems, already operating at a given time in a partially or fully overlapping spatial as well as spectral region are PUs and any new system that wishes to operate at some later time in that spatial-spectral region is a SU.
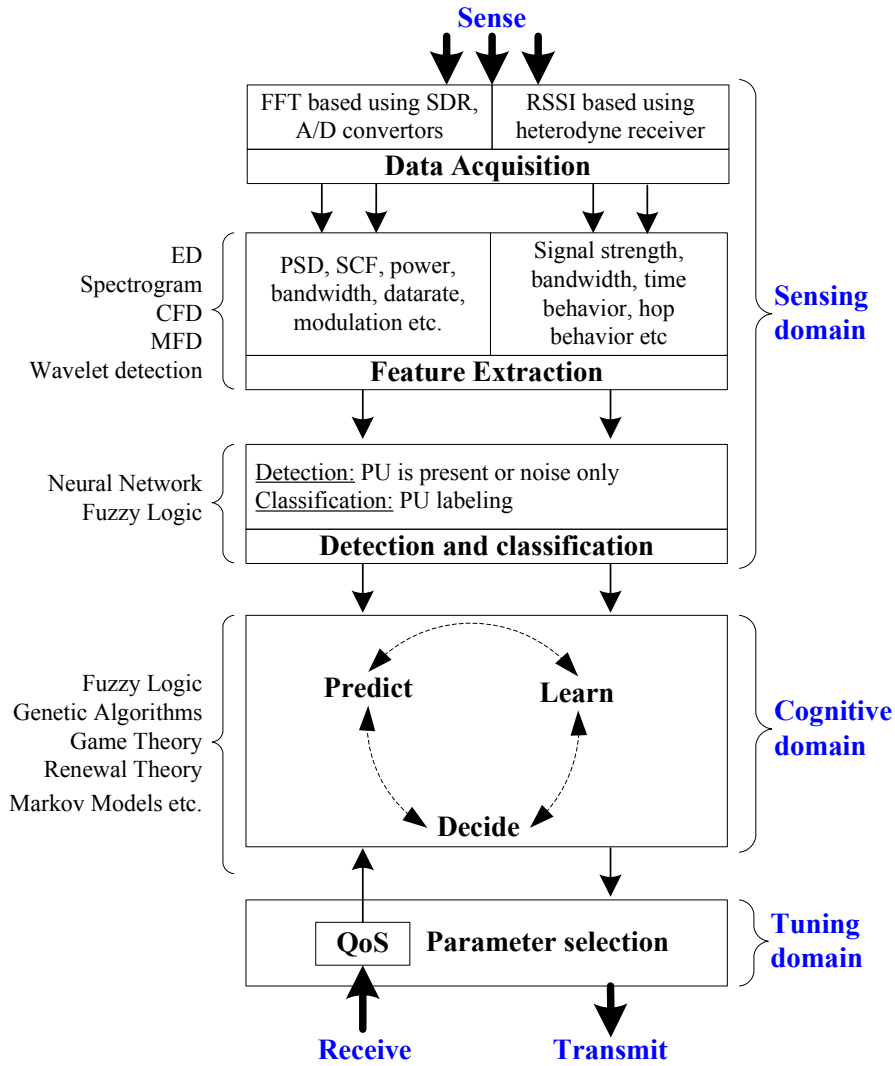
Figure 2.2: *The hierarchical model of a CR system. Popular state-of-the-art methods for each task are also listed at the left hand side. Energy detection (ED), cyclostationary feature detection (CFD), matched feature detection (MFD), power spectral density (PSD) and spectral correlation function (SCF) are explained later in this chapter.*

Functions of a CR can be divided into sensing, cognitive and tuning domains [AHM10] as shown in Fig. 2.2. The terms *knobs* and *meters* are borrowed from [THO07] to explain the functionality of these domains. These terms originally come from classical transceivers with adjustable controls (knobs) that control the radio's operating parameters and meters which display certain performance or operating parameters of the system. For instance, one can tune a knob in an FM radio to select a specific frequency in order to tune to a specific station, or, tune a knob to adjust the sound of the radio. Whereas, the meter can be the small screen showing the current frequency. The sensing domain deals with meter readings, the cognitive domain is responsible for decision making and the tuning domain deals with knob control type tasks. A brief explanation of functions, related problems, and existing solutions of these domains is provided in the following.

2.1.1 Sensing Domain

The sensing domain keeps the CR aware of electromagnetic (EM) activities in its surroundings. It consists of *data acquisition*, *feature extraction*, and *detection/classification* components. Collectively, these tasks are referred as spectrum sensing. Typically, a CR acquires samples of an entire band of interest and uses these samples to extract particular signal features and in turn uses some predefined threshold values to detect or classify the radio signals.

Detection or often referred as *hole detection* is the minimum required goal of the spectrum sensing process. The term hole refers to an arbitrarily wide part of the spectrum and there can be white and black holes indicating free and busy spectral areas, respectively. Grey hole is also often used to refer to a partially free subband. The hole detection method merely speaks about the presence or absence of primary signals and is formulated by the following binary hypotheses:

$$H_0 \ : \ y(n) = w(n)$$

$$H_1 : \ y(n) = x(n) + w(n) \tag{2.1}$$

where $y(n)$, $x(n)$ and $w(n)$ represent time domain samples of the received signal y, primary signal x and additive white Gaussian noise (AWGN) w, respectively. H_0 and H_1 denote the hypothesis corresponding to the absence and presence of a primary signal, respectively.

In addition to the binary hypothesis, the classification of distinct PU signals, formulated by M-ary hypotheses in eq. (2.2), enables a better decision making in subsequent domains of the CR system.

$$H_0 \ : \ y(n) = w(n)$$

$$H_i \ : \ y(n) = x_i(n) + w(n) \qquad\qquad i = 1,\ldots,M. \tag{2.2}$$

Where M is the total number of distinct signals, $x_i(n)$ represents samples of a particular PU signal, i.e. PU_i and H_i denote the hypothesis corresponding to the presence of that PU signal.

Classical spectrum sensing strategies include energy detection (ED), cyclostationary feature detection (CFD), and matched filter detection (MFD) as discussed in the following.

ED is the most basic spectrum sensing technology [CAB08]. It is the only choice when there is no knowledge about the received signal. The decision rule in this approach is given by:

$$T(y) = \sum_{n=1}^{N} |y(n)|^2 \underset{H_1}{\overset{H_0}{\underset{>}{\lessgtr}}} \gamma$$

(2.3)

where $T(y)$ is the test statistic of the received signal y, N is the sampling size in the time domain and γ is a predefined threshold value. It can be implemented like a spectrum analyzer by averaging frequency bins of the fast Fourier transform (FFT) of the received signal. Processing gain in this technique is proportional to the FFT size N and observation/averaging time. By increasing N one can improve the frequency resolution to better detect narrowband signals.

If a priori knowledge of modulation or signal features is available, CDF can also be a choice. It can utilize built-in hidden periodicity, e.g. sine wave carriers, pulse trains, repeated spreading, hopping sequences, or cyclic prefixes of modulated primary signals for more accurate detection. Due to this hidden periodicity the autocorrelation function of such signals is periodic and is called cyclic autocorrelation function. It can be used to calculate the spectral correlation function (SCF) to detect signal features. The cyclic autocorrelation function and the SCF are given in eq. (2.4) and eq. (2.5), respectively [WAG92].

$$R_y^\alpha(\tau) = \lim_{T \to \infty} \frac{1}{T} \int_T y\left(t + \frac{\tau}{2}\right) y^*\left(t - \frac{\tau}{2}\right) e^{-j2\pi\alpha t} dt$$

(2.4)

$$S_y^\alpha(f) = F\{R_y^\alpha(\tau)\}$$

(2.5)

Where, the operator $F\{\cdot\}$ denotes the Fourier transform. If a signal is cyclostationary with the period T then the cyclic autocorrelation function has a component at $\alpha = 1/T$ where α is the cycle frequency. The binary hypothesis of eq.(2.1) can be rewritten as follows:

$$H_0 : S_y^\alpha(f) = S_w^\alpha(f)$$
$$H_1 : S_y^\alpha(f) = S_x^\alpha(f) + S_w^\alpha(f)$$

(2.6)

Since the noise is in general not periodic, we have $S_w^\alpha(f) = 0$ for $\alpha \neq 0$. It leaves only signal features in the α domain which makes this technique a better candidate in noisy environments. The decision rule in this strategy is given by the following equation:

$$T(y) = \sum_{n=1}^{N} S_y^\alpha(f)\left[S_y^\alpha(f)\right]^* \overset{\overset{H_0}{\lessgtr}}{\underset{H_1}{}} \gamma \tag{2.7}$$

The optimal strategy for any signal detection is MFD [SMK98], where the unknown received signal $x(n)$ is correlated with a known replica $y(n)$ of the signal. It maximizes the received SNR. However, it is a coherent detection strategy and is not suitable in very low SNR regimes since it is difficult to achieve the required synchronization.

So far only a binary hypothesis is considered. However, these strategies can be used for M-ary hypothesis testing by extracting and distinguishing particular signal features. In this regard, ED can be used to compute the power spectral density (PSD) or spectrogram of signals to extract signal features such as bandwidth (BW), center frequency, hop behavior, duty cycle and time behavior of signals. Modern A/D based sensing platforms, such as an SDR or a so-called real-time spectrum analyzer (RSA), are often employed for ED based spectrum sensing. Traditional heterodyne receivers can also be employed where a received signal strength indicator (RSSI) has to be used as proxy to ED.

In contrast to it CFD and MFD perform more sophisticated signal processing. Consequently, more complex signal features such as modulation, bitrate, symbol rate, spreading, chip rate etc. can also be extracted in addition to the above mentioned signal features. For example symbol rate based feature detection is addressed in [CAB08] and modulation detection in [FEH05, KYO07, HAN08] using CFD. Eventually, it results in better detection and classification of the PU signals but at the expense of increased system complexity and processing time. Signal classification is discussed in detail in chapter 4.

Note that data acquisition is the job of the underlying radio platform, whereas the remaining components of the sensing domain can be implemented either in the CE or as part of the underlying radio or can be distributed in both.

2.1.2   Cognitive Domain

The cognitive domain plans optimal usage of radio resources in order to satisfy the performance requirements of the underlying SU radio system. It constitutes most of the CE and is solely responsible for the decision-making process. There is no single well accepted model of cognition. However, learning with experience and strategic decision making is the overall goal of it. There is a long list of machine learning (ML) strategies which can be used to realize specialized tasks at the cognitive domain. However, genetic algorithms (GA), neural networks (NN), Bayesian inference, fuzzy logic (FL) and game theory are the most popular methods for learning and strategic decision making tasks in cognitive radios. Hybrid

approaches based on these techniques are also used often to either minimize limitations of individual technologies or to exploit accumulative gains. Neuro-Fuzzy approach, GA for weight allocation in NN, fuzzy games are some examples of hybrid technologies.

Modeling of real-time situations and predicting future outcomes is also a well accepted job of the cognitive domain as it significantly enhances the decision making capabilities of the cognitive system. Traditional methods for modeling and prediction include autoregressive (AR) and time series modeling, Markov models and NNs. Furthermore, channel occupancy and transmission occurrences of radio systems are often modeled as Poisson process which is also recommended by the International Telecommunication Union's (ITU) handbook on Teletraffic Engineering [SIT10]. Therefore, several methods derived from Poisson arrival processes are also used in literature for modeling and prediction of radio signals, e.g. renewal theory or Markov-modeled Poisson process. Appendix A1 includes a survey of learning and modeling strategies in existing CR systems. Whereas, ML strategies that are used in this thesis work are discussed in detail in section 2.2 and statistical modeling of radio signals is further discussed in chapter 5.

Typical challenges and limitations involved at this domain are inherited from its constituent ML techniques. The most prominent of which are computational complexity, high demand of computational resources especially memory, difficulty in modeling real world problems and reasoning in uncertain and unfamiliar situations [HEA10, MUS95, JUE08, SED03].

2.1.3   Tuning Domain

It consists of a software-controlled radio platform, which offers flexible tuning of communication parameters. USRP series [ETTUS], FlexRadio [FLEXR] and Sundance's SDR-DS [SUNDA] are some popular SDR architectures commercially available for research purposes. However, there are countless hardware defined radios (HDR) which can be used as tuning domain.

Limitations and challenges at this domain are basically related to the underlying radio platform. The tuning domain is not in the scope of this thesis. Interested readers are referred to [DAN05, MIT09].

2.2   Machine Learning Fundamentals

Machine learning (ML) covers a broad range of computer programs. In general, it is the study of computer algorithms that improve their performance automatically through experience [TMM97]. The fundamental task in ML is to model a real-world problem or in other words determine the estimate $\hat{y}$ of a function $y = f(x)$. Where x is the input variable and describes features and attributes of the problem, y is

the outcome and f is the relation between input variable and outcome. In real applications, most learning tasks can be formulated as one of the following two problems [YIH07]:

Regression: It is about inferring a function $f(X)$ so that a given value x of the input variable X, generates a good prediction $\hat{y} = f(x)$ of the true value y of the output variable Y.

Classification: Given a finite set of classes $C = \{1,2,\ldots,K\}$ and a value x of random variable X, infer a function $l = g(x)$ to label x such that $l \in C$.

In fact, both the regression and classification problems can be formulated using the same framework and the only difference between them is in terms of the dependent variable, i.e. Y in regression and l in classification. It requires nominal, discrete values in classification, while continuous, real values in regression [YIH07].

Why is ML a natural choice for a coexistence problem? Generally, ML is useful in the following situations:

- Environments change with time.
- A task cannot be mathematically defined but only by example.
- Large piles of data include some important hidden relationships.
- The amount of available knowledge is too large for interpretation by a human.

Refractions, diffractions, reflections, and moving objects make the response of a radio channel highly dynamic and vague. Whereas, versatile and conflicting requirements of applications make the transmission patterns of the radio systems highly uncertain. This does not only make the coexistence environments hard to model but also requires a continuous and dynamic decision making under multiple constraints and objectives. Furthermore, regulatory policies, increasing number and usage of radio systems and new radio technologies are adding more to the existing radio knowledge. All these reasons make the coexistence problem a good application of ML.

Following is a brief overview of ML strategies and concepts which are used later in this dissertation.

2.2.1 Fuzzy set theory

Fuzzy Logic (FL) uses human like reasoning to deal with uncertainties and ambiguities in a given problem. There is a smooth and gradual transition from true to false and the truth of each statement is a matter of degree. Important components of a FL based system, as shown in Fig. 2.3, are:

- The fuzzy representation of I/O parameters (fuzzification/defuzzification) and relationship between them.

- Membership functions (MF) for input space.

- Antecedents and consequents

- Decision rules
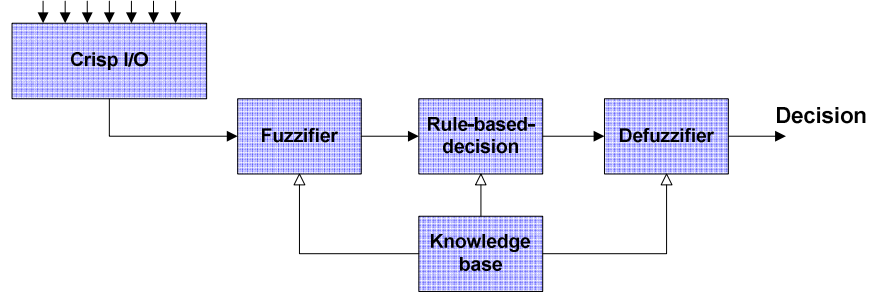
Figure 2.3: *Model of a FL based system.*

The rule-based decision is the heart of a fuzzy model and contains the set of *if-then* rules. Such rule sets are flexible and new rules can easily be added to extend the functionality of the system. For example, the following simple rule can be used to classify some well-known non-hopping radio systems having distinct BW and/or centre frequency f_c in the 80 MHz wide 2.4 GHz ISM band.

if BW ***matched*** BW_{PUi} **AND** f_c ***matched*** to $f_{\text{jth channel}}$ of PU_i

   then PU_i ***operating*** in j^{th} channel

The following new rule, to analyze the hopping behavior of signals, can be added without changing the existing functionality of the classifier.

if BW ***matched*** BW_{BT} **AND** f_c is ***hopping***

   then BT based PU is ***operating***

The if-part of above rules is called the antecedent and the then-part is called the consequent.

Note that all bold-italic words are *fuzzy* or *linguistic variables* defined over some *base variables*. The set of possible values is called the *term set*. For instance a term set *T* for fuzzy variable *matched* can be defined on the base variable "$|BW_{PUi} - BW|$" as follows:

$$T = \left\{ \begin{array}{l} matched, strongly\ matched, almost \\ matched, weakly\ matched, not\ matched \end{array} \right\}$$

Where, "$BW_{PUi} - BW$" is the difference of bandwidth of ith PU system and bandwidth of input signal and | | represents the absolute value.

Fuzzy set and singleton: A fuzzy set '*A*' is a collection of ordered pairs represented as $A = \{(x, \mu(x))\}$, where item *x* belongs to the universe of discourse and $\mu(x)$ is the degree or grade of membership. A single pair $(x, \mu(x))$, in a fuzzy set is called a fuzzy singleton. Since frequency is the central resource in radio environment, we can replace *x* with frequency *f* to define our fuzzy radio set as $F = \{(f, \mu(f))\}$.

Universe of discourse: The input space, where elements of a fuzzy set are taken from, is called universe of discourse or universe and is often represented by *u* or *U*. The entire radio frequency is the universe in our fuzzy radio model.

Membership function (MF): A MF is a curve that defines how each point in the input space is mapped to a membership value (or degree of membership - DoM) between 0 and 1. It is conventionally denoted as $\mu(x)$ or equivalently as $\mu(f)$ in the fuzzy radio set. The set of elements that have a non-zero membership is called the support of the fuzzy set. Note that a fuzzy set can be equivalently represented by its MF.

Standard Fuzzy Operators: Boolean operators AND, OR, and NOT are interpreted as intersection or min ($\cap$), union or max ($\cup$), and fuzzy complement ($1 - A$), respectively.

Similarity measure (SM): SM is used in fuzzy mathematics to measure the similitude between two fuzzy sets. Several definitions of *SM* have been presented. This thesis adapts [HAS06], which states that *SM* of fuzzy sets *A* and *B* is based on the minimum relative sigma count of *A* in *B* (and *B* in *A*) as follows:

$$SM(A, B) = \frac{|A \cap B|}{\max(|A|, |B|)} \tag{2.8}$$

Where $|A| = \sum_{x \in U} \mu_A(x)$. Hence eq. (2.8) can be written as,

$$SM(A, B) = \frac{\sum_{x \in U} \min(\mu_A(x).\mu_B(x))}{\max(\sum_{x \in U} \mu_A(x), \sum_{x \in U} \mu_B(x))} \tag{2.9}$$

2.2.2 Neural Network

Modeled on a nerve plexus, a neural network (NN) is nothing more than a set of nonlinear functions with adjustable parameters to give a desired output. Different types of NNs are separated by their network configurations and training methods, allowing for a multitude of applications. However, they are all comprised of processing elements (PEs), called neurons, which are interconnected to form a layered network. Each PE usually produces a single output value by accumulating inputs from other PEs. While there are many types of NNs available in the literature, multi-layer linear perceptron networks (MLPNs), nonlinear perceptron networks (NPNs) and radial basis function networks (RBFNs) are most common and

applicable for CR systems [HEA10]. Fig. 2.4 provides an example NN of a hypothetical signal classifier. Note that a PE in a NN can itself be a NN.

A neuro-fuzzy (NF) model is often used to combine the advantages of both FL and NNs. It adapts a NN based connectionist approach to exploit parallelism and adaptation, while individual PEs use FL based linguistic rules from human experts to deliver outputs.
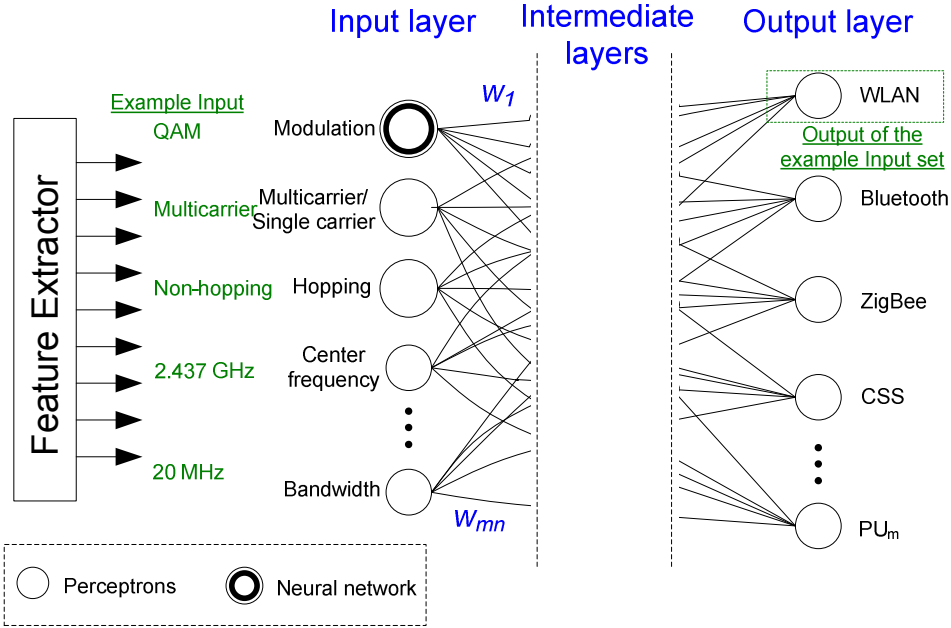
Figure 2.4*: Example NN of a radio signal classifier. Different features of an incoming signal are extracted and fed to NN which in turn identifies the signal. Note that a PE in NN can itself be a NN.*

2.2.3 Markov Models

Consider a stochastic process that is in one of N distinct states at any given time where distinct states are represented by a set $S = \{S_i: i = 1,2,\ldots,N\}$. If the state at time $t = n$ is denoted as q_n, where $n = 1,2,\ldots$, then at regularly spaced discrete times, the process constantly undergoes a transition from one state to another with a set of probabilities associated with each state. A full probabilistic description of the process requires specification of the current state (i.e. at time t), as well as all predecessor states, as follows [LAW89]:

$$P(q_n = S_n | q_{n-1} = S_{n-1}, q_{n-2} = S_{n-2}, \ldots)$$

where $S_n \in S, n \geq 0$, and '|' is the conditional probability. The process is said to follow a Markov model (MM) of order m if the next state depends only on preceding m states, where m is finite valued. The probabilistic description can then be truncated to only m previous states, as follows:

$$P(q_n = S_n | q_{n-1} = S_{n-1}, q_{n-2} = S_{n-2}, \dots) =$$

$$P(q_n = S_n | q_{n-1} = S_{n-1}, q_{n-2} = S_{n-2}, \dots, q_{n-m} = S_{n-m}), \text{for } n > m \tag{2.10}$$

For the special case of a first order MM, this probabilistic description is limited to just the current and the predecessor state, as follows:

$$P(q_n = S_n | q_{n-1} = S_{n-1}, q_{n-2} = S_{n-2}, \dots) = P(q_n = S_n | q_{n-1} = S_{n-1}) \tag{2.11}$$

In order to better incorporate the concept of prediction, this description can be equivalently described in terms of the present and the future states as given in the following:

$$P(q_{n+1} = S_{n+1} | q_n = S_n, q_{n-1} = S_{n-1}, \dots) = P(q_{n+1} = S_{n+1} | q_n = S_n) \tag{2.12}$$

Which means that, given the present state, the future is independent of the past. From now onwards this form of first order Markov model will be used in the rest of the text. Furthermore, a process is considered a time-homogeneous Markov process if:

$$P(q_{n+1} = S_{n+1} | q_n = S_n) = P(q_{n+1+m} = S_{n+1} | q_{n+m} = S_n), \text{where } m \text{ represents a time shift} \tag{2.12a}$$

Furthermore, it is assumed that the right-hand side of above equations is independent of time, which leads to the set of state transition probabilities a_{ij} of the following form:

$$a_{ij} \equiv P(q_{n+1} = S_j | q_n = S_i), \text{where } S_i, S_j \in S \tag{2.13}$$

The matrix $A = \{a_{ij}\} = \left\{\frac{\text{Total number of trnsitions from state } S_i \text{ to state } S_j}{\text{Total number of transitions from } S_i}\right\}$ is an $N \times N$ transition matrix. Since its entries are probabilities, its rows sum to 1 and there must be a transition from a state S_i to another state. It follows that:

$$a_{ij} \geq 0 \text{ and } \sum_{j=1}^{N} a_{ij} = 1 \tag{2.14}$$

So from any state S_i, the process moves to the state S_j with probability a_{ij}, and this probability remains the same for any n. The only special case is the first state of a discrete sequence, called initial state.

The probability distribution of the initial state, called initial probabilities is represented as follows:

$$\pi_i = P(q_1 = S_i) \tag{2.15}$$

where $\pi = \{\pi_i\}$ is a vector of N elements satisfying the following identity:

$$\sum_{i=1}^{N} \pi_i = 1 \tag{2.16}$$

An example two state Markov model of a noisy radio signal is shown in Fig. 2.5. The sensed signal is converted to a binary stream (also shown in Fig. 2.5) by using a threshold value, where 1 and 0 represent

ON and OFF states respectively at discrete time steps. Where, a time step is defined by the sample time. Hence, using this 23 samples long binary time series one can compute the following:

$E[\text{ON}] = sum(\text{one runs})/number\ of\ one\ runs = average\ packet\ size = 3.2$ time units

$E[\text{OFF}] = sum(\text{zero runs})/number\ of\ zero\ runs = average\ interarrival\ time\ between\ packets$
$= 1.75$ time units

$S = \{S_1 = 0, S_2 = 1\}$, $\pi = \{\pi_0, \pi_1\}^T = \{0.30, 0.70\}^T$ and $A = \begin{Bmatrix} a_{00} & a_{01} \\ a_{10} & a_{11} \end{Bmatrix} = \begin{Bmatrix} 0.43 & 0.57 \\ 0.26 & 0.74 \end{Bmatrix}$
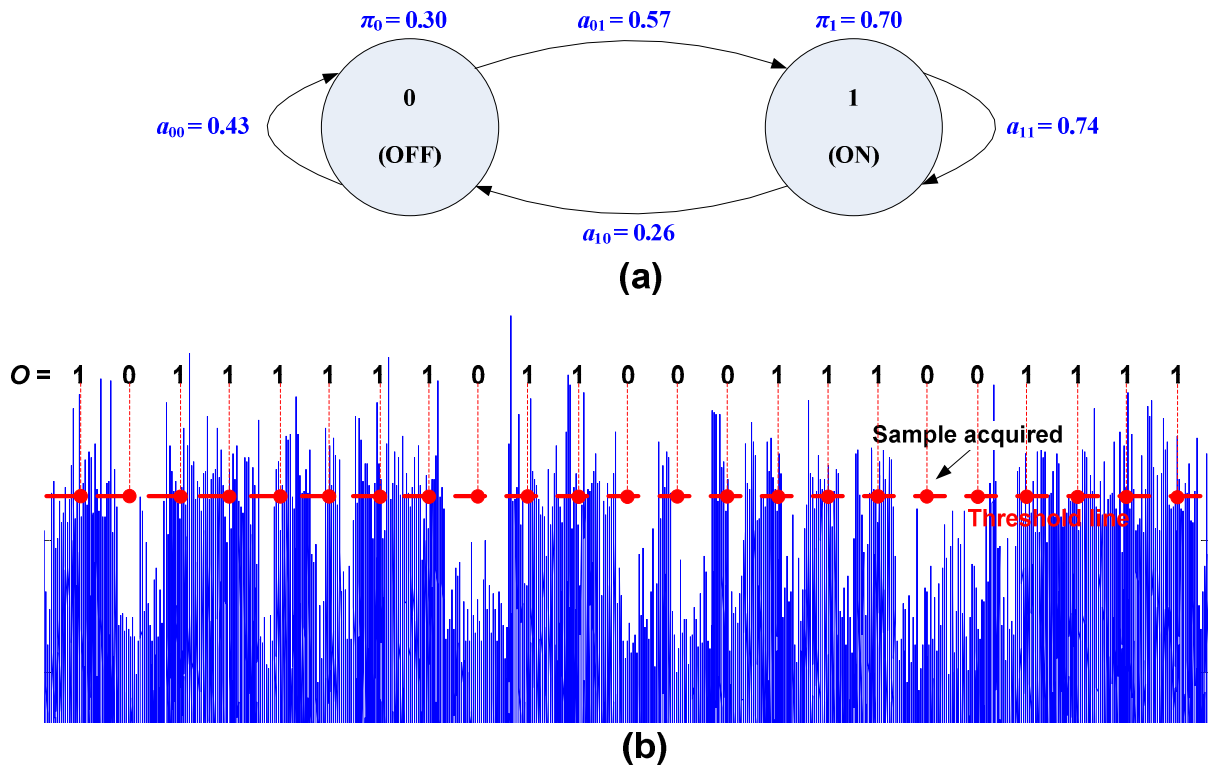
Figure 2.5: a) *A two state MM for a noisy radio signal. b) Corresponding radio signal and binary series.*

Given the model, one can ask some useful questions. For example, what is the probability that the usage of the channel for the next five time units will be "ON, ON, OFF, OFF, ON"? More formally it can be stated as an observation sequence $O = \{1, 1, 0, 0, 1\}$. Its probability is as follows:

$P(O|A,\pi) = P(1,1,0,0,1|A,\pi) = P(1) \cdot P(1|1) \cdot P(0|1) \cdot P(0|0) \cdot P(1|0) = \pi_1 \cdot a_{11} \cdot a_{10} \cdot a_{00} \cdot a_{01}$
$= 0.70 \cdot 0.26 \cdot 0.74 \cdot 0.43 \cdot 0.57 = 0.033$

One can also be interested in knowing that if the channel is busy (signal is ON) at a current time then what is the probability that it will remain busy for exactly d time units? This question can be answered by evaluating the probability of the observation sequence $O = \{1_1, 1_2, 1_3, \ldots, 1_d, 0_{d+1}\}$ as follows:

$$P(O|A, \pi, q_1 = 1) = P(1) \cdot \left(\prod_{j=2}^{d} P(1_j|1_{j-1})\right) \cdot P(0_{d+1}|1_d) = 1 \cdot (a_{11})^{d-1} \cdot a_{10} = (a_{11})^{d-1} \cdot (1 - a_{11})$$

(2.17)

Note that $P(1) = 1$ in this equation as it is given that $q_1 = 1$. If q_1 is not known then $P(1) = \pi_1$. The above probability can be generalized as follows:

$$P(O|A, \pi, q_1 = S_i) = (a_{ii})^{d-1} \cdot (1 - a_{ii}) = p_i(d)$$

(2.18)

The quantity $p_i(d)$ is the discrete probability density function (PDF) of duration d in state S_i. It describes the exponential duration characteristic of the state duration in a Markov process. Using $p_i(d)$ one can estimate the expected number of observation in a state, conditioned on starting in that state:

$$\hat{d}_i = \sum_{d=1}^{\infty} d \cdot p_i(d) = \sum_{d=1}^{\infty} d \cdot (a_{ii})^{d-1} \cdot (1 - a_{ii}) = \frac{1}{1-a_{ii}}$$

(2.19)

where $\sum_{d=1}^{\infty} d \cdot (a_{ii})^{d-1} = \frac{1}{(1-a_{ii})^2}$ and $\hat{\ }$ denotes the expected or average value. Thus, for our example Markov model shown in Fig. 2.5a, the expected packet duration is $1/(0.26) = 3.84$ time units and expected inter-arrival time of packets is $1/(0.57) = 1.75$ time units. For sufficiently large number of samples, the estimated values matches to the directly computed values, which are also given in Fig. 2.5b.

Summarizing this discussion, an observable Markov model is uniquely determined by the following three components:

1. A state space vector S
2. An initial state distribution π
3. A state transition matrix A

Moreover, the reason to call it an observable MM is because at any discrete time n, the state q_n is observable.

2.2.4 Hidden Markov Model

The Markov model explained so far is called observable MM because the states of the underlying system are clearly observable. However, an observable MM is too restrictive to be applicable in many real world problems since the states may be hidden and therefore not directly observable or some samples are missing because they could not be collected at some times for any reasons. In either of these cases an applied Markov model is called Hidden Markov model (HMM). In a HMM the observation or the missing

part is a probabilistic function of the state. The remaining text in this section will not differ between missing and hidden scenarios and will refer them as hidden. However, section 2.3 and chapter 6 will address the issues of missing data samples in detail.

In a HMM the discrete observations in each state come from a set of M symbols, denoted by $V = \{v_1, v_2, \ldots, v_M\}$. There is an observation or emission probability that a symbol v_m at time n is observed in the state S_i. This emission probability is specified as:

$$b_i(m) \equiv P(O_n = v_m | q_n = S_i) \tag{2.20}$$

Moreover, the emission probability matrix is $B = \{b_i(m)\}$. The observed values constitute the observation sequence O and the actual state sequence Q is hidden. The task is then to infer the state sequence from the observation sequence.

Formulizing an HMM is uniquely determined by the following elements:

1. State space $\mathbf{S}$ of N states

2. M number of distinct observation symbols

3. State transition probabilities $\mathbf{A}$

4. Emission probabilities $\mathbf{B}$

5. Initial state probabilities $\boldsymbol{\pi}$

Since, N and M are implicitly defined in other parameters, an HMM is shortly denoted as $\boldsymbol{\lambda} = (A, B, \pi)$[5]. Furthermore, given a number of observation sequences, there are three types of problems where HMMs can be applied. These are listed in the following:

1. Evaluation: Given the model $\boldsymbol{\lambda}$ and an observation sequence O, efficiently evaluate the probability $P(O|\boldsymbol{\lambda})$.

2. Decoding: Given a model $\boldsymbol{\lambda}$ and an observation sequence O, decode the most probable state sequence Q that has generated the observation sequence. Formally, we are interested in finding Q^* that maximizes $P(Q|O, \boldsymbol{\lambda})$, i.e. $Q^* = \arg\max_Q P(Q|O, \boldsymbol{\lambda})$. The Viterbi algorithm is a popular dynamic programming based method to compute such single best state paths and is widely used in decoding the convolution codes of communication systems.

3. Learning: Given k observation sequences $L = \{O^k\}$, learn the optimal parameters of $\boldsymbol{\lambda}$. i.e. $\boldsymbol{\lambda}^* = \arg\max_{\boldsymbol{\lambda}} P(L|\boldsymbol{\lambda})$. This thesis work will deal with such kind of problem. A popular approach

---

[5] Note that $\boldsymbol{\lambda}$ (**bold**, non-italic) is used to denote a HMM whereas, λ (non-bold, *italic*) is used to represent the rate parameter of exponential and Poisson distributions in this document.

called Baum-Welch algorithm, a maximum-likelihood estimation method for learning parameters of HMMs will be used in this thesis for learning HMM parameters and is discussed in detail in Section 2.3. Additionally, a renewal theory based maximum-likelihood parameter estimation method will also be used for this task.

2.2.5   Treating Missing Data

Learning, inference and prediction in the presence of missing data is a popular research problem in machine learning and statistical data analysis. Meanwhile, there can be a variety of reasons for missing data. Limiting the discussion strictly to sensor actuator and communication systems, some example reasons of missing data can be:

- Some sensors in a sensor network may stop functioning.
- The sensor can observe only a part of a larger target space.
- The acquired samples could not be successfully transmitted due to high noise or interference.
- The sensor could not see the target signals because of unfavorable channel conditions at arbitrary points in time (typically known as hidden node problem).

Abstractly, the generative process of data acquisition may be decomposed into a complete data process that generates complete data sets and a missing data process that determines which parts of the acquired data are missing. The problem of interest is the analysis of missing data process to estimate unbiased model parameters of the generative process. In order to avoid biased estimations in the presence of missing data several methods have been developed where each of which has a limited application range depending on the application area (finance, medical, engineering etc.) and pattern of missing data. Roughly, the pattern of the missing data can be random or deterministic. In this thesis the problem of spectrum sensing will be later on formalized as missing data problem with deterministic periodic patterns of missing data. State-of-the-art techniques to treat missing data can be grouped as following [MYR01]:

Techniques ignoring incomplete observations: The simplest technique is to ignore missing observations. It is usually satisfactory with small amounts of missing data but its major drawback is that its application may result in too small data sets if the percentage of missing data is too high, eventually resulting in biased estimates.

Imputation-based techniques: Imputation based methods replace missing parts of data sets with some suitable estimates to generate imputed data sets. In turn standard complete data parameter estimation methods such as ordinary least squares method can be applied to the imputed data set. Some common methods to compute imputation value include overall mean of complete part of data, some appropriate

subgroup mean, logical rule based estimated value and last value carried forward. However, the main drawback of imputation is that artificially substituted values may lead to biased results if the imputation method is not appropriate.

Model based methods: Model based methods do neither remove missing parts of data nor replace missing values. Rather, these methods define a model for the partially missing data and base their inference under the likelihood of that model. A full information maximum likelihood (FIML) method, multiple-group likelihood method and expectation-maximization (EM) algorithms are three popular maximum likelihood estimation methods [CRA01] that are often available in software packages. The first two algorithms are considered as direct approaches in a sense that model parameters are estimated directly from the available data without any preliminary preparation step (e.g. imputation). In contrast, the EM algorithm is an indirect approach since an additional preparation phase is required before the parameter estimation. This method will be briefly discussed in the following paragraphs because a particular variant of it, known as Baum-Welch algorithm, will be used in this thesis for learning HMM parameters.

Expectation-Maximization (EM) algorithm: The EM method [JEF98] is an iterative technique of finding the maximum-likelihood estimate of the parameters of an underlying distribution when the given data set has missing values. In order to understand the algorithm assume that X is an observed random variable with probability density function $P(X|\Phi)$ generated from some distribution with parameter set Φ (e.g. P can be a Poisson distribution and Φ can be the arrival rate λ). Let's call X the incomplete data set (with missing values) and the likelihood function of it, i.e. $\mathcal{L}(\Phi|X) = P(X|\Phi)$, the incomplete likelihood function. Now assume that there exists a complete data set $Z = (X, Y)$, where Y is another random variable corresponding to missing data. The joint density function of Z is given by:

$$P(Z|\Phi) = P(X,Y|\Phi) = P(Y|X,\Phi) \cdot P(X|\Phi) \tag{2.21}$$

Where the likelihood function of this joint density function is given as:

$$\mathcal{L}(\Phi|Z) = \mathcal{L}(\Phi|X,Y) = P(X,Y|\Phi) \tag{2.22}$$

This is called a complete likelihood function. The EM algorithm first finds the expected (E) value of the complete-data log-likelihood i.e. $\log(P(X,Y|\Phi))$ with respect to missing data Y given the observed data X and current parameter estimates. This is called E-step and is specified as follows:

E-step: $Q(\Phi, \Phi^l) = E[\log(\mathcal{L}(\Phi|X,Y)|X, \Phi^l)]$ \hfill (2.23)

Where Φ^l is the current parameter set estimate and Φ is the new parameter set that will be optimized to increase Q. Estimation in E-step is done on the basis of either marginal distribution of observed

incomplete data or some past knowledge or some logical assumptions about missing data or merely some random guess. It is worth noting that X and Φ^l are constants and Y is a random variable in Eq. (2.23). The next step is the iterative maximization (M) of the expectation computed in E-step. It is described as:

M-step: $\Phi^{l+1} = \arg \max_\Phi Q(\Phi|\Phi^l)$ $\hspace{5cm}$ (2.24)

where the superscript l is the index of iteration.

It is proved in [DEM77] that an increase in Q implies an increase in the likelihood of missing data, i.e. $\mathcal{L}(\Phi^{l+1}|X) \geq \mathcal{L}(\Phi^l|X)$ and also that the algorithm is proved to converge to a local maximum of the likelihood function.

2.2.6   Renewal Theory

Renewal theory [COX67] emerged from the study of self-renewing aggregates and was initially used in problems of probability theory related to failure and replacement of some components. Soon it became a tool for investigation of probability of general problems connected with sums of independent non-negative random variables. The theoretical concept of *failure* can be given any interpretation depending upon the context of its application. For example in this thesis packet size and inter-packet arrival times will be used instead of this bookish term.

The fundamental model of renewal theory is based on the definition of an *ordinary renewal process*. Suppose in a mechanical system we have a population of components, each component has a *life-time* specified by a random variable X with PDF $f(x)$. The mechanical system starts with a new component with life-time X_1 at time zero. Assume the component fails at time X_1. It is immediately replaced by another new component which has the life-time X_2. Next failure will occur exactly at $X_1 + X_2$. The process continues and the failure time of the rth component with life-time X_r is specified as follows:

$S_r = X_1 + X_2 + ... + X_r$ $\hspace{5cm}$ (2.24)

If $\{X_i\}$ are independent and identically distributed (i.i.d.)[6] random variables the system is called an ordinary renewal process. As a special case, if X is exponentially distributed with PDF $\lambda e^{-\lambda x}$, the ordinary renewal process is called a Poisson process. In communication systems, a PU radio system transmitting fixed sized data packets with i.i.d. random inter-packet times can be modeled as an ordinary renewal process.

---

[6] In probability theory a collection of random variables is considered i.i.d. if all random variables belong to the same probability distribution and are independent from each other.

The definition of an ordinary renewal process provides the base for defining *alternating renewal processes* that can better explain many real world systems where the concept of immediate replacement is not applicable. Suppose there are two types of components with life-times given by i.i.d. random variables *X* and *Y* with PDF's *f(x)* and *f(y)* respectively. Let say the process starts with a new component of type-X and whenever a component fails, it is replaced by a new component of the opposite type. Then the resulting process is called a alternating renewal process. For example, the radio traffic of an IEEE 802.11 based WLAN network as captured by a sensor (e.g. a spectrum analyzer), where many users are surfing internet, is a good example of an alternating renewal process as shown in Fig. 2.6 for simulated signals. See Appendix A3 for real-time WLAN signals.
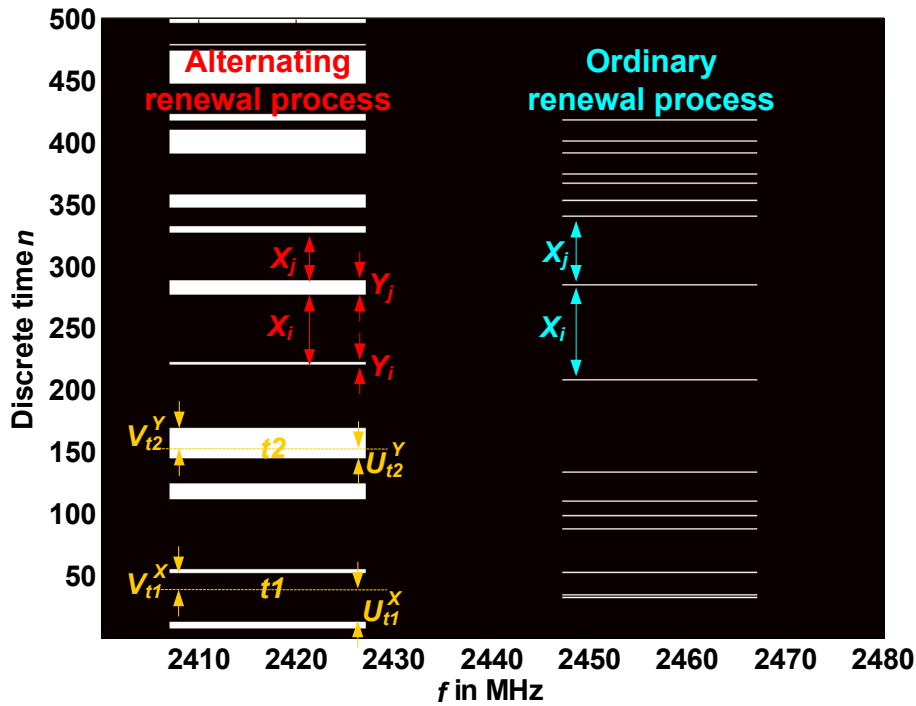
Figure 2.6: *A combined spectrogram of two IEEE 802.11 based 20 MHz wide simulated signals. The packet size of signal at $f_c = 2457$ MHz is equal to one unit of time and inter-packet arrival times are exponentially distributed, that makes it an ordinary renewal process. The other signal, at $f_c = 2417$ MHz demonstrates a more realistic scenario, where both packet sizes (signal ON time) and inter arrival times (signal OFF time) are exponentially distributed, hence an alternating renewal process.*

Furthermore, if the system has been already running since a long time when it is first observed then it is called an *equilibrium* (ordinary or alternating) renewal process. It is more applicable to real world problems since it does not require the system to be observed from the beginning.

By modeling a signal as an ordinary or alternating renewal process, one can use the concepts of renewal theory in order to solve problems of the following types:

- Time up to the rth renewal: If the renewal process is the PU transmission sensed by a sensor, then this can be interpreted as estimating time for transmission of r packets.

- Number of renewals in time t: One is interested in a random variable N_t, which specifies total number of packet transmissions occurring in a time interval (t_1, t_2).

- The moments of the number of renewals in time t: The moments such as mean and variance of number of packets can be computed that can eventually provide an estimate of the transmission rate of a PU system. The first moment, i.e. the mean, of a renewal process is particularly emphasized and is given by:

$$H(t) = E[N_t] \tag{2.25}$$

where $H(t)$ is called the renewal function. This renewal function is used in more general form as $E[N_{t_1, t_2}] = H(t_2) - H(t_1)$, to compute the *renewal density* or the mean number of packets to be expected in a narrow time interval Δt, As follows:

$$h(t) = \lim_{\Delta t \to 0+} \frac{E[N_{t, t+\Delta t}]}{\Delta t} \tag{2.26}$$

- Forward recurrence time (V_t) or backward recurrence time (U_t): The forward and backward recurrence times give the measure of remaining and passed life of a component at any given time t respectively. It can be used to estimate the remaining or passed length of an ongoing packet transmission or conversely, the time that has passed in last transmission or expected remaining time in next transmission by simply exchanging the roles of X and Y.

- The type of component in use at time t: This gives the probability $\pi_i(t)$ that component of type-i is in use at time t. For an alternating renewal process with two types of components i and j it is given as:

$$\pi_i = \frac{E[i]}{E[i]+E[j]} \text{ and } \pi_j = \frac{E[j]}{E[i]+E[j]} \tag{2.27}$$

For the PU signal with ON and OFF component types:

$$\pi_{\text{ON}} = \frac{E[\text{ON}]}{E[\text{ON}]+E[\text{OFF}]} \text{ and } \pi_{\text{OFF}} = \frac{E[\text{OFF}]}{E[\text{ON}]+E[\text{OFF}]} \tag{2.28}$$

- *Survivor function:* Given the cumulative distribution function, $F(x)$, of the current state (let say ON state) of the renewal process, the survival function is the probability that the process has not changed its state since the last known time x. It is specified as follows:

$$\mathbb{F}(x) = \Pr(X > x) = 1 - F(x) = 1 - \int_0^x f(u)du \qquad (2.29)$$

Where $F(x)$ is the cumulative distribution function and $f(u)$ is the PDF of the corresponding state of the renewal process. The survivor function can be used for some useful derivations about the state of the renewal process. For example, an alternating renewal process that has been started a long time ago, the remaining time $\bar{x}$ (see Fig. 2.7) in the current state (let say ON state) from the sampling time t_s is given by $\frac{\mathbb{F}(\bar{x})}{E[ON]}$.

- Transition probabilities of replacement of components: In an equilibrium alternating renewal process with i and j component types, at any given time t if type i component is in use then the probability that type j component will be replaced can be computed as transition probability.
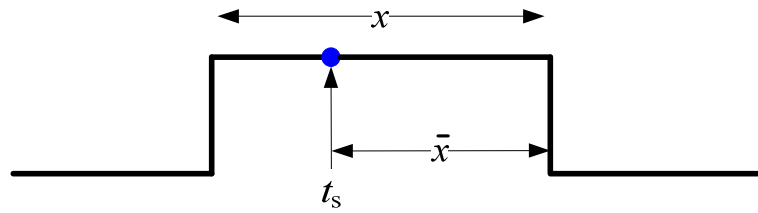
Figure 2.7: *Illustration of the remaining time in ON state.*

2.3 Standard Wireless Technologies Used as Primary User Systems

The following standard wireless technologies are used in this research work as primary user (PU) systems and are described in detail in Appendix A3 with respect to selected PHY/MAC layer parameters. Selected PHY/MAC parameters are channel definition (bandwidth (BW), center frequency (f_c)), pulse shape, modulation, hopping pattern, time behavior, bitrate, symbol rate and transmission power. Moreover, all these technologies operate in the 2.4 GHz ISM band.

1. IEEE 802.15.1 based technologies

    a. Bluetooth

    b. Wireless Interface for Sensors and Actuators (WISA)

      c.   Wireless Sensor Actuator Networks for Factory Automation (WSAN)

2. IEEE 802.15.4 based technologies

      a.   ZigBee/ZigBee Pro (non-hopping system)

      b.   WirelessHART

      c.   ISA100.11a

      d.   IEEE 802.15.4a based NanoNET

3. IEEE 802.11 based Wireless Local Area Networks (WLAN)

4. Atmel's ATR2406 based proprietary transceiver. Note that this technology will be referred as 'Atmel' throughout in this document. Although it is not a standard technology, it will be used in this thesis as a non-hopping system that is very similar to Bluetooth in terms of channel definitions.

Chapter 3

Problem Definition and Proposed Solution

The coexistence of wireless devices can be studied with respect to the following three issues:

- *Collaborative* vs. *non-collaborative*: A coexistence mechanism in which coexisting systems can exchange information is known as collaborative. For coexisting systems that can't exchange any information, only non-collaborative coexistence mechanisms can be employed.

- Coexistence of *heterogeneous* or *homogeneous* devices. Heterogeneous radio systems use different technologies, whereas homogeneous radio systems make use of the same radio technology.

- *Collocation* vs. *proximity*: Collocation is the case when multiple radios are in a single physical unit so that mutual interference can be caused by conduction, parasitic radiation or antenna near field radiation. The recommended practice by IEEE 802.15.2 regards the interference between IEEE 802.11 and IEEE 802.15.1 based devices as collocation when their device antennas are placed less than 0.5 meters apart. On the other hand, proximity considers larger distances, where interfering effects are only caused by radiation. The devices are typically located in the antenna far field range.

Since there are better chances to exchange information among homogeneous devices, therefore their coexistence can almost always be dealt by using collaborative means. Whereas, the coexistence of collocated devices is mainly a concern of device manufacturers. This dissertation proposes cognitive strategies to improve the coexistence behavior for non-collaborative heterogeneous and homogenous radio systems operating in proximity scenarios.

This chapter discusses major challenges involved to realize these cognitive strategies and proposes suitable solutions. Table 3.1 briefly summarizes the concepts presented in this chapter while Fig. 3.1 presents a flow diagram of existing and proposed strategies in a comparative manner. Later on, section 3.1 confines limitations of existing cognitive methods. Section 3.2 presents proposed solutions and section 3.3 proposes a cognitive engine that incorporates the proposed solutions.

Table 3.1: *Summary of limitations of existing cognitive strategies and solutions proposed in this thesis.*

	Existing approach	**Proposed approach**
Predictive modeling	*Multi-channel predictive modeling:* Reactive / proactive sensing can't anticipate the primary user activity and results in harmful collisions between primary and secondary signals. In order to coup with this problem predictive modeling based OSA has already been proposed. Multi-channel view of traditional predictive sensing approaches doesn't account for missing information caused by limited sensor bandwidth. Therefore, accuracy of model parameter estimation remains a critical limitation of existing predictive modeling based OSA approaches in real-time applications. **(section 3.1.1)**	*Multi-PU predictive modeling:* Multi-PU view of proposed predictive sensing approach supported by a radio knowledge base (RKB) performs *bandwidth independent parameter estimation* to treat the missing data caused by limited sensor bandwidth. Individual PU streams are extracted from the amalgamated coexistence stream and are modeled individually. Hence, statistical parameters are estimated for individual PU systems instead of individual channels. **(section 3.2.1),** **(chapter 4, chapter 5)**
Decision making for resource allocation	*Dumb hole detection (DHD):* Decision making about radio resource allocation is done on the basis of spectral holes. Where, a spectral hole is the result of binary hypothesis testing (Eq. 2.1) based spectrum sensing. It merely carries information about the presence or absence of a primary signal and doesn't provide detailed coexistence behavior of primary signals. Eventually, opportunities in the coexisting environment can't be fully exploited because of limited knowledge provided by the spectral holes, therefore the existing hole detection approach is dumb. **(section 3.1.2)**	*Intelligent hole detection (IHD):* M-ary hypothesis testing (Eq. 2.2) is proposed to classify the primary signals with respect to standard technologies. The identification of primary signals in turn can be used to learn transmission characteristics of the signal from documented standards that better explains the coexistence behavior of signals. RKB can be maintained that includes documented knowledge of primary systems and secondary system's operating history. Signal identification is then used to index useful information in RKB to explore hyper-spatial holes to better exploit opportunities in the coexisting environment in an intelligent way. **(section 3.2.2),** **(chapter 4, chapter 6)**

3.1 Shortcomings of Existing Cognitive Strategies
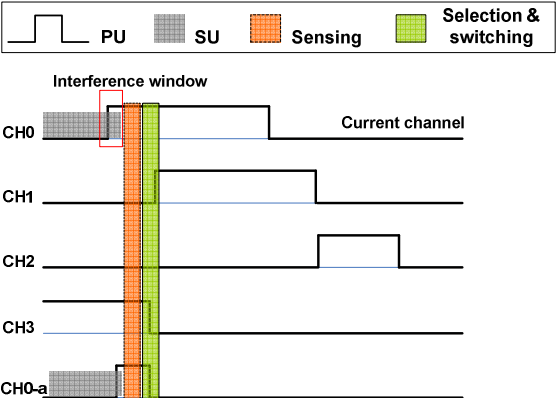
A SU requires efficient situational awareness to utilize cognitive measures against harmful interference to/from PU systems. Where, situational awareness includes sensing the environment followed by a hypothesis testing for detection of available opportunities in the shared radio environment. In predictive modeling based approaches, the situational awareness is further enriched by forecasting the primary activities in the radio environment. Improved knowledge about the coexisting environment essentially means better decision making for secondary resource allocation. The following subsections identify shortcomings of existing situational awareness and cognitive decision making mechanisms.

3.1.1   Multi-channel Predictive Modeling

Typically, a CR system either senses a channel just before starting its desired transmission or performs this task periodically in order to remain aware about the operational environment. The former method is typically known as reactive sensing, while the latter one as proactive sensing [GHA08, HYO08]. Apart from *when to sense*, both methods are similar in nature, because both decide about the availability of the sensed channel merely on the basis of information obtained during the sensing process as illustrated in Table 3.2. These approaches can be regarded as *collision detection* strategies, since preventive measures can only be taken upon detecting a collision. Consequently both approaches suffer from the following problems:

1. It is not possible to anticipate the usage of a spectral area, which hinders optimal decision making for channel selection. For instance, selection of CH1 and CH2 in Table 3.2 is equally likely, although CH1 will result soon in an extra switching. Similarly, CH3 can be an excellent choice, since it is available for the longest time in future, but a conventional sensing method will always detect it as a black hole.

Table 3.2: *Conventional reactive/proactive sensing vs. predictive sensing*

		Conventional sensing		Predictive sensing	
		classification	switching	classification	switching
		black hole	yes	black hole	yes
		white hole	yes	black hole	-
		white hole	-	white hole	-
		black hole	-	white hole	-
		black hole	yes	white hole	no

2. There is always an interference window before a collision is detected, as shown at 'current channel - CH0' in Table 3.2.

3. SU transmission often suffers unnecessary interruptions. For instance, if CH0-a is the current channel, then the selection of a new channel may not be an optimal decision since the interference is for such a short time that it will be ended just after the switching is done. Similarly, selection of CH1 will result in an unnecessary interruption soon after switching is completed.

The limitations of reactive/proactive sensing approaches can be overcome by predictive modeling based OSA[7] which is also referred as predictive sensing. It uses statistical modeling of the channel usage and employs probabilistic methods to predict those spectral-temporal areas where collisions are least likely to occur. Therefore, it can be regarded a *collision avoidance* (CA) approach. A comparison of predictive sensing with conventional methods is presented in Table 3.2 and further discussed in section 3.1.1.2.

3.1.1.1   Sensor Bandwidth Limitation

In order to completely understand the working and limitation of state-of-the-art predictive modeling based OSA approaches it is necessary to first recognize a fundamental limitation of sensing platforms. The sensing platforms that can be used for data acquisition can be categorized as *wideband* or *narrowband* with respect to the bandwidth of sensor (B_s) relative to the bandwidth of interest (B_W). Where, $B_s < B_W$ and $B_s \geq B_W$ correspond to the narrowband and wideband sensing platforms, respectively. Due to technological limitations a narrowband sensor is employed quite often in existing real-time applications. A standard method to scan the entire band of interest with a narrowband sensor is swept sensing [TEK04-AGI04] as illustrated by Fig. 3.1.

However, swept sensing can easily miss primary radio systems resulting in a loss of valuable spectral-temporal information which is vital for predictive modeling and parameter estimation. A solution, to improve the detection probability, is to sense for a longer time at a single frequency as shown by triangles in Fig. 3.1. However, this solution can only improve the detection probability in situations where a single frequency has to be particularly stressed e.g. if the CR system is already transmitting in a channel and it wants to continue in the same channel and just wants to make sure after some time that the channel is still free. The overall probability of data loss does not improve across the entire band of interest. Furthermore, this solution directly conflicts with the efficiency requirements particularly in real-time applications with low latency requirements, especially because the task of sensing is already quite time consuming as compared to other tasks of a radio system. Cooperative sensing using multiple sensors can be another

---

[7] It is also referred as MAC-layer sensing or MAC-PHY sensing or cross layer sensing in the literature

solution, e.g. as used in [XIZ11], but at an expense of increased system complexity, cost and resources. This thesis will present non-cooperative cognitive strategies using a single narrowband antenna.
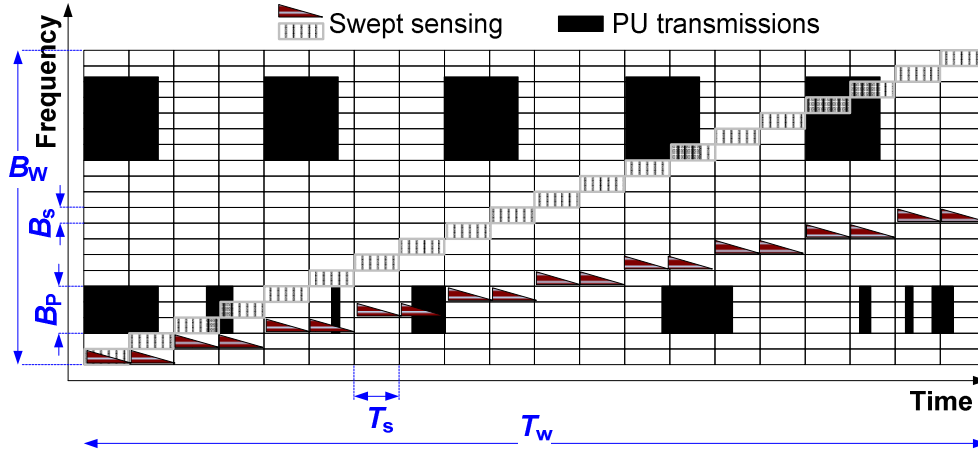
Figure 3.1: *Illustration of swept sensing. Where, T_s = sample time, T_w = time required to sweep the entire band of interest, B_P = bandwidth of primary radio system.*

3.1.1.2 Predictive Sensing: Multi-channel Predictive Modeling Approach

In general, given that the SU is not able to sense the entire band of interest at once, the existing predictive sensing strategies view the spectrum as a collection of multiple non-overlapping channels and model the PU activity in each of these channels. The model is then either used to directly choose a channel with least probability of interference instead of sensing before each secondary transmission or is used to sense the channels in an optimal order with an objective to detect maximum opportunities. Following is a short literature overview of predictive sensing approaches:

In [HYO08], a sensing-period optimization mechanism, a channel-sequencing algorithm and an environment adaptive channel-usage parameter estimation method are presented. The PU traffic is assumed independent identically distributed ON/OFF patterns and is modeled using a semi-Markov process. It proposes a maximum likelihood parameter estimation method using four transition probabilities (ON→ON, ON→OFF, OFF→ON, OFF→OFF) of the channel usage which have to be computed from samples acquired for each channel. The predictive modeling based method is reported finding 22 % more opportunities with smaller channel discovery delay than the conventional sequential sensing method.

In [HAI09], the optimal sensing order problem is formulated as a multi-armed bandit problem for multiple channels. The busy/free status of each channel is independent from other channels. Statistical parameters of primary transmissions in each channel are computed online using a gradual sensing

method. As a starting point, each channel is sensed once and an initial estimation of parameters is obtained which is then gradually improved as the sensing time grows.

An extended knowledge based reasoning (EKBR) is presented in [XIA10]. A secondary user initially possesses no statistical information about the primary traffic which is assumed an i.i.d. Poisson arrival process. It performs fine sensing in a proactive manner to determine an initial set of probabilities regarding channel availability. Upon the request of data transmission, the SU retrieves its short-term statistics, and initiates fast sensing immediately on all channels to obtain the instantaneous statistical information. The short-time and instantaneous statistics are then used with knowledge based reasoning to maximize the detection probability of opportunities. OSA using EKBR is reported to have outperformed the traditional approaches in terms of sensing delay, transmission rate and percentage of missed opportunities.

In [HOY08], sensing information is stored in a channel history database in order to retrieve it later to compute statistical parameters of channel usage, where multiple channels are sensed sequentially. Primary traffic in each channel is first classified as one of four patterns which are, periodic traffic with fixed ON+OFF time, fixed OFF and random ON times, fixed ON and random OFF times, both ON and OFF random times. Probabilistic availability of each channel is then computed using the identified patterns of ON and OFF states of the channel. It is demonstrated using simulations that the channel switch rate is reduced up to 55 % in comparison to the traditional reactive methods.

In [QIN07], the theory of a Partially Observable Markov Decision Process (POMDP) is used to provide an analytical framework for opportunistic spectrum access. The usage of each channel is assumed to follow a Markov chain, whose transition matrix is already known to the secondary users. Using POMDP an opportunistic user makes optimal decisions for sensing and access based on the belief vector that summarizes the knowledge of the network state based on all past decisions and observations.

In [XIZ11], a Cognitive Radio-EnAbled Multi-channel MAC (CREAM-MAC) protocol with cooperative sequential spectrum sensing scheme with multiple channels is presented. The channel usage pattern of the PUs follows an i.i.d. ON/OFF renewal process. Multiple nodes of the SU network cooperate to maximize the detected opportunities where each SU is equipped with multiple sensors.

In [GEI07], a Poisson distributed IEEE 802.11 based WLAN network traffic is modeled using a semi-Markov process in order to exploit temporal opportunities. Spectrum sensing and predictive modeling are performed for only one channel where the WLAN based PU is active. An enhanced hopping scheme is then presented for Bluetooth systems to coexist with the WLAN primary system. It is demonstrated that

the predictive modeling based hopping scheme outperforms the traditional counterpart in terms of collision rate and throughput.

All this work reports promising results and highlights the usefulness of predictive modeling to realize opportunistic spectrum access. However, model generation and parameter estimation methods of these strategies face at least one of the following limitations:

1. All primary channels are sequentially sensed to acquire the training data such as in [HYO08]. However, as the number of channels increases the sampling interval between two consecutive samples of a particular channel increases as illustrated in Fig. 3.2, which decreases the accuracy of estimated model parameters.
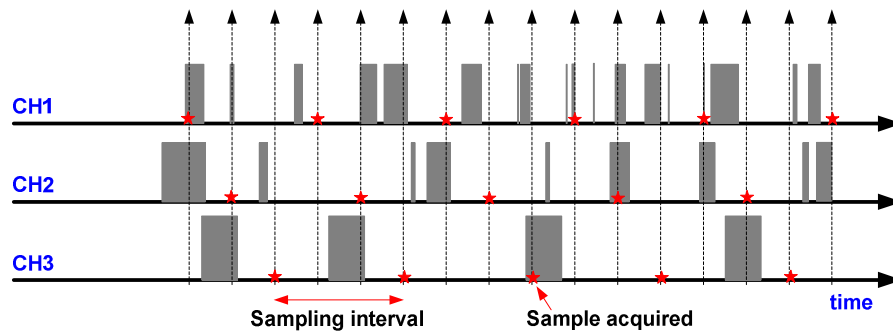
Figure 3.2: *Sequential sampling of three channels*

2. It is sometimes assumed that statistical parameters of the primary traffic are known to the cognitive system, e.g. in [QIN07], which is an unrealistic assumption for time varying environments.

3. Sometimes, only a small set of channels is considered for modeling where it is very easy to collect statistical parameters of the PU system. E.g. [GEI07] where only active channels of IEEE 802.11 are modeled.

4. Multiple multi-sensor or single sensor nodes cooperate to acquire samples of multiple sensors [XIZ11]. Firstly, it requires more resources and secondly, the data acquisition problem becomes trivial at each individual node similar to the one mentioned in 3.

5. A gradual learning approach, e.g. [HAI09, XIA10], shows potential for real-time parameter estimation. However it also relies on assumptions and limitations stated in 1-3.

6. Sensing information is stored, e.g. in [XIA10, HOY08], and used later for statistical parameter estimation. However, the dynamic nature of real-time environments may not be accurately represented with previously stored information.

Summarizing the entire discussion presented in section 3.1.1 it can be concluded that despite the effectiveness of existing predictive modeling in OSA based approaches there is still a great need for advanced methods that can provide up-to-date and accurate model parameter estimation when the wider band of interest is comprised of multiple channels accompanied by a narrow bandwidth of the SU sensor. Section 3.2.1 proposes identifying and extracting individual PU systems from the coexisting environment to perform bandwidth independent parameter estimation using non-cooperative sensing with a single antenna. In turn, transmission characteristics of each PU should be modeled separately giving a multi-PU view of the spectrum instead of the traditional multi-channel perspective.

3.1.2   Dumb Hole Detection

Conventionally, the hole detection process merely identifies the presence or absence of the PU signals as it is formulated by the binary hypotheses given in eq. (2.1). Such a hole detection process provides information about:

1.   The instant occupancy status of the scanned spectral area.
2.   The signal strength of the PU signals.

It can be argued that this information is not enough to tune the cognitive radio system to optimally exploit the multi-dimensional opportunities. Therefore, it shall be named a dumb hole detection (DHD) method. In order to understand this notion, it is important to understand the concept of *coexistence margin*, which can be defined as follows:

Coexistence margin: *"Coexistence margin is the measure of ability of a SU radio system to tolerate interference or accommodate interference if it is intolerable."*

It is a combination of *the perspective of the harmful interference and reconfigurability* of a radio system, *physical strength of interfering signal* and *appropriateness of situational knowledge acquired by the SU system*. These parameters are explained in the following:

Perspective of the harmful interference: As already mentioned in the first chapter, harmful interference, i.e. the level of interference where the performance degradation is felt by a radio system, depends on operational circumstances and goals of the radio system. A robust communication system may tolerate high interference because error handling methods employed across different layers of its protocol stack are able to keep the influence of interference hidden from its end users. It can do so by either error correcting codes or retransmissions at the data link layer or routing around areas of high interference at the network layer or by using more buffering at the application level etc. However, consequences of these error handling methods such as reduced battery life, increased delay, reduced

system capacity or coverage may themselves be significant performance degradation factors for other systems. Systems that can't compromise on these factors may require a lightweight stack, consequently lacking such cross layer error handling capabilities which make them unable to tolerate even low to medium levels of interference. Eventually, there is a greater need of coexistence management strategies for such radio systems.

Physical strength of interference: Physical strength of interference over the time interval, in which the cognitive SU is interested to transmit, is the result of interferer's bandwidth, received power at recipient's antenna and duty cycle. Although, channel parameters such as path loss and fading effects also significantly influence the physical strength of interference, but these are beyond the scope of this thesis. Meanwhile, the duty cycle itself is a function of many other signal parameters such as symbol rate, packet length, retransmissions, overhead bytes, preamble length, total number of network nodes etc.

Reconfigurability: A SU radio platform offering more configurable orthogonal parameters will be able to exploit more dimensions of the hyperspace (see Table 3.3 for a short list of important hyperspace dimensions). Note that these hyperspace dimensions are orthogonal opportunities from the SU's perspective but are operational parameters of primary systems that influence their coexistence behavior. For example, a CDMA based PU system offers an orthogonal opportunity in the code dimension but only a CDMA enabled SU system can avail this opportunity.

Appropriateness of situational knowledge: The hyperspace dimensions are directly related to the operating parameters of the PU system that define its coexistence behavior. Consequently, a particular hyper-spatial opportunity emerges only if the PU system is operating using certain parameters. A CR system needs sufficient knowledge about operational parameters of the PU systems in order to optimally tune the underlying radio system. For instance, a SU capable of transmitting using CDMA can justifiably choose this option only if it knows that the PU system is a CDMA based system. However, the DHD method considerably lacks such situational knowledge. In addition to this, the DHD method also has the following limitations:

1. The DHD method can't even completely evaluate the physical strength of interference because of its inability to detect several important parameters such as symbol rate, packet length, retransmissions, overhead bytes, preamble length, total number of network nodes etc.

2. Different hopping systems have different hopping characteristics. For example, a Bluetooth system offers very short lived interference since it stays for only $625\ \mu s - 1875\ \mu s$ in a single channel as compared to several milliseconds of a slow hopping ISA100.11a system. Some hopping systems may be simultaneously using several channels; an example of which is Wireless Interface for Sensors and Actuators (WISA) using 5 channels (see Appendix A3). Knowledge of

such hopping characteristics can be very helpful in the decision making process but it can't be provided by the DHD method as it merely detects the instant occupancy status.

Table 3.3: *Selected dimensions of hyperspace and related coexistence opportunities. A comprehensive list of communication parameters that can affect coexistence behavior and operation of radio systems is provided by IEEE 1900.2 [STD28] and is included in Appendix A1.*

General class	Hyperspace dimension	Opportunity
Frequency	Frequency	Utilize frequency multiplex.
Time	Time	Utilize time multiplex.
Space	Location	Utilize MIMO features, i.e. make use of directional transmitting and/or receiving abilities.
	Angle of arrival (AoA)	
Additional signal features	Code	These items can be viewed as secondary dimensions of hyperspace but can help to achieve simultaneous transmission without interfering primary users.
	Polarization	
	Power	Concepts such as an ultra-wideband underlay, spread spectrum, and interference temperature [HAY05] are all methods that manage transmit power to improve coexistence with other radio systems.

In short, more knowledge of the coexisting environment enables the cognitive system to perform better decision making to optimally exploit available opportunities in a multi-dimensional hyperspace. Although the DHD method if using some sophisticated spectrum sensing methods, e.g. CFD, can detect few additional parameters such as modulation, symbol rate, chip rate etc., only at a cost of increased overhead and complexity. Yet it is impossible to detect all communication parameters using this approach. However, the complete set of communication parameters of the primary systems will better express their coexistence behavior. Hence, there is a need to find methods that can enable the CR system to acquire enough knowledge of the transmission characteristics of primary systems. Section 3.2.2 proposes to classify the PU systems with respect to standard technologies. The standard based identification of PU systems can then be used to learn the complete communication parameter set of the corresponding PU systems from documented standards.

3.2 Proposed Solutions

3.2.1 Multi-PU Predictive Modeling

Instead of dividing the entire band of interest into multiple channels with respect to the bandwidth of SU sensor and modeling the usage of each individual channel, this dissertation suggests modeling the transmission pattern of each coexisting system separately. In order to do so the coexisting systems have to be first identified. Once identified, transmission streams of individual PU signals have to be extracted from the amalgamated coexisting environment. The extracted signals of s_i a-priori known technologies can then be individually modeled and due to the linear proximity environment the accumulative response of these individual models can be used to approximate the overall statistical behavior of the coexisting environment x, as specified by eq. (3.1) and eq. (3.2) in time and frequency domains respectively.

$$x(t) = s_1(t) + s_2(t) + \cdots + s_n(t) \tag{3.1}$$

Taking the FFT of eq. (3.1) results in eq. (3.2):

$$X(f) = S_1(f) + S_2(f) + \cdots + S_n(f) \tag{3.2}$$

The main advantage of identifying and modeling individual primary signals over traditional multi-channel based approaches is that it enables to use known signal features for reliable modeling and parameter estimation.

3.2.1.1   Bandwidth Independent Parameter Estimation

In order to put the narrowband sensors to the same grade of performance as of wideband sensors bandwidth independent parameter estimation methods are proposed in this thesis work. The term bandwidth independent in the context of predictive modeling means that the estimation error should be independent of the sensor bandwidth (B_S), PU bandwidth (B_P) and the width of entire band of interest (B_W). As an example, consider that two PU systems with bandwidths $B_{P1} = 1$ MHz and $B_{P2} = 20$ MHz and arrival rates λ_{P1} and λ_{P2} are coexisting in the 2.4 GHz band ($B_W = 80$ MHz) and two sensors with bandwidths $B_{s1} = 1$ MHz and $B_{s2} = 80$ MHz are independently used to sense the radio environment. The bandwidth independent estimation ideally means that the estimated values of λ_{P1} and λ_{P2} should be the same for both sensors. The proposed approach involves two major concepts; these are, viewing the shared spectrum from the multi-PU perspective instead of multi-channel perspective and treating the problem of modeling using narrowband sensing as a problem of learning from missing data.

3.2.1.2 Parameter Estimation using Narrowband Sensors - a Missing Data Problem

Since narrowband sensing always misses some useful data, the parameter estimation problem using a narrowband data acquisition platform has to be treated as a problem of learning from missing data. The eventual target is to estimate statistical parameters such as mean, arrival rate etc., of the primary signals of diverse bandwidths with the same level of accuracy using wideband as well as narrowband sensing platforms. Primary transmissions are modeled using first order Markov model in chapter 5 and HMM and renewal theory based methods are used to estimate model parameters in the presence of missing training data.

3.2.2 Intelligent Hole Detection

In order to equip the CR system with sufficient situational knowledge this thesis suggests an *intelligent hole detection* (IHD) method. In a broader sense, IHD means cognitive decision making for radio resource allocation has to be performed on the basis of complete knowledge of the PU systems. The idea is to use a radio knowledge base (RKB) to include information extracted from documented standards for all systems of interest. The extracted information such as bandwidth, channel frequencies, modulation, data rate, spreading, hopping etc. can better explain the coexistence behavior of the primary system in contrast to only considering the signal strength and instant occupancy status of the spectrum. In turn, the CR system can identify the coexisting systems and relate the already stored information to acquire enough situational knowledge to perform optimal tuning as illustrated by Fig. 3.3. Additionally, the CR system can evolve its RKB by collecting its own working experience with respect to different coexisting systems if it is aware of the identity of the PU systems.
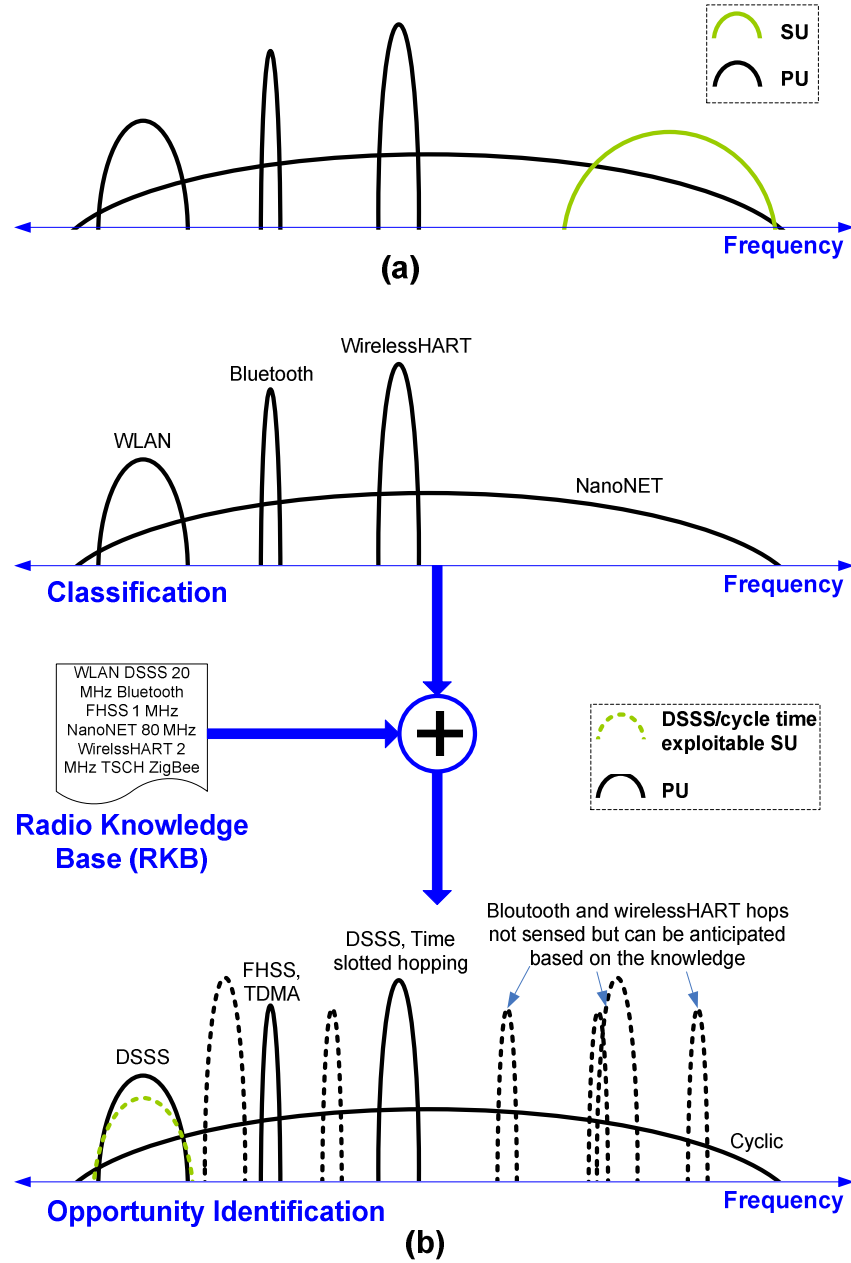
Figure 3.3: *A hypothetical example of coexistence management of DHD and IHD based CR systems in a crowded environment.* **a)** *If a white hole is not detected then the DHD based CR system decides to transmit at a frequency where the amplitude of the interfering signal is weakest,* **b)** *An IHD based CR system can reject interference of all four PU systems as follows. It chooses a DSSS based waveform to reject WLAN interference and transmits in idle times between consecutive cyclic transmissions of a NanoNET based interferer. The knowledge of the CR system about the ability of Bluetooth and wirelessHART to blacklist active WLAN channels can be another motivation of choosing to coexist with the WLAN system and avoid both other systems.*

3.2.2.1   A Real-time Example

A simple cognitive test-bed, based on USRP2 [ETTUS], is implemented to demonstrate the decision making based on dumb and intelligent hole detection methods. There are four channels for the SU test-bed defined over 10 MHz bandwidth at 2.407 GHz, 2.422 GHz, 2.44 GHz, and 2.455 GHz center frequencies. Three different PU systems are used to create a coexistence scenario in the 80 MHz wide 2.4 GHz band as shown in Fig. 3.4a. Based on prior experimental results, the CR system has learnt (in fact this information is hardcoded in SU to substitute a real RKB) that an Atmel system (PU$_1$ in Fig. 3.4) is a very high duty-cycle periodic system and the worst interferer for it. IEEE 802.11 based PU$_2$ is a mediocre interferer and CSS based PU$_3$ is a wideband low duty-cycle system and offers almost negligible interference to it. To realize the DHD method, the test-bed needs no knowledge about the PU systems and simply scans the entire band to find available holes. After finding the entire band equally occupied it decides to transmit in the first channel as shown in Fig. 3.4b and suffers very high interference from PU$_1$ and PU$_2$. In order to realize the IHD method, the cognitive test-bed identifies the coexisting radio systems (using the NFSC classifier presented later in chapter 4) and uses its stored (hardcoded) knowledge about the strength of these interferers to take a decision about tuning itself. Eventually, the SU chooses the last channel, where the interference is negligible (Fig. 3.4c).

(a) Coexistence environment

(b) Dumb hole detection based operation

(c) Intelligent hole detection based operation
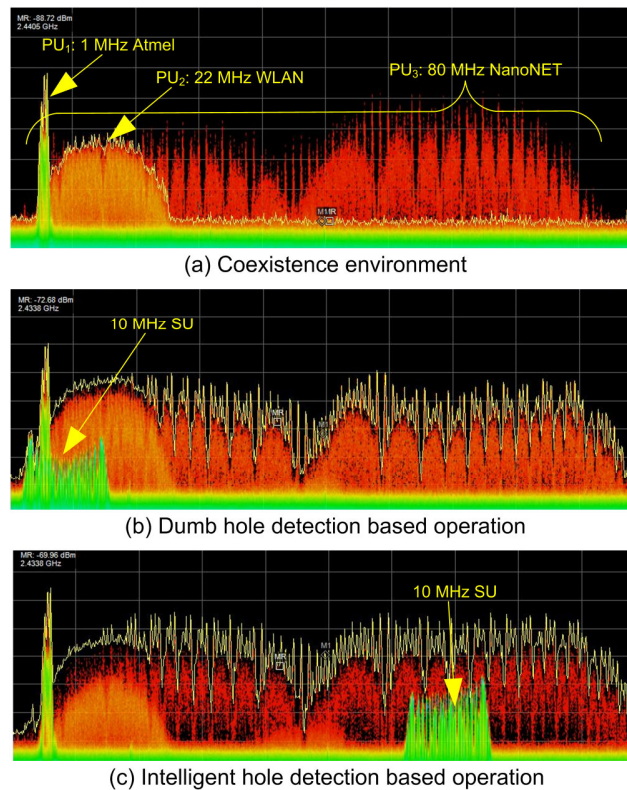
Figure 3.4: *Opportunistic operation of a USRP2 based SU using DHD and IHD based methods.*

Obviously, this example scenario is limited but at this point it is sufficient because the main purpose is to illustrate the concept. In real-time situations the optimal parameter selection can itself be a significant challenge because the coexistence of radio systems is a multi-objective optimization problem [THO07]. Hence, the CR system should be able to plan a set of operating parameters that meet all conflicting objectives under imposed constraints. In this simple example the parameter selection or more formally the resource allocation problem is mere frequency selection. However, in real-time scenarios the resource allocation problem is expected to be much more complicated than this example because the CR system has to evaluate all possible orthogonal opportunities with respect to the given coexistence scenario and reconfiguration capabilities of itself.

Overall, there are three constituents of the proposed IHD method. These are *classification of primary signals*, *maintenance of RKB* and *optimal resource allocation*. This dissertation will address the problem of signal classification in chapter 4. The remaining aspects of IHD are addressed in chapter 6 for some selected scenarios.

3.2.3   Classification of PU Signals with Respect to Known Standards

Classification of primary signals is basic to multi-PU predictive modeling and intelligent hole detection methods. It has already gained much attention but the majority of the stat-of-the-art radio signal classifiers such as [FEH05, KYO07, HAN08, WUD05, CAT07, JOL08, WEN99], lie in the category of automatic modulation classification (AMC)[8] as shown in Table 3.4. However, in order to usefully utilize the documented knowledge of standard technologies it is essential to classify the signals with respect to known standards. While, modulation alone cannot be used for this purpose because many standard technologies can employ the same modulation e.g. ZigBee, ISA100.11a and WirelessHART all use O-QPSK modulation. Therefore, the classification of coexisting signals with respect to known standards is an essential part of this dissertation. A neuro-fuzzy signal classifier (NFSC) is presented in chapter 4 to classify the primary radio systems with respect to known standards. It uses operating frequency, bandwidth, pulse shape, hoping behavior and time behavior of primary systems as distinct features.

However, a few contributions presented in recent years have already addressed the classification of signals with respect to standard technologies, such as [SHR11, PAL03]. The work presented in [SHR11] uses a WiFi based Airshark card, capable of acquiring RSSI based spectrum sensing using 20 MHz bandwidth, to classify several state-of-the-art hopping and non-hopping standard radio technologies. The overall approach looks somewhat similar to that of the NFSC though it uses a decision tree based classifier unlike the neuro-fuzzy approach of the NFSC. However, the NFSC had already been partially

---

[8] AMC is the automatic identification of the modulation of the received signal without any prior knowledge.

reported in [AHD10, AHA10] before [SHR11]. Furthermore, a 20 MHz sensor is already wide enough to acquire good training data in an 80 MHz target bandwidth. In comparison to it the NFSC does not limit itself to a sensor of any particular bandwidth and treats the classification problem generally in the context of sensor bandwidth. The work presented in [PAL03] addressed the problem of standard classification using a two parameter (pulse shape, BW) NN based classifier. In contrast to it, firstly, the NFSC includes more parameters i.e. f_c, hopping behavior, temporal behavior in addition to pulse shape and BW, as distinct features providing better discriminating capabilities. Secondly, the fuzzy logic based approach of the NFSC strengthens discriminating capabilities of the classifier because fuzzy-logic provides robustness against noise and other anomalies caused by multipath and fading effects of real-time environments.

Table 3.4: *A survey of radio signal classification methods*

References	Parameter extraction method	Parameter extracted	Learning method	Labeling
[FEH05]	SCF	$\propto$-profile[2]	MLPN[1]	Modulation
[KYO07]	SCF	$\propto$-profile[2]	HMM	Modulation
[HAN08]	SCF	$\propto$-profile[2]	SVMFM[1]	Modulation
[WUD05]	Wavelet analysis	Localized frequency	WSVM[1]	Modulation
[CAT07]	PDF[1] of frequencies	Frequency distribution features[3]	Multiple NN	Modulation
[JOL08]	PSD, SWWVD[1]	Modulation type, modulation parameters, Instantaneous frequency	Rule based classifier	Modulation
[WEN99]	Constellation diagram	Constellation points	Fuzzy logic	Modulation
[QIN08]	Universal classifier	BW, symbol timing	Sample, symbol and frame based reasoning	Analog-digital categorization, modulation
[SHR11]	RSSI based frequency-time representation	BW, f_c, Spectral signature, Duty cycle, Pulse signature, Pulse spread, Pulse distribution	Decision tree	Standard
[PAL03]	PSD	BW, Pulse shape	RBF[1] NN	Standard

1. Wavelet SVM (**WSVM**), Support vector machine and feature matching (**SVMFM**), Multilayer Linear perceptron network (**MLPN**), Temporal width (**TW**), Smooth-windowed Wigner-Ville distribution (**SWWVD**), Probability density function (**PDF**), Radial Basis Function (**RBF**)

2. $\propto$-**profile** is the highest value of the spectral correlation function (**SCF**) for a given cyclic frequency '$\propto$'

3. **Frequency distribution features** used are mean frequency and standard deviation of frequency

Furthermore, to the best of my knowledge the influence of bandwidth of data acquisition platform is never studied in the context of radio signal classification. The NFSC explicitly addresses the role of sensor bandwidth and studies test case scenarios using narrowband as well as wideband sensing platforms. Unlike supervised learning approaches, the NFSC follows an un-supervised approach and does not need explicit training. The need for training is not only a complicated job because it is difficult to obtain the training data of all real-time scenarios but it also causes the overfitting problem. Finally, the NN based architecture offers scalability. To add a new radio technology or a new signal feature PE's corresponding to newly desired functionality have to be added without disturbing the existing structure. As an example a state-of-the-art modulation classifier can be added to the NFSC by merely adding new processing elements.

3.3 Coexistence Optimized Cognitive Engine

The proposed model of a coexistence optimized cognitive engine (COCE) combines all suggested ideas as shown in Fig. 3.5. Its functionality can be divided into five main components: *signal classifier*, *predictor*, *opportunity locator*, *sensing organizer* and *parameter selector.* Additionally, these components share a *radio knowledge base (RKB)* which stores 'expert knowledge' about radio systems and channels. This expert knowledge includes extracted information from documented standards and cognitive radios' own working experience and can be maintained manually or automatically by the system through an evolution process.
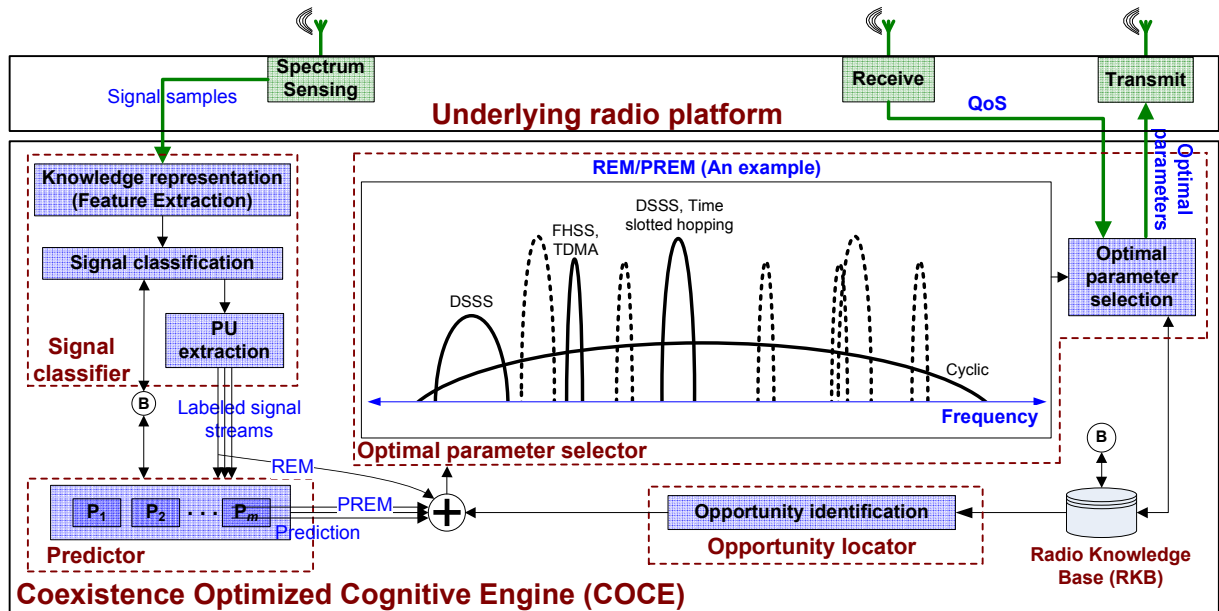
Figure 3.5: *Conceptual model of the proposed coexistence optimized cognitive engine*

As a first step, unknown radio systems are labeled by the signal classifier. Based on this labeling information the signal classifier decomposes the incoming coexisting stream and outputs the individual signal streams. These streams represent the ON and OFF patterns of spectral usage at respective discrete time steps. Where sample time T_s of the underlying sensor provides the fundamental step size in all components of COCE.

The extracted signals of a-priori known technologies can be individually modeled and the accumulative response of these individual models can be used to approximate the overall statistical behavior of the coexisting environment, as specified by eq. (3.1) and eq. (3.2). A bank of predictors, which includes one predictor corresponding to each distinct radio technology, receives the extracted signal streams. Each predictor models the incoming signal and generates probabilistic prediction of temporal-spectral behavior of the corresponding PU system.

Furthermore, a radio environment map (REM) or a predicted REM (PREM) can be generated by combining the expert knowledge from RKB with either labeled signal streams or prediction, respectively, depending on the needs of the underlying radio platform. For instance, a SU radio platform capable of exploiting only frequency and time dimension may find it useful to use prediction to subsidize its limited reconfigurability. On the other hand, a platform richer in terms of reconfigurability, may already have enough leverage and can choose merely a REM to omit the modeling overhead to increase its efficiency. Finally, this REM/PREM is used by a parameter selection method to choose an optimal combination of parameters for safe transmission.

Chapter 4

Classification and Extraction of Primary User Systems

The process of signal classification typically consists of a feature extraction phase followed by a classification or labeling phase as shown in Fig. 4.1. Where, prominent signal features often used as distinct features for signal classification are modulation, data rate, symbol rate, bandwidth (BW), center frequency (f_c), signal power, time and hopping behavior.
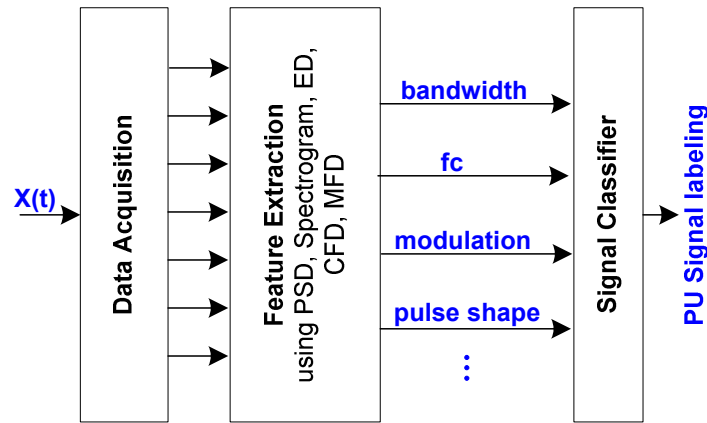
Figure 4.1: *Signal classification process*

Generally, the extraction of certain signal features needs complex and expensive signal processing. For instance, a popular method for this purpose is the computation of the spectral correlation function (SCF) which requires the FFT computation of order N followed by cross-correlation of order N^2. Such challenging computational effort is not feasible in existing radio platforms. On the other hand, some of these signal features can be extracted without going into internal details of the signal, e.g. by using power spectral density (PSD) or frequency-time representation of signals. It merely needs FFT processing of order N. Table 4.1 lists important MAC/PHY layer parameters and methods used in popular literature to extract these parameters.

This chapter presents a neuro-fuzzy signal classifier (NFSC) which uses a-priori known signal features to classify the PU systems and extract them from an incoming coexisting stream as earlier mentioned by eq. (3.1) and eq. (3.2).

Table 4.1: *Prominent signal features and corresponding extraction methods*

Feature	Parameter extraction method
Channel definition (Bandwidth, center frequency f_c)	Power spectral density (PSD)
Pulse shape (shape filter)	Power spectral density (PSD)
Modulation	Cyclostationary feature detection
Hopping pattern	Time-frequency representation such as spectrogram
Temporal pattern	Time-frequency representation such as spectrogram
Bitrate/Symbol rate	Cyclostationary feature detection
Mono/Multi carrier	Cyclostationary feature detection

4.1 Neuro-Fuzzy Signal Classifier

A neuro-fuzzy signal classifier (NFSC), partially reported in [AHD10, AHA10], is implemented in order to classify the PU radio systems with respect to radio standards and extract individual systems from the coexisting environment. It uses bandwidth (BW), center frequency (f_c), pulse shape, time behavior (TB) and hop behavior (HB) of primary signals as distinct features. All experiments are done in the 80 MHz wide 2.4 GHz ISM band using PU technologies presented in section 2.3. Thus, in terms of FL, the universe of discourse, U_f, is as follows:

$$U_f = \{2400 \text{ MHz} \leq f \leq 2483 \text{ MHz}\} \tag{4.1}$$

The block diagram of the NFSC is shown in Fig. 4.2. It consists of PEs distributed in six layers where each layer is specialized for a single task. The data acquisition and fuzzification layers consist of only one PE each. The inference layer consists of one PE for each PU, thus for n PUs there are n PEs in this layer. There is exactly one PE corresponding to each channel of each PU in all other layers. Consequently, if M_i denotes the total number of frequency channels of a particular PU, then each of these layers contains $\sum_{i=1}^{n} M_i$ PEs. The functionality of these layers is briefly discussed in the following paragraphs.

4.1.1 Data Acquisition

Wideband data acquisition: A real-time spectrum analyzer, Tektronix RSA6114A, is used as RF front end for capturing the entire 2.4 GHz ISM band as a single frame. It can process a bandwidth up to

110 MHz (sensor bandwidth B_s) using 14 bit/300 MHz analog-to-digital (A/D) convertors. It performs ED based sensing and generates the PSD by computing the FFT of the acquired frame. The left hand side plot in Fig. 4.3b and Fig. 4.3c display individual frames containing nanoNET, WLAN, Atmel, and Bluetooth signals, whereas, a combination of several frames, a spectrogram, is shown in Fig. 4.3a. The sample time (T_s) for data acquisition is 625 μs for one frame in order to keep exactly one Bluetooth hop in a single frame.

In addition to real-time data, simulated wideband data will also be used in this chapter. Some example spectrograms are included in Fig. A3.2, Fig. A3.6 and Fig. A3.9 for Bluetooth, WISA/WSAN and wirelessHART/ISA100.11a systems respectively in Appendix A3. The sample time for simulated data acquisition is 10 μs for one frame in order to enable the NFSC distinguishing between minor variations in slot lengths of very identical systems such as between WISA (64 μs) and WSAN (72 μs) or wirelessHART (10 ms) and ISA100.11a (10…15 ms).
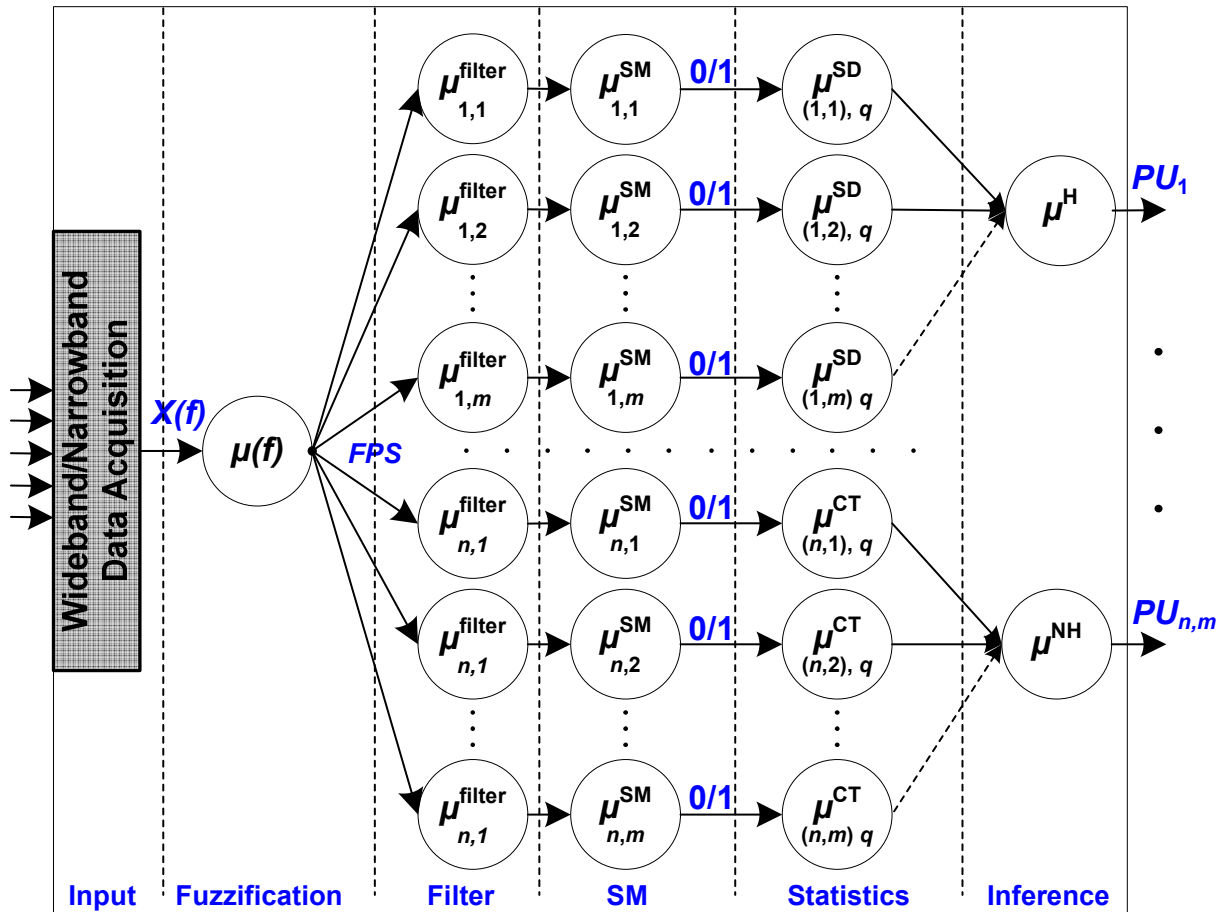
Figure 4.2: *Block diagram of the NFSC (PU$_H$: frequency hopping PU, PU$_{NH}$: PU without frequency hopping, SM: similarity measure, SD: statistical dispersion, CT: central tendency)*

Narrowband data acquisition: A CC2500 transceiver from TI is used to perform RSSI based narrowband sensing. It can acquire only 0.812 MHz bandwidth. Exactly 80 channels are sensed in the 2.4 GHz ISM band with 1 MHz channel spacing. It performs swept sensing to generate a complete frame of the entire ISM band. The conventional MaxHold spectrum analyzer mode is applied to acquire a high resolution picture. However, as a disadvantage, the MaxHold mode looses all time related information. Therefore, this data can be used to process only two features, BW and f_c, for signal classification. However, chapter 6 includes methods to improve the quality of narrowband data acquisition to provide somewhat equivalent information to the wideband data acquisition. Two example RSSI based frames, sensed using CC2500, are shown in the right hand side plot of Fig. 4.3. The sample time for the narrowband data acquisition method is approximately 100 µs.
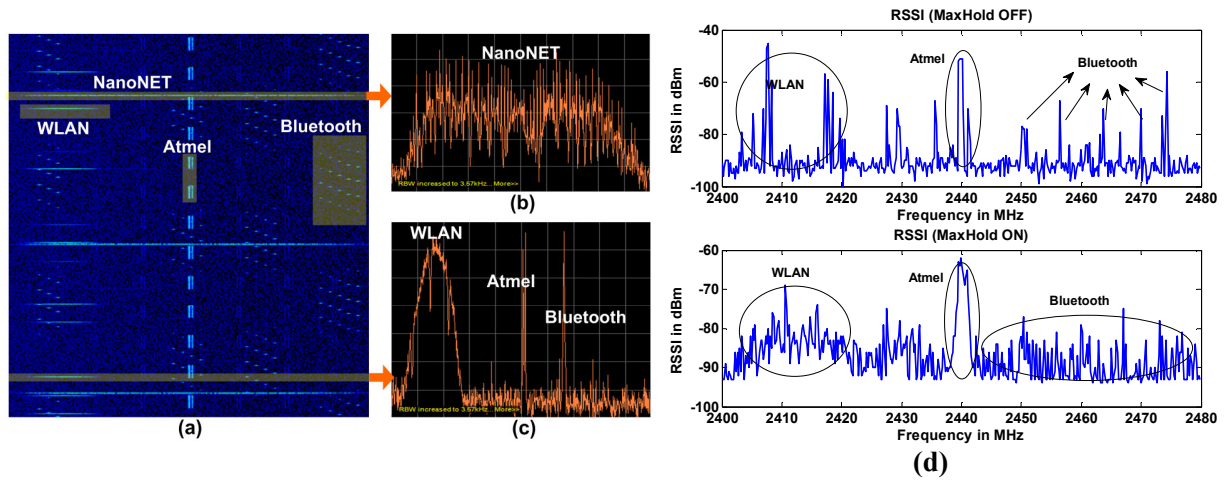
Figure 4.3: (a) *A spectrogram acquired with a real-time spectrum analyzer using 80 MHz acquisition bandwidth. (b) and (c) are PSD plots. The Bluetooth hop sequence captured in the spectrogram is a 'page hop sequence' that uses only 32 channels (Appendix A3). (d) Swept spectrum analyzer scanning. Single sweep (top) vs. MaxHold mode (bottom)*

4.1.2   Fuzzification

The incoming frame $X(f)$ containing n dBm based frequency bins is mapped to a membership value between 0 and 1 as shown in Fig. 4.4 using the following MF:

$$\mu(f) = \left| \frac{P_{min} - P_x}{w} \right| \tag{4.2}$$

Where w is the total range of the received dBm distribution ($w = P_{min} - P_{max}$) within a single frame. P_{min} and P_{max} are the minimum and the maximum dBm values and P_x represents dBm value

corresponding to individual frequency bins. The resulting frame, fuzzy power spectrum (FPS), is a fuzzy set and can be written as:

$$FPS = \{(X(f), \mu(f)) | f \ in \ U_f\} \tag{4.3}$$

(a) *Strong signals*   **(b)** *Weaker signals*
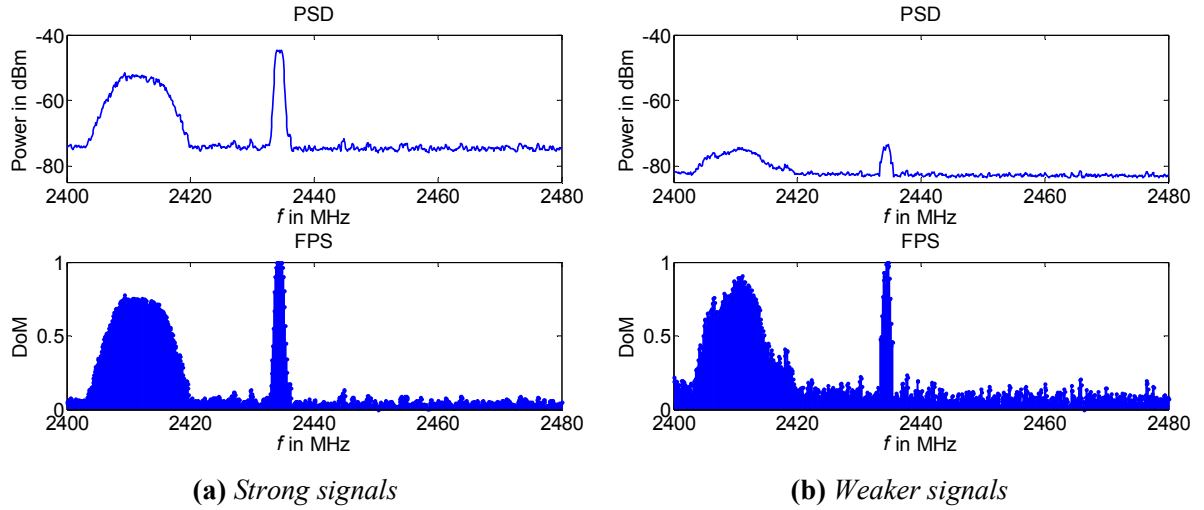
Figure 4.4: *A PSD frame acquired by real-time spectrum analyzer (top) and the corresponding fuzzy power spectrum (bottom). The PSD frame includes WLAN and Atmel based primary signals. DoM: degree of membership.*

(a)   **(b)**
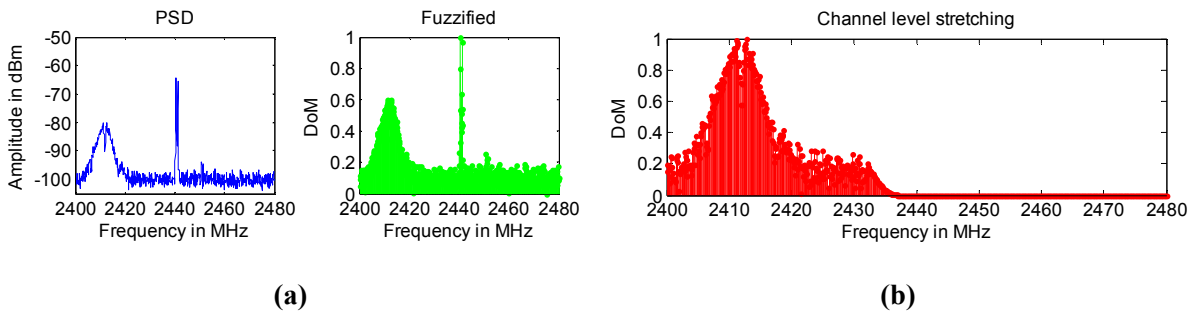
Figure 4.5: (a) *Fuzzification of strong signals acquired by the wideband platform. The WLAN and the Atmel systems are operating. Note that presence of a stronger signal (Atmel) reduces the extent of stretching of other coexisting signals (WLAN). To solve this problem, a channel level stretching is done after filtering.* **(b)** *Channel level stretching for first channel of WLAN*

As discussed earlier in section 2.2.1 fuzzy representation of inputs is mandatory to perform fuzzy operations later on. Additionally, in NFSC, this process provides functionality similar to adjusting the reference amplitude in a spectrum analyzer in order to improve the 'peak prominence' or visibility of weaker signals. The fuzzification process stretches the signal in the fuzzy interval (0, 1) to hide major anomalies in the original dBm data caused by channel impairments, path loss and diverse characteristics of different underlying data acquisition RF front ends. Consequently, it provides a fairly normalized data stream, for different channel conditions and sensing platforms, to its subsequent layers as shown in plots of two very different signal strengths presented in Fig. 4.4. For further illustration, some special cases are discussed in Appendix A4 using signals acquired in various bad channel conditions, with different sensing platforms.

Furthermore, P_{min} and P_{max} in eq. (4.2) are selected at the frame level therefore the fuzzification process does not stretch all coexisting signals equally when the amplitudes of PU signals are considerably different from each other. To solve this problem I performed another stretching at the channel level after filtering, using the same MF as given in eq. (4.2). This phenomenon is shown in Fig. 4.5.

4.1.3   Filtering

Each PE emulates a band-pass filter functionality and allows frequency bins of the corresponding channel only. For instance, the two top plots in Fig. 4.6a and Fig. 4.6b show filtered parts of the input FPS corresponding to two selected channels of WLAN (1$^{\text{st}}$ and 6$^{\text{th}}$) and Atmel (15$^{\text{th}}$ and 39$^{\text{th}}$) PU systems. The incoming frame, *FPS*, filtered over the jth channel of PU$_i$ is represented as:

$$FPS_{i.j} = \left\{ FPS, \ \mu_{i,j}^{\text{filter}}(f) \right\} \tag{4.4}$$

where, $\mu_{i,j}^{\text{filter}}(f)$ is the fuzzy MF used as filter. It is the pulse shape of the corresponding PU signal. Commonly used pulse shaping filters in communication systems are raised cosine, the root raised cosine and the Gaussian filters. However, pi-curve is used to design filters for all PUs in experiments reported in this document because it provided sufficient approximation for experimental purposes. It is given below:

$$\mu_{i,j}^{\text{filter}}(f) = \pi\text{Curve}\left(BW_i^{\text{PU}} \times D, \ f_j \right) \tag{4.5}$$

where BW_i^{PU} is the bandwidth and f_j is the center frequency of jth channel of PU_i. D is a constant, which can be selected to adjust the width of pass-band of the filter for each PU. In presence of coexisting systems with diverse bandwidths, it is noted during experiments that 'narrower' systems should always be filtered with relatively wider bandwidths than their actual channel bandwidths. Otherwise, a wider-band signal is incorrectly detected as a narrower-band signal. The following values were determined during

simulations and used for specified systems in the rest of document: $D_{\text{NanoNET}} = 1$, $D_{\text{WLAN}} = 2$, $D_{\text{IEEE 802.15.4}} = 4$ and $D_{\text{Atmel}}/D_{\text{IEEE 802.15.1}} = 8$ as optimal values during experiments.
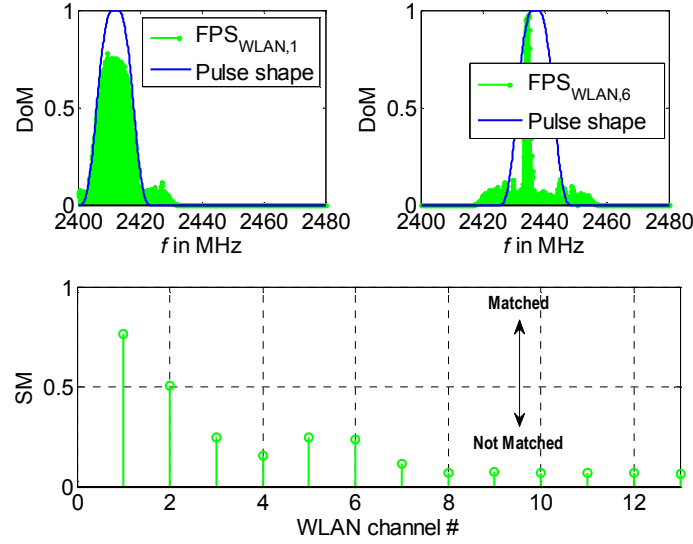
(a): $\mu_{\text{WLAN}}^{\text{pulse shape}}$ *and* FPS_{WLAN} *for two selected channels (top) and SM score of all 13 channels (bottom)*
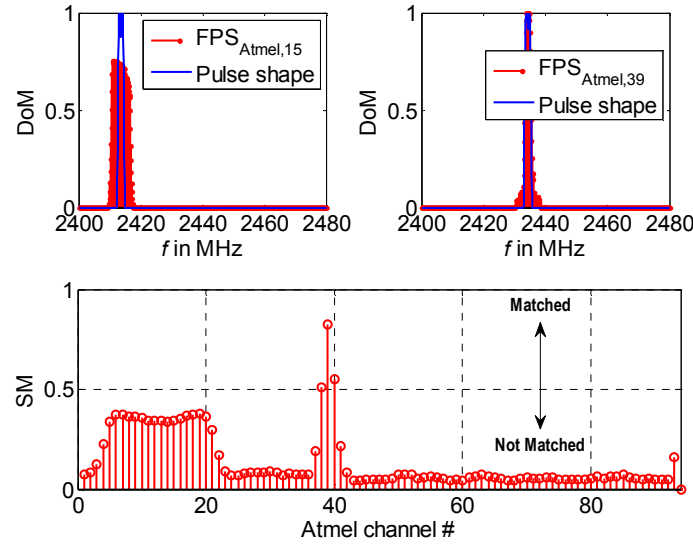
(b): $\mu_{\text{Atmel}}^{\text{pulse shape}}$ *and* FPS_{Atmel} *for two selected channels (top) and SM score of all 94 channels (bottom)*

Figure 4.6: *Results at filtering and SM layer using the FPSs shown in Fig. 4.4. Note that the fuzzification process results in identical SM scores for stronger and weaker signals shown in Fig. 4.4.*

4.1.1   Similarity Measure

It compares the incoming filtered FPS, $\mu^{\text{filter}}(f)$, with the ideal pulse shape of the respective PU signals to generate a similarity measure (SM) score. The resulting SM score can be either defuzzified using a MS like the one shown in Fig. 4.7 or simply compared with a predefined threshold value to evaluate the presence or absence of the corresponding PU signal. For instance, for both FPSs shown in Fig. 4.4, the SM score for 13 WLAN and 94 Atmel channels is plotted in Fig. 4.6.
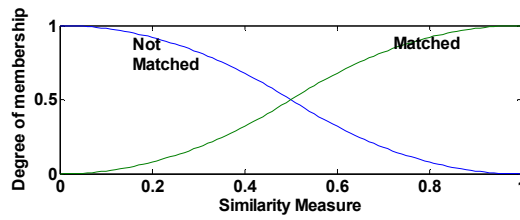
Figure 4.7: *The membership function to grade the SM score*

In terms of BW and f_c, the PU systems presented in section 2.3 can be divided into four distinct classes, which are NanoNET, IEEE 802.11, IEEE 802.15.4 and Atmel/IEEE 802.15.1 based systems. At the SM layer the NFSC successfully distinguishes between these classes. However, signals which are identical in terms of these parameters, e.g. different variants of a standard such as WISA and Bluetooth, can't be differentiated from each other at this layer. The MF used as ideal pulse shape is given by eq. (4.6) while the pulse shapes used for WLAN and Atmel signals are also shown in the top plots in Fig. 4.6a and Fig. 4.6b.

$$\mu_i^{\text{pulse shape}}(f) = \pi Curve\left(\text{BW}_i^{\text{PU}}\right) \tag{4.6}$$

The comparison of the filtered FPS with an ideal pulse shape is done by computing the SM. Thus, eq. (2.9) can be written as follows:

$$SM_{i,j} = \mu^{SM}(f) = \frac{\sum_{f \in U} \min(\mu^{\text{filter}}(f).\mu^{\text{pulse shape}}(f))}{\max(\sum_{f \in U} \mu^{\text{filter}}(f), \sum_{f \in U} \mu^{\text{pulse shape}}(f))} \tag{4.7}$$

where $SM_{i,j}$ is a fuzzy singleton, computed in a single PE and is a measure of the PU$_i$ presence in one of its channels, i.e. the jth channel. The complete fuzzy set for PU$_i$, i.e. the SM over all M$_i$ channels computed by M$_i$ PEs, is as follows:

$$SM = \left\{\left(FPS, \mu^{SM}(f)\right)\right\} \tag{4.8}$$

The fuzzy set, *SM* or *SM$_i$* for *PU$_i$*, only contains a DoM. It is compared with a predefined threshold value for each PU system represented by γ^{SM}, to categorically label the presence or absence of a PU using the following MF:

$$LABEL_{i,j}^{SM} = \mu^{LABEL^{SM}}(SM_{i,j}) = \begin{cases} 1 & \text{if } SM_{i,j} \geq \gamma_i^{SM} \\ 0 & \text{otherwise} \end{cases} \tag{4.9}$$

where, LABEL^{SM} is a binary time series representing SM layer labeling. Using fuzzy set notation it can be represented as:

$$LABEL^{SM} = \left\{ \left(SM, \mu^{LABEL^{SM}}(SM) \right) \right\} \tag{4.10}$$

Example SM sets for WLAN and Atmel systems using two FPSs presented in Fig. 4.4 are plotted in Fig. 4.6a and Fig. 4.6b respectively. The SM score for four selected PU systems for FPS presented in Fig. 4.5 are shown in Fig. 4.8.
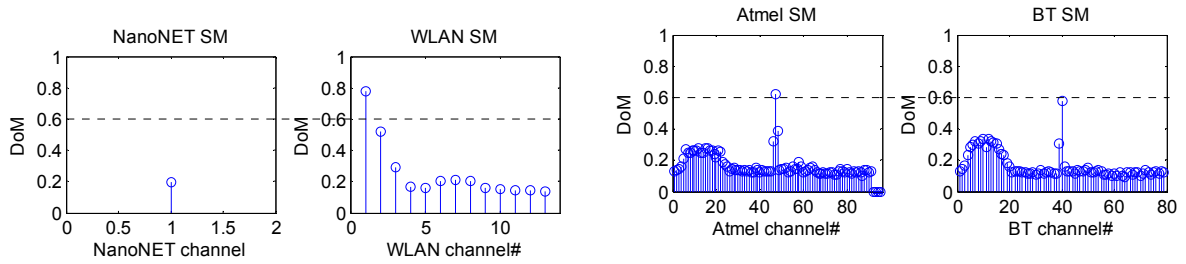
Figure 4.8: *SM of four specified systems using FSP shown in Fig. 4.5. Since only WLAN and Atmel systems are active in the input FPS, these results correspond to true negative for NanoNET, true positive for WLAN and Atmel systems and false positive for Bluetooth. A threshold line at $\gamma^{SM} = 0.6$ is also visible.*

Note that $LABEL_i^{SM}$ completely preserves frequency and time related information of an individual PU system and acts as extracted binary time series. Operating parameters, such as center frequency of the active channel or hop, duty cycle, period (in case of cyclic systems, e.g. NanoNET and Atmel in these experiments) etc. can easily be deducted from it to model the transmission of respective PU systems. For sake of illustration the extracted binary time series for four PU systems are plotted in Fig. 4.9a with real-time acquired data and for two hopping systems in Fig. 4.9b using simulated wideband data. However, it should be noticed that incorrectly identified entries for identical systems are still there in $LABEL_i^{SM}$.

Section 4.2.2 presents a detailed performance analysis of the detection probability of the NFSC at the SM layer using receiver operating characteristic (ROC) curves.
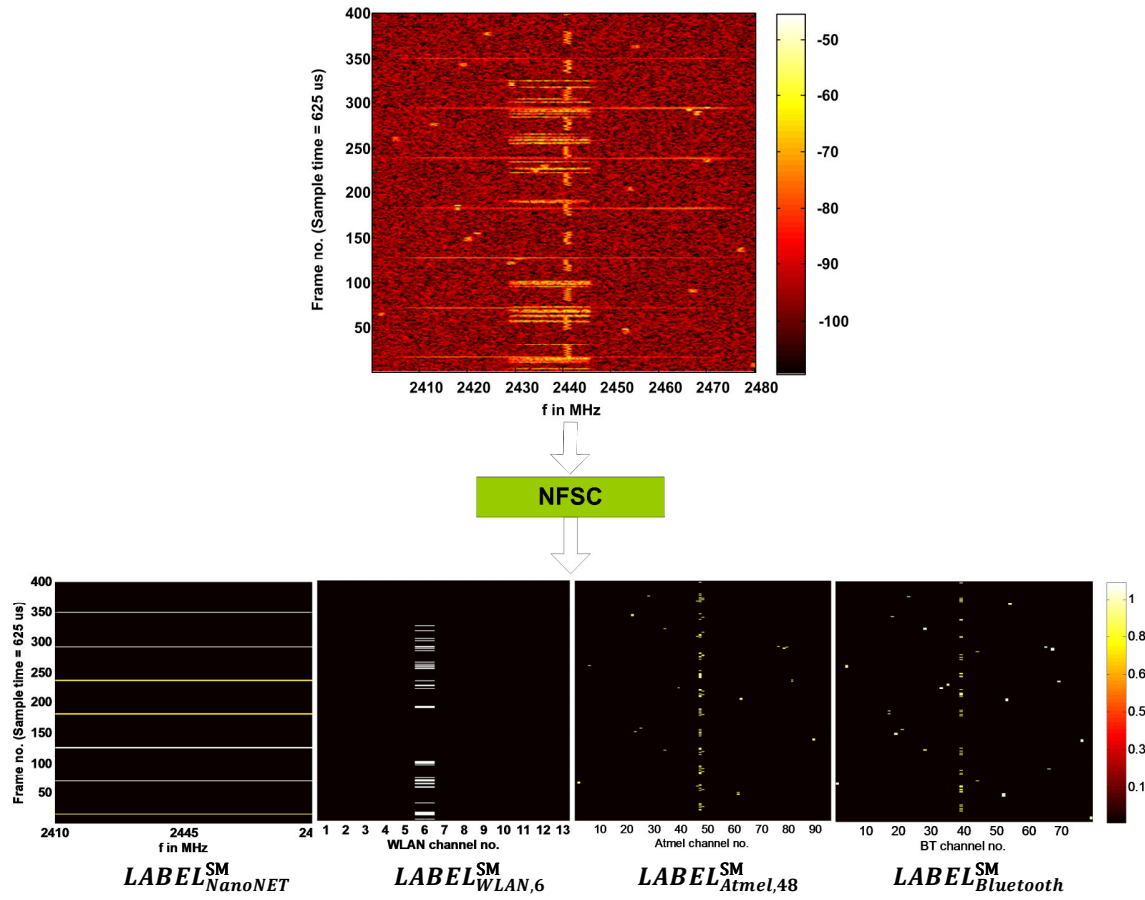
(a) *Real-time wideband data acquisition. Note that the Atmel and Bluetooth systems are very identical in terms of channel definitions therefore the SM layer can't differ between these signals.*
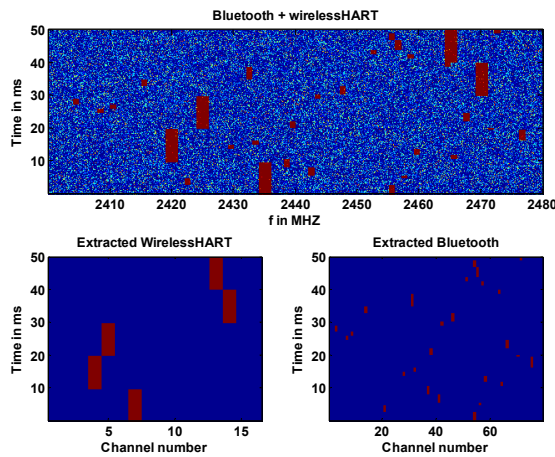
(b) *Simulated wideband data. Identification and extraction of multiple hopping systems with distinct channel definitions. WirelessHART and Bluetooth are used as PUs at SNR = 2dB.*

Figure 4.9: *PU classification and extraction at SM layer*

4.1.2   Distinguishing Between a Hopping and a Non-Hopping System

In order to discriminate between a hopping and a non-hopping system with identical channel definition, the last two layers of NFSC are implemented as follows.

4.1.2.1   Statistics Layer

Descriptive statistics summarize an entire data set to describe the main features of it. Statistical dispersion (SD) and central tendency (CT) are two of several measures of it. The former measures the spread of data and the latter measures how the data is clustered around a single value. Transmissions of a hopping system are reasonably spread over its hopping channels and have high SD as long as the total number of captured hops is fairly large. On the other hand a non-hopping system exhibits high CT, since all occurrences are expected to be at a single channel.

PEs corresponding to non-hopping PU systems maintain cumulative moving average of incoming binary values as a measure of CT as given by the following MF:

$$CT_{i,j} = \mu^{CT}\left(LABEL_i^{SM}\right) = \frac{LABEL_{(i,j),q}^{SM} + ((q-1) \times CT_{(i,j),q-1})}{q} \tag{4.11}$$

where q is the total number of processed frames. On the other hand, only the first occurrence over each hopping channel is remembered for a hopping PU system as a measure of SD. It is given by the following MF:

$$SD_{i,j} = \mu^{SD}\left(LABEL_i^{SM}\right) = \begin{cases} 1 & \text{if } LABEL_{i,j}^{SM} = 1 \\ \text{unchanged} & \text{otherwise} \end{cases} \tag{4.12}$$

where $\left\{\left(LABEL^{SM}, \mu^{CT}\left(LABEL^{SM}\right)\right)\right\}$ and $\left\{\left(LABEL^{SM}, \mu^{SD}\left(LABEL^{SM}\right)\right)\right\}$ are fuzzy CT and fuzzy SD sets, respectively.

4.1.2.2   Inference

The following MF is used to evaluate the presence of a non-hoping PU:

$$\mu^{NH}(CT_i) = \begin{cases} 1 & \text{if } \max(CT_i) \geq \gamma_i^{CT} \\ 0 & \text{otherwise} \end{cases} \tag{4.13}$$

Whereas, presence of a hopping system is evaluated using the following MF:

$$\mu^{H}(SD_i) = \begin{cases} 1 & \text{if } \text{mean}(SD_i) \geq \gamma_i^{SD} \\ 0 & \text{otherwise} \end{cases} \tag{4.14}$$

Illustration: Fig. 4.10 illustrates how descriptive statistics are used to distinguish between hopping and non-hopping systems. Both systems are identical in terms of BW and f_c and have ten channels each. Both

are incorrectly identified as each other by the SM layer. The threshold sets, $LABEL^{SM}$, for eight consecutive frames are shown, which include TP as well as FP occurrences of both systems. Fig. 4.10a shows how $\max(CT_i)$ and $\text{mean}(SD_i)$ remains fairly high for respective systems. Fig. 4.10b illustrates a case when there is only 'correctly detected' PU operating and the cheating PU is OFF. While, Fig. 4.10c illustrates the case when only cheating PU is operating. Note that, fuzzy threshold sets, $LABEL^{SM}$, for later two cases are not shown in this figure. Real-time results at inference layer of PU systems earlier extracted in Fig. 4.9a, are plotted in Fig. 4.11.
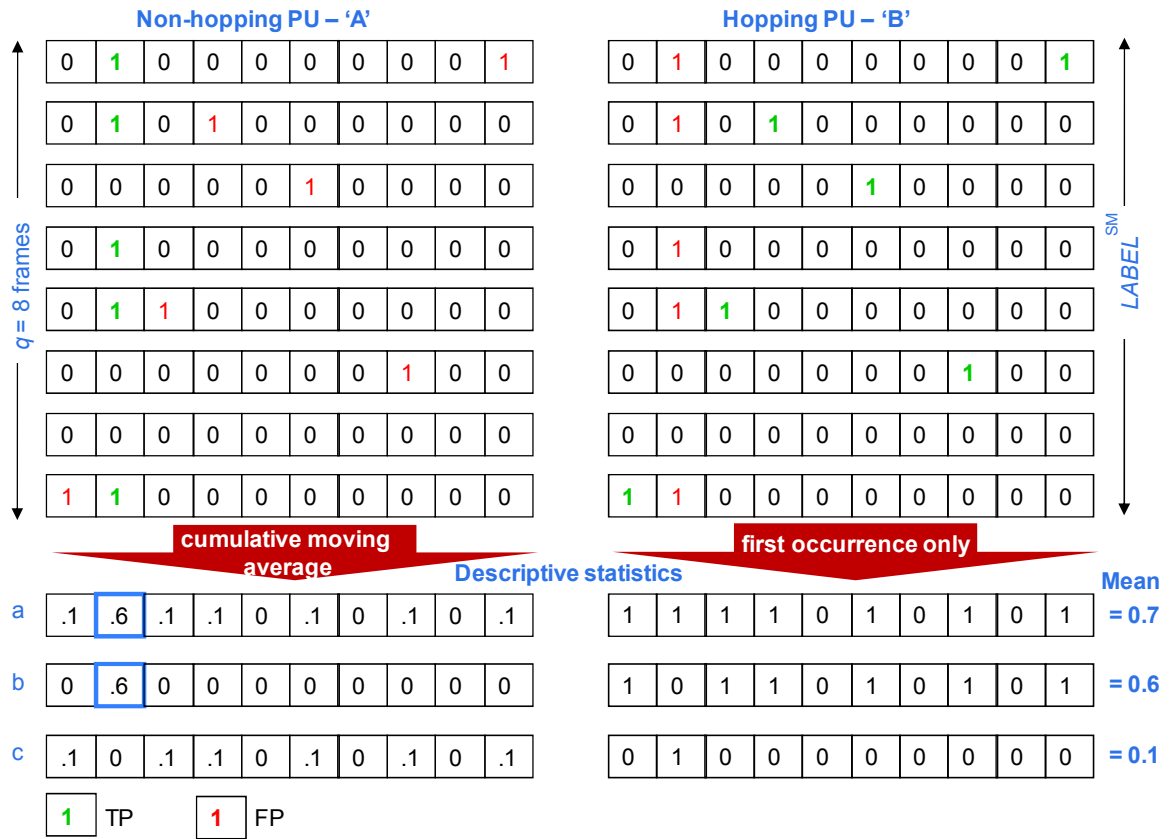
Figure 4.10: *An illustration of distinguishing hopping and non-hopping PU systems at the inference layer.*
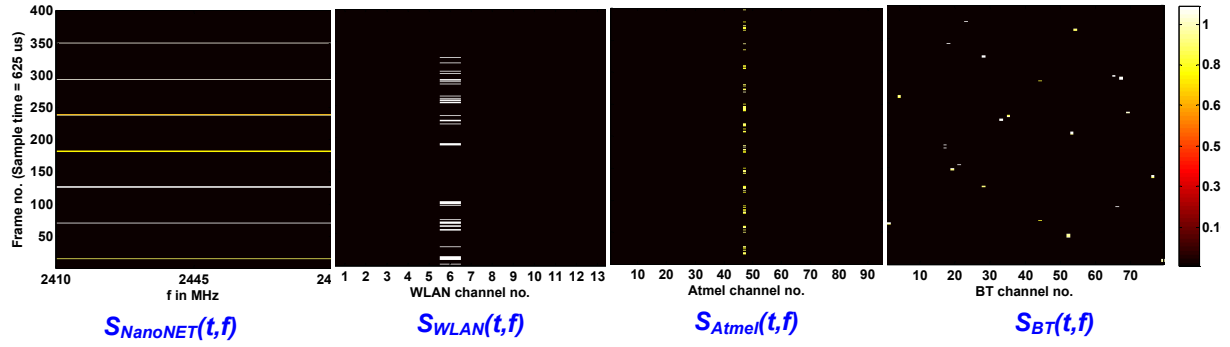
Figure 4.11: *Inference layer PU classification and extraction extended from Fig. 4.9a.*

4.1.2.3   Distinguishing between multiple hopping systems

In order to distinguish between coexisting hopping PU systems with very identical channel definitions both temporal and hop behavior have to be studied. Section 4.2.2.3 presents three example scenarios to illustrate the concept.

4.2 Performance Evaluation

4.2.1   Performance evaluation tools

The diagnostic performance of a classifier is often evaluated using the receiver operating characteristic (ROC) curve. The scores generated by the classifier are considered in two populations. One population corresponds to the presence of a particular class (positive case) and the other corresponds to the absence of that class (negative case). The distribution of scores is used to study the separation between the two populations. The better the classifier, the more separated scores of both populations can be achieved. Indeed, the distribution of the scores often overlaps to some extent. Fig. 4.12 provides an illustration of interpretation of score distribution of a classifier and corresponding ROC curve using two hypothetical classifiers. In this figure, the classifier B is a better classifier since the score distributions of positive and negative classes generated by it has less overlapping.

A suitable threshold or cut-off point is then chosen in order to discriminate between the two populations. For every possible cut-off point, there will be some results corresponding to correctly classified as positive (TP = True Positive), wrongly classified as negative (FN = False Negative), correctly classified as negative (TN = True Negative) and wrongly classified as positive (FP = False Positive). *Sensitivity* and *specificity* of the classifier are then computed as True Positive Rate (TPR) and True Negative Rate (TNR)

to plot ROC curve as shown in Fig. 4.12 and further explained in Appendix A5. Instead of specificity, *1-specificity* or False Positive Rate (FPR) is often considered as more expressive parameter in a ROC curve and will be used for the NFSC performance evaluation. Moreover, a classifier, which can perfectly discriminate between distinct classes, has no overlapping in score distributions of negative and positive classes and has an ROC curve that passes through the upper left corner of the plot and is interpreted as having 100% sensitivity and 100% specificity. Hence, the closer the ROC curve is to the upper left corner, the higher is the area under the curve (AUC) and the higher is the accuracy of the classifier. Conversely, the closer the curve comes to the 45-degree diagonal of the ROC space, the less accurate is the classifier with less AUC.
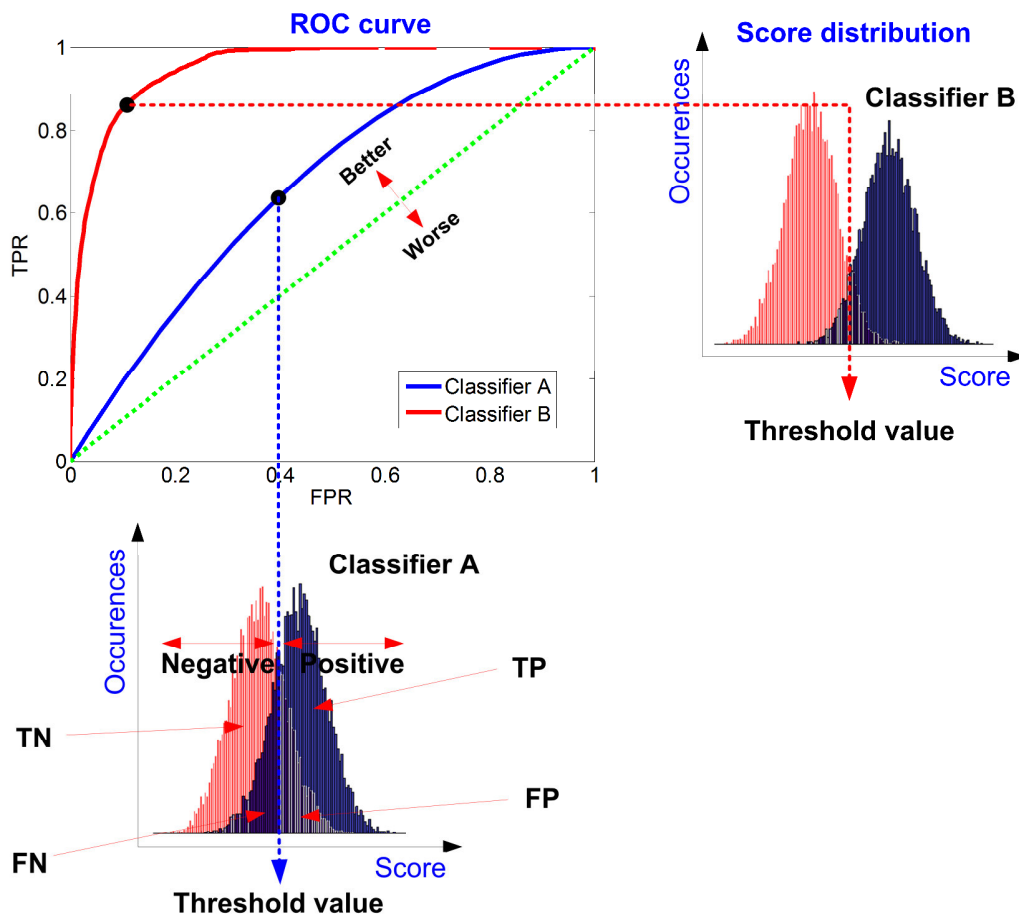
Figure 4.12: *Interpretation of distribution of scores and ROC using two hypothetical classifiers.*

In detection theory TPR and FPR are better known as probability of detection (P_{d}) and probability of false alarm (P_{FA}). A useful measure of performance of detectors and classifiers is the probability of detection (PoD) curve which is obtained by plotting P_{d} at a fixed P_{FA} value against some signal or sensor parameters such as *SNR*, sensing time, BW etc. If the probability of deciding H_i when H_k is true, is represented by $P(H_i; H_k)$ [STE11] then P_{d} and P_{FA} for the NFSC can be written as follows:

$$P_{\mathrm{d}} = P(H_i\;;\;H_i) = \Pr\{SM_{i,j} > \gamma_i^{\mathrm{SM}};\,H_i\} = \frac{TP}{TP+FN} \tag{4.15}$$

$$P_{\mathrm{FA}} = P(H_i\;;\;H_k) = \Pr\{SM_{i,j} > \gamma_i^{\mathrm{SM}};\,H_k\} = \frac{FP}{FP+TN}\;;\;\;i = 1,2,3\ldots N \text{ and } k = 0,1,2\ldots N \text{ and } i \neq k \tag{4.16}$$

4.2.2   Performance Evaluation at SM Layer

The PoD curve for four PU classes with respect to different SNR values is shown in Fig. 4.13a. Fig. 4.13b shows corresponding optimal threshold values (γ_i^{SM}) for $P_{\mathrm{FA}} = 0$ and $P_{\mathrm{FA}} = 0.1$. Fig. 4.14 presents distribution of NFSC scores for three different SNR values. Both these figures include results based on simulated data. Whereas, results using real-time acquired wideband and narrowband data are presented in Fig. 4.15 and Fig. 4.16. All these results are discussed in the following paragraphs.

Choosing a threshold is always a tricky problem in classification and detection theory. Choosing a high threshold value will decrease the probability of detection whereas lowering the threshold will increase the probability of false alarm. Eventually, a compromise has to be done between P_{FA} and P_{d}. A good idea is to choose a threshold value corresponding to a certain value of P_{FA} or P_{d} depending on the requirements of application. The selection of optimal threshold also depends on the value of SNR of the underlying signal. Fig. 4.13b plots optimal thresholds at different SNR values for different radio systems corresponding to two typical values of P_{FA}.

(a)

(b)
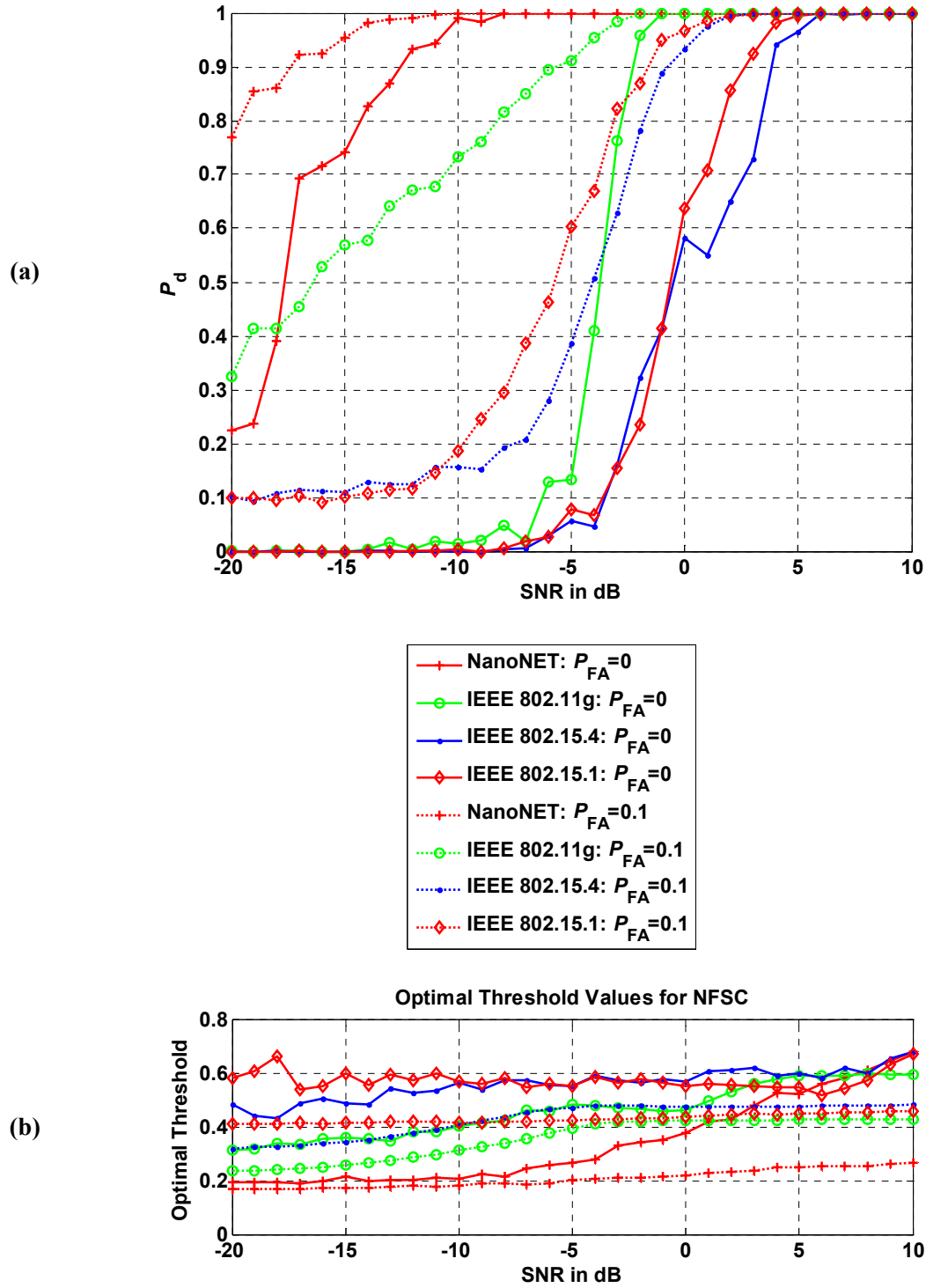
Figure 4.13: *Performance analysis of NFSC using simulated wideband data* **a)** *The probability of detection at SM layer* **b)** *Corresponding optimal threshold values.*
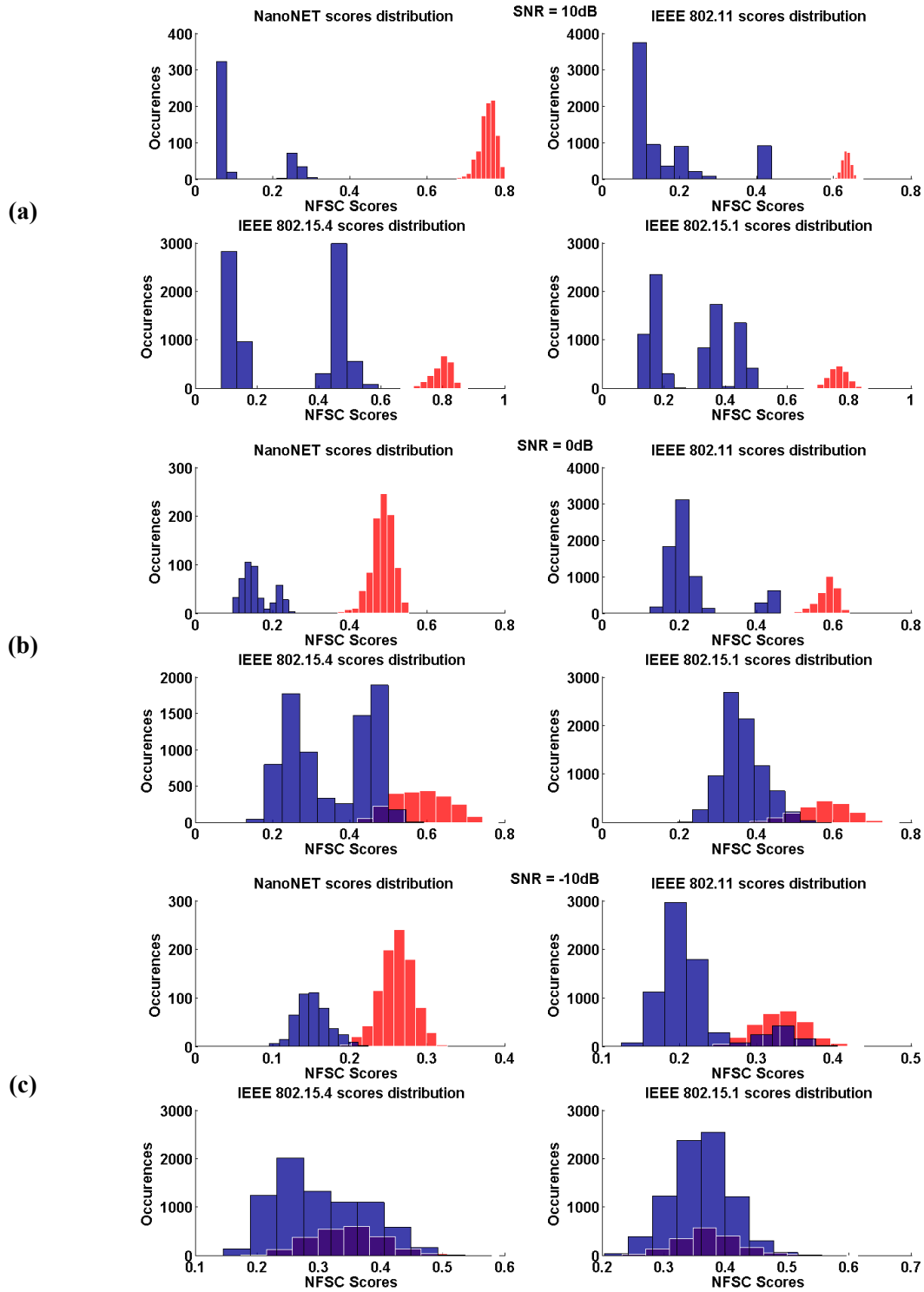
Figure 4.14: *NFSC score distribution for three different SNR values. Red and blue histograms correspond to the presence and absence of respective PU signal. (a) SNR = 10 dB, (b) = 0 dB, (c) = -10 dB.*

Looking at the probability of detection curve shown in Fig. 4.13a and distribution of scores in Fig. 4.14 it can be concluded that:

- The PU systems with wider bandwidths are better distinguished than their narrower band counterparts. A NanoNET signal is identified at as low as SNR = -10 dBm, an IEEE 802.11 based system at SNR = -2 dBm and both IEEE 802.15.4 and IEEE 802.15.1 based systems at approximately SNR = 2 dBm with 100 % probability of detection ($P_d = 1$).

- Optimal thresholds of wider signals are more dependent on the value of SNR. For instance, the optimal threshold value is 0.2 at SNR = -10 dB and 0.6 at SNR = 10 dB for NanoNET system at $P_{FA} = 0$. However, at $P_{FA} = 0.1$, the threshold value remain stable at ~0.2 for the nanoNET system. For an IEEE 802.11 WLAN system, the threshold value varies between 0.4 at SNR = -10 dB...0.6 at SNR = 10 dB against $P_{FA} = 0$. The threshold value is almost stable for the WLAN system at $P_{FA} = 0.1$. For narrower systems the threshold remains stable at different SNR values.

  However, instability of threshold values is mainly observed at $P_{FA} = 0$, which is an ideal case and is often not required in real-time situations. For $P_{FA} = 0.1$, the threshold value is stable but choosing a different threshold value for each primary systems can be a reasonable idea instead of a single threshold for all systems. A reasonable estimation of set of threshold values for all SNR values obtained from Fig. 4.13b and Fig. 4.14 is $\gamma_{NanoNET}^{SM} = 0.25$, $\gamma_{IEEE\ 802.11}^{SM} = 0.3$, $\gamma_{IEEE\ 802.15.4}^{SM} = 0.45$ and $\gamma_{IEEE\ 802.15.1}^{SM} = 0.45$ against $P_{FA} \sim 0.1$.

Furthermore, the NFSC demonstrates excellent performance with both wideband as well as narrowband data real-time data acquisitions as shown by the ROC curves in Fig. 4.15 and Fig. 4.16, respectively. For wideband acquisition, the AUC is approximately 100 %, 98 %, 93 %, and 94 % for nanoNET, IEEE 802.11, Atmel, and Bluetooth signals respectively. It is important to note that Bluetooth and Atmel systems are not operating simultaneously in these results. In case of simultaneous operation of these systems it is not possible to distinguish them from each other because of highly identical channel definition as already specified in Fig. 4.9a.

On the other hand, for narrowband data acquisition, the NFSC also performs excellently as long as the signal is acquired with an optimal MaxHold time as shown in Fig. 4.16a. The AUC is approximately 100 %, 98 %, 94 %, and 96 % for nanoNET, IEEE 802.11g, Atmel, and Bluetooth PU signals respectively with MaxHold time, $T_{MaxHold} = 40$ ms (Single sweep $= T_s * $ Total no. of channels $= 8$ ms , five consecutive sweeps are held). However in the presence of hopping systems, the MaxHold operation can seriously degrade the performance, if it is applied for a longer time. It is because several hops, frozen together, give an impression of a wideband signal and cheats the NFSC. Fig. 4.16b presents P_{FA} of

nanoNET and IEEE 802.11 signals computed for $P_d = 1$, when $T_{MaxHold}$ is gradually increased. The ROC curve labeled as 'NanoNET [BT working]' in Fig. 4.16a corresponds to $T_{MaxHold} \sim 2$ s. On the other hand, narrowband Bluetooth and Atmel systems do not require MaxHold operation as for the used narrowband sensor. However, the MaxHold operation will not degrade the results as long as several consecutive hops are not frozen together. Two almost equal ROC curves plotted in Fig. 4.16a, labeled as 'BT [single trace]' and 'BT [MaxHold]' supports this argument.
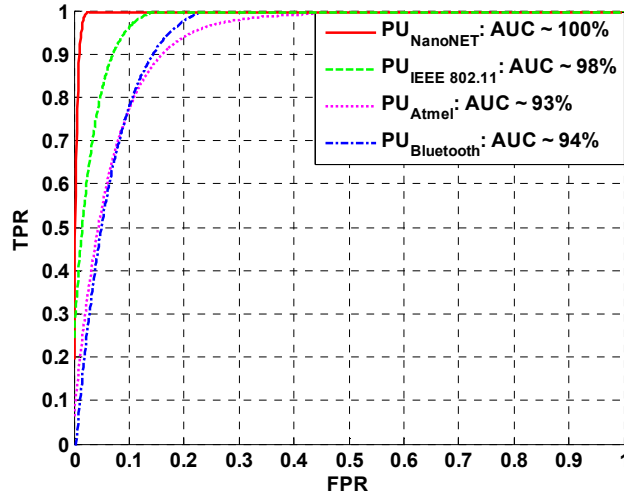
Figure 4.15: *ROC at SM layer using real-time wideband data acquisition.*

(a)   **(b)**
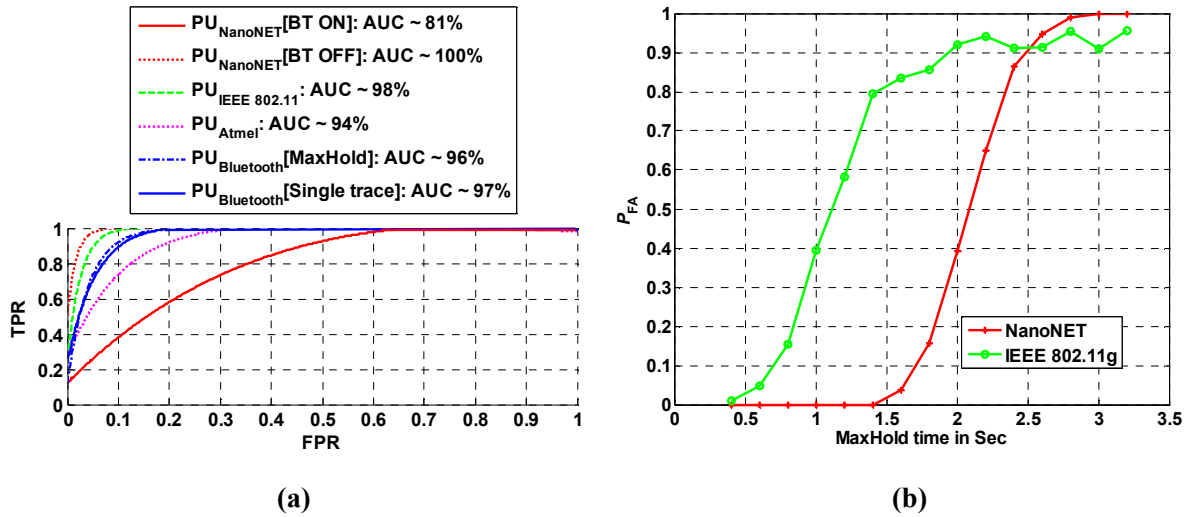
Figure 4.16: a) *ROC at SM layer using real-time narrowband data acquisition.* **b)** *Influence of MaxHold time in the presence of a narrowband hopping system on P_d of non-hopping wider band systems. A Bluetooth PU is actually operating but increasing MaxHold time beyond a certain limit increases P_{FA} against a fixed P_d for wider band PU systems. $P_d = 1$ in this plot.*

4.2.3   Performance Analysis at Inference Layer

4.2.3.1   Distinguishing between multiple hopping systems

The ROC curves for Atmel and Bluetooth at the inference layer are shown in Fig. 4.17. The NFSC exhibits perfect performance as long as the duty cycle of Atmel is sufficiently high and fairly large number of frames are processed. These parameters strongly effect the values of $\max(CT_i)$ and $\text{mean}(SD_i)$. In order to achieve sufficient separation in terms of these measures the duty cycle of the PUs should be high enough and/or more frames should be processed to compute the descriptive statistics. Additionally, extensive blacklisting or smaller number of active hops of a hopping system may also make the separation of values of $\max(CT_i)$ and $\text{mean}(SD_i)$ less separable.
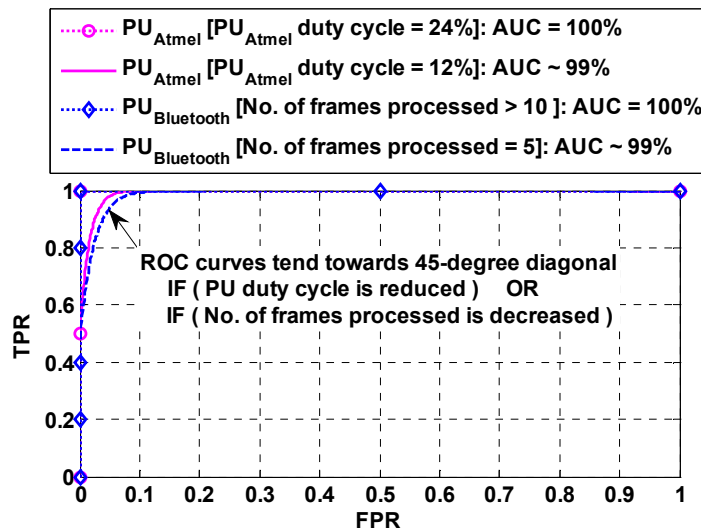
Figure 4.17: *Identifying coexisting hopping and non-hopping PU systems with identical channel definitions using real-time wideband data acquisition*

4.2.3.2   Distinguishing between multiple hopping systems

When multiple hopping systems are expected to coexist, the statistical analysis of their hopping and/or time behavior can help to reveal their identities. Following three example scenarios illustrate the idea.

Note: It is important to mention that only simulated data are used for simulations in this section because real-time devices for WISA, WSAN, wirelessHART and ISA100.11a were not available.

4.2.3.3   Example 1: Coexistence of Bluetooth and WISA/WSAN

Statistics Layer: The hopping pattern used in WISA/WSAN is fairly different from that of the Bluetooth PU system. The WISA/WSAN specification divides the entire ISM band into seven sub-bands. Four uplinks lie in a single sub-band whereas there is a separation of at least two sub-bands in uplinks and downlink. Based on this information the algorithm given in Table 4.2 can accurately distinguish a WISA/WSAN PU system from a Bluetooth system.

Table 4.2: *WISA/WSAN statistics layer*

1: Since uplinks are three channels apart from each other, define a theoretical template for WISA/WSAN uplink hop pattern as $\text{WISA}_{\text{UL\_hop\_pattern}} = 1001001001$.

2: Check each frame in incoming $LABEL^{\text{SM}}$ for 3 sub-bands separation in uplink and downlink frequencies.

3: Compute cross-correlation ($R_{xy}^{s}(l)$ - where *'s'* specifies WISA/WSAN sub-band index) of $\text{WISA}_{\text{UL\_hop\_pattern}}$ with $LABEL^{\text{SM}}$ at each WISA/WSAN sub-band. Where cross-correlation is defined as:

$$R_{xy}(l) \equiv \frac{1}{M}(x * y)[l] \equiv \frac{1}{M}\sum_{m=0}^{M-1} \bar{x}[m]y[m+l]; \qquad l = 0,1,2,\dots M-1 \tag{4.17}$$

where $x = LABEL_{\text{WISA},\, s}^{\text{SM}}$ is the truncated part of $LABEL^{\text{SM}}$ corresponding to sub-band *s*, and $y = \text{WISA}_{\text{UL\_hop\_pattern}}$

4: Take average of maximum cross-correlation value of each frame for *q* frames, as follows:

$$R^{\text{AVG}} = \frac{sum(\max(R_{xy}^{i,s}(l)))}{q}; \quad \text{where } i = 1,2,3,\dots,q \text{ and } s = 1,2,3,\dots,7 \tag{4.18}$$

Note: Step-2 in Table 4.2 is not performed in results presented in later sections. However, it can be easily implemented to better discriminate the signals.

Inference Layer: Following MF is used to evaluate the presence of a WISA/WSAN PU system:

$$\mu^{\text{WISA/WSAN}}(R^{\text{AVG}}) = \begin{cases} 1 & \text{if } \max(R^{\text{AVG}}) \geq \gamma^{R} \\ 0 & \text{otherwise} \end{cases} \tag{4.19}$$
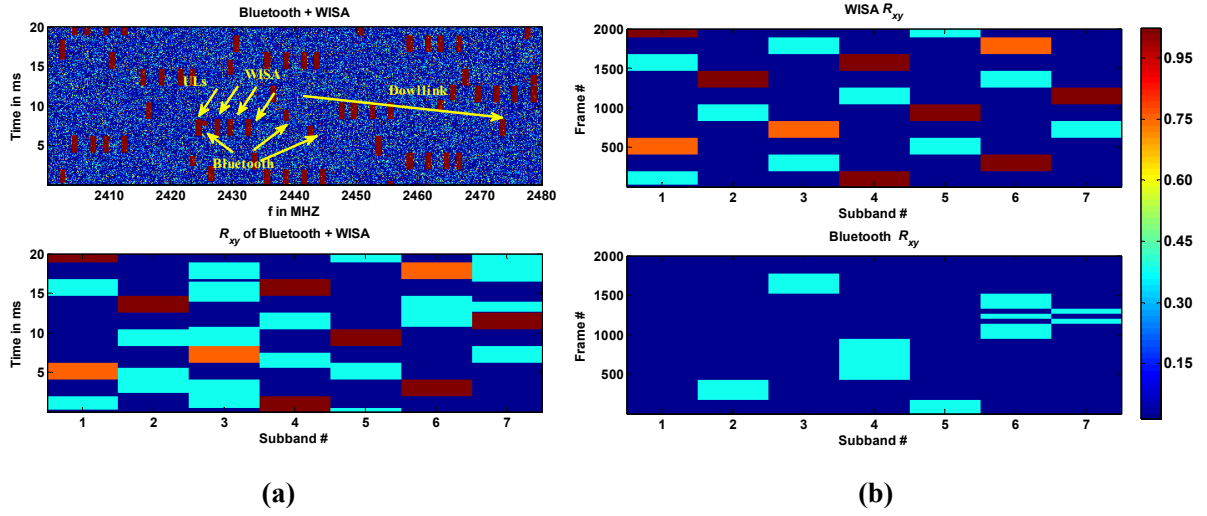
Figure 4.18: a) *(top) Spectrogram of coexisting WISA and Bluetooth systems and (bottom) the corresponding correlation matrix* **b)** *Cross correlation matrix for WISA and Bluetooth systems when operating alone while spectrograms of these two plots are not shown.*
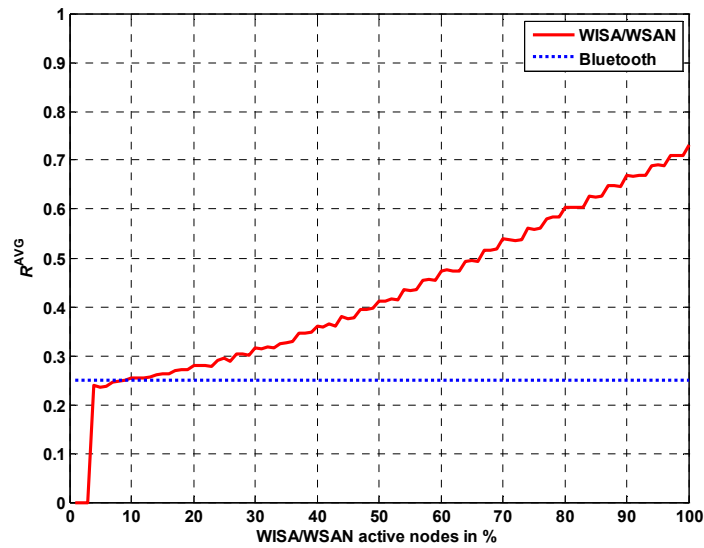
Figure 4.19: *NFSC cross-correlation scores with varying traffic loads for WISA/WSAN system. For Bluetooth system 100 % traffic load is considered here which means that plotted line indicates the maximum possible R^{AVG} value for the Bluetooth system.*

Fig. 4.18a plots a coexisting spectrogram and its corresponding correlation matrix, while Fig. 4.18b plots cross-correlation matrices for simulated spectrograms with WISA and Bluetooth systems operating alone.

It can be seen that fairly high correlation value is generated when a WISA frame is encountered. However, the correlation value can be lower if WISA/WSAN traffic load is smaller. Where, traffic load is defined by the total number of active nodes in the WISA network. Fig. 4.19 plots the R^{AVG} values against varying traffic loads. The maximum possible value of R^{AVG} for Bluetooth system is also plotted in this figure, which shows that WISA/WSAN network load as small as 20 % can be distinguished from a Bluetooth PU system.

Furthermore, there is a small contradiction in WISA/WSAN specification and the method provided for computation of uplink hop sequence which can also affect the maximum value of correlation. It is stated that the uplink frequencies should be exactly three channels apart from each other. However, the computed sequences often include one uplink frequency which is at only two channels separation from one of its neighbor frequencies. It means that WISA$_{UL\_hop\_pattern}$ is not fixed as used in Table 4.2 and can be a varying sequence e.g. 101001001 or 100100101 etc. However, the used fixed pattern provides sufficiently high correlation value even in the presence of varying patterns as shown in Fig. 4.18 and Fig. 4.19.

4.2.3.4   Example 2: Coexistence of WSAN and WISA

These two systems can only be discriminated from each other by measuring the super-frame length using very small sample time in the order of tens of microseconds. However, lower traffic load can make it further challenging to find the boundaries of super-frames as shown in Fig. 4.20b with 50 % traffic loads for both systems.

4.2.3.5   Example 3: Coexistence of WirelessHART and ISA100.11a

These systems can be differentiated from each other only in the following situations as shown in the simulated coexisting spectrogram in Fig. 4.21:

- The ISA100.11a system is using hybrid or slow hopping then measuring the slot/frame length can help identifying the ISA100.11a system.

- The ISA100.11a system has not blacklisted the 26th channel.
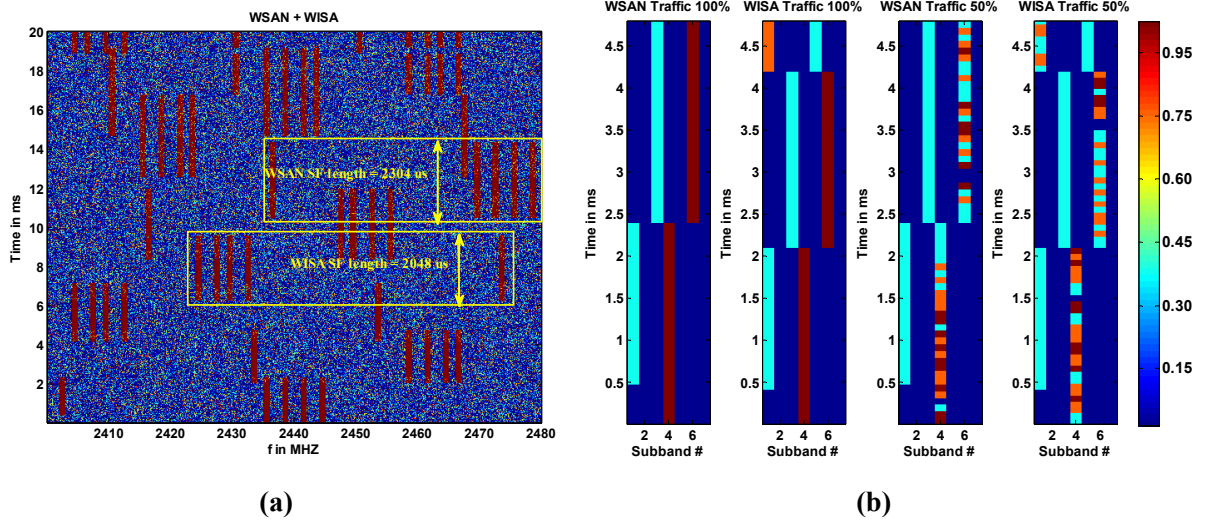
Figure 4.20: *Coexisting WISA and WSAN systems. Super frame length is the only discriminating feature in these systems.*
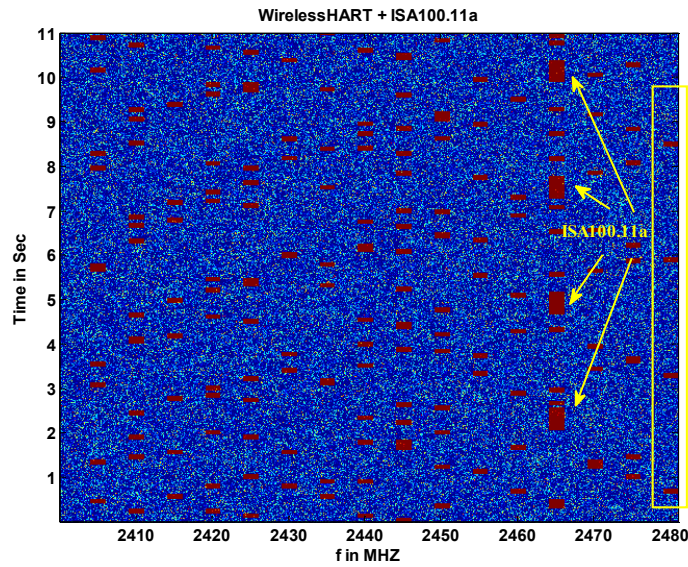
Figure 4.21: *Coexisting WirelessHART and ISA100.11a systems. These systems can only be distinguished from each other if ISA100.11a is using 26th channel or hybrid/slow hopping.*

Chapter 5

Bandwidth Independent Predictive Modeling

A secondary CR system equipped with capabilities to capture statistical characteristics of PU systems can model the behavior of coexisting environment that empowers its decision making process for opportunistic spectrum access (OSA). Overall, the goal of predictive modeling in cognitive radio systems is to forecast primary traffic variations and future traffic patterns. This in turn, enables the SU system to estimate the duration for which a vacant channel left by the incumbent PU system is expected to be available or an occupied channel is expected to remain busy. In wireless environments, the following two types of traffic patterns are recognized [HAY05]:

Deterministic traffic: The PU system, exhibiting such type of traffic is assigned a fixed time slot for transmission. When the primary system is switched OFF, the frequency band remained vacant for some fixed amount of time and can be used by the SU system. Cyclic traffic, often used in industrial sensor-actuator systems lies in this class. The deterministic transmission times can easily be calculated using methods such as cycle-time detection [AHM10] and global maximum of the autocorrelation function [HOY08].

Stochastic traffic: This type of radio traffic can only be described in statistical terms. Typically, the arrival times of data packets are modeled as a Poisson process [ZAN01]. IEEE 802.11 based internet traffic is a famous example of this kind that can be found in most offices and industrial areas. An interesting approach to model IEEE 802.11b based internet traffic is presented in [GEI07]. It uses the knowledge of different types of inter-frame (IF) spaces[9] specified in the IEEE 802.11b standard to model the internet traffic as a semi-Markov model[10] as shown in Fig. 5.1. The appropriateness of Markov models to model the stochastic radio traffic has been widely demonstrated in literature, some of which are mentioned in section 3.1.2.3.

The model parameters of stochastic traffic have to be estimated using historical data. However, in the presence of limited sensor bandwidth with respect to the entire band of interest, the job of acquiring historical data becomes very challenging as already discussed in section 3.1.2. This chapter presents 'bandwidth independent' parameter estimation strategies for Markov modeled PU traffic in order to put

---

[9] For example short inter-frame space (SIFS), contention window (CW) etc.
[10] A semi-Markov process can be viewed as a continuous-time Markov chain (CTMC) [GEI07]

the narrowband sensors to the same grade of performance as of wideband sensors. The term bandwidth independent in the context of predictive modeling means that the model parameter estimation error should be independent of the sensor bandwidth (B_S), PU bandwidth (B_P) and the width of entire band of interest (B_W).
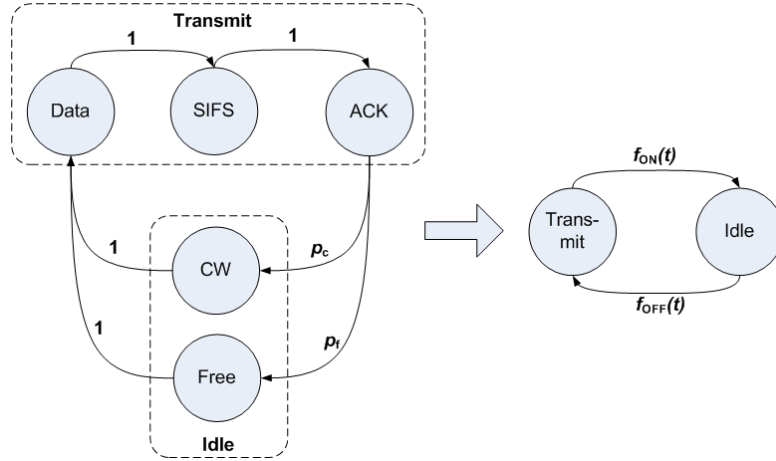
Figure 5.1: *IEEE 802.11b based internet traffic modeled as semi-Markov model, adapted from [GEI07]. An expanded version of the model is shown on the left hand side and a simplified version on the right hand side. p_c: probability of contention, p_f: probability of free, $f_{ON}(t)$: pdf of ON state, $f_{OFF}(t)$: pdf of OFF state.*

The idea is to estimate model parameters (e.g. transition probabilities, mean etc.) of each coexisting PU systems using its identification and extracted binary time series provided by the NFSC presented in chapter 4. The NFSC provides binary time series of coexisting systems without losing any temporal-spectral information of the original constituent signals as long as the bandwidth of the sensor is large enough to capture the entire band of interest (Wideband NFSC case). Hence, the estimation problem is straightforward in this case and estimated values can be used as reference for sake of comparison. However, narrowband sensing devices can't capture the entire band of interest at once that results in loss of vital temporal-spectral information therefore, parameter estimation in this case is the main focus of this chapter.

Overall, this chapter is structured as follows. Section 5.1, published in [AHM12], compares the performance of traditional OSA strategies with Markov modeling based OSA strategies using MATLAB simulations in order to highlight the significance of predictive modeling. Furthermore, this section will also help to introduce some concepts which are essential for the rest of this chapter. Section 5.2 formulates the problem, describes the system model and finally provides methods to improve the missing information and parameter estimation.

5.1 Comparative Analysis of Traditional and Predictive Modeling Based OSA Strategies

5.1.1 Simulation Setup

The entire band of interest is divided into M (where $M > 1$) channels with identical bandwidths $B_{channel}$. Each channel is occupied with primary traffic which means that there is no completely free channel and the SU has to accommodate its transmission by finding some temporal gaps in one of these channels. The primary traffic in each of these channels, as observed by the SU sensor, is merely a sequence of ON (PU is active) and OFF (PU is inactive) states (see Fig. 2.4 for binary series generation using the binary hypothesis testing given by eq. (2.1)). The ON and OFF states are modeled by two i.i.d. random variables T_{ON} and T_{OFF} respectively. Both T_{ON} and T_{OFF} are exponentially distributed random variables with rate parameters λ_{ON}, λ_{OFF} and pdf's as given by the following set of equations [COX67]:

$$\begin{cases} T_{ON} \sim f_{ON}(t) = \lambda_{ON} e^{-\lambda_{ON} t} \\ T_{OFF} \sim f_{OFF}(t) = \lambda_{OFF} e^{-\lambda_{OFF} t} \end{cases} \tag{5.1}$$

where expected lengths of ON (packet length) and OFF (inter packet arrival time) states are given by $E[ON] = 1/\lambda_{ON}$ and $E[OFF] = 1/\lambda_{OFF}$ respectively.

Such alternating behavior is a combination of two Poisson processes and is also known as renewal process as already discussed in chapter 2, section 2.2.5. Furthermore, because of the exponential state distribution it can also be modeled as a first order Markov process with state space S = {0,1}. Meanwhile, the rate parameters λ_{ON} and λ_{OFF} are specified in inverse time units. Further assumptions made for the simulation setup are listed in Table 5.1.

5.1.2 Opportunistic Spectrum Access Methods

The following three OSA methods are used for comparison:

1) First free: It is a traditional *reactive sensing* method in which sensing is performed before each transmission in order to find a suitable channel. Its algorithm is given below:

  i. Start sensing channels in a sequential order using the narrowband sensor and choose the first one where the average signal value is less than a predefined threshold value, as follows:

$$\frac{1}{N_{AVG}} \sum_{i=1}^{N_{AVG}} r_i^m < Threshold$$

where r_i^m are sensed samples in m^{th} channel and N_{AVG} is the total number of samples acquired for averaging for a channel.

ii.   If no channel is selected in step 1 then transmit in the channel with $\min(\frac{1}{N_{AVG}}\sum_{i=1}^{N_{AVG}} r_i^m)$.

Table 5.1: *Important assumptions made for the simulation setup of section 5.1*

1: The primary traffic rate in each channel is independent of all other channels.

2: The radio environment is noiseless and ON and OFF states of the PU signal can be clearly distinguished from each other using the binary hypothesis given by eq. (2.1) to generate the binary series with $P_{miss} = 0$ and $P_{fa} = 0$.

3: It is assumed that data transmission and sensing operation of the SU system can't be done simultaneously because there is only one narrowband transceiver with bandwidth $B_S = B_{channel}$ for both of these tasks.

4: Training data to estimate the model parameters are acquired using an ideal wideband sensor with bandwidth $B_S = M \cdot B_{narrowband}$. Hence, the training data for all channels is acquired at once which ensures the completeness of the data for all channels. Eventually, the parameter estimates are very accurate. It is once again stressed that this wideband sensor is only used for acquisition of training data and regular sensing and transmission will be done only using the narrowband transceiver. The purpose to have this assumption is to investigate the performance of predictive modeling using narrowband devices assuming that accurate model parameters are available. Later on, this chapter will present parameter estimation methods using narrowband devices with an objective to achieve the same level of estimation accuracy as wideband devices.

5: Energy detection based spectrum sensing is used.

6: The SU transmits a fixed sized packet periodically. The size of packet and the period length also remains fixed for a single measurement.

2) MM2: The PU traffic is modeled as a Markov process with only two types of transitions. Self-state transitions are not considered. In such a model the initial state distribution probability matrix $\pi = \{f_{\text{ON}}(t), f_{\text{OFF}}(t)\} = \{\pi_0, \pi_1\}$ defines the state transition probabilities as shown in the simplified version of model in Fig. 5.1.

Meanwhile, the initial state distribution matrix will be referred as $\pi = \{P(i)\} = \{P_{\text{OFF}}, P_{\text{ON}}\}$ from now onwards throughout in the text because of being more expressive about the context. The algorithm of MM2 based OSA is as follows:

i. Sense M channels at once using the wideband sensor for a fixed time interval T_{learning}. Use this data to learn Markov model parameters, $\pi = \{P_{\text{OFF}}, P_{\text{ON}}\}$.

ii. Transmit using the channel which has the lowest probability that the PU system is active, i.e. the one with $\min(P_{\text{ON}})$.

iii. Continue step-ii until a measurement is complete in case of stationary random traffic or go to step-i in case of non-stationary random PU traffic after every T_{window}. Where, the measurement is defined in terms of a fixed no of secondary transmissions.

Note: The non-stationary traffic is simulated in a way that the ON/OFF patterns of the primary traffic vary with time but remain fixed at least within a very small time window T_{window}. Hence, the estimation process must be performed frequently enough to capture the variation of primary statistics.

3) MM4: The PU traffic is modeled as a Markov process considering all four state transitions hence, it is specified by an initial state distribution matrix π and a state transition matrix A. Two different algorithms are used for the channel selection, which are described in the following.

TYPE-I:

i. Sense M channels at once using the wideband sensor for a fixed time interval T_{learning}. Use this data to learn the Markov model parameters, $\pi = \{P(i)\}$, and $A = \{a_{ij}\}$.

ii. Transmit using the channel which has the longest OFF state in comparison to its ON state. The difference of ON and OFF state is specified as:

$\max(\hat{d}_0 - \hat{d}_1)$, where $\hat{d}_i = \frac{P(i)}{1 - a_{ii}}$ is specified by eq. (2.19).

iii. Continue step-ii until a measurement is complete in case of stationary random traffic or go to step-i in case of non-stationary random PU traffic after every T_{window}.

TYPE-II:

    i.   Sense M channels at once using a wideband sensor for a fixed time interval T_{learning}. Use this data to learn the Markov model parameters, $\pi = \{P(i)\}$, and $A = \{a_{ij}\}$.

    ii.   Perform sequential sensing of all channels using the narrowband sensor to acquire the actual state of each channel given by r^m.

    iii.   Compute $\hat{d}_i = \frac{1}{1-a_{ii}}$ for each channel where i is specified by the actual state, r^m, of the corresponding channel. For example, compute $\hat{d}_0$ for all those channels whose sensed state is OFF (i.e. $r^m = 0$) and vice versa. Transmit using the channel where the least PU activity is expected during the transmission of the SU packet. For p channels with actual OFF state and q channels with actual ON state, the decision parameter is given as:

$$\max\left(\hat{d}_0^p - packet\ size, packet\ size - \hat{d}_1^q\right) \text{ where } p + q = M.$$

    iv.   Continue steps ii-iii until a measurement is complete in case of stationary random traffic or go to step-i in case of non-stationary random PU traffic after every T_{window}.

Note that unlike MM2 and MM4 TYPE-I methods, this approach requires the acquisition of the actual state of the channel in order to predict the state of the channel. Such predictive approaches are only suitable when there is a small number of channels, i.e. when M is small. The reason is illustrated in Fig. 5.2 with $M = 3$ and explained in the following paragraphs.
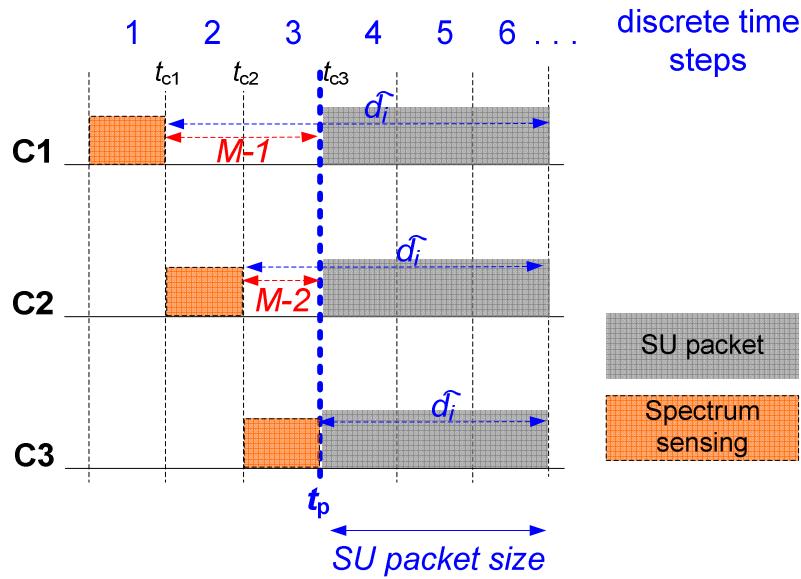
Figure 5.2: *Illustration of the prediction process using three channels.*

In order to accommodate a SU packet one has to predict the state of the channel for a time interval $\hat{d}_i =$ packet size on the basis of q previous states acquired by the sensor, where q is the order of the model. Since future depends only on present but not on past in the case of a first order MM, only the *current state* of the channel has to be acquired i.e. $q = 1$.

Meanwhile, the prediction can be generated in following two ways:

ii.   Firstly, the state of the channel can be predicted right after the *current state* of that channel is sensed (i.e t_{c1}, t_{c2} and t_{c3} in Fig. 5.2) but for a time longer than the SU packet size by a factor '*M-i*', where i is the index of the channel in sequential order. The prediction time in this case is given by $\hat{d}_i =$ packet size $+ (M - i)$.

iii.   Secondly, the prediction for all channels can be deferred till the sensing to acquire the *current state* of all channels is finished i.e. at t_p in Fig. 5.2. In this approach the so called *current state* of each channel is *M-i* time units old indeed. However, in this case prediction needs to be done only for a fixed time i.e. $\hat{d}_i =$ packet size.

In the first case, as the number of channels increases, the predicted time for each preceding channel is increased while longer prediction is naturally less reliable. The fact that packet will be transmitted in the latest part of the prediction further reduces the reliability because later parts of the prediction are less reliable than the former ones. In the second case, the prediction is done on the basis of *current state* that has been acquired some time ago and the statistical significance of this *current state* reduces for each preceding channel when the value of M increases. Eventually, less reliable prediction will be generated on the basis of less significant 'current' channel state. However, the tolerable value of M will also depend on the sample rate of the SU sensor as well as on PU traffic dynamics. For example, sensing with higher sample rate or the PU traffic with slower state changes (i.e. longer T_{ON} and T_{OFF}) will tolerate higher values of M than their contrary counterparts.

At this point it is worth mentioning that auto-regression (AR) based prediction strategies were also studied during the work done for this thesis. The results are reported in [AHM11 SHR12,]. In case of an AR model, the order q is often larger than 1, e.g. $q = 10$ is suggested for IEEE 802.11 based WLAN primary signals in [AHM11]. Where, larger values of q further lower down the tolerable maximum limit of M making the application of the AR model limited to only those scenarios where there is very small number of selectable channels, ideally for a single channel.

On the other hand, some variants of MM based models can be implemented without acquiring the current state of the channel making it suitable for even very large values of M. Only MM4 TYPE-II method performs spectrum sensing before every SU transmission to acquire the current state of the

channel, whereas the other two methods are completely probabilistic in nature since decision is made only on the basis of prior probabilities. Table 5.2 summarizes main parameters of investigated OSA methods.

Table 5.2: *The OSA methods used in simulation*

Method		Decision rule	Sense before every transmission?	Training required?
First free		$\frac{1}{N_{AVG}}\sum_{i=1}^{N_{AVG}} r_i^m < threshold,$ Or $\min(\frac{1}{N_{AVG}}\sum_{i=1}^{N_{AVG}} r_i^m)$	Yes	No
MM2		$\min(P_{ON})$	No	Yes
MM4	TYPE-I	$\max(\hat{d}_0 - \hat{d}_1),$	No	Yes
	TYPE-II	$\max(\hat{d}_0^p - packet\ size, packet\ size - \hat{d}_1^q)$	Yes	

5.1.3 Quality of Service Parameters

The QoS of different OSA methods is measured in terms of *'collision rate'*. It is computed as follows:

$$collision\ rate = \frac{Collision\ count}{total\ number\ of\ SU\ transmission}$$

where 'collision count' is measured as follows (see Fig. 5.3):

Collision count: $\frac{size\ of\ collided\ part\ of\ PU\ packet}{SU\ packet\ size}$, where size is measured as a multiple of fundamental step size of simulation.
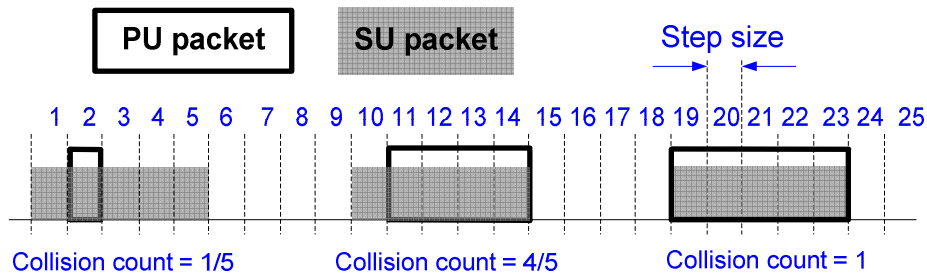
Figure 5.3: *Collision count*

5.1.4   Simulation results

The fundamental step size of the simulation is 1 ms and 5000 points are generated using this step size for each measurement which results in 5 seconds duration for one measurement unless time is explicitly specified. It also means that all quantities such as packet size or sample time are multiple of this step size. In case of stationary traffic λ_{ON} and λ_{OFF} do not change for one measurement. In order to simulate non-stationary traffic the rate parameters are randomly changed after every 2000 points (2 sec), which also defines the value of T_{window}. It is also worth mentioning about these results that the point of interest is the difference in collision rate of different OSA methods but not the absolute value of the QoS parameter. This is because, the collision rate does not directly reflect the traditional BER and PLR type parameters that are used to measure the data loss in communication systems. By using the state-of-the-art transmission schemes (modulations, error correction mechanisms etc.), the actual data loss can be considerably less than the collision rate measured in this section.

The first subsection compares the results of first free method with MM2 and MM4 TYPE-I for stationary and non-stationary PU traffic. Whereas, the second subsection compares the performance of MM2 and MM4 TYPE-II methods.

First free vs. MM2/MM4 TYPE-I: The investigated parameters in this section are number of channels, PU traffic type and the SU packet size. Fig. 5.4a and Fig. 5.4b show results for stationary and non-stationary PU traffics respectively whereas important observations are summarized in the following:

- The difference in collision rate of first free and modeling based methods significantly increases with increase in number of channels. The difference is as small as ~10 % at smallest packet size with only 3 channels and as large as ~50 % with 80 channels. One major reason of this large difference is the fact that the traffic rate is randomly chosen in M channels and the higher the number of channels, the higher are the chances to have some channels with a very small traffic rate. Hence, if all channels would be using a very high traffic rate then Markov based methods may also perform in the same order as the traditional OSA methods. However, the main success of modeling based method is that they always successfully choose the optimal channel whereas, the traditional sensing approaches often fails to exploit such opportunity because mere sensing is not enough to learn the rate of the PU activity in a channel.

- The MM2 and MM4 methods exhibit identical performance. It can be concluded that prediction done in MM4 without explicitly sensing the current state of the channel does not provide better results than the simpler MM2 variant of it.

- Markov based methods demonstrate a performance of the same scale even in the case of non-stationary random PU traffic as long as model parameters are re-estimated at reasonably frequent intervals (see Fig. 5.4b).

a) *Stationary random PU traffic.*

$M = 13$ (e.g. IEEE 802.11a/b/g defines 13 channels)

$M = 79$ (e.g. IEEE 802.15.1 based Bluetooth defines 79 channels)
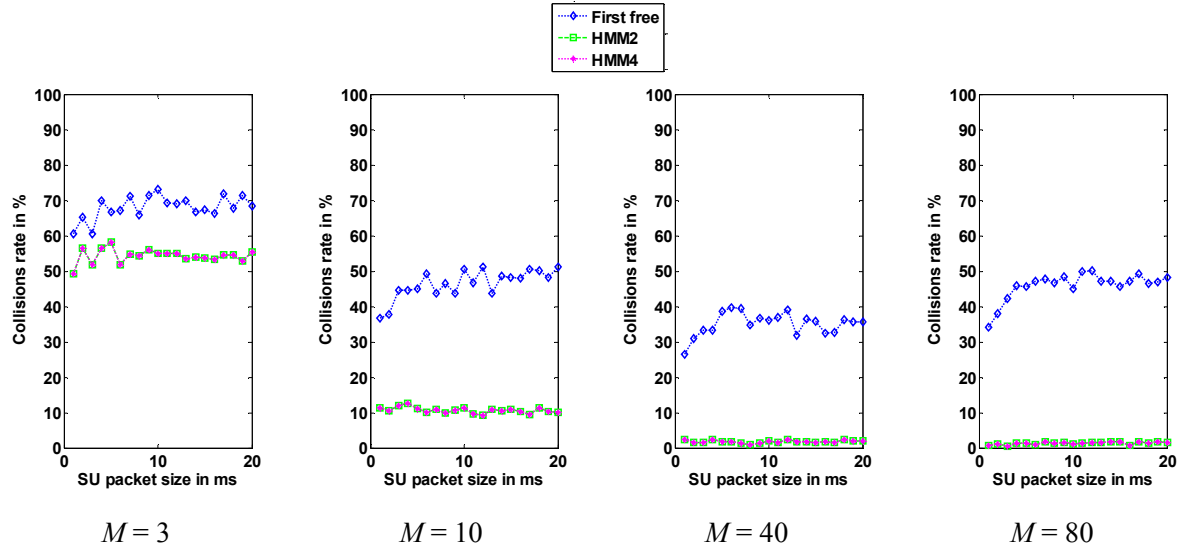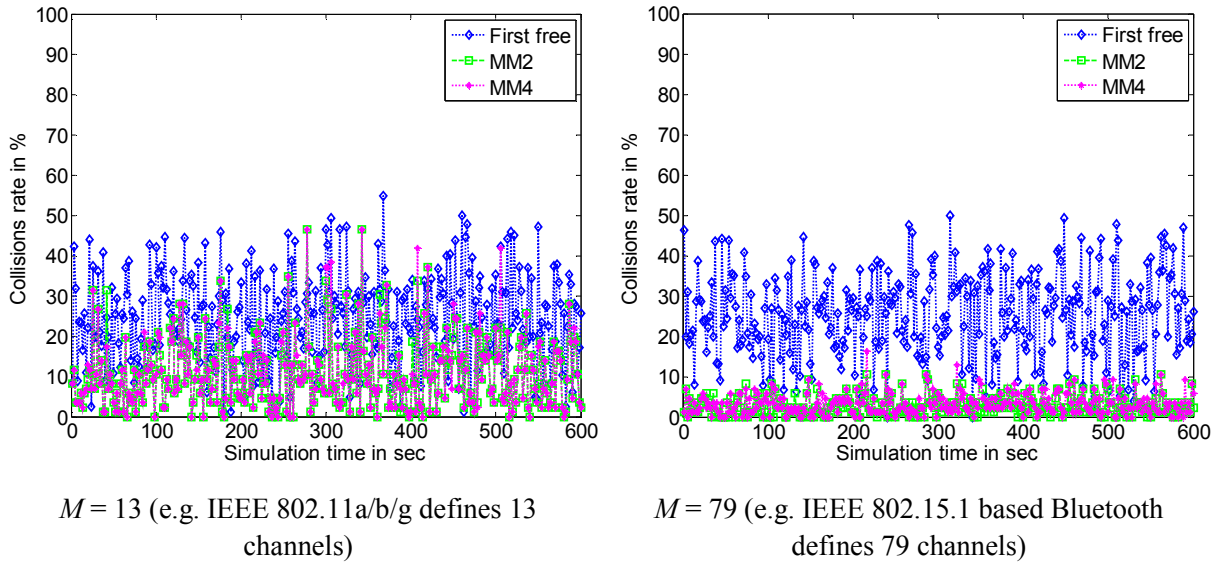
b) *Non-stationary random PU traffic. Traffic rate (λ_{ON}, λ_{OFF}) changes randomly after every 2 seconds.*

Figure 5.4: *Performance analysis of first free, MM2 and MM4 TYPE-I based OSA methods. The MM based methods clearly outclass the traditional methods particularly at higher values of M.*

MM2 vs. MM4 TYPE-II: The previous section concluded that if the state of the channel is predicted merely on the basis of prior probabilities, as in the TYPE-I method, then the MM4 and MM2 methods perform identically. However, this section will argue that the MM4 method is richer in decision making because it has more information than the MM2 type variant of it. In order to demonstrate this argument, the collision rate for MM2 and MM4 TYPE-II OSA methods with four different values of M is plotted in Fig. 5.5.

It is important to note that the PU traffic is chosen in such a way that P_{ON} is identical in all channels but half channels have long packets arriving less often (i.e. both λ_{ON} and λ_{OFF} are large) while the other half channels have very small packets occurring very often (i.e. both λ_{ON} and λ_{OFF} are small). The reason to choose such traffic is to investigate if the MM4 TYPE-II method can differentiate in equally used channels merely on the basis of highly diverse transition probabilities. As shown in Fig. 5.5 the collision rate is 13 % lower for MM4 TYPE-II method than MM2 when there are only 2 channels. However, this difference is reduced with increase in number of channels because the prediction is less reliable for large number of channels as already discussed in section 5.1.2 (Fig. 5.2). Once again it is stressed that it is not the absolute value of collision rate that should be noted but the difference of collision rates of different methods. This is because the absolute value of collision rate depends on the PU traffic rate and for channels with lesser PU activity this value will be obviously lower as shown in Fig. 5.6 in comparison to first plot in Fig. 5.5.

5.1.5 Conclusion

It can be concluded from these results that the predictive modeling based OSA approach will surely choose the channel which has least probability of interference whereas, the conventional reactive/proactive OSA approaches have no means to give such guarantee. Therefore, it can often happen that a reactive/proactive approach would miss a less active channel by choosing a busier channel. Furthermore, the performance difference becomes more profound when the number of channels is increased because a higher number of channels generally increases the chances to find a less active channel. It means that in case of predictive modeling based OSA, it would be more beneficial to widen our search for opportunities to all available channels, i.e. having more channels in opportunity search space is better. However, the difficulty of obtaining an up-to-date and accurate estimation of the model parameters also increases with the increase in number of channels. Hence, an important challenge to realize the predictive modeling based approach is to include maximum number of channels in the search space without compromising on the quality of estimation of model parameters. The remaining part of the chapter takes on this challenge and provides bandwidth independent parameter estimation methods for MM2 and MM4 based OSA approaches.
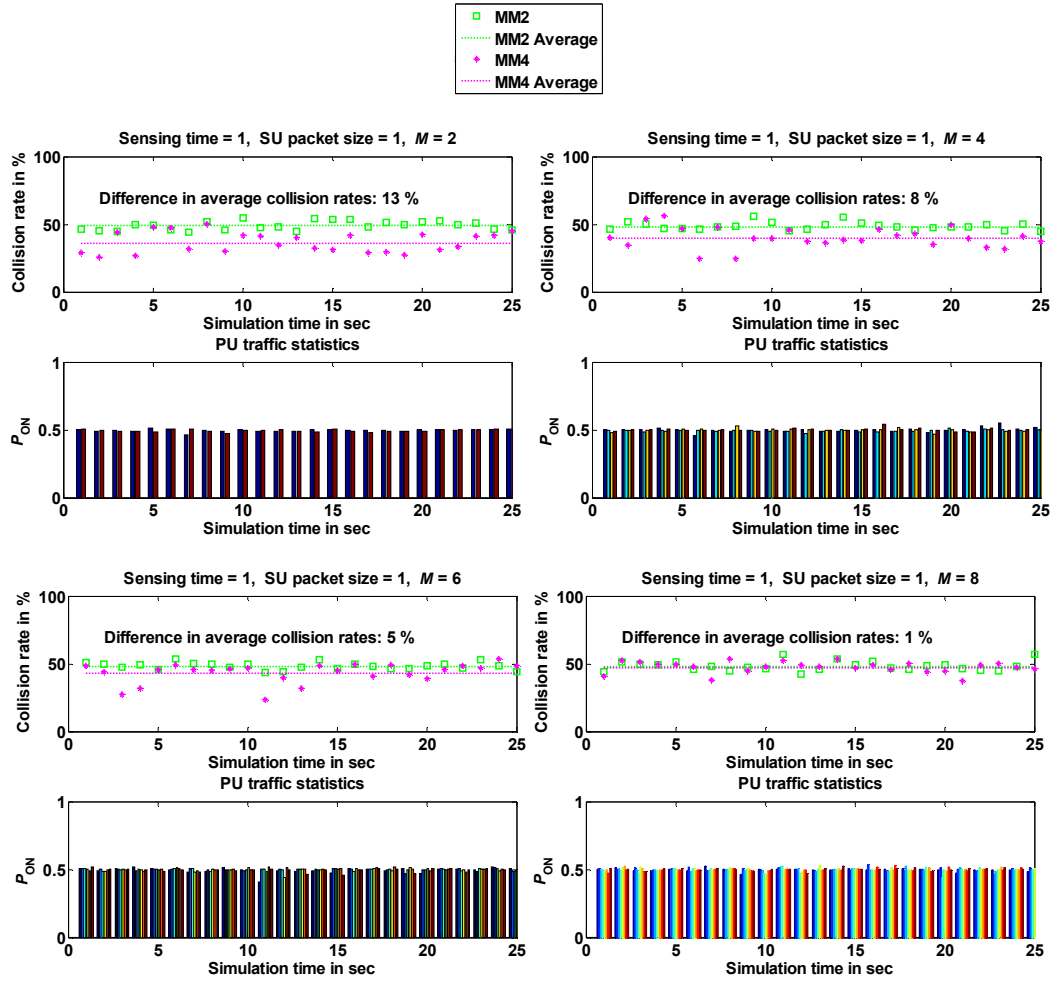
Figure 5.5: *Collision rate of MM2 and MM4 TYPE-II with different values of M and non-stationary random traffic. $P_{ON} \sim 50\%$ for all M channels is also plotted for each case.*
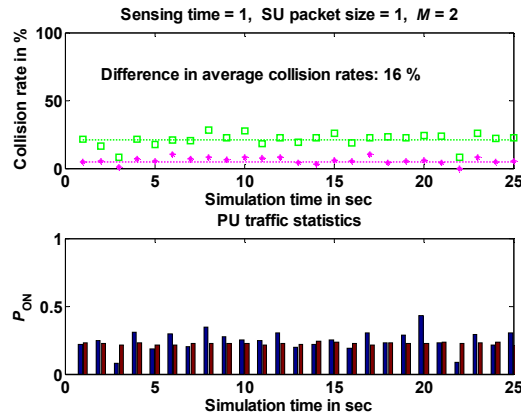
Figure 5.6: *Collision rate with $P_{ON} \sim 25\%$ in both PU channels.*

5.2 Bandwidth Independent Parameter Estimation

Fundamental assumptions regarding data acquisition for parameter estimation made in the previous section are quite unrealistic for real-time scenarios. Firstly, obviously radio systems would often have to work in low signal-to-noise ratio (SNR) regimes in different types of fading environments. Secondly, the entire band of interest in a coexisting environment can be better modeled as divided into overlapping PU channels of different bandwidths rather than into equal bandwidth non-overlapping channels because of coexisting PU systems of diverse bandwidths. Thirdly, and most important, the data acquisition bandwidth B_S is often smaller than the width B_W of the band of interest and the entire band of interest cannot be sensed at once. These factors will result in non-zero P_{fa} and P_{miss} which makes the task of parameter estimation very challenging.

The factors contributing to P_{miss} and P_{fa} can be mainly divided into two categories, environmental effects such as fading, noise and interference and sensor bandwidth limitation. The treatment of missing information because of sensor bandwidth limitation is the focus of this chapter. Note that sensors with $B_S < B_W$ and $B_S \geq B_W$ will be referred as narrowband and wideband sensors respectively in this document.

Traditionally, only a part of the entire band of interest that is equal to the data acquisition bandwidth is sensed continuously for $T_{learning}$ and parameters are estimated for that part only. This process is then repeated for the entire band of interest. However, this approach does not effectively capture up-to-date statistics of the PU traffic because the estimation becomes outdated for earlier channels particularly when the number of channels is higher or the PU traffic is non-stationary. Using more than one narrowband sensor obviously is a solution at an expense of increased system resources and network level cooperation between multiple sensors. This chapter presents parameter estimation methods using a single narrowband sensor for data acquisition. Where, the parameters to be estimated are P_{ON} which also gives $P_{OFF} = 1 - P_{ON}$ and the transition probability matrix A.

5.2.1 System Model

The coexisting environment is constituted by N PU systems of diverse bandwidths represented by B_P. The primary channels may or may not be overlapping. Each PU generates i.i.d. exponential traffic as specified by eq. (5.1). A narrowband sensor is used to sequentially sweep the entire band of interest and multiple consecutive sweeps are combined to generate a spectrogram as shown in the right hand side plot in Fig. 5.7. This swept spectrogram includes two types of incomplete information of actual PU signals which are shown in the wideband spectrogram in the left hand side plot in Fig. 5.7. Firstly, whenever the PU signal is partially acquired it results into a spectrally incomplete signal. Secondly, whenever the PU signal is completely missed it generates a temporal missing.
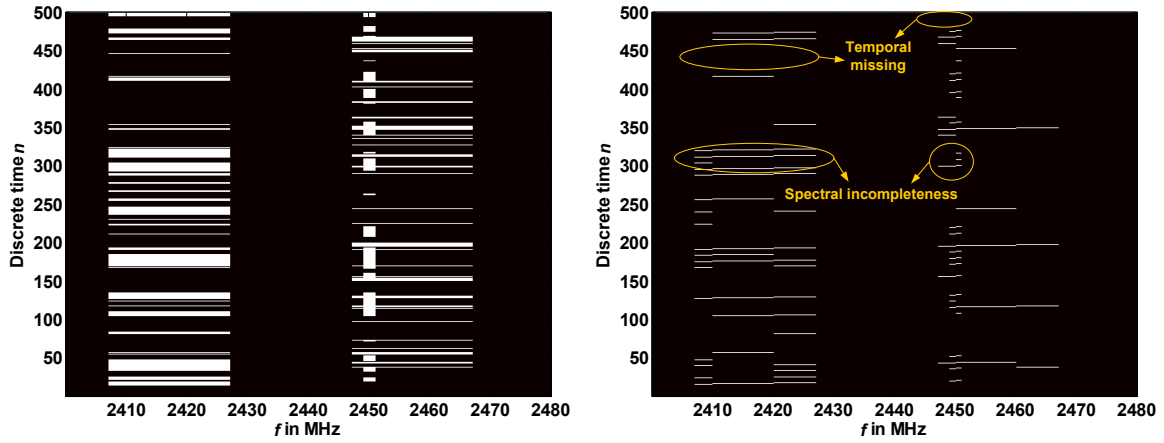
Figure 5.7: *Spectrogram of a simulated coexisting environment constituted by one IEEE 802.15.4 and two IEEE 802.11 based PU signals in the 2.4 GHz ISM band. The swept spectrogram shown in the right hand side plot is generated using a 10 MHz sensor.*
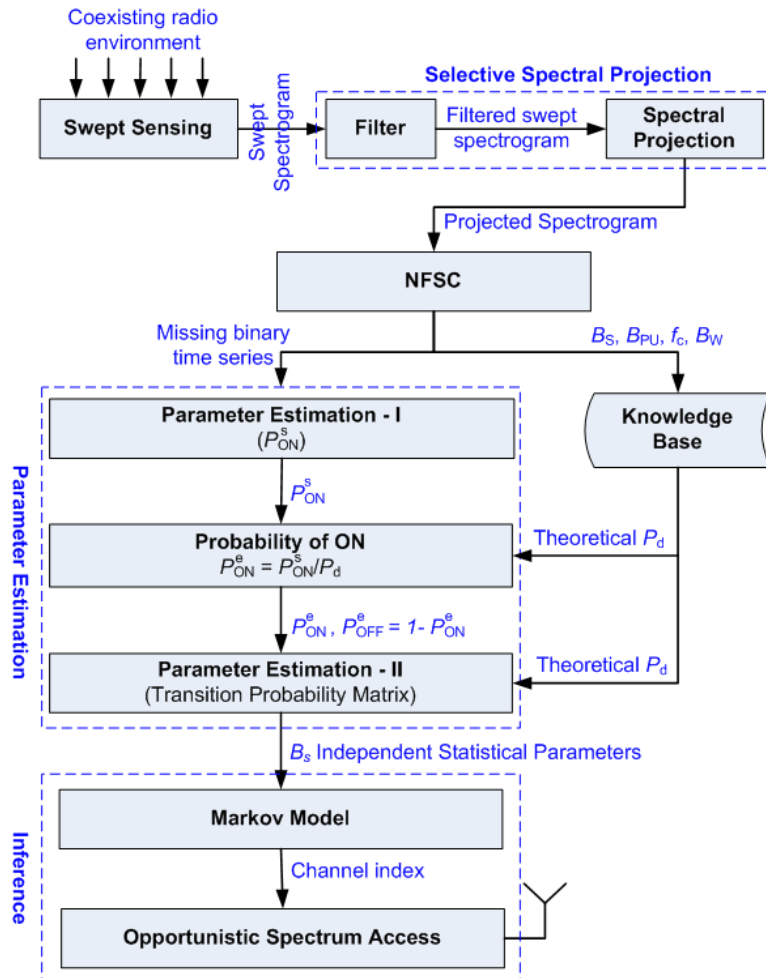
Figure 5.8: *OSA using bandwidth independent parameter estimation*

First of all, given the swept spectrogram, a binary series for each PU signal has to be generated which in turn will be used for parameter estimation. The NFCS presented in chapter 4 will be used for this task. However, the spectral incompleteness hardens the classification task and increases the values of P_{fa} and P_{miss}. Hence, the first task is to process the swept spectrogram in order to handle the spectral incompleteness and generate the binary time series with minimal P_{fa} and P_{miss}. Note that there is yet another factor of P_{miss} caused by temporal missing therefore this binary time series will be referred as *missing binary series*. The next step is to treat the missing binary time series to reduce the effect of temporal missing and obtain unbiased parameter estimation. The system model of OSA using bandwidth independent parameter estimation is presented in Fig. 5.8.

Section 5.2.2 presents an analysis of detection probability of the swept sensing method and also introduces a method named as selective spectral projection to treat the spectral incompleteness. Section 5.2.3 to section 5.2.5 present methods to minimize the impact of temporal missing in order to obtain an unbiased parameter estimation.

5.2.2   Detection Performance of Swept Sensing

The probability to detect a transmission (i.e the ON state) of a PU signal is specified as probability of detection P_{d}. It will be used as the measure to analyze the performance of swept sensing. In case of a binary hypothesis of signal detection given by eq. (2.1), a signal is considered as detected no matter whether its bandwidth is captured completely or partially. However, in case of an *M*-ary hypothesis given by eq. (2.2) using NFSC, a signal is considered detected only if enough spectral part of it is captured to identify the signal on the basis of its bandwidth. Although, this chapter considers *M*-ary hypothesis and attempts to identify the signals using NFSC but for the time being let's assume the binary hypothesis case until explicitly specified.

Binary hypothesis case: The detection probability of a PU signal using swept sensing depends on four system parameters which are sensor bandwidth B_{S}, total bandwidth B_{W} and bandwidth B_{P} and center frequency f_{c} of the PU signal. Mathematically, it is specified by the following equation.

$$P_{\text{d}}^{PU_i} = \frac{\text{Total number of sensor crossings in } PU_i \text{ signal}}{\lceil B_{\text{W}}/B_{\text{S}} \rceil} \tag{5.2}$$

Where $\lceil\ \ \rceil$ is the ceil function and the value of 'total number of censor crossings' depends on B_{s} and the location (f_{c}) of the signal within total band of interest and its width (B_{p}). It is the count of total number of times the sensor samples within the PU channel during one sweep as shown in Fig. 5.9a. In order to grasp the concept let say that if B_{S}, B_{W}, B_{P} and f_{c} are known then one can exactly compute the detected (P_{d}) and missing ($P_{\text{miss}} = 1 - P_{\text{d}}$) proportions of the sensed signal using eq. (5.2). Detected and missing parts of

missing binary series for PU_1 are shown in Fig. 5.9b. Table 5.3 includes algorithm for computation of theoretical detection probability given by Eq. (5.2).
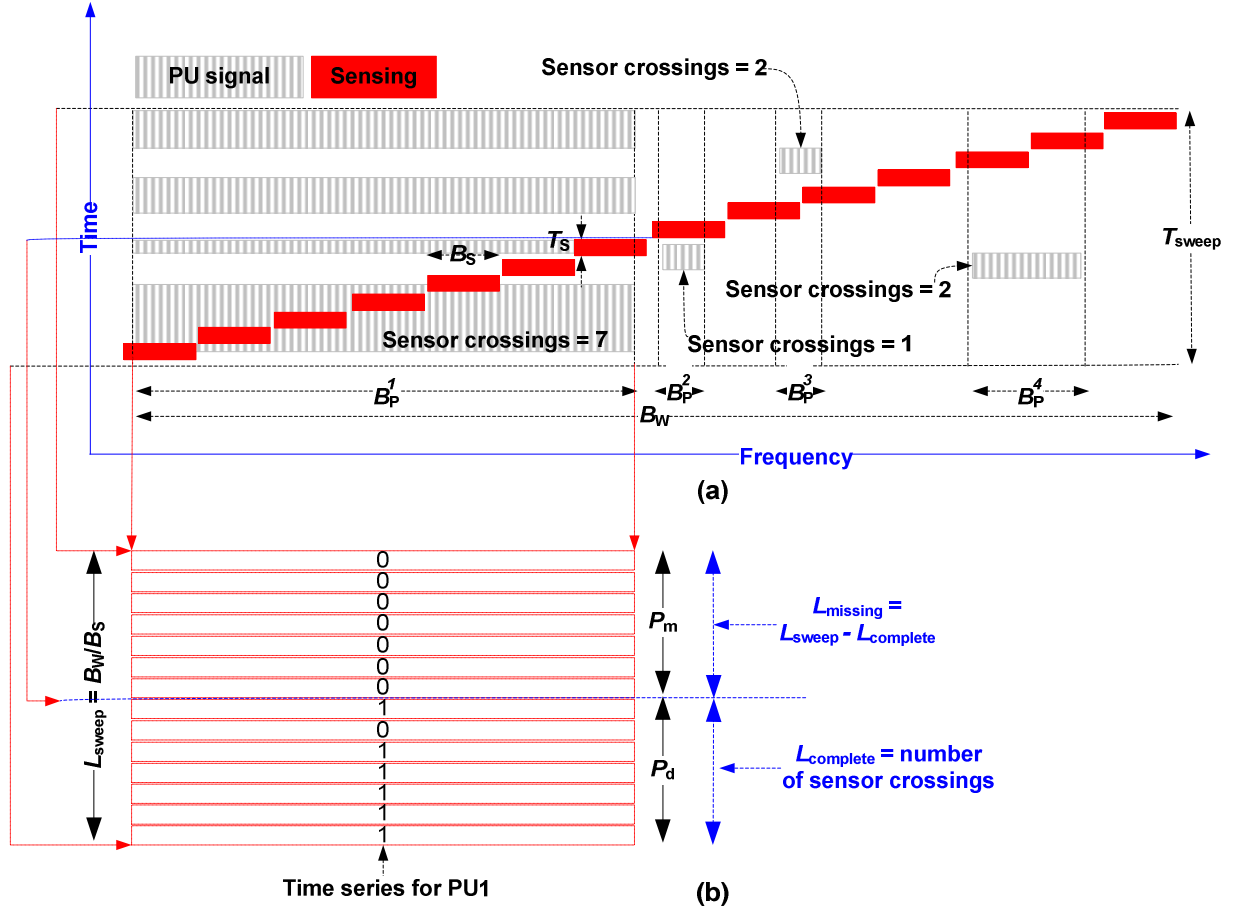
Figure 5.9: (a) *Illustration of computation of total number of sensor crossings using swept sensing* **(b)** *Illustration of the proportion of missed and detected parts in the missing binary series of PU_1 for one sweep. Note that a 0 represent a truly detected OFF state as well as the missed parts.*

Table 5.3: *MATLAB code for computation of theoretical detection probability.*

```
Bw = 80, Bs = specify;
[fc,Bp]= NFSC();
sensor_crossings = count_crossings(Bw,Bs,Bp,fc);
Pd = sensor_crossings / [Bw/Bs];

function sensor_crossings = count_crossings(Bw,Bs,Bp,fc)
sensor_crossings = 1;
for i = 1 to [Bw/Bs] - 1
    if ((fc - Bp)/2) < (i × Bs)) && ((i × Bs) < ((fc + Bp)/2))
        sensor_crossings = sensor_crossings + 1;
    end
end
```

Proof-of-concept: In order to prove this argument, theoretical results generated using eq. (5.2) are compared with simulation results in Fig. 5.10.

(a) *Single PU is operating at $f_c = 2440$ MHz*

(b) *Single PU is operating at $f_c = 2400 + \frac{B_P}{2}$ MHz*
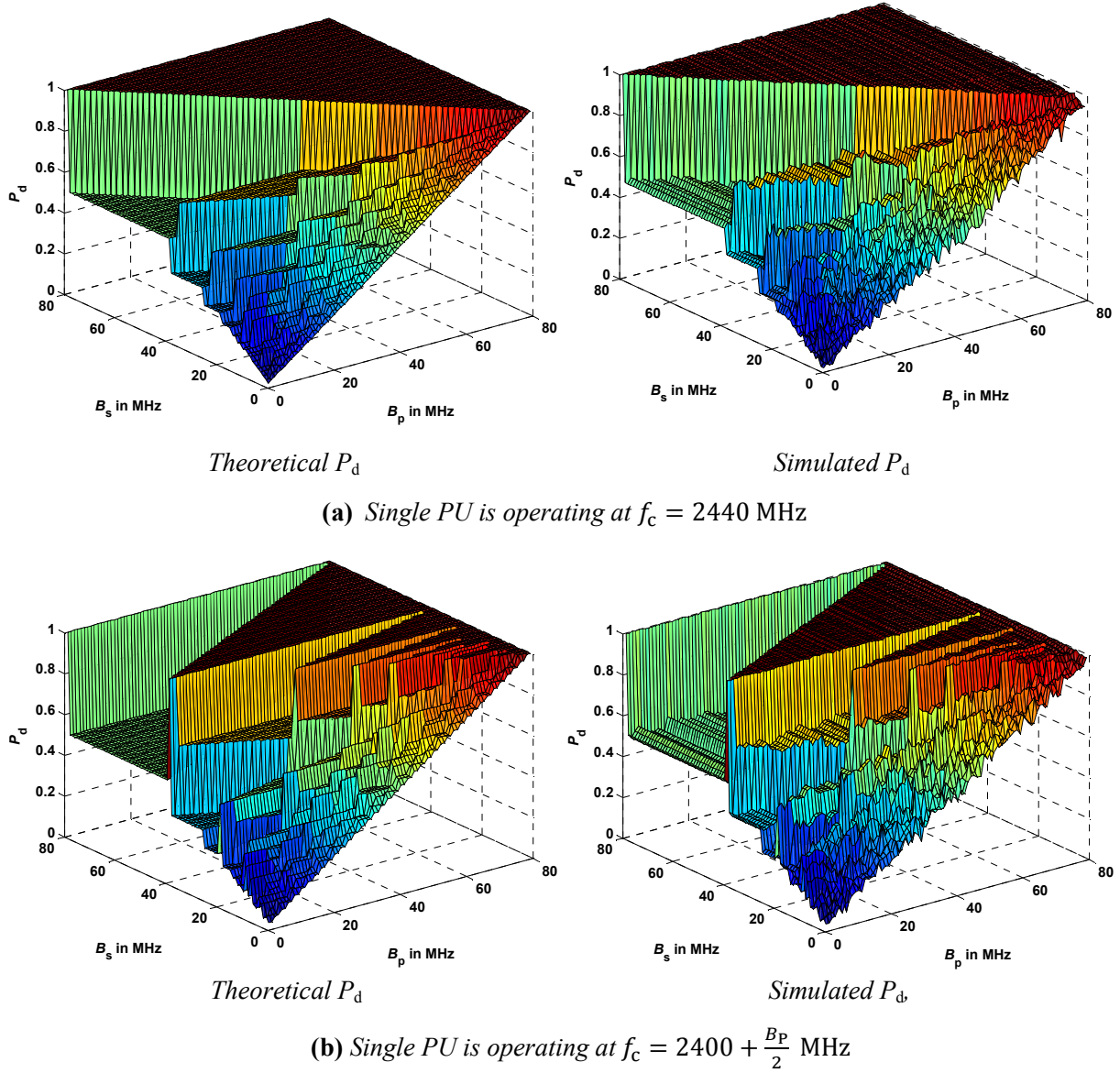
Figure 5.10: *Simulated results vs. theoretical values of the detection probability of swept sensing. $B_W = 80$ MHz in 2.4 GHz ISM band, PU duty cycle ~ 20 %, $T_S = 625$ μs, random PU traffic.*

These results are generated in the 2.4 GHz ISM band ($B_W = 80$ MHz) for two different values of f_c in a standalone noiseless environment. While, both B_P and B_S are in the range 1 MHz, 2 MHz,...,B_W and are specified on corresponding axis. The primary traffic is random as specified by eq. (5.1) and the average

ON time or duty cycle of the primary traffic is approximately 20 %. However, it is worth mentioning that this computation of detection probability of swept sensing method is not limited to the random primary traffic only and is equally valid for any type of primary traffic.

In order to further investigate the accuracy of eq. (5.2), Fig. 5.11 plots percentage error for IEEE 802.11g and IEEE 802.15.4 based signals against different sensor bandwidths and duty cycles. The error is computed as follows:

$$\text{error in \%} = \left| P_d^{\text{theoretical}} - P_d^{\text{simulation}} \right| \times 100 \tag{5.3}$$

The value of error remains less than 2 % for all values of sensor bandwidth except for extremely low duty cycle systems. When the PU duty cycle is less than 5 %, the worst case error is ~4.5 %. Furthermore, the value of error does not depend on which channel the IEEE 802.11/IEEE 802.15.4 based PU system is operating. Moreover, by comparing both error plots it can be observed that the value of error is also independent of bandwidth of PU system since both systems have very different bandwidths but are generating very similar error plots.
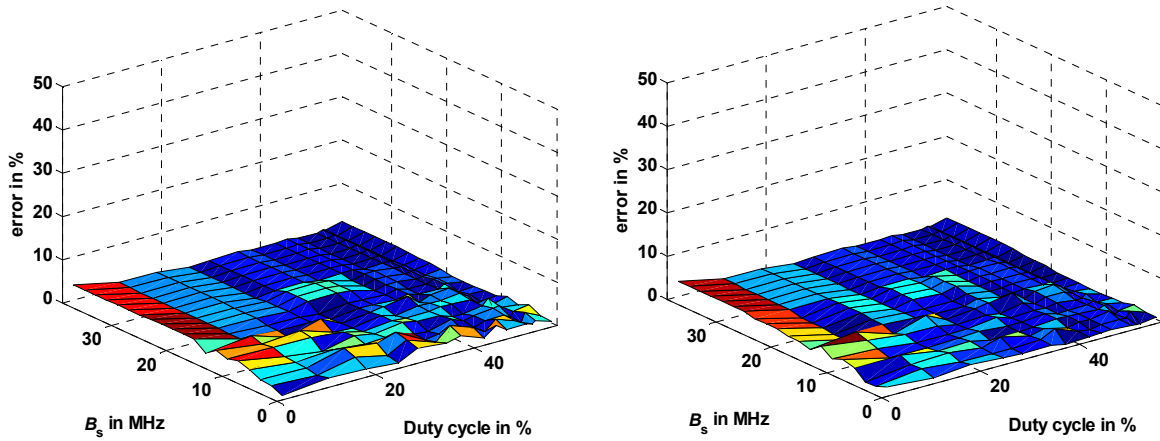
Figure 5.11: *Detection probability error for IEEE 802.11 signal (left) and IEEE 802.15.4 (right) with respect to different duty cycles and B_S values. The error is computed using eq. (5.3).*

M-ary hypothesis case: So far the probability of detection is considered in the context of binary hypothesis. However, if we assume that an ideal method is available that can handle the spectral incompleteness by converting every partial acquisition into a spectrally complete signal in such a way that the NFSC can identify the signal with $P_{\text{fa}} = 0$, then the probability of detection of the binary hypothesis remains valid for the *M*-ary hypothesis case. It means that if there are no spectrally incomplete signal occurrences in a swept spectrogram then the detection probability of the PU signal using the NFSC is given by eq. (5.2). In other words, for a binary series generated by the swept sensing based NFSC,

$P_{miss} = 1 - P_d$ specifies the missing information because of the temporal missing phenomenon as illustrated by Fig. 5.9b.

Meanwhile, in order to compute the detection probability, the values of B_P and f_c can be obtained from the NFSC along with the binary series while the values of B_W and B_S are already known (see MATLAB based algorithm of eq. (5.2) in Table 5.3 and the system model in Fig. 5.8). The next section describes how the spectral incompleteness can be treated using the selective spectral projection method whereas sections 5.2.3 and onwards use the knowledge of P_d/P_{miss} to estimate parameters of the MM2 and MM4 based OSA methods.

5.2.3   Treatment of Spectral Incompleteness Using Selective Spectral Projection

Since bandwidth and center frequency of the PU signals are key distinct features used by the NFSC to classify the PU signals, a spectrally incomplete signal may result in incorrect identification. It will raise P_{fa} for incorrectly detected signal and P_{miss} for actual signal that remains undetected. As discussed earlier in section 4.1.1 the MaxHold operation can be used to improve the spectral incompleteness. In order to realize the MaxHold operation, a sensor sweeps through the entire band of interest and records only the maximum value at each spectral point resulting in a single frame no matter what is the total sensing duration (or time window). In this way it loses all temporal information of the signal which is vital for the statistical estimation and modeling. In order to preserve the time related information, the MaxHold operation is altered to realize a new concept named as selective spectral projection.

The idea of selective spectral projection is different from the traditional MaxHold operation in a sense that instead of holding the running maximum value, post processing of the swept spectrogram is done to compute the maximum value within a time window for only a filtered part of the swept spectrogram. Where, filtering is done over each channel of every PU system. The maximum value is then projected to all those frames where the signal partially occurs. Meanwhile, the partial occurrence of the signal simply means that at least one spectrogram bin is higher than the expected noise floor as shown in Fig. 5.12. Fig. 5.13 shows filtered projected spectrograms for the first 12 channels of the IEEE 802.11 based signal and Fig. 5.14 shows three projected spectrograms with different window sizes. The swept spectrogram used in these two figures is shown in Fig. 5.7. This projected swept spectrogram can be fed to NFSC to generate the *missing binary series* for all coexisting PU signals. Note that in the best case scenario, this missing binary series includes detected occurrences of the corresponding PU system with probability P_d while the occurrences with probability $P_{miss} = 1 - P_d$ are still missing because of the temporal missing phenomenon. However, in real-time scenarios one should also expect some false alarms (represented by P_{fa}), therefore the target of selective spectral projection method is to generate a binary series with missing

data as close as possible to P_{miss} with minimum P_{fa}. Section 5.2.2.1 investigates the performance of the selective spectral projection method in detail.

It is worth mentioning that major beneficiaries of this method are the PU systems with bandwidth larger than the bandwidth of sensor. A PU system with bandwidth smaller than that of sensor will only need spectral projection if it lies somewhere on the boundary of two steps of the sensor such as the third PU in Fig. 5.9a. Hence, it should be applied only when partial occurrences are expected, where the possibility of presence of partial occurrences can be tested using the method *count_crossing*(B_P, B_S, B_P, f_c) given in Table 5.3. If this method returns a value greater than 1, only then selective spectral projection should be performed for that channel of that PU system.
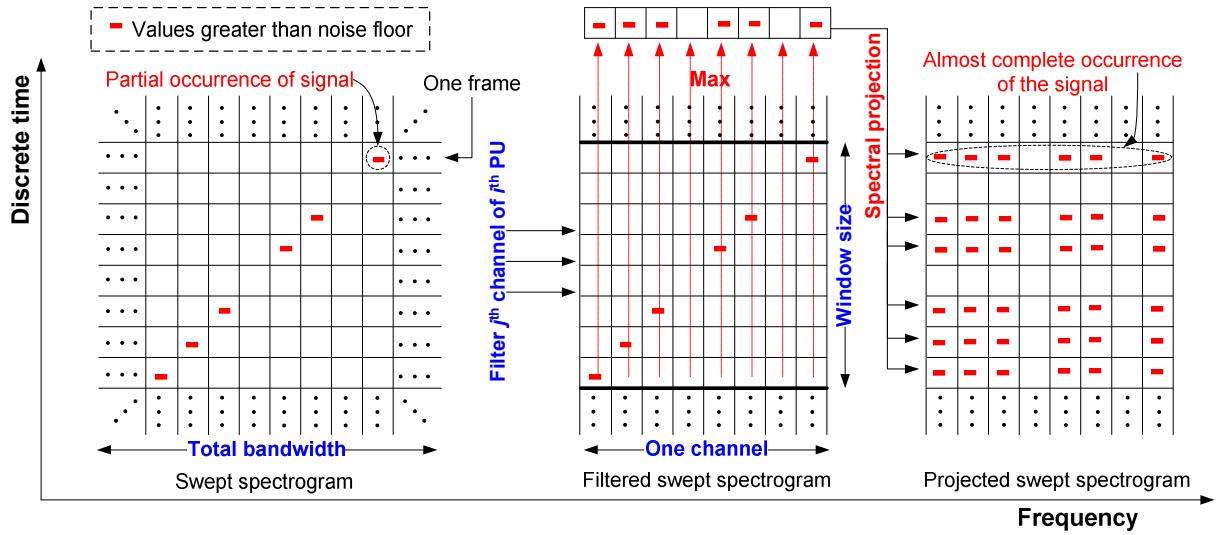
Figure 5.12: *Illustration of the selective spectral projection method. The reason to use the prefix 'selective' is to stress that spectral projection is performed separately within each channel for each PU system.*
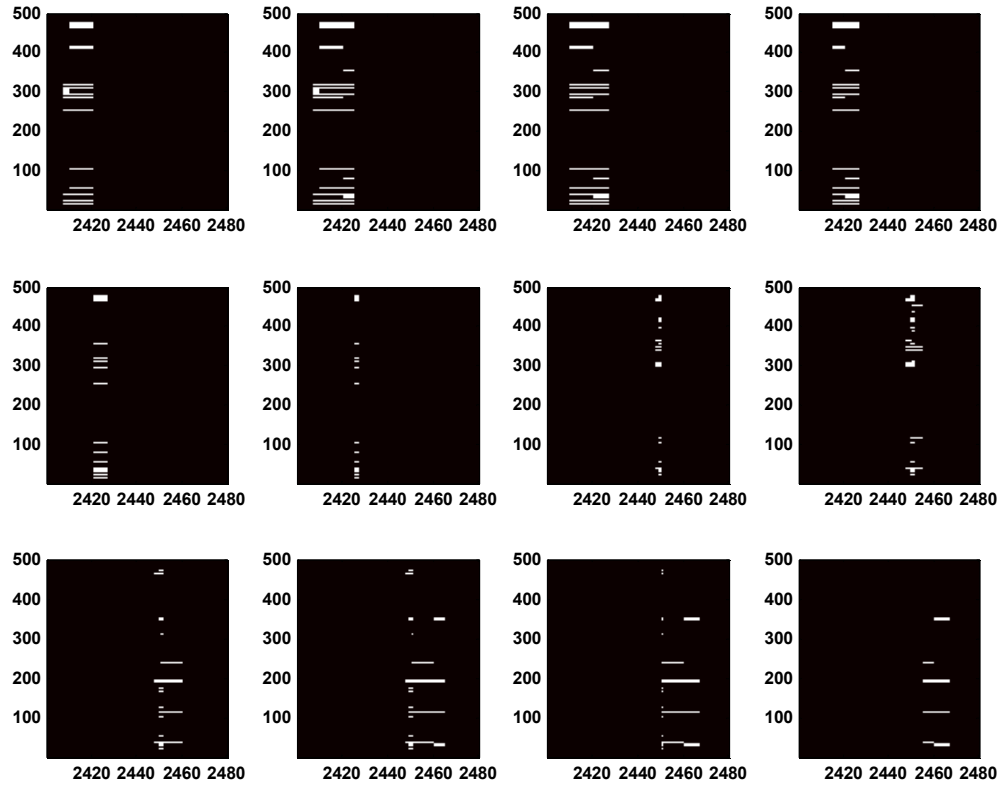
Figure 5.13: *Spectral projection of swept spectrogram shown in Fig. 5.7 in first 12 channels of the IEEE 802.11 based signal with window size = 10. The x-axis corresponds to frequency in MHz and the y-axis to the discrete time n in all these plots.*
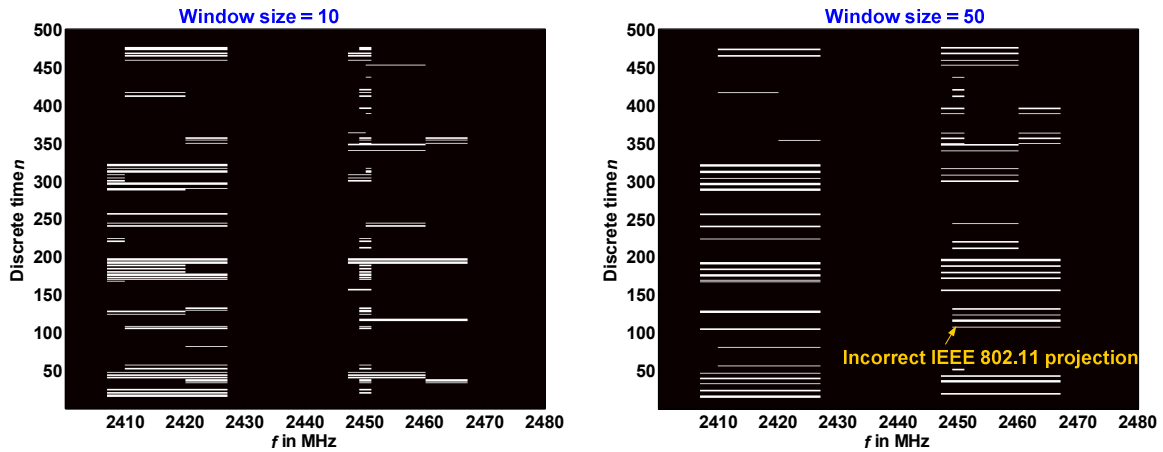
Figure 5.14: *The selective spectral projection of the spectrogram shown in Fig. 5.7 with two different window sizes. Each of these plots is a merger of 29 plots out of which, 16 plots corresponds to IEEE 802.15.4 channels and 13 plots to IEEE 802.11 channels. 12 constituent plots of the left most plot are shown in Fig. 5.13.*

5.2.3.1   Performance Analysis of the Selective Spectral Projection

As mentioned earlier, in a noiseless standalone environment, if an ideal method can treat all spectrally incomplete occurrences of the PU signal with $P_{fa} = 0$ then the probability of detection (*M*-ary context) is given by eq. (5.2). Such ideal method can be the selective spectral projection method, if primary signals do not overlap each other and number of frames in the swept spectrogram is statistically large enough and the length of the swept spectrogram is chosen as window size. The results presented in previous section in Fig. 5.10c, Fig. 5.10d and Fig. 5.11 are generated using such scenarios. However, such a large window size can only be used if the PU signals are not overlapping. The possibility of overlapping signals demands choosing the window size carefully because the spectral projection method can incorrectly project the overlapping PU signals on each other raising the value of P_{fa}. Furthermore, the duty cycle of the PU systems will also influence the choice of widow size because more frequent signals are expected to generate spectrally complete signal in less time than the signals occurring less often. Fig. 5.15 – Fig. 5.17 present detection probability of three scenarios that can influence the window size as discussed in the following:

A hopping system occasionally overlaps a non-hopping primary system: Fig. 5.15 plots P_{miss} and P_{fa} of an IEEE 802.11 based PU system operating in the coexistence of a Bluetooth system for different window sizes. The duty cycles of IEEE 802.11 and Bluetooth systems are ~20 % and 100 % respectively. The blacklisting procedure using adaptive frequency hopping is turned off for the Bluetooth system.
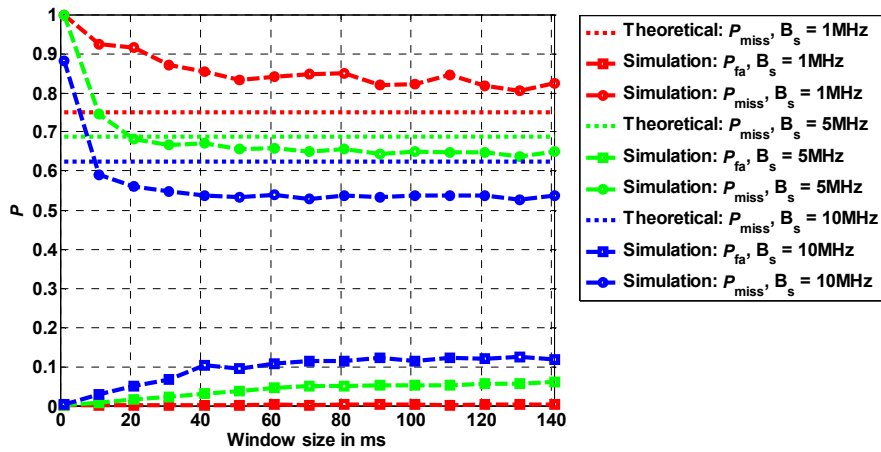
Figure 5.15: *Impact of spectral projection on detection probability of an IEEE 802.11 based WLAN system in coexistence of a Bluetooth system. $T_s = 625 \mu s$, $\gamma^{SM} = 0.4$, duty cycle of WLAN ~ 20 %, duty cycle of Bluetooth ~ 100 %, $T_{training} = 0.625$ sec.*

At very small window size P_{miss} is too biased in comparison to the theoretical values. However, as the window size increases, the value of P_{fa} also increases because some Bluetooth hops are also swept and projected incorrectly as the wider signal of the IEEE 802.11 based PU. Furthermore, the value of P_{fa} is higher for larger sensor bandwidths because there are more chances to acquire the hopping signals and hence more chances to incorrectly project them. A window size of 20 frames will be used as optimal value in rest of this chapter where worst case P_{fa} is ~5 % for $B_{\text{S}} = 10$ MHz and worst case detection error is ~15 % for $B_{\text{S}} = 1$ MHz. It is important to note that since duty cycle of the Bluetooth PU is 100 % therefore it gives the worst case scenario and one can expect less interference with smaller duty cycles. Furthermore, there can be no overlapping at all in real-time coexistence scenario of these two systems because of the Bluetooth system's capability to blacklist active channels of the IEEE 802.11 based system.

Non-hopping overlapping systems: Fig. 5.16 a & b plots the detection probability of IEEE 802.11 and IEEE 802.15.4 based non-hopping systems in an overlapping scenario for different window sizes and a fixed ~20 % duty cycle. It is to be noted that the wider IEEE 802.11 signal can't be incorrectly projected as the narrower IEEE 802.15.4 signal hence, the value of P_{fa} of the narrower signal is not influenced by the selective spectral projection method. However, since the reverse of it is possible, i.e. the narrower signal can be incorrectly projected as the wider signal therefore, the measured value of P_{miss} is expected to increase for narrower signal. On the other hand, both P_{miss} and P_{fa} are expected to be influenced for the wider signal, P_{miss} can be lower than the theoretical value at an expense of increased value of P_{fa} because many narrower signals are incorrectly projected and identified. Another reason for the value of P_{miss} of narrower signal to be higher than the theoretical value is the fact that all simultaneous occurrences of narrower signal are buried under wider signal because of the inability of energy detection method to dig into to find the buried signals. Only a more complicated spectrum sensing strategy such as the CFD method can detect these buried signals. The results plotted in Fig. 5.16 a & b support these arguments. Once again, a window size of 20 frames is found optimal for both systems with P_{fa} less than 1 % for all investigated scenarios and worst case detection error ~10 % with $B_{\text{S}} = 1$ MHz for the IEEE 802.11 based system.

Very low duty cycle systems require larger window size to produce optimal results and vice versa as shown in Fig. 5.16 c & d for IEEE 802.11 and IEEE 802.15.4 based signals with window size = 20 frames. Increasing the duty cycle of narrower signal increase the value of P_{fa} for wider signal whereas increasing the duty cycle of wider signal buries more occurrences of narrower signal resulting in higher P_{miss} for the narrower signal. However, in real-time scenarios it is unlikely to have multiple systems with high duty cycles operating in overlapping channels (except systems with some

robust strategies such as TDMA, CDMA etc.) because high data loss due to high interference will possibly force them to choose safer channels.

(a) *PU = IEEE 802.11, channel # = 2.*   (b) *PU = IEEE 802.15.4, channel # = 3*

(c) *PU = IEEE 802.11, channel # = 2.*   (d) *PU = IEEE 802.15.4, channel # = 3*
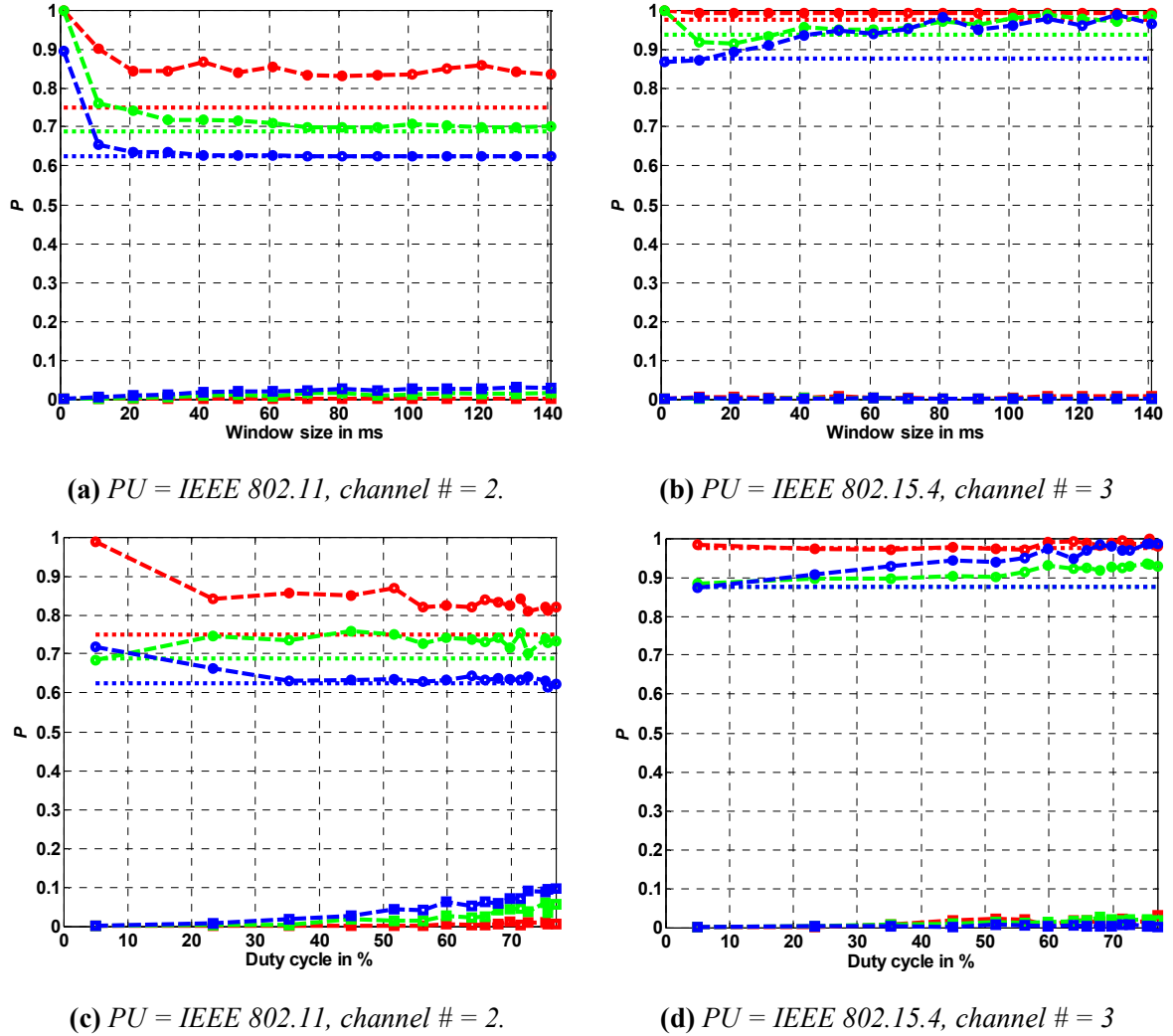
Figure 5.16: *Detection probability of the specified PU systems coexisting in overlapping channels using selective spectral projection with **a) & b)** window size = x-axis, duty cycle of both PU systems ~ 20 %, **c) & d)** window size = 20, duty cycle of both PU systems is specified on x-axis. Moreover, $T_s = 625\ \mu s$, $\gamma^{SM} = 0.4$, $T_{training} = 0.625\ sec$ (see Fig. 6.15 for legend).*

The window size will also be influenced by the sample time and for higher sample rates a smaller window size has to be chosen and vice versa for same reasons as given for the duty cycle of PU systems. The influence of noise is not considered on the detection probability of signals firstly because noise has to be dealt at NFSC or earlier stages which has already been discussed in chapter 5. Another reason to ignore

noise related issues is because the goal of this chapter is to handle missing data caused by bandwidth limitations but not by noise.

5.2.4   Estimation of P_{ON} ($P_{OFF} = 1 - P_{ON}$)

It is the measure of average time the primary signal remains in ON state and is required by both MM2 and MM4 based OSA methods. It is given by:

$$P_{ON} = \hat{x} = \frac{1}{n}\sum_{k=1}^{n} x_k \text{ ; where } x_k \in \{0,1\} \tag{5.4}$$

Where $\widehat{}$ is the average operator, n is the total number of samples or the length of the missing binary series X and x represents a single sample. If this average value is computed using the missing binary series then it will be a biased value because of temporal missing information with probability P_{miss}. Let's call this average value P_{ON_S} when it is computed using missing binary series, where superscript 's' stands for swept. This value can be combined with P_d to get an unbiased estimation, P_{ON_e}, of the average ON state of the corresponding PU signal, as specified by the estimation process given in Table 5.4.

5.2.4.1   Analysis of Results

The percentage error as an absolute difference of true and computed values is plotted in Fig. 5.17a and Fig. 5.17b for P_{ON} directly computed from missing binary series using eq. (5.4) and estimated using method in Table 5.4 respectively. Non-overlapping scenario is considered in these plots with varying values of B_S and B_P. The primary statistics are randomly changed every second and with $T_{training} = 0.625$ sec, a single point in these plots is an average of 10 consecutive measurements. The average error remains higher than 20 % for computed P_{ON_S} as long as P_{miss} is 0.5 or higher. For very small combinations of B_P and B_S the average error up to 40 % can be expected. On the other hand, the average error remains below 2 % except for very small values of B_P and B_S for P_{ON_e}. The worst case estimation error is almost 5 % when both B_P and B_S are 1 MHz.

Running results for two standard technologies are plotted in Fig. 5.18 for non-overlapping and overlapping scenarios. It can be seen from these plots that the error in P_{ON_S} is higher for higher duty cycles hence average error can be much higher than the one stated in last paragraph if the primary signal remains highly active all the time.

On the hand the value of P_{ON_e} is expected to be overestimated with an increase in the value of P_{fa}. For example consider plots shown in Fig. 5.18c & d for two specified standard technologies coexisting with a Bluetooth system. It can be seen that higher values of B_P and B_S increase the chances of incorrect detection of Bluetooth hops that eventually result into overestimation of P_{ON}.

Table 5.4: *Algorithm for estimation of* P_{ON_e}. *SS: swept spectrogram, FSS: filtered swept spectrogram, PFSS: projected FSS, PSS: projected swept spectrogram.*

	Process	**Output**
1	Perform swept sensing for T_{learning} to acquire the training data.	*SS*
2	**for** $PU_i \in \{\text{all expected PUs}\}$ and $f_\text{c} \in \{\text{all channels of } PU_i\}$, $\quad FSS = \text{filter}(B_\text{P}, f_\text{c}, SS)$ $\quad$ **if** $count\_crossing(B_\text{P}, B_\text{S}, B_\text{P}, f_\text{c}) > 1$ $\quad\quad PFSS_j = selective\_spectral\_projection(B_\text{P}, f_\text{c}, FSS)$ $\quad$ **else** $\quad\quad PFSS_j = FSS$ $\quad$ **end** **end** $PSS = \sum_{j=1}^{total\ number\ of\ PUs\ \times\ number\ of\ channels\ of\ each\ PU} PFSS_j$	*PSS*
3	$\{X^i, B_\text{P}^i, f_\text{c}^i\} = NFSC(PSS)$	$\{X^i, B_\text{P}^i, f_\text{c}^i\}$ *
4	$P_{\text{ON}_\text{S}}^i = \frac{1}{T_{learning}} \sum_{k=1}^{T_{learning}} x_k^i$; where T_{learning} is discrete valued.	$P_{\text{ON}_\text{S}}^i$
5	Compute the value of P_d^i for $B_\text{P}^i, f_\text{c}^i$ using eq. 5.2.	P_d^i
6[11]	$P_{\text{ON}_\text{e}}^i = \dfrac{P_{\text{ON}_\text{S}}^i}{P_\text{d}^i}$	$P_{\text{ON}_\text{e}}^i$

* X is the random variable represented as missing binary series extracted by NFSC and its realizations are represented by x.

---

[11] If two events *A* and *B* are defined as, *A* = sensor detects the primary occurrence, and *B* = PU is in ON state, then P_d, the conditional probability of detecting PU occurrences given the PU is in ON state, is given as follows:

$P_\text{d} = P(A|B) = \frac{P(A \cap B)}{P(B)} = \frac{P_{\text{ON}_\text{S}}}{P_{\text{ON}}} \Rightarrow P_{\text{ON}} = \frac{P_{\text{ON}_\text{S}}}{P_\text{d}}$, where P_{ON} is in fact the estimated value i.e. P_{ON_e}.

(a) *Error in computation of* P_{ON_s}

(b) *Estimation error for* P_{ON_e}
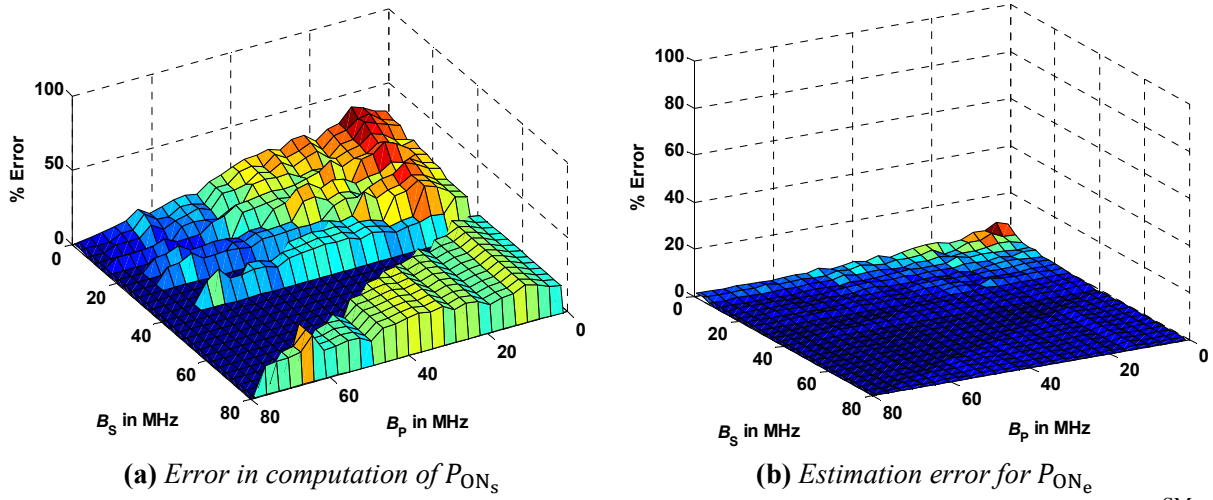
Figure 5.17: *Comparison of % error in* P_{ON_s} *and* P_{ON_e} *in non-overlapping scenario.* $T_s = 625\ \mu s$, $\gamma^{SM} = 0.4$, *Window size = 20,* $T_{learning} = 0.625\ sec$, $f_c = 2.44\ GHz$.

(a) *IEEE 802.11, no overlapping*

(b) *IEEE 802.15.4, no overlapping*

(c) *IEEE 802.11, BT overlapping*

(d) *IEEE 802.15.4, BT overlapping*
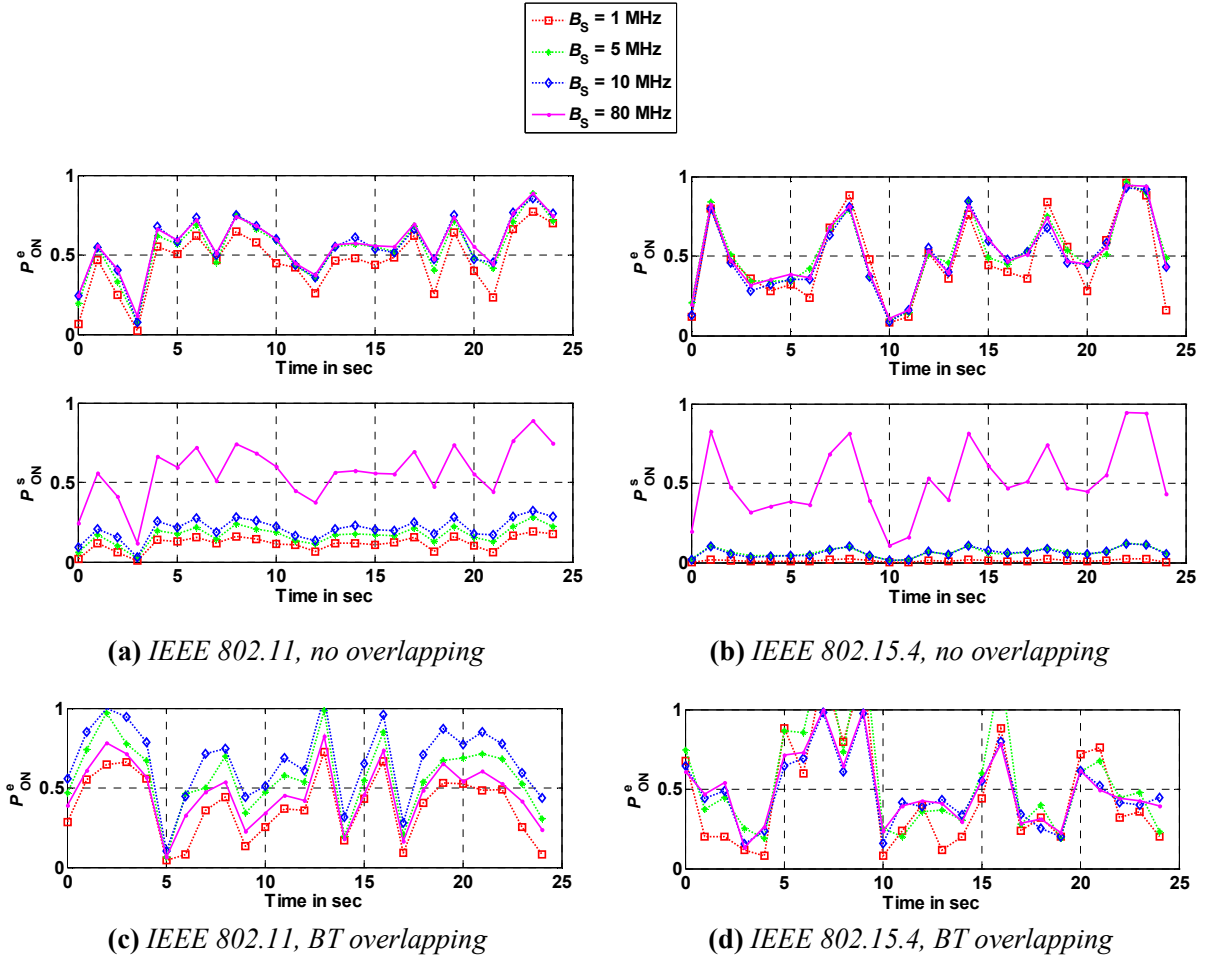
Figure 5.18: *Running results of estimated, swept and actual values of* P_{ON} *in* **a) & b)** *non-overlapping scenario* **c) & d)** *Bluetooth overlapping.* $T_{learning} = 0.625\ sec$, $\gamma^{SM} = 0.4$, $T_S = 625\ \mu s$, *window size = 20,* B_S *is specified in legend, values corresponding to* $B_S = 80\ MHz$ *are true values.*

5.2.5   Estimation of the Transition Probability Matrix, $A = \{a_{ij}\}$

5.2.5.1   Renewal theory based approach

According to renewal theory [COX67], the equilibrium probability of an alternating renewal primary signal, given that the signal is in ON state at the time of origin, to be in ON state at some later time t is given by:

$$a_{11}(t) = \int_t^\infty \frac{\mathbb{F}_1(x)}{E[T_{ON}]} du + \int_0^t h_{10}(x)\, \mathbb{F}_1(t-x) dx \tag{5.5}$$

Where $\mathbb{F}(\cdot)$ is the survivor function given by eq. (2.29) and $h_{10}(x)$ is the renewal density of the OFF state of the primary signal, given that the renewal process started from the ON state. The eq. (5.5) can be written as follows by using the Laplace transform:

$$a_{11}^* = \frac{\{E[T_{ON}]s - 1 + f_{ON}^*(s)\}}{E[T_{ON}]s} + h_{10}^*(s) \cdot \frac{1 - f_{ON}^*(s)}{s} \tag{5.6}$$

Where $(\cdot)^*$ is the Laplace transform. It is also proved in [COX67] that:

$$h_{10}^*(s) = \frac{f_{OFF}^*(s)\{1 - f_{ON}^*(s)\}}{E[T_{ON}]s\{1 - f_{ON}^*(s)f_{OFF}^*(s)\}} \tag{5.7}$$

Substituting the value of $h_{10}^*(s)$ in eq. (5.6) and simplifying gives:

$$a_{11}^*(s) = \frac{1}{s} - \frac{\{1 - f_{ON}^*(s)\}\{1 - f_{OFF}^*(s)\}}{E[T_{ON}]s^2\{1 - f_{ON}^*(s)f_{OFF}^*(s)\}} \tag{5.8}$$

Where f_{ON} and f_{OFF} are specified by eq. (5.1) and their corresponding Laplace transforms are $f_{ON}^* = \frac{\lambda_{ON}}{\lambda_{ON}+s}$ and $f_{OFF}^* = \frac{\lambda_{OFF}}{\lambda_{OFF}+s}$ respectively. By substituting these values, eq. (5.8) becomes:

$$a_{11}^*(s) = \frac{1}{s} - \frac{\left\{1 - \frac{\lambda_{ON}}{\lambda_{ON}+s}\right\}\left\{1 - \frac{\lambda_{OFF}}{\lambda_{OFF}+s}\right\}}{E[T_{ON}]s^2\left\{1 - \left(\frac{\lambda_{ON}}{\lambda_{ON}+s}\right)\cdot\left(\frac{\lambda_{OFF}}{\lambda_{OFF}+s}\right)\right\}} \tag{5.9}$$

Taking inverse Laplace transform of eq. (5.9):

$$a_{11}(t) = 1 - \frac{1}{E[T_{ON}]}\left(-\frac{1}{(\lambda_{ON}+\lambda_{OFF})}e^{-(\lambda_{ON}+\lambda_{OFF})t} + \frac{1}{(\lambda_{ON}+\lambda_{OFF})}\right) \tag{5.10}$$

For exponential distribution $E[ON] = \frac{1}{\lambda_{ON}}$ and $E[OFF] = \frac{1}{\lambda_{OFF}}$ hence, eq. (2.28) can be written as:

$$\pi_{ON} = P_{ON} = \frac{\lambda_{OFF}}{\lambda_{ON}+\lambda_{OFF}}, \pi_{OFF} = P_{OFF} = \frac{\lambda_{ON}}{\lambda_{OFF}+\lambda_{OFF]}} \tag{5.11}$$

Where P_{ON} is already estimated in section 5.2.4. Hence, the transition probability from ON state to ON state is given by:

$$a_{11}(t) = P_{ON_e} + (1 - P_{ON_e}) \cdot e^{-(\lambda_{ON} + \lambda_{OFF})t} \tag{5.12}$$

By merely exchanging the roles of ON and OFF in eq. (5.5) to eq. (5.10) one can obtain the transition probability from OFF state to OFF state which is given as follows:

$$a_{00}(t) = (1 - P_{ON_e}) + P_{ON_e} e^{-(\lambda_{ON} + \lambda_{OFF})t} \tag{5.13}$$

The remaining two transition probabilities can be simply obtained by using eq. (5.12) and eq. (5.13) with the fact that summation of each row of the transition probability matrix is equal to 1 as specified by eq. (2.14). These are given in the following:

$$a_{10}(t) = 1 - a_{11}(t) = (1 - P_{ON_e}) - (1 - P_{ON_e}) \cdot e^{-(\lambda_{ON} + \lambda_{OFF})t} \tag{5.14}$$

$$a_{01}(t) = 1 - a_{00}(t) = P_{ON_e} - P_{ON_e} \cdot e^{-(\lambda_{ON} + \lambda_{OFF})t} \tag{5.15}$$

However, these equations also need the knowledge of λ_{ON} and λ_{OFF} in order to estimate the transition probabilities and both of these parameters are unknown. Knowledge of one of these parameters is enough as the other can be computed using eq. (5.11).

Maximum Likelihood Estimator (MLE): The likelihood function of the parameter set θ is specified as follows:

$$\mathcal{L}(\theta|X) = \Pr(X|\theta) = \prod_{i=1}^{r} \Pr(x_i|\theta) \tag{5.16}$$

Where r is the total number of samples or the length of the missing binary series. The MLE estimate can be obtained by solving the following partial differential equation:

$$\frac{\partial \mathcal{L}(\theta|x)}{\partial \theta_i} = 0; \text{where } \theta = \{\theta_1 = \lambda_{ON}, \theta_2 = \lambda_{OFF}\} \tag{5.17}$$

$\prod_{i=1}^{r} \Pr(x_i|\theta)$ in eq. (5.16) is the joint probability mass function of all samples and can be expressed as a function of initial probability distribution and the transition probability matrix for a Markov process. Using the Markovian property specified by eq. (2.11), eq. (5.16) can be written as:

$$\mathcal{L}(\theta|X) = \Pr(x_1; \theta) \cdot \prod_{k=2}^{r} \Pr(x_k|x_{k-1}; \theta) \text{ where } x_i \in \text{the state space vector } S \tag{5.18}$$

Using eq. (2.13) and eq. (2.15) the above equation can be written as:

$$\mathcal{L}(\theta|X) = \pi_i \cdot [a_{00}(t)]^{n_{00}} \cdot [a_{01}(t)]^{n_{01}} \cdot [a_{10}(t)]^{n_{10}} \cdot [a_{11}(t)]^{n_{11}} \tag{5.19}$$

Where $n_{00}, n_{01}, n_{10}, n_{11}$ give the count of corresponding state transitions from a total of $r - 1$ transitions in a binary series of r samples. The initial state probability π_i is P_{ON_e} or $P_{OFF_e} = 1 - P_{ON_e}$ depending on the value of the first sample.

Substituting the values given by eq. (5.12) – eq. (5.15) in eq. (5.19) and solving the differential equation given by eq. (5.17) for λ_{ON} or λ_{OFF} gives the estimation of corresponding parameter. In [HYO08], the solution of these equations is given for λ_{OFF} as follows:

$$\hat{\lambda}_{OFF} = -\frac{P_{ON_e}}{T_S} \ln\left[\frac{-B+\sqrt{B^2-4AC}}{2A}\right]; \text{ where } \begin{cases} A = \left(P_{ON_e} - \left(P_{ON_e}\right)^2\right)(r-1) \\ B = -2A + (r-1) - n_{00}\left(1 - P_{ON_e}\right) - P_{ON_e} \cdot n_{11} \\ C = A - P_{ON_e} \cdot n_{00} - n_{11}\left(1 - P_{ON_e}\right) \end{cases} \quad (5.20)$$

where T_S is the time between two consecutive samples and can also be used in eq. (5.12) – eq. (5.15) instead of t.

State Transition Count: In order to estimate λ_{OFF} using eq. (5.20) the count of state transitions i.e. n_{00}, n_{01}, n_{10}, n_{11} is still to be estimated. Let say n_{ij}^s = total number of trnsitions from state S_i to state S_j, is the state transition count obtained from the missing binary series. It can be used with already known values of P_d and P_{ON_e} to estimate true count of state transitions, n_{ij}^e as discussed in the following.

Note that a '1' in the missing binary series never corresponds to a missed value. Although the processing at NFSC or selective spectral projection may generate '1' with some P_{fa} however, for sake of simplicity it is assumed that $P_{fa} = 0$. On the other hand, the missing binary series includes 0 for both correctly detected OFF states and the missing values (see Fig. 5.9b).

Consequently, a state transition count to and from state 1 in the missing binary series can never be wrong whereas, all state transition counts to and from state 0 may contain an incorrectly counted factor proportional to P_{miss}. It means that some counts in n_{00}^s can be actually either n_{10} or n_{01} if one of the 0's corresponds to a missed ON state or n_{11} if both consecutive 0's are missed occurrences. Similarly, both n_{10}^s and n_{01}^s may contain some incorrect parts of n_{11} if 0 is actually a missed ON state.

Moreover, according to the memoryless property of exponential distribution, the occurrence of any state at t-1 does not change the probability of occurrence of the state at next time t, i.e.

$$P(x_t = S_i|x_{t-1} = S_i) = P(x_t = S_i|x_{t-1} = S_j) = P(S_i) = \pi_i \quad (5.21)$$

In other words, the probability of occurrence of a state is given by the initial probability irrespective of the neighboring state. Hence, in a given missed binary series, the probability of '00' being truly '00' is P_{OFF_e} and being any of '01' or '10' or '11' is P_{ON_e}. Similarly, the probability of '10' being truly '10' is P_{OFF_e} and being '11' is P_{ON_e} and the probability of '01' being truly '01' is P_{OFF_e} and being '11' is P_{ON_e}.

Based on the above discussion, it is concluded that n_{00}^s includes truly detected OFF states as well as the missing part whereas, the missing part also includes n_{00} with probability P_{OFF_e}. Hence, the estimation of n_{00} is given as follows:

$$n_{00}^e = n_{00}^s \times P_d + (n_{00}^s \times P_{miss}) \times P_{OFF_e} \qquad (5.22a)$$

However, it is observed that following provides better estimation in most cases:

$$n_{00}^e = n_{00}^s \times P_{OFF_e} \qquad (5.22b)$$

Similarly, the occurrence of '0' in n_{01}^s and n_{10}^s include true OFF states with probability P_{OFF_e} and missed ON states with P_{ON_e}. Finally, missed ON states in n_{00}^s represented by $\left[P_{ON_e}(n_{00}^s \times P_{miss})\right]$ has to be distributed among n_{10}, n_{01} and n_{11}. One possibility is to distribute this part equally in these three counts however, it often generates biased results. Another solution, which gave promising results during simulations, is to distribute this factor proportional to the 'so far' estimated counts of the respective state transitions as specified by the following three equations:

$$n_{01}^e = n_{01}^s \times P_{OFF_e} + \left[P_{ON_e}(n_{00}^s \times P_m)\right] \frac{n_{01}^s \times P_{OFF_e}}{\left[(n_{01}^s \times P_{OFF_e}) + (n_{10}^s \times P_{OFF_e}) + \left(n_{11}^s + (n_{01}^s \times P_{ON_e}) + (n_{10}^s \times P_{ON_e})\right)\right]} \qquad (5.23)$$

$$n_{10}^e = n_{10}^s \times P_{OFF_e} + \left[P_{ON_e}(n_{00}^s \times P_m)\right] \frac{n_{10}^s \times P_{OFF_e}}{\left[(n_{01}^s \times P_{OFF_e}) + (n_{10}^s \times P_{OFF_e}) + \left(n_{11}^s + (n_{01}^s \times P_{ON_e}) + (n_{10}^s \times P_{ON_e})\right)\right]} \qquad (5.24)$$

$$n_{11}^e =$$
$$n_{11}^s + (n_{01}^s \times P_{ON_e}) + (n_{10}^s \times P_{ON_e}) +$$
$$\left[P_{ON_e}(n_{00}^s \times P_m)\right] \frac{[n_{11}^s + (n_{01}^s \times P_{ON_e}) + (n_{10}^s \times P_{ON_e})]}{\left[(n_{01}^s \times P_{OFF_e}) + (n_{10}^s \times P_{OFF_e}) + \left(n_{11}^s + (n_{01}^s \times P_{ON_e}) + (n_{10}^s \times P_{ON_e})\right)\right]} \qquad (5.25)$$

Analysis of results: Two of the four state transition probabilities computed using eq. (5.12) – eq. (5.15), eq. (5.20), eq. (5.22) – eq. (5.25) for different sensor and PU bandwidths are plotted in Fig. 5.19. The remaining state transition probabilities can be computed by using the identity given by eq. (2.14).

It can be observed from these plots that the estimation error remains well below 10 % for both transition probabilities for any values of B_P and B_S. However, at all those places where P_d is 0.5 (e.g. $B_P = 1$ MHz, $f_c = 2.44$ GHz, 80 MHz $< B_S > 40$ MHz), n_{11} is slightly overestimated causing comparatively higher estimation error for a_{11} and obviously for a_{10} too. Fortunately, this overestimation only occurs when $B_S \geq 50$ % of B_W. Clearly, such situations are not the actual target area of estimation methods presented in this chapter because with so large B_S any traditional parameter estimation approach will provide reasonable estimation accuracy.

(a) *Estimation error for a_{00}*

(b) *Estimation error for a_{11}*
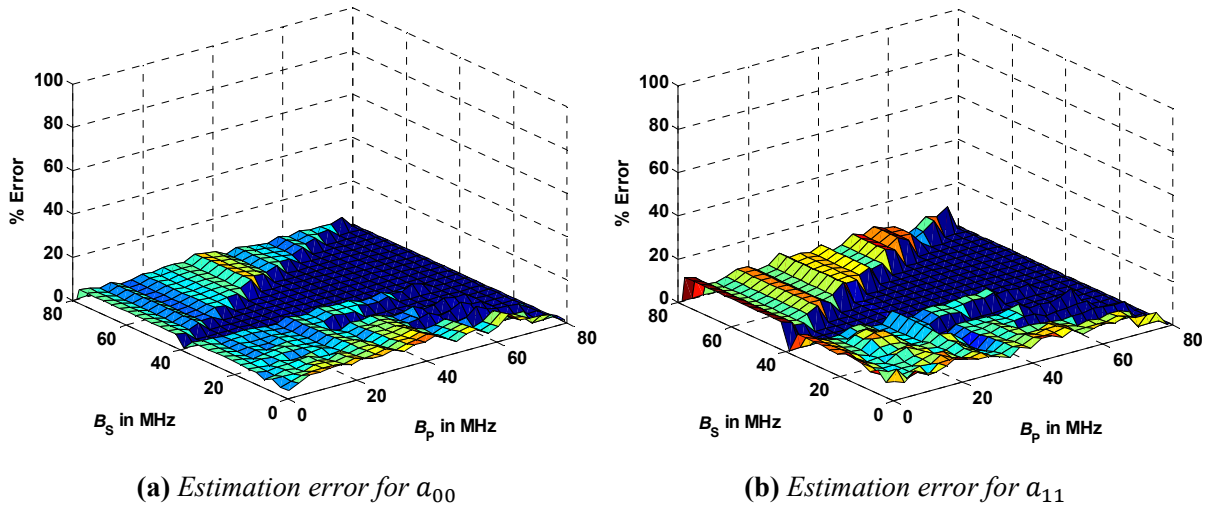
Figure 5.19: *The percentage estimation error for a_{00} and a_{11} using renewal theory based approach in non-overlapping scenario with non-stationary primary traffic. The primary statistics are changed and re-estimated after every second hence, the % error is the average value computed over 10 measurements. $r = 1000$, $f_c = 2.44$ GHz, $T_{learning} = 0.625$ sec, $\gamma^{SM} = 0.4$, $T_S = 625$ μs, window size = 80.*

(a) *PU = IEEE 802.11*

(b) *PU = IEEE 802.15.4*
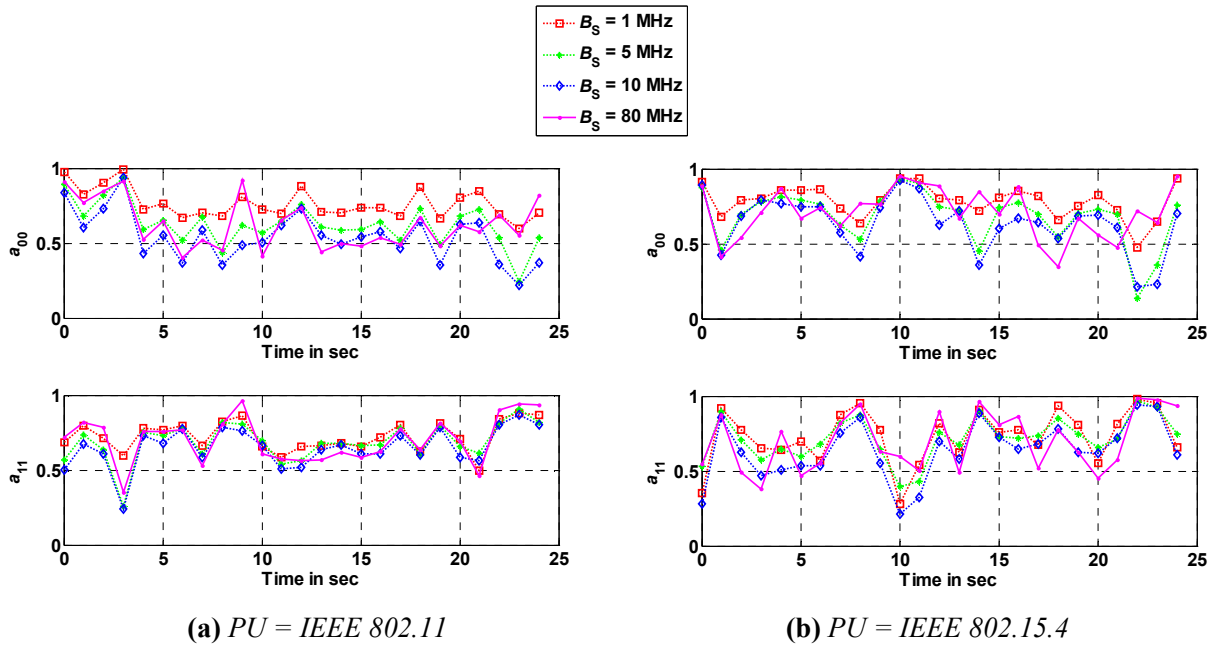
Figure 5.20: *Estimation of specified state transition probabilities using renewal theory approach in a non-overlapping scenario. Non-stationary primary traffic is used where traffic statistics i.e. λ_{ON} or λ_{OFF} vary after every one second. The respective values of P_{ON} (estimated) are plotted in Fig. 5.18 a&b. The values corresponding to $B_S = 80$ are true values used for reference. Total number of samples for each point i.e. $r = 1000$, $T_{training} = 0.625$ sec, $\gamma^{SM} = 0.4$, $T_S = 625$ μs, window size = 20, B_S is specified in legend.*

Running results of two standard wireless technologies are presented in Fig. 5.20. A significant observation is the occurrence of large estimation error in a_{00} when duty cycle is too high (higher than ~90 %) and large error in a_{11} when the duty cycle of the primary signal is too low (lower than 10 %). For example, time 10, 22 and 23 for IEEE 802.15.4 signal plot in Fig. 5.20b. Meanwhile, corresponding running results of P_{ON} are already plotted in Fig. 5.18 a & b.

5.2.5.2   HMM based approach

Baum-Welch algorithm, an EM procedure, is a maximum-likelihood approach for HMM parameter learning. Given observation sequences $L = \{O^k\}$, it learns the optimal parameters of λ i.e. $\lambda^* = \arg\max_\lambda P(L|\lambda)$. The idea is to divide the observation sequence, O, into two parts, the first part is from time 1 to time t and the other part is from time $t+1$ to time T as shown in Fig. 5.21. A so-called *forward-backward* procedure [ETH10] is used to compute two variables $\alpha_i(t)$ and $\beta_i(t)$ for these parts of the observation sequence which are then used for estimation of λ^*.

$\alpha_i(t)$ is called the forward variable and is defined as the probability of seeing the partial sequence $o_1, \ldots, o_t$ and ending up in state S_i at time t, i.e.

$$\alpha_i(t) = P(O_1 = o_1, \ldots, O_t = o_t, q_t = S_i | \lambda) \tag{5.26}$$

It can be recursively calculated as follows:

Initialization: $\alpha_i(1) = \pi_i b_i(o_1)$ $\hphantom{xxxxxxxxxxxxxxxxxxxxxxxxxxxxxxxxxxxxxxxxxx}$ (5.27)

Recursion: $\alpha_j(t + 1) = \left[\sum_{i=1}^N \alpha_i(t) a_{ij}\right] b_j(o_{t+1})$ $\hphantom{xxxxxxxxxxxxxxxxxxxxxx}$ (5.28)

where π_i, a_{ij} and $b_i(o_1)$ are initial, state transition and emission probabilities specified by eq. (2.15), eq. (2.13) and eq. (2.20) respectively and N is the number of states.
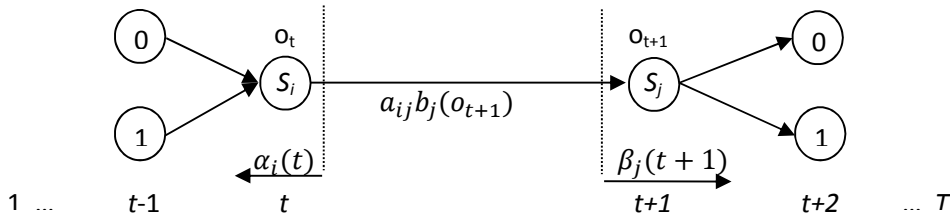
Figure 5.21: *Illustration (concept from [LAW89]) of the computation process of probability of joint event that the system is in state S_i at time t and S_j at time t+1 for a two state Markov process with symbol set V ={0, 1}.*

Similarly, $\beta_i(t)$, called the backward variable, is the probability of being in state S_i at time t and observing the partial sequence $o_t+1,\ldots,o_T$ i.e.

$$\beta_i(t) = P(O_{t+1} = o_{t+1}, \ldots, O_T = o_T, q_t = S_i | \lambda) \tag{5.29}$$

It can be recursively computed as follows:

<u>Initialization:</u> $\beta_i(T) = 1$ (5.30)

<u>Recursion:</u> $\beta_i(t) = \sum_{j=1}^{N} a_{ij} b_j(o_{t+1}) \beta_j(t+1)$ (5.31)

As per Rabiner's HMM tutorial [LAW89], Baum-Welch algorithm defines $\xi_{ij}(t)$ as the probability of being in state S_i at time t and in state S_j at time $t+1$ given the model and the observation sequence, i.e.

$$\xi_{ij}(t) = P(q_t = S_i, q_{t+1} = S_j | O, \lambda) \tag{5.32}$$

This equation can be expanded as[12]:

$$\xi_{ij}(t) = \frac{P(q_t = S_i, q_{t+1} = S_j, O | \lambda)}{P(O | \lambda)} \tag{5.33}$$

Where numerator is the joint probability as illustrated by Fig. 5.21. By using the forward and the backward variables eq. (5.33) can be written as:

$$\xi_{ij}(t) = \frac{\alpha_i(t) a_{ij} b_j(o_{t+1}) \beta_j(t+1)}{\sum_{i=1}^{N} \sum_{j=1}^{N} \alpha_i(t) a_{ij} b_j(o_{t+1}) \beta_j(t+1)} \tag{5.34}$$

Note that summation of eq. (5.34) over time is the expected number of transitions from state S_i to state S_j for observation sequence O, i.e.

$$n_{ij} = \sum_{t=1}^{T-1} \xi_{ij}(t) \tag{5.35}$$

Furthermore, the probability of being in state S_i at time t for the observation sequence O can be calculated by summing up the probabilities for all possible next states from state S_i, i.e.

$$\gamma_i(t) = P(q_t = S_i | O, \lambda) = \sum_{j=1}^{N} \xi_{ij}(t) \tag{5.36}$$

Summation of eq. (5.36) across time gives the expected number of times in state S_i and hence the expected number of transitions from state S_i, as given below:

---

[12] If two events A and B are defined as, A = Being in state S_i at time t and in state S_j at time $t+1$ given the model, and B = observing the sequence O given the model, then $\xi_{ij}(t)$ is the conditional probability of being in state S_i at time t and in state S_j at time $t+1$ given the observation sequence and the model, and is given as follows:

$$\xi_{ij}(t) = P(A|B) = \frac{P(A \cap B)}{P(B)}$$

$$n_i = \sum_{t=1}^{T} \gamma_i(t) \tag{5.37}$$

The goal is to use ξ_{ij} and γ_i to estimate the parameters of the HMM, $\lambda = (A, B, \pi)$, for observation sequence O, which are given in the following:

$$\hat{\pi}_i = expected \text{ number of times in state } S_i \text{ at time } (t = 1) = \gamma_i(1) \tag{5.38}$$

$$\hat{a}_{ij} = \frac{n_{ij}}{n_i} = \frac{\sum_{t=1}^{T-1} \xi_{ij}(t)}{\sum_{t=1}^{T-1} \gamma_i(t)} \tag{5.39}$$

$$\hat{b}_i(m) = \frac{expected \text{ number of time in state } j \text{ and observing symbol } v_m}{n_i} = \frac{\sum_{t=1}^{T-1} \gamma_i(t) 1(o_t = v_m)}{\sum_{t=1}^{T-1} \gamma_i(t)} \tag{5.40}$$

Now the model parameters are computed as follows:

<u>E-Step:</u> Let say an initial guess of model parameters is defined as $\lambda = (A, B, \pi)$.

<u>M-Step:</u> Use the initial guess in eq. (5.38) – eq. (5.40) to obtain a re-estimation of model parameters specified by $\hat{\lambda} = (\hat{A}, \hat{B}, \hat{\pi})$. Iteratively use $\hat{\lambda}$ instead of λ in these equations until some limiting point is reached.

In order to apply the Baum-Welch algorithm to the problem of parameter estimation using swept sensing, the missing binary series is considered as the observed sequence O. While, the complete state sequence that can only be observed by a wideband sensor is the hidden sequence Q. Initial guess of parameters is given in the following:

$$\pi_i = (P_{ON}^e, 1 - P_{ON}^e) \tag{5.41}$$

$$a_{ij} = \begin{bmatrix} \dfrac{n_{00}^e}{(1-P_{ON}^e) \times \text{length of missing binary series}} & \dfrac{n_{01}^e}{(1-P_{ON}^e) \times \text{length of missing binary series}} \\ \dfrac{n_{10}^e}{P_{ON}^e \times \text{length of missing binary series}} & \dfrac{n_{11}^e}{P_{ON}^e \times \text{length of missing binary series}} \end{bmatrix} \tag{5.42}$$

Where n_{ij}^e is given by eq. (5.22) - eq. (5.25).

$$b_j(m) =$$

$$\begin{bmatrix} \text{probability to observe a 0 given an OFF state} & \text{probability to observe a 1 given an OFF state} \\ \text{probability to observe a 0 given an ON state} & \text{probability to observe a 1 given an ON state} \end{bmatrix} \tag{5.43}$$

Assuming that $P_{fa} = 0$, it is known that an OFF state always generates a '0' in O. On the other hand, an ON state can be missed with P_{miss} generating a '0' or can be detected with P_d generating a '1' in O as illustrated by HMM model for swept sensing in Fig. 5.22. Hence, the matrix in eq. (5.39) can be written as:

$$b_j(m) = \begin{bmatrix} 1 & 0 \\ P_{miss} & P_d \end{bmatrix} \tag{5.44}$$

If there is some false alarm probability that can be estimated then the emission probability matrix can be adjusted accordingly however, false alarms are not considered in this document.
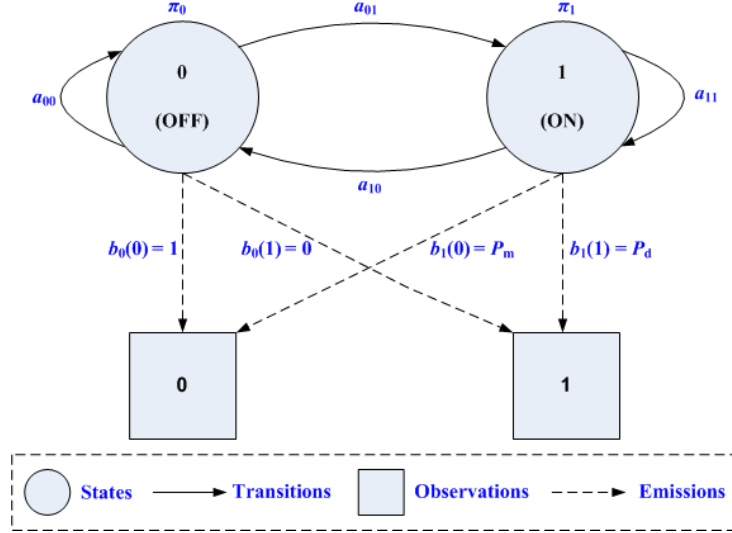
Figure 5.22: *The HMM model for swept sensing.*

(a) *Estimation error for a_{00}*

(b) *Estimation error for a_{11}*
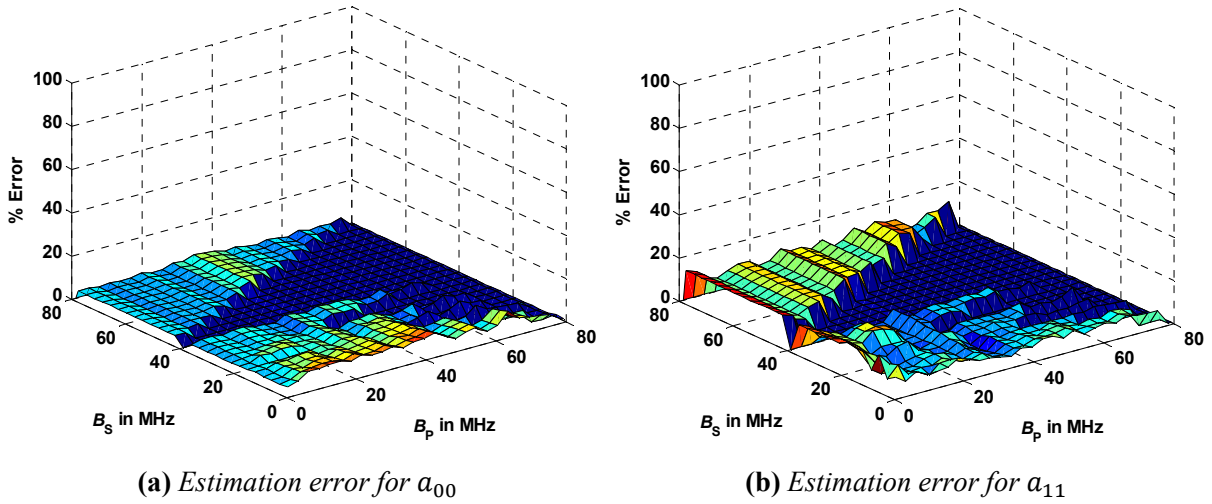
Figure 5.23: *The percentage estimation error for a_{00} and a_{11} using Baum-Welch algorithm in non-overlapping scenario with non-stationary primary traffic. The primary statistics are changed and re-estimated after every second hence, the % error is the average value computed over 10 measurements. $r = 1000$, $f_c = 2.44$ GHz, $T_{learning} = 0.625$ sec, $\gamma^{SM} = 0.4$, $T_S = 625$ μs, window size = 80.*

Analysis of results: The average estimation error in a_{00} and a_{11} using Baum-Welch algorithm is presented in Fig. 5.23. The results are very identical to those produced by renewal theory based approach with slight differences. For higher values of P_{miss}, i.e. for smaller values of B_{P} and B_{S}, the estimation of a_{11} is $\sim$ 2-3 % better than the renewal theory based estimation. However, at $B_{\text{S}} \geq 50\%$ of B_{W} and $P_{\text{d}} = 0.5$, the overestimation of n_{11} is $\sim$ 2-3 % worse than the estimation done by renewal theory. Finally, the estimation of a_{00} is also $\sim$2 % worse than that of renewal theory based approach for larger values of P_{miss}.

5.2.5.3   Renewal theory based approach vs. Baum-Welch algorithm

Since both methods relays on same parameters i.e. P_{ON}^{e} and n_{ij}^{e} and produces almost identical results, the only significant point of comparison is the computational time required to estimate the model parameters. The renewal theory based approach has to compute only five equations (eq. (5.20), eq. (5.22) – eq. (5.25)). On the other hand, the computational time required to calculate the forward and the backward variables is $\mathcal{O}(N^2 T_{\text{training}})$ [ETH10]. It further requires K number of iterations in M-Step to reach to the convergence point. Hence, the computation complexity of the Baum-Welch algorithm is $K \times \mathcal{O}(N^2 T_{\text{training}})$. Because of such large computational time this method may not be feasible at all with traditional microcontroller/FPGA based platforms particularly in situations where either large training time is required e.g. in the presence of primary signals with low duty cycles or when the model parameters has to be re-estimated very often e.g. in case of non-stationary traffic.

Chapter 6

Implementation of Selected Scenarios

A COCE based SU demonstrator is presented in this chapter for proof-of-concept of some selected scenarios. The overall chapter is divided into two sections. Section 6.1 explains implementation details and the experimental setup while section 6.2 discusses experimental results of the SU in coexistence of IEEE 802.11g WLAN, IEEE 802.15.1 BT and nanoNET based PU systems.

6.1 Implementation

An HDR based CC2500 transceiver and a MSP430 microcontroller from Texas Instruments (TI) are employed to implement the SU testbed. SDR based systems are still in their research phase and almost all existing automation systems are implemented using HDR based platforms. Therefore, instead of choosing a modern SDR platform, which is often preferred to realize proof-of-concept demonstrators in CR research, a traditional HDR based platform is chosen to demonstrate the suitability of the proposed cognitive strategies with platforms that are still dominant in real world applications.

A master-slave setup (see Fig. 6.1) using cyclic round-trip communication is realized. All cognitive tasks are implemented in the SU master device as illustrated by flow graphs shown in Fig. 6.3. The main features of the SU demonstrator are summarized in Table 6.1.

The master node senses the spectrum, measures the QoS, and decides about necessary tuning. It controls tuning of the slave node via special control packets. The slave acknowledges after executing the tuning command of the master. Eventually, the master tunes its own parameters to the new values.

Transmitted data packets of the master node with fixed size and contents are always echoed back by the slave node. The master node calculates the QoS from this round-trip communication in terms of BER and PLR.

6.1.1 Experimental setup

The SU master and slave nodes are placed 6 m apart from each other with non-line-of-sight as shown by the constellation of the experimental setup in Fig. 6.1. An IEEE 802.15.1 based frequency hopping SDR system named SDR-BT, a nanoNET system and three IEEE 802.11g based WLAN APs are used as PU

systems as briefly described in table 6.2. The WLAN APs are installed at different locations and are operating at channel no. 1, 6 and 11. The AP at channel 1 is closest to the SU and is also the busiest one and hence is the worst interferer among all three WLAN networks. The cyclic nanoNET and the BT-SDR systems are manually turned on and off at random times.

Table 6.1: *Main features of the SU Testbed*

Platform	CC2500 TRX + MSP430 µC	
Spectrum sensing	RSSI	
Sample time (RSSI read time)	~ 100 µs	
Frequency switching time	~ 90 µs	
Operating band	2.4 GHz ISM band	
Bandwidth	812 kHz	
Total no. of channels*	**Data transmission**	70 channels are used for data transmission with $f_c = 2405 + k$ in MHz; where $k = 1,2,3,…,70$
	Spectrum sensing	407 channels are used for spectrum sensing with $f_c = 2400 + channel\_spacing \times k$ in MHz; where $channel\_spacing = 200$ kHz, $k = 1,2,3,…,400$
TX power	0 dBm	
Modulation	MSK	
Bitrate	500 kbps	
Traffic type	Cyclic	
CRC	CRC-16	
QoS	BER, PLR	

Table 6.2: *PU systems used to create the experimental coexisting environment. See Appendix B for a detailed description of these radio systems.*

WLAN	Several IEEE 802.11 based networks are active in channel numbers 1, 6 and 11. Fig. 6.2 presents a snapshot of WLAN activity in the experimental area captured at the location of the SU master device. It is worth noting that the WLAN network in CH1 is the worst interferer for the SU system because it is the closest to SU transceivers as well as the busiest system. The farthest and the least busy, hence the weakest interferer among all three is the one active in CH6.
SDR-BT	A USRP2 based SDR is used to employ an adaptive hopping system as described by IEEE 802.15.1 standard. It blacklists active WLAN channels. However, this system significantly differs from the standard BT system in terms of length of a single time slot. Because of a slow host PC, the SDR-BT transmits for ~20 ms at each hop frequency instead of traditional 625 μs time slot based 1-slot, 3-slot and 5-slot packets. Only one transmitter of this system is used.
NanoNET	A nanoNET master-slave pair is used. The master device transmits cyclically. Each transmission is echoed back by the nanoNET slave device.
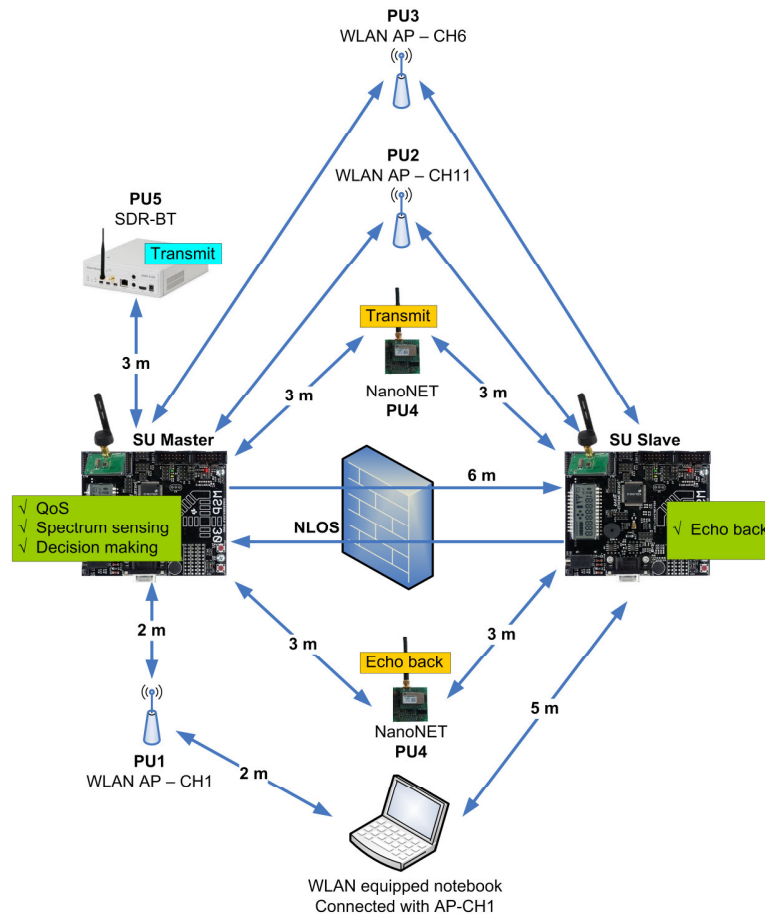
Figure 6.1: *Node constellation of the experimental setup. In fact there are more WLAN APs operating in three specified channels as listed in Fig. 6.2. However, this picture only depicts the position of the closest, hence the most influential AP in each active channel.*

SSID	C...	Speed	Type	SNR	Signal+	Noise-	First Seen	Last Seen
eduroam	1	54 Mbps	AP	26	-66	-100	12:59:33	13:03:13
S(kim)	1	54 Mbps	AP		-66	-100	12:59:27	13:03:09
	1	54 Mbps	AP		-68	-100	12:59:27	13:03:12
S(kim)_Hotspot	1	54 Mbps	AP	30	-66	-100	12:59:19	13:03:13
dlink	1	54 Mbps	AP	60	-34	-100	12:59:18	13:03:13
S(kim)	1	54 Mbps	AP	48	-48	-100	12:59:18	13:03:13
	1	54 Mbps	AP	48	-50	-100	12:59:18	13:03:13
eduroam	1	54 Mbps	AP	40	-50	-100	12:59:17	13:03:13
S(kim)_Hotspot	1	54 Mbps	AP	42	-52	-100	12:59:17	13:03:13
	6	54 Mbps	AP	24	-70	-100	12:59:17	13:03:13
S(kim)_Hotspot	6	54 Mbps	AP	26	-72	-100	12:59:17	13:03:13
eduroam	6	54 Mbps	AP	28	-70	-100	12:59:17	13:03:13
ISIIntern	6	48 Mbps	AP	26	-70	-100	12:59:17	13:03:13
S(kim)	6	54 Mbps	AP	24	-70	-100	12:59:17	13:03:13
S(kim)_Hotspot	11	54 Mbps	AP	54	-46	-100	12:59:17	13:03:13
eduroam	11	54 Mbps	AP	56	-44	-100	12:59:17	13:03:13
S(kim)	11	54 Mbps	AP	54	-46	-100	12:59:17	13:03:13

Figure 6.2: *WLAN activity in the experimental area.*

Figure 6.3: *Flow graph of the proof-of-concept SU demonstrator.*

6.1.2   Opportunistic Spectrum Access Algorithms

The SU calculates its QoS after each transmission and compares this QoS with a predefined threshold value periodically after every N^{QoS} transmissions. It initiates the sensing and decision making process whenever the measured QoS is worse than the threshold value. Intelligent hole detection (IHD), first free (FF) and Markov model (MM) based methods are used for decision making. Where, FF, MM2 and MM4 TYPE-I based OSA algorithms, presented in section 5.1.2 are incorporated with suitable amendments needed for real-time implementation as described in the following:

6.1.3   First Free

Starting from the first channel, the RSSI reading for a channel is acquired and averaged over a time T_{AVG}, and this process is performed for all channels in a sequential order until a channel (first free channel) is found that has an average RSSI value smaller than a predefined threshold value $THRESHOLD^{\text{RSSI}}$. If such a channel is not found in one scan then the entire process is repeated until a free channel is found.

6.1.4   MM2, MM4 TYPE-I

The Markov model parameters, $\pi = \{P(i)\}$, and $A = \{a_{ij}\}$ of the PU systems, are computed using the bandwidth independent parameter estimation method (BIPE) presented by the flow graph in Fig. 5.8. The SU first attempts to find a channel for its transmission with $P_{\text{ON}} < THRESHOLD^{\text{ON}}$, if such a channel is not found then the channel with $\max(\hat{d}_0 - \hat{d}_1)$ is chosen.
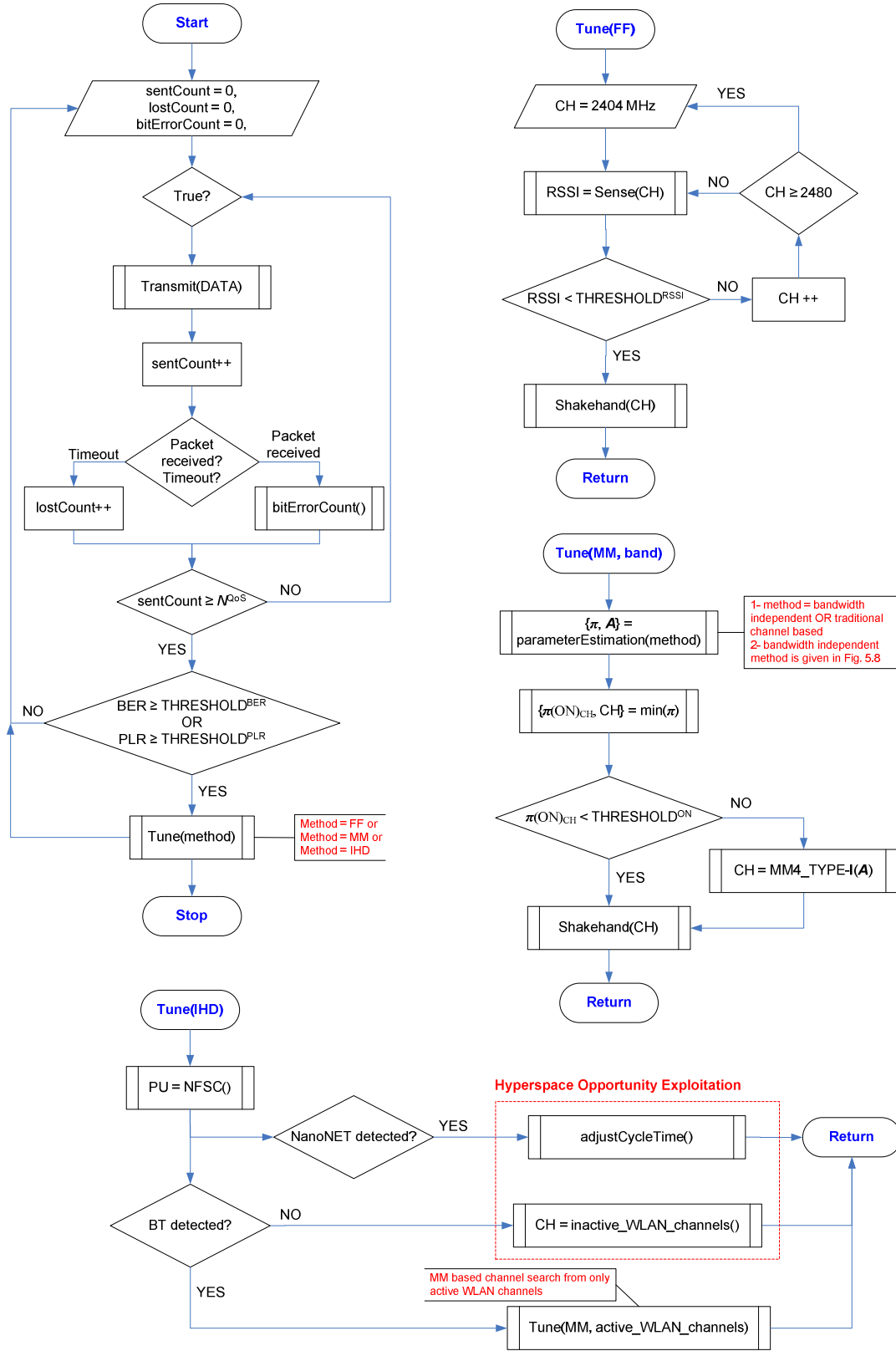
Furthermore, Markov model parameters are estimated using either the traditional multi-channel approach or the multi-PU approach presented in chapter 5.

6.1.5   Intelligent Hole Detection

As already discussed in chapter 3, the IHD method classifies coexisting systems and uses the existing knowledge of features of the detected PU systems to explore hyperspace opportunities. Its performance depends on reliable classification and the extent of reconfigurability of the underlying SU radio platform. The CC2500 transceiver does not offer much reconfigurability and only operating frequency, transmission time and transmission power can be reconfigured by the cognitive engine. In order to demonstrate the significance of classification based cognitive decision making using this limited reconfigurability, the selected PU systems are accommodated using methods explained in the following:

SDR-BT: The SU system knows the blacklisting feature of the SDR-BT system. The narrowband sensor of the SU system cannot detect all hops of the SDR-BT system. However, based on its prior knowledge it assumes that all inactive WLAN channels are being used by the hopping system whenever even a single

SDR-BR hop is detected. Furthermore, on the basis of prior experimentation (presented later in Fig. 6.7) it is known to the cognitive engine that the SDR-BT system is a worse interferer to the SU than the boundary areas (see Fig. 6.6) of the WLAN system no matter what is the strength of WLAN interference at the SU antenna. Where, the strength of the WLAN interference depends on the traffic load of the WLAN network and distance of WLAN nodes form the SU antenna. Hence, in the presence of an SDR-BT system, transmitting at the boundary of an active WLAN channel is a safer option for the SU system.

WLAN:

- If SDR-BT is not active then an inactive WLAN channel is selected.
- If SDR-BT is active then the cognitive engine uses MM2/MM4 method to find the least active WLAN channel. Based on prior experiments (presented later in Fig. 6.6) it is known to the SU that choosing a channel at the boundary of an active WLAN channel offers much weaker interference than at closer to that channel's center frequency (see Fig. 6.7b and related discussion). Where, precise interpretation of center and boundary of a 22 MHz IEEE 802.11g channel is given in Fig. 6.6. Thanks to the signal classification, it is possible for the SU to identify center and boundary areas of a PU system. Eventually, the cognitive engine chooses a channel at the boundary of the WLAN channel selected by MM2/MM4 based method.
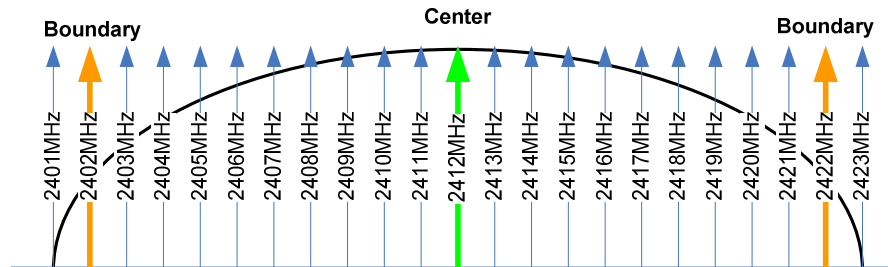
Figure 6.4: *Interpretation of center and boundary of a 22 MHz IEEE 802.11g channel.*

NanoNET: It covers the entire ISM band and virtually leaves no free spectral space. Consequently, traditional predictive and non-predictive OSA methods fail to find a safe channel. A method named *cycle time configuration*, proposed in [AHM10], is used to locate opportunities in time domain to accommodate the SU system. It is explained in the following paragraphs.

Most of the communication in industrial automation systems works cyclically where fixed small data packets are exchanged after a predefined fixed time interval called the *cycle time*. There is some *white space* between the start of the next packet transmission and the completion of the previous transmission which can be used as temporal gap by the SU. However, the length of this useful white space can be variable and is calculated as follows (see Fig. 6.4):

white_space = cycle_time - max_packet_delay - packet_size

Where max_packet_delay depends on the following:

- Max. number of retransmissions

- Response time of the transceiver

The CR system knows a-priori that the nanoNET based PU system is a cyclic system; however the cycle time is not known. Whenever, the CR detects a nanoNET system it attempts to reconfigure its own cycle time to exploit the available temporal gaps as explained in the following.
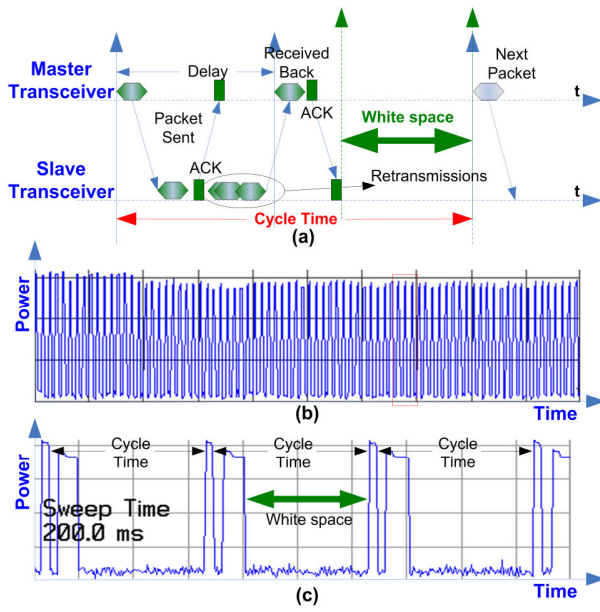
Figure 6.5: *a) Depiction of cyclic transmission. b) 4 seconds transmission trace of a cyclic master-slave system measured by a spectrum analyzer in zero-span mode. The cycle time is 50 ms. c) Enlarged view of consecutive packets.*
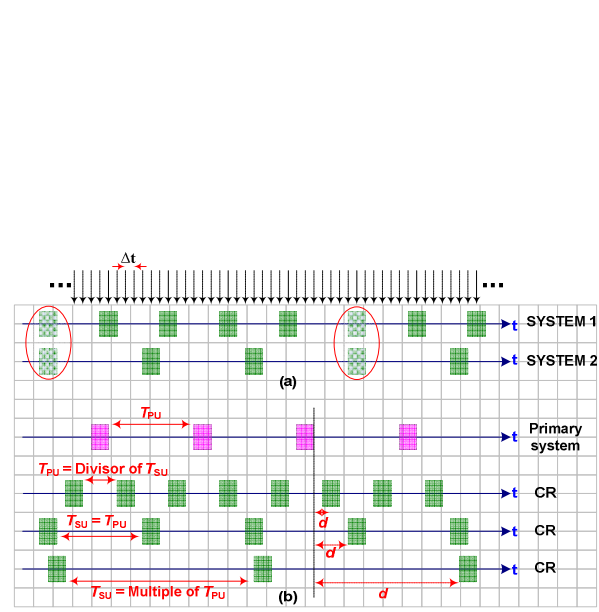
Figure 6.6: *Cycle time configuration. a) Appearance of collisions; b) collision avoidance*

The idea is to detect the cycle time T_{PU} of the PU and choose the cycle time T_{SU} of the secondary CR user as follows:

$$T_{SU} = \begin{cases} T_{PU} & \text{or} \\ \text{an integer multiple or divisor of } T_{PU} \end{cases}$$

Once T_{SU} is selected the CR can slide its transmission by inserting and controlling a delay d to provide an optimal synchronization between the CR and the coexisting system as illustrated by Fig. 6.5.

6.2 Results

In the absence of any PU system, the SU system sees a 'coexistence free channel'. The QoS achieved in such a coexistence free channel is considered optimal. The optimal QoS of the CC2500 TRX is $BER \sim 10^{-3}$ and $PLR \sim 10^{-3}$ measured at 6 m transmitter-receiver separation with NLOS in same experimental vicinity where all experiments reported in this section are done. Moreover, coexistence optimization in the context of these experiments means to find an *optimal channel* for the SU radio system with an aim to achieve QoS better than a predefined threshold QoS. Table 6.3 lists different threshold values used in experiments.

Description of experimental results is divided into three subsections as listed in Table 6.4. Section 6.2.1 presents QoS of the SU platform in coexistence of selected interferers without any coexistence management. These results are used as reference in later sections to compare improvement in QoS of the SU system caused by various OSA approaches. Section 6.2.2 evaluates the performance of different predictive modeling based OSA approaches and section 6.2.3 compares the performance of IHD and DHD based OSA approaches.

Table 6.3: *Different threshold values set in the SU testbed*

Threshold	Selected value
$THRESHOLD^{RSSI}$	-80 dBm
N^{QoS}	50 packets
$THRESHOLD^{ON}$	0.1
$THRESHOLD^{BER}$, $THRESHOLD^{PLR}$	1%, 2%
$THRESHOLD^{SM}$	0.5

Table 6.4: *Summary of section 6.2*

| 1	Reference measurements	No coexistence management is used by the SU system	Section 6.2.1
2	Performance analysis of predictive modeling based OSA	Traditional reactive/proactive OSA approach (FF) vs Multi-channel predictive modelling based OSA	Section 6.2.2.1
		Multi-channel predictive modelling based OSA vs Multi-PU predictive modelling based OSA	Section 6.2.2.2
3	IHD based OSA vs. DHD based OSA		Section 6.2.3

6.2.1   Reference measurements: SU employs no coexistence management strategy

Figure 6.7a plots QoS of the SU system measured when the non-cognitive SU system is operating in the coexistence of exactly one of the selected PU systems. These results are considered reference measurements and explain the impact of each interferer on the performance of the SU system. Both nanoNET and SDR-BT systems are used with fixed transmission power and are placed at fixed distance in the experimental constellation as already shown in Fig. 6.1. PLR of the SU system is recorded 6.4 % and 4.3 % in the presence of nanoNET and SDR-BT interferers respectively. BER is 0.52 % and 0.29 % in the presence of nanoNET and SDR-BT interferers respectively.

Since, there are several WLAN APs operating in the experimental area at different distances from the SU system, different values of RSSI are felt at SU antenna because of different locations of the WLAN APs. Furthermore, traffic load (or duty cycle) of WLAN networks felt by the SU system in different WLAN channels is also highly variable. Because of these reasons, interference strength of the WLAN system is time varying in nature unlike fixed interference strength of nanoNET and SDR-BT systems. Therefore, it is useful to plot SU QoS measurements with all possible values of RSSI and duty cycle of the WLAN system. These measurements are taken by changing the location and traffic load of an AP. The reason to choose the RSSI value instead of the distance of the AP from SU is the fact that it is the RSSI value that defines the strength of interference not the distance. But the RSSI value is not merely varied by the distance but also with the locality of the AP because of different obstacles and channel conditions between the WLAN AP and the SU nodes. Experimental results show that the PLR value is almost proportional to both RSSI and the duty cycle of the WLAN system. As long as RSSI < -50 dBm and duty cycle < 80 % the WLAN system offers less interference than both SDR-BT and nanoNET systems. The highest value of PLR is almost ~13 % at maximum observed RSSI and duty cycle. On the other hand BER remains between 0.5 % - 1.8 % except for lower values of RSSI. For RSSI < -60 dBm, the value of BER remains well below 0.5 %.

Furthermore, the observed value of PLR at the boundary of an active WLAN channel is approximately 4 times less than at the center of that channel as shown by Fig. 6.7b. The value of BER at the boundary of an active WLAN channel is approximately 2-3 times less than at the center of that channel particularly in high BER scenarios i.e. when the values of RSSI and/or duty cycle are high. In order to generalize this observation to use later during coexistence optimization using IHD it is concluded that the QoS of the SU system operating at the boundary of a WLAN channel is always better than the QoS achieved while operating in a channel occupied by the SDR-BT system.

These reference measurements and related observations are stored in the radio knowledge base of the IHD based SU. Using these measurements, the cognitive engine can estimate the expected QoS at different spectral areas in a given coexistence scenario if the PU systems are correctly classified.
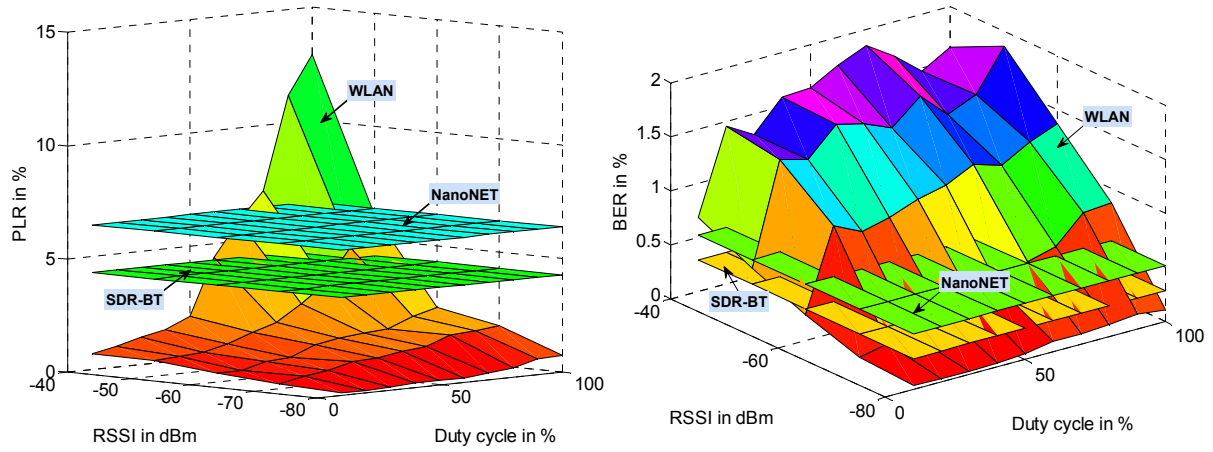
(a) *Reference QoS measurements of the SU system in the presence of selected interferers. The names of interferers are specified on respective plots. NanoNET and SDR-BT systems operate with fixed transmission power at fixed distances as specified in Fig. 6.1, therefore, the axis corresponding to RSSI and duty cycle are only meaningful for measurements with WLAN as an interferer.*

<u>Note:</u> *PLR in % and BER in % are QoS parameters of the SU system. RSSI in dBm and Duty cycle in % are features of the PU system.*
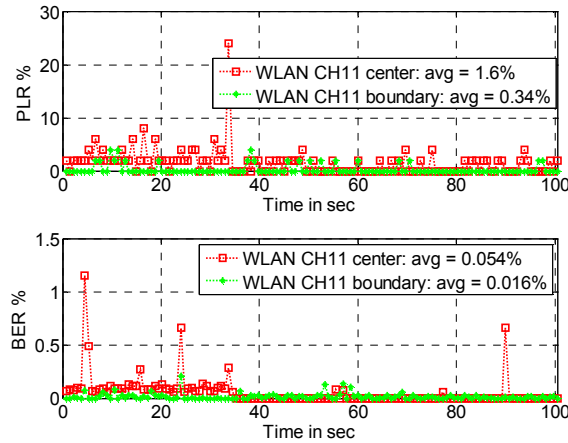
(b): *Comparison of the SU system at center and boundary areas of an active WLAN channel (CH11).*

Figure 6.7: *Reference QoS measurements of the SU system in the presence of selected interferers.*

6.2.2   Performance analysis of predictive modeling based OSA

6.2.3   FF vs multi-channel MM

Experimental results using FF and multi-channel MM based SU testbeds in coexistence of WLAN and SDR-BT systems are presented in Fig. 6.8. For each OSA method four different parameters are plotted for two different averaging/training time values. First of these parameters is a binary variable that marks the discrete points of time when spectrum sensing and decision making is performed to find a new channel. It describes how frequently the SU system has to spend its resources for channel selection. Second parameter is the channel number used for next N^{QoS} transmissions. Last two parameters describe the rate of data loss.

(a) *Performance trace of the FF based SU*

(b) *Performance trace of the Multi-channel MM based SU*
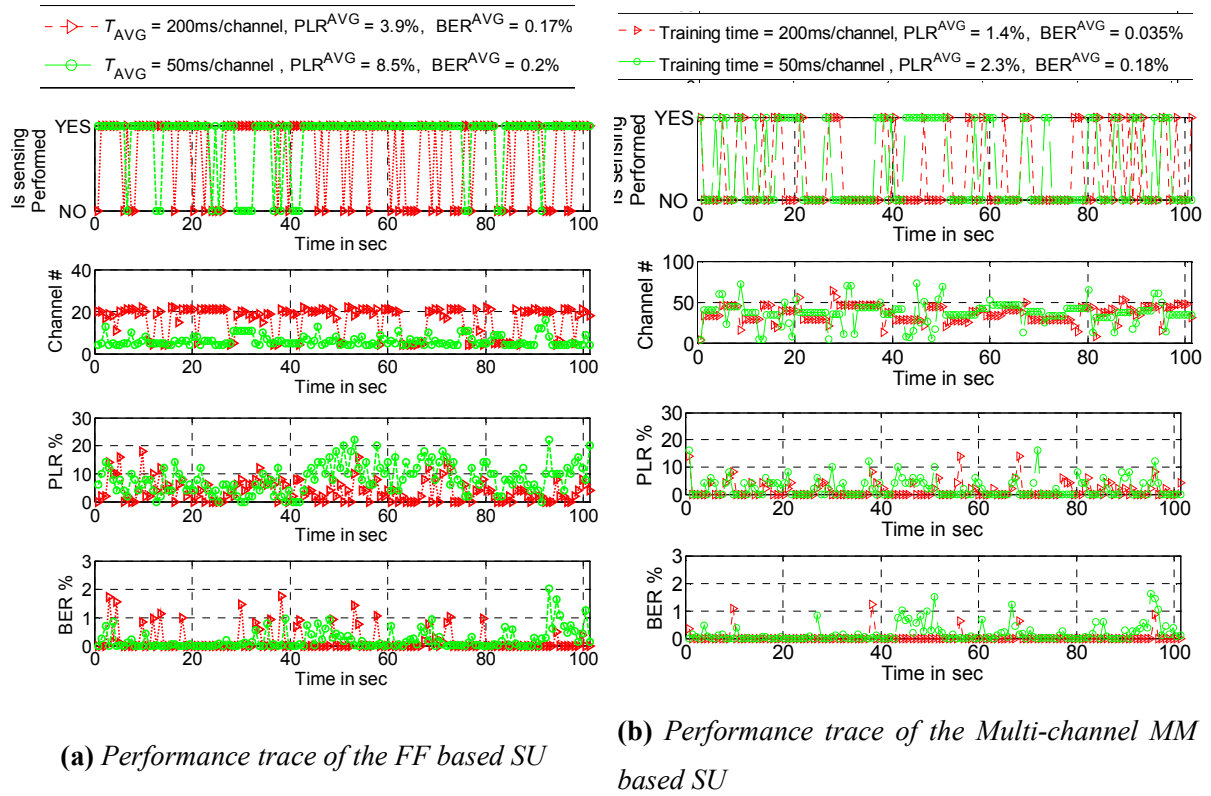
Figure 6.8: *FF vs Multi-channel MM.*

The SU system always starts operating at first channel (f_c = 2.406 GHz) which overlaps the first channel of the WLAN based PU. Hence, it immediately suffers severe interference and starts searching for a safer channel. It can be seen from results presented in Fig. 6.8a that the channel selected by the FF method is not always optimal and consequently the SU system often suffers high performance degradation. In fact

6th channel of the WLAN system is the least used part of the spectrum but the FF based CR system never continues its search till that part of the spectrum as shown by the spectral traces of the coexistence environment in Fig. 6.9. It always chooses a channel that overlaps either with the first channel of the WLAN system or with SDR-BT hops. Even averaging over longer time does not always guarantee that an optimal channel is selected. For instance, with T_{AVG} = 50 ms (500 samples), the CR system mostly chooses a channel overlapping with first channel of the WLAN system which offers very strong interference. The average values of PLR and BER are 8.47 % and 0.21 % respectively in this case. Furthermore, it can be noticed by comparing top two plots of Fig. 6.8a that many times the spectrum sensing process proves to be a useless practice because the SU kept operating in the same channel rather to find a better one.

On the other hand, with T_{AVG} = 200 ms (2000 samples), the CR system mostly chooses a channel that is actually occupied by the hopping SDR-BT system. It generates slightly better results with PLR^{AVG} = 3.91 % and BER^{AVG} = 0.16 %, but still fails to find the optimal solution. It proves the fact that even high averaging time does not guarantee an optimal solution in traditional FF type OSA approaches.

Although, further increasing the averaging time may leads the SU system to an optimal solution yet it depends on the transmission pattern of the PU system. For instance, bursty nature of the WLAN traffic may contain very long inactive periods between successive data transmissions and sensing the channel during that inactive period even for very long time may fail to detect the PU system. However, despite these long inactive periods, such PU systems can still offer considerable interference to the coexisting system.

On the other hand, the multi-channel MM based approach is almost always able to choose the optimal channel if it exists or the best channel otherwise. However, the performance of this approach also highly depends on the training time. With larger values of the training time the SU achieves better estimation of the model parameters resulting in better decision making. For instance, with a training time of 200 ms/channel, the SU system achieves PLR^{AVG} = 1.4 % and BER^{AVG} = 0.035 % and needs less frequent channel switching in comparison to 50 ms training time that achieves PLR^{AVG} = 2.3 % and BER^{AVG} = 0.18 % with more frequent channel selection as shown in Fig. 6.8b. The spectral trace of the coexisting environment when the multi-channel MM based SU is operating is plotted in Fig. 6.9.
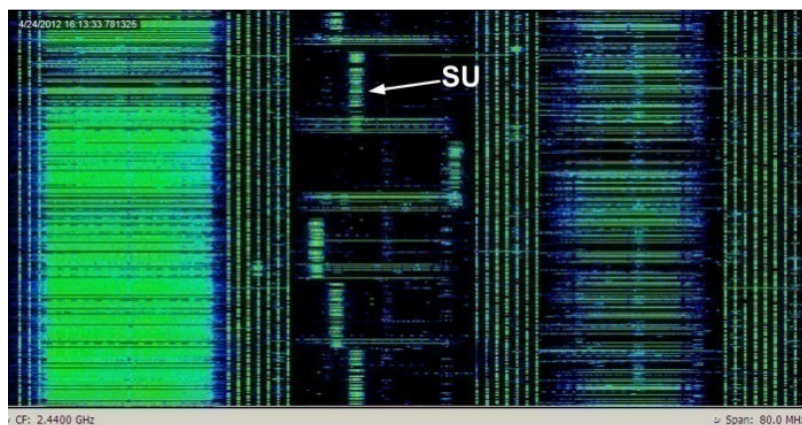
Figure 6.9: *The multi-channel MM based SU operates in the coexisting environment using training time = 200ms/channel.*

6.2.4   Multi-channel MM vs Multi-PU MM

Performance trace of multi-PU MM based SU is presented in Fig. 6.10 for two different training times.
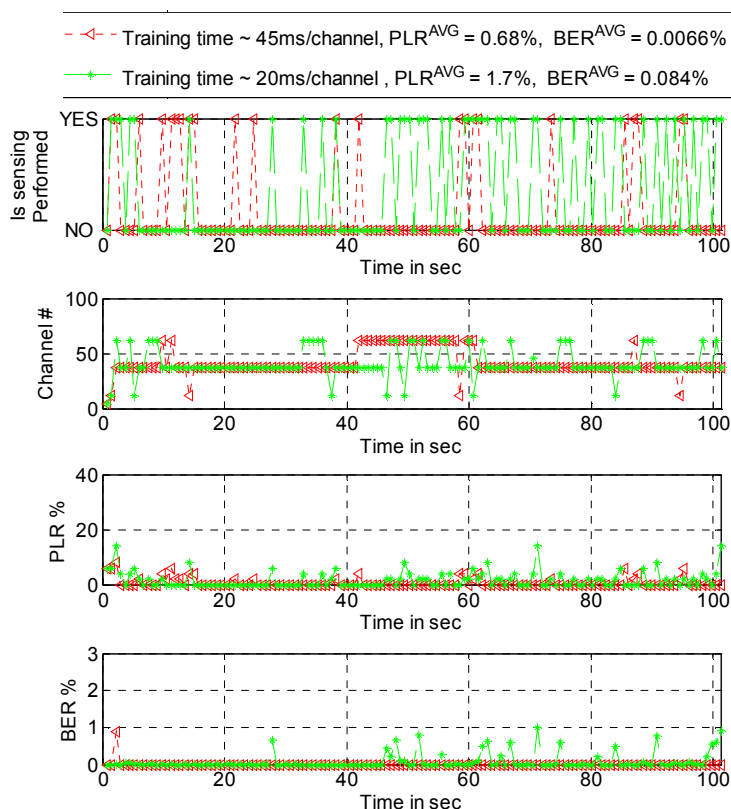

Figure 6.10: *Performance trace of multi-PU MM.*

It is worth noting that multi-PU uses identification of PU systems to compute MM model parameters. Hence, parameters are computed only at center frequencies of detected PU systems unlike multi-channel MM approach that compute parameters for all 70 channels. The coexistence environment being discussed in section 6.2.2 only consists of three WLAN instances (WLAN$_{CH1}$, WLAN$_{CH6}$, WLAN$_{CH11}$) and SDR-BT as already mentioned in the beginning of this section. Eventually, model parameters are only computed at center frequencies of three active WLAN channels. SDR-BT is stronger interferer than WLAN system in most cases (except for very strong WLAN signals) therefore the SU system never attempts to transmit in a channel that is occupied by it. Eventually, the SU system always chooses one of three active WLAN channels as can be seen in channel # plot in Fig. 6.10.

The SU system achieves PLR = 1.7%, BER = 0.084 and PLR = 0.68%, BER ~ 10^{-3} for 20ms and 45ms training times respectively, which is better than the QoS of multi-channel MM based SU presented in section 6.2.2.1. Because of better decision making for channel selection, channel switching is also performed less often than multi-channel MM based approach as shown in top two plots of Fig. 6.10.

Coexistence of the SU system using FF and MM based OSA approaches in the presence of the nanoNET PU is not included here because all channels are equally occupied by the nanoNET system and these methods always struggle to find an optimal channel. Coexistence of the SU system with nanoNET PU will be further discussed in section 6.2.3.

6.2.5   Intelligent Hole Detection vs. Dumb Hole Detection

The opportunistic operation of the IHD based SU relies on the classification information provided by the NFSC and the information stored in the radio knowledge base about the transmission characteristics of the PU systems extracted from documented standards. Furthermore, the reference measurements presented in Fig. 6.7 are also stored in the radio knowledge base which helps the cognitive engine to estimate the expected level of interference in different channels in a given coexistence scenario. It is further strengthened by multi-PU MM based OSA. On the other hand DHD approach could only employ either FF or multi-channel MM and the better of these is selected. Table 6.5 lists down constituents of IHD and DHD based approaches.

Coexisting environment: The coexisting environment used for measurements in this section includes three WLAN networks, one SDR-BT transmitter and a nanoNET master-slave system (see Fig. 6.1).

Since spectral projection and classification provide foundation of the IHD method, results of these two processes are presented in the next subsection. Coexistence performance of IHD and DHD methods will be discussed afterwards.

Table 6.5: *Constituents of IHD and DHD based OSA approaches*

IHD	DHD
Identification of PU systems	Multi-channel MM
Multi-PU MM	
Cycle time detection	
Knowledge of reference measurements	

Spectral projection and classification: Fig. 6.11 presents a swept spectrogram and the corresponding selective projected spectrogram generated by the SU system using a window size of 1 sec. The NFSC score of the SU testbed for all PU systems for three possible scenarios is plotted in Fig. 6.12. Note that classification is first done using MaxHold operation as described in chapter 4 and the selective spectral projection method is only performed for active WLAN channels, which significantly reduces the computational complexity. Selective spectral projection is not performed for nanoNET and SDR-BT systems because the MM based approach is never used for these two PU systems.
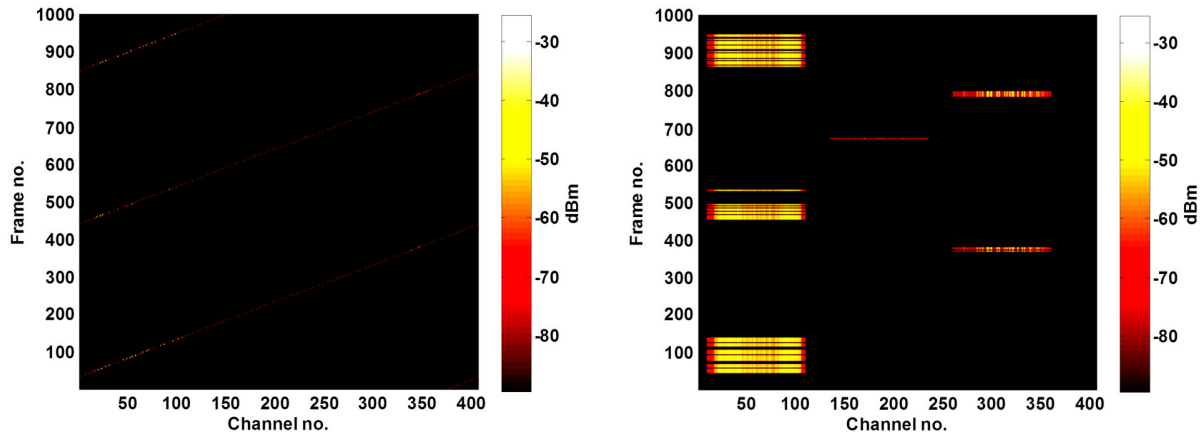
Figure 6.11: *Swept spectrogram (left plot) and the selective projected spectrogram (right plot). Projection is performed only for active WLAN channels. Where active WLAN channels are found using MaxHold based NFSC. Window size = 1 sec, however, only 100 ms fraction of the complete spectrogram is displayed.*

Fig. 6.12a plots the SM score when WLAN and SDR-BT PU systems are operating simultaneously. The SU system generates reasonably prominent scores for the SDR-BT signals although there are also some false alarms for the SDR-BT system in the presence of the wider IEEE 802.11 based signals. A false

alarm for the SDR-BT system will force the cognitive engine to choose a WLAN boundary channel although a completely free spectral area is present. These false alarms can be reduced by choosing a higher *THRESHOLD*^{SM} but it will obviously increase the probability of miss detection for the SDR-BT system. However, as discussed earlier failing to choose the completely free channel because of a false alarm is less costly than choosing a channel that is actually occupied by the SDR-BT system because of a miss detection. On the other hand, channels of the IEEE 802.11g based PU overlap each other therefore, the SM score for the neighboring channels of a truly active channel is also very high but surly smaller than the truly active channel. For instance, in Fig. 6.12a channel 2 is not active but its SM score is higher than the other inactive channels. It is assumed during these experiments that WLAN systems are never active in adjacent channels which, is mostly true in real-time environments. Therefore, local maximum value of the SM score is computed to find the truly active WLAN channel whenever multiple adjacent channels generate scores higher than *THRESHOLD*^{SM}. The nanoNET PU system can be clearly distinguished as inactive in this scenario even though more or less the entire 80 MHz band is occupied by WLAN and SDR-BT systems.

Fig. 6.12b plots the SM score of a scenario when only IEEE 802.11 based PU is active. Once again there are few false alarms for the SDR-BT system. The IEEE 802.11 PU system is correctly identified whereas the nanoNET system is also clearly identified as inactive.

Fig. 6.12c plots the SM score for scenario when all three PU systems are active simultaneously. Very prominent SM scores are generated for the SDR-BT system at the boundary areas of the ISM band because the wider nanoNET system is very weak at these points. However, in other spectral areas the SDR-BT signals are somewhat buried under the nanoNET signal and the resulting SM score is not very prominent but still mostly above the threshold value. The IEEE 802.11 based signals are still distinguishable although the SM score corresponding to the inactive WLAN signals is slightly raised because of the wider nanoNET signals. Finally, the truly active nanoNET system is always clearly detected.
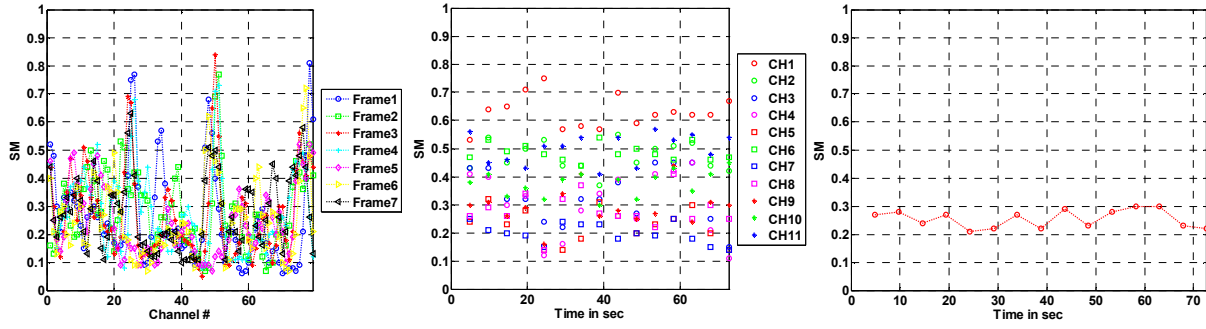
(a) *SDR-BT is also active, IEEE 802.11 is active in CH1, CH6 and CH11, NanoNET is inactive*
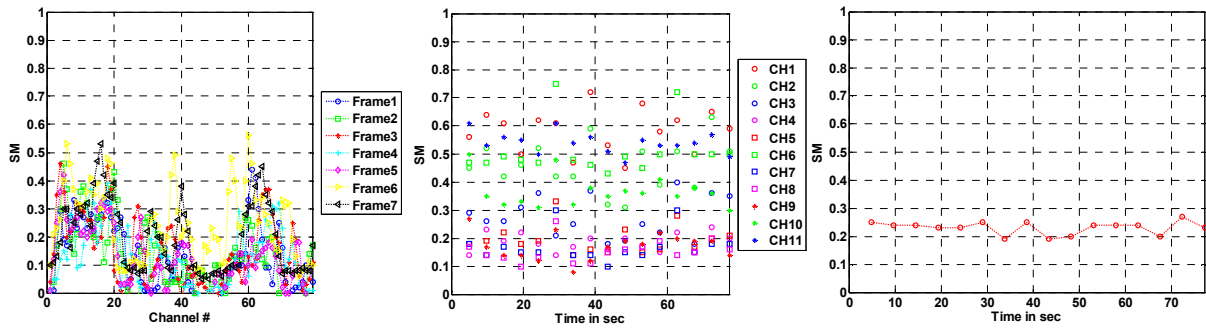
(b) *Only IEEE 802.11 is active in CH1, CH6 and CH11, SDR-BT and NanoNET are inactive*
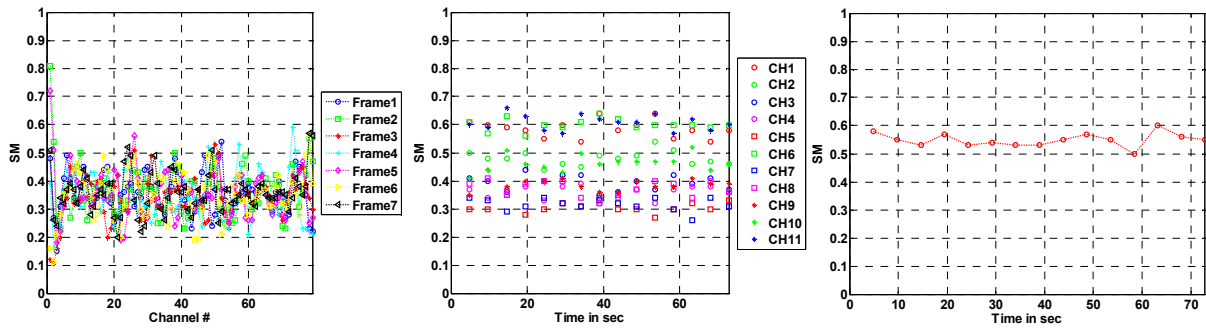
(c) *SDR-BT is active, IEEE 802.11 is active in CH1, CH6 and CH11, NanoNET is active*

Figure 6.12: *The SM score generated by the SU demonstrator for three different scenarios. Note that the SM score of the SDR-BT system is only plotted for 7 selected frames instead of plotting against time like other two PU systems because plotting all 79 channels in a single graph makes it impossible to understand the plot.*
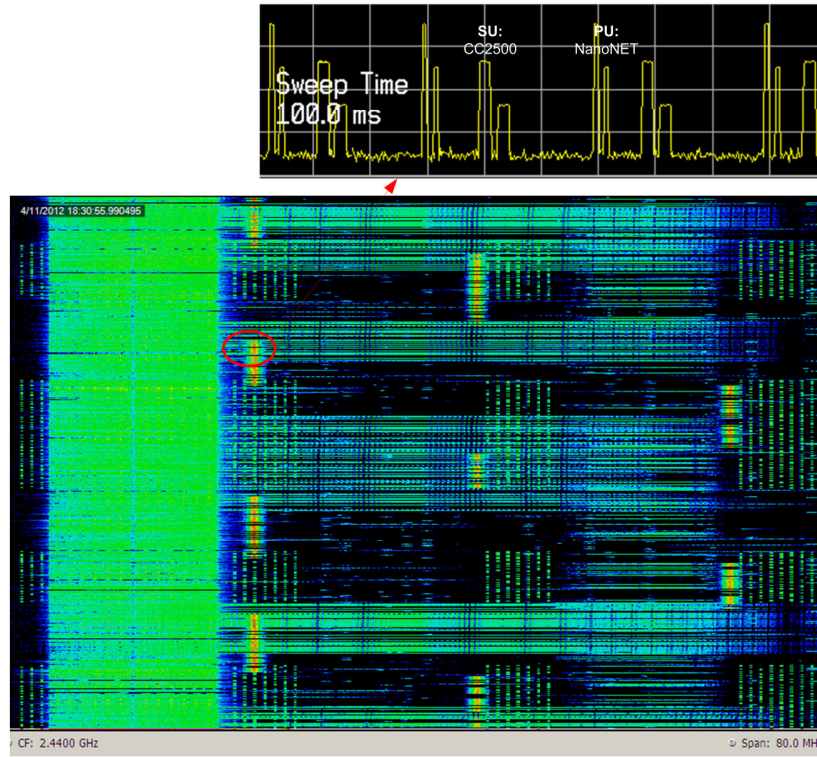
Figure 6.13: *5 minutes long spectral trace of 80 MHz wide 2.4 GHz ISM band taken by a real-time spectral analyzer. The IHD based SU operates in the coexisting environment where WLAN, SDR-BT and nanoNET systems are operating. Because of very low resolution in time domain cyclic activity is not visible. The smaller plot taken in zero span mode shows how SU is accommodated using cycle-time exploitation method whenever it has to coexist with the nanoNET system.*

Performance analysis: Spectral trace of working of the IHD based SU in coexistence of all three PU systems is shown in Fig. 6.13. It can be seen in this spectral trace that the SU switches to only some selected channels. If an SDR-BT system is not detected then the SU transmits at $f_c = 2.424$ GHz which is a completely free channel in this case. However, if the SDR-BT system is detected then the SU uses multi-PU approach to find the least used but active WLAN channel. Once the least used channel is found the SU opts to transmit on the boundary channel of the selected WLAN channel. It can be seen from the spectral trace that either a boundary channel of $WLAN_{CH6}$ or of $WLAN_{CH11}$ is mostly selected. It is also worth noting that the WLAN system at CH6 is not very active and the signal is also too weak to be always detected. Whenever a WLAN system at CH6 is not detected the cognitive engine assumes that it is also occupied by the SDR-BT system because it is known to the cognitive engine that only active WLAN channels are skipped by the hopping system. Hence, a miss detection of the WLAN PU leads to the

selection of a channel that may not be optimal because in fact $WLAN_{CH6}$ is the least active channel and is also not occupied by the hooping system as can be seen from the spectral trace. A solution is to lower down the threshold values of the NFSC to decrease the probability of miss detection but obviously at the expense of increased false alarms. However, the cost that has to be paid in the case of a miss detection is smaller than the cost in case of a false alarm. It is because transmitting at the boundary of even a very active WLAN channel offers less interference than the SDR-BT system as it is already known from the reference measurements. Hence, failing to choose the boundary of the least active channel is better than falsely detecting a WLAN system where actually the hopping system is operating.

Fig. 6.14 presents results of the IHD based SU in left hand side plots and DHD based SU in right hand side plots. During these experiments nanoNET and SDR-BT based PU systems are switched ON and OFF randomly while the SU is running. Fig. 6.14a presents classification trace of the coexistence environment generated by the SU system. Top most plot in Fig. 6.14b presents the decision method used to choose the channel at any discrete time, middle plot in Fig. 6.14b presents the selected channel. Fig. 6.14c plots estimated values of three Markov model parameters. Once again it is stressed that in case of IHD, the MM method is only used to find the least used WLAN channel when an SDR-BT based PU is active. Therefore, MM parameter values are only plotted at times when SDR-BT is marked active in Fig. 6.14a. Left hand side plot of Fig. 6.14c presents the MM parameters for all active WLAN channels. On the other hand, in right hand side plot of Fig. 6.14c, the MM parameters of only selected SU channel are plotted. Fig. 6.14d presents parameters describing the rate of data loss.

The SU has to find an optimal channel using only MM based approach in right hand side plots and using a combination of MM, radio knowledge and cycle time detection in left hand side plot in Fig. 6.14. In the absence of the nanoNET PU system, the MM based approach always successfully steers the SU systems to an optimal channel as shown by the QoS plotted in right plot in Fig. 6.14d. However, the presence of nanoNET system creates a situation where all channels are apparently equally busy as it covers the entire ISM band and leaves no completely free spectral area. In such situations neither the traditional OSA methods like FF nor the predictive models such as MM can find an optimal channel. In Fig. 6.14 right hand side plots, it can be seen that whenever a nanoNET system is turned ON the SU struggles to find a good channel and keeps on switching to a new channel at each discrete step without any improvement in the QoS. However, the SU equipped with IHD successfully accommodates itself in the current channel by merely adjusting its cycle time whenever a nanoNET PU is active as shown in left hand side plot of Fig. 6.14.
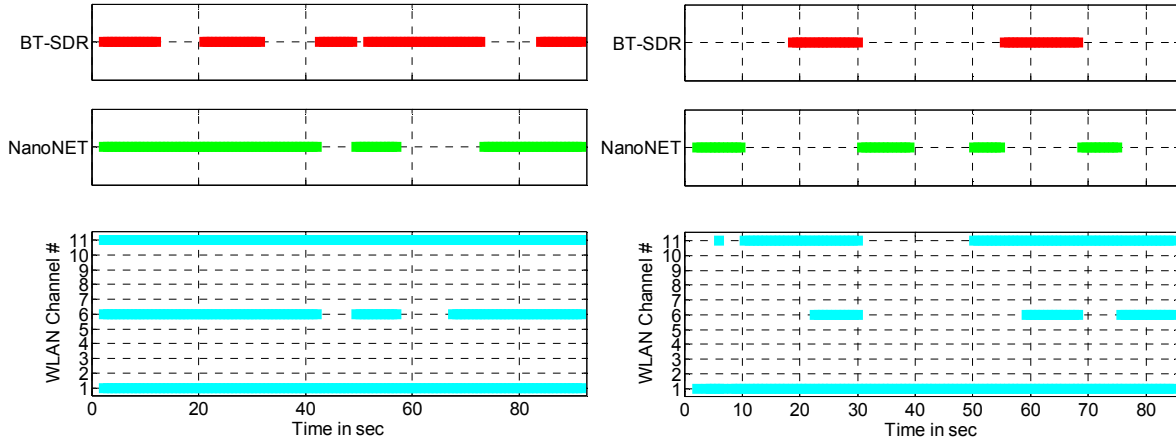
(a) *Detection trace of PU systems*
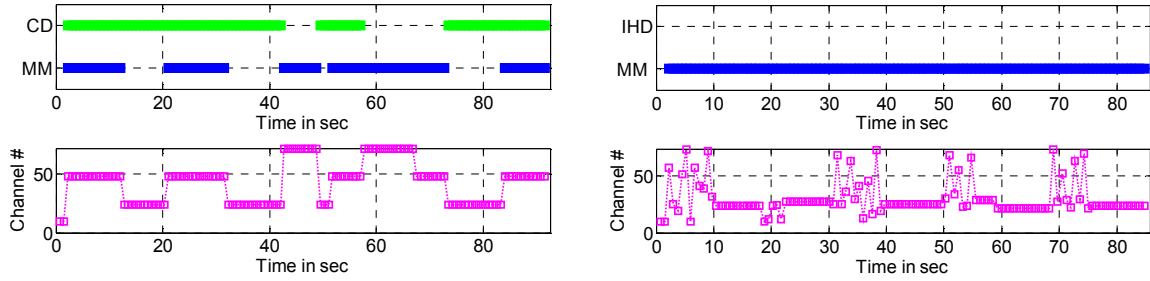
(b) *Decision method, selected channel and total time taken to take the decision (from top to bottom)*
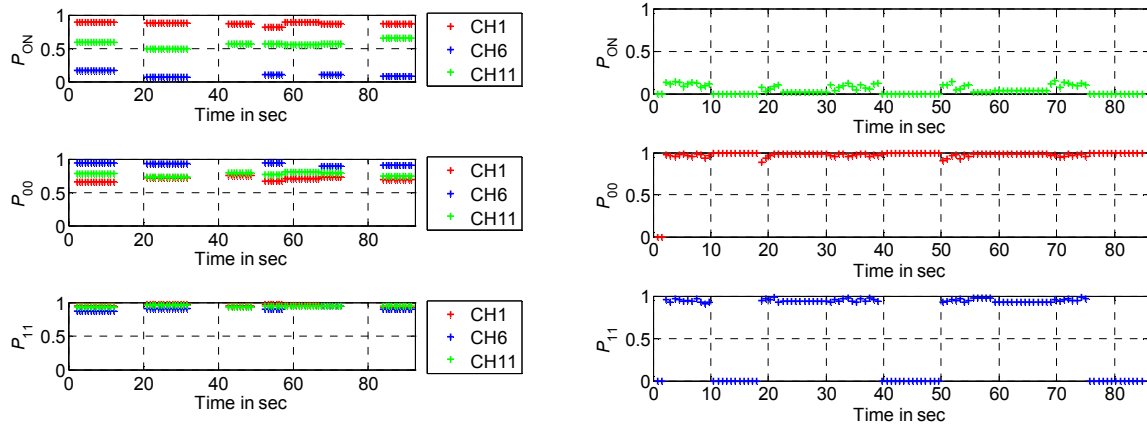
(c) *Estimated MM parameters. Estimated parameters of three active WLAN systems using multi-PU method (left plot), estimated parameters of only the selected channel where estimation is done using traditional multi-channel based parameter estimation method (right plot).*
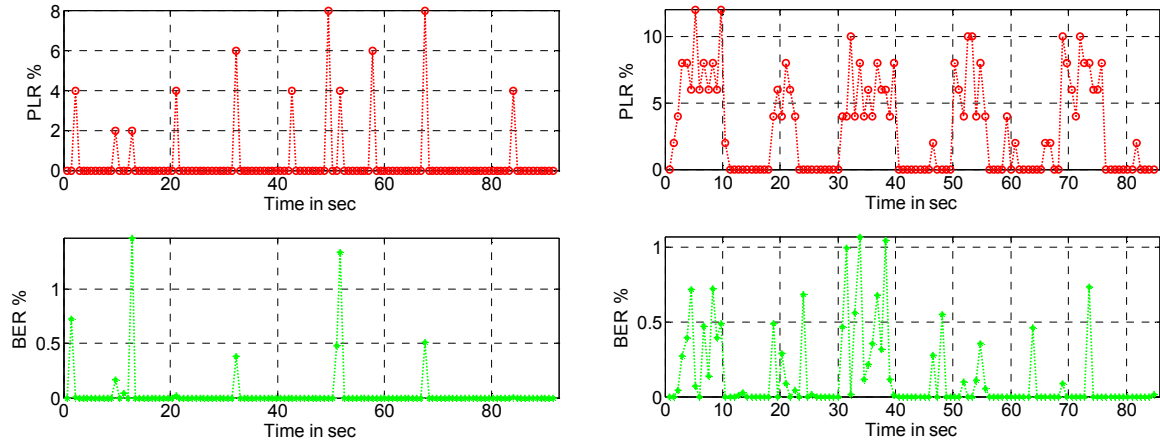
(d) *QoS*

Figure 6.14: *Performance analysis of IHD based SU (left plot) and DHD based SU (right plot). 1 sample ~ 100 us, first channel = 4.*

Note: Note that identity of the coexisting systems presented by the detection trace shown in part 'a' of this figure is only used by IHD for decision making. DHD method does not use this information and it is plotted here only for better understanding of other DHD based results.

6.3 Conclusion

Predictive OSA methods perform better than the traditional non-predictive methods because they always choose the optimal channel if it exists and the best channel otherwise. On the other hand traditional non-predictive approaches often fail to find the optimal/best channel. However, predictive approaches also fail to optimally exploit available hyperspace opportunities because of their inability to learn the complete coexistence behavior of the coexisting radio systems. In contrast to the traditional non-predictive and predictive approaches, the IHD based OSA approach can better plan opportunistic operation of a SU radio system in a coexistence environment where primary systems with diverse radio characteristics are operating.

The proof-of-concept IHD based SU system presented in this chapter uses prior knowledge of two transmission characteristics, i.e. adaptive hopping and cyclic transmission, of primary systems for decision making. Furthermore, it is equipped with reference measurements, which helps the cognitive system to estimate the expected strength of interference at different spectral areas in a given coexistence scenario. The SU system classifies the primary systems and relates all this information in order to optimally tune the SU radio platform. The CC2500 TRX used as SU radio platform is a traditional HDR platform and doesn't offer much flexibility. But the proof-of-concept SU system demonstrates the fact

that the ideas involved in IHD based OSA can be successfully employed even with traditional HDR based rigid platforms. However, more flexible software radio platforms will certainly be able to better exploit the advantages of the IHD based OSA scheme.

Chapter 7

Conclusion and Future Work

7.1 Conclusion

Cognitive radio is being considered as a platform to realize strategies to improve the wireless coexistence. It operates as a secondary user (SU) and opportunistically fits its transmission to spectral holes left by the coexisting primary user (PU) systems. Despite the promising results shown so far, the existing opportunistic spectrum access strategies suffer from some critical limitations. Firstly, proactive and reactive types of spectrum sensing limit the vision of a cognitive radio system making it unable to reliably gauge the activity of primary systems resulting in harmful collisions and unnecessary interruptions in secondary transmissions. Predictive approaches have already been suggested to improve the deficiencies of proactive and reactive spectrum sensing methods but the presence of data loss due to limited sensor bandwidth, and false alarms and miss detections because of difficult environmental conditions makes the modeling task very challenging in real-time environments. Secondly, the existing dumb hole detection (DHD) methods do not provide enough knowledge for optimal cognitive decision making. This thesis work presents cognitive strategies that use documented knowledge of coexisting radio systems to overcome these two limitations.

Neuro-Fuzzy Signal Classifier (NFSC): A common requirement of the proposed cognitive strategies is the classification and extraction of primary systems. A NFSC is presented in chapter 4 that uses bandwidth, operating frequency, pulse shape, hop behavior and time behavior of radio systems as distinct features. It uses fuzzy logic based rules and a neural network based connectionist structure to classify primary radio systems with respect to standard technologies. Furthermore, it disintegrates the amalgamated coexisting environment and extracts distinct radio systems from a given spectrogram without losing any spectral and temporal information of the original signals.

Bandwidth Independent Parameter Estimation: A bandwidth independent parameter estimation method is presented in chapter 5 that enables a cognitive radio system to estimate model parameters accurately in the presence of missing data because of limited sensor bandwidth. This bandwidth independent parameter estimation method enables a multi-PU modeling approach instead of a traditional multi-channel approach. Meanwhile, the PU signals are modeled as Markov processes and estimated

parameters are the duty cycle and transition probabilities of the primary signals. Given an extracted binary stream provided by NFSC along with identification of the corresponding PU system, theoretical value of probability of detection of a primary system is computed. This theoretical value is in turn used to estimate the model parameters using Baum-Welch algorithm and Renewal theory based approaches.

Intelligent Hole Detection (IHD): IHD based opportunistic spectrum access is proposed to overcome the limitations of conventional DHD based opportunistic spectrum access approaches. It suggests radio resource allocation on the basis of a-priori known technologies in order to optimally utilize available opportunities in the multidimensional coexisting environment. Fundamental problems to realize this idea are classification of signals and multi-objective resource allocation to tune the underlying SU radio platform. This thesis work uses the NFSC for the PU classification part and addresses the resource allocation in coexisting environment for some limited scenarios in chapter 6 using a hardware defined radio based platform.

Proof-of-concept: A CC2500 TRX and MSP430 μC based platform is used to implement a testbed that uses bandwidth independent parameter estimation and classification information of radio systems to accommodate itself in the presence of WLAN, SDR-BT and nanoNET based primary systems. An IHD based SU demonstrator clearly outperforms a conventional DHD based demonstrator by successfully finding an optimal channel in all presented situations.

7.2 Future Work

Radio Resource Allocation and RKB maintenance: Given the environmental knowledge using presented strategies it will be interesting to research efficient methods to tune the SU radio system to optimally utilize the hyper-spatial opportunities in more generic scenarios under conflicting goals and constraints. Genetic algorithms and game theory based methods can be particularly focused since their effectiveness have already been demonstrated successfully for resource allocation problems in cognitive radio systems, e.g. in [MAC09, THO07]. Furthermore, techniques to maintain a useful radio knowledge base (RKB) is another important area which require more focused research in subjects like data mining and artificial intelligence.

Extending NFSC: The functionality of the NFSC can be further extended to distinguish between overlapping signals by employing cyclostationary feature detection (CFD) based spectrum sensing strategies. The existing connectionist structure of the NFSC can be extended by adding new CFD based processing elements. However, because of very high computational complexity of CFD, it should be used as an optional feature. The cognitive radio can be empowered to enable or disable the CFD based processing elements on demand.

Investigation of Influence of channel conditions: Influence of channel conditions such as noise and fading is not particularly focused. It can be interesting to study the parameter estimation methods presented in chapter 5 for time varying channels under different fading conditions. The false alarm and miss detection probabilities should be estimated for different types of fading environments and estimated parameters should be compensated accordingly.

Chapter 8

References & Bibliography

8.1 References

[A4779]   http://www.atmel.com/dyn/resources/prod_documents/doc4779.pdf

[AGI04]   Agilent Technologies, Inc., Spectrum Analyzer Basics, www.agilent.com. 2004.

[AGU07]   Ana Aguiar, A. W.; "Channel Prediction Heuristics for Adaptive Modulation in WLAN", IEEE 65th Vehicular Technology Conference, April 2007, pages 1091 - 1095

[AHA10]   Ahmad, K.; Meier, U.; Kwasnicka, H.; , "Fuzzy logic based signal classification with cognitive radios for standard wireless technologies," Cognitive Radio Oriented Wireless Networks & Communications (CROWNCOM), 2010 Proceedings of the Fifth International Conference on , vol., no., pp.1-5, 9-11 June 2010

[AHD10]   Ahmad, K.; Shresta, G.; Meier, U.; Kwasnicka, H.; , "Neuro-fuzzy signal classifier (NFSC) for standard wireless technologies," Wireless Communication Systems (ISWCS), 2010 7th International Symposium on , vol., no., pp.616-620, 19-22 Sept. 2010

[AHM10]   Ahmad, Kaleem; Ostfeld, Philip; Meier, Uwe; Kwasnicka, Halina: Exploitation of Multiple Hyperspace Dimensions to Realize Coexistence Optimized Wireless Automation Systems. In: IEEE Transactions on Industrial Informatics S.: 758 - 766, Special Section on: Industrial Communication Systems, Aug 2010

[AHM11]   Ahmad, Kaleem; Shrestha, Ganesh Man; Meier, Uwe: Real-Time Issues of Predictive Modeling for Industrial Cognitive Radios. In: IEEE 9th International Conference on Industrial Informatics - INDIN 2011 Lisbon, Portugal , Jul 2011.

[AHM12]   Ahmad, Kaleem; Meier, Uwe; Witte, Stefan: Predictive Opportunistic Spectrum Access Using Markov Models. In: 17th IEEE Conference on Emerging Technologies and Factory Automation (ETFA 2012) Krakow, Poland, Sep 2012.

[BER06]   Berlemann, L.; Hoymann, C.; Hiertz, G.; Walke, B.; "Unlicensed Operation of IEEE 802.16: Coexistence with 802.11(A) in Shared Frequency Bands," IEEE 17th International

Symposium on Personal, Indoor and Mobile Radio Communications, 2006, 11-14 Sept. 2006 Page(s):1 – 5

[BTS01]   BLUETOOTH SPECIFICATION Version 1.1, February 22 2001

[BUL09]   S.Buljore, H.Harada, S.Filin, P.Houze, K.Tsagkaris, O.Holland, T.Farnham, K.Nolte and V.Ivanov, "An Architecture and Enablers for Optimized Radio Resource usage: The IEEE P1900.4 Working Group", IEEE Communications Magazine, vol. 47, no. 1, pp. 122-129, Jan. 2009

[CAB08]   Cabric, D.; , "Addressing feasibility of cognitive radios," Signal Processing Magazine, IEEE , vol.25, no.6, pp.85-93, November 2008

[CAS07]   Cassioli, D.; Giuliano, R.; Mazzenga, F.; "Analysis of UWB system capacity in a realistic multipath environment with coexistence constraints", IET Communications, Volume 1, Issue 3, June 2007.

[CAT07]   Cattoni, Andrea F.; et al.; "Neural networks mode Classification based on Frequency Distribution Features," CrownCom 2007

[CHR10]   Christin, D.; Mogre, P.S.; Hollick, M.; "Survey on Wireless Sensor Network Technologies for Industrial Automation: The Security and Quality of Service Perspectives,; Future Internet 2010, 2, 96-125.

[COX67]   D. R. Cox, "Renewal Theory," Butler & Tanner Ltd, London, 1967.

[CRA01]   Craig K. Enders; "A primer on maximum likelihood algorihms available for use with missing data," Structural Equation Modeling, 8(1), 128-141, 2001

[DAN05]   Danijela Cabric, Robert W. Brodersen. "Physical Layer Design Issues Unique to Cognitive Radio Systems". 16th IEEE International Symposium on Personal Indoor and Mobile Radio Communications, (PIMRC 2005), September, 2005.

[DEH09]   Dehner, H.-U.; Linde, M.; Moorfeld, R.; Jakel, H.; Burgkhardt, D.; Jondral, F.; Finger, A.; "A low complex and efficient coexistence approach for non-coherent multiband impulse radio UWB," IEEE Sarnoff Symposium, 2009. SARNOFF '09, March 30 2009-April 1 2009, Page(s):1 – 5.

[DEJ10]   Deji Chen, Mark Nixon, Aloysius Mok; WirelessHART: "Real-Time Mesh Network for Industrial Automation", published by Springer 2010.

[DEM77]   A. P. Dempster; N. M. Laird; D. B. Rubin; "Maximum Likelihood from Incomplete Data via the EM Algorithm," Journal of the Royal Statistical Society. Series B (Methodological), Vol. 39, No. 1. (1977), pp. 1-38

[DRO05]   L. Drozd, et al., "Computational electromagnetics applied to analyzing the efficient utilization of the RF transmission hyperspace," IEEE/ACES Int., Honolulu, USA, Apr. 2005, page(s) 1077-1085

[ETH10]   Ethem Alpaydin, "Introduction to machine learning", The MIT press, 2010.

[ETTUS]   http://www.ettus.com/

[EUROP]   http://www.onlineconversion.com/downloads/european_frequency_allocations.pdf

[FEH05]   Fehske, A.; Gaeddert, J.; Reed, J.H.; , "A new approach to signal classification using spectral correlation and neural networks," New Frontiers in Dynamic Spectrum Access Networks, 2005. DySPAN 2005. 2005 First IEEE International Symposium on , vol., no., pp.144-150, 8-11 Nov. 2005

[FLEXR]   http://www.flex-radio.com/Default.aspx

[FOR02]   A. Forenza and R. W. Heath, Jr., "Link adaptation and channel prediction in wireless OFDM systems," in Proc. 45th Midwest Symposium on Circuits and Systems, August 2002, pp. 211–214.

[GEI07]   Geirhofer, S.; Lang Tong; Sadler, B.M.; , "COGNITIVE RADIOS FOR DYNAMIC SPECTRUM ACCESS - Dynamic Spectrum Access in the Time Domain: Modeling and Exploiting White Space," Communications Magazine, IEEE , vol.45, no.5, pp.66-72, May 2007

[GEI08]   Geirhofer, S.; Lang Tong; Sadler, B.M.; "Cognitive Medium Access: Constraining Interference Based on Experimental Models," IEEE Journal on Selected Areas in Communications, Volume 26, Issue 1, Jan. 2008 Page(s):95 - 105

[GHA08]   Ghasemi, A.; Sousa, E.S.; , "Spectrum sensing in cognitive radio networks: requirements, challenges and design trade-offs," Communications Magazine, IEEE , vol.46, no.4, pp.32-39, April 2008

[GIO06]   Giorgetti, Andrea; Chiani, Marco; Dardari, Davide; "Coexistence Issues in Cognitive Radios Based on Ultra-Wide Bandwidth Systems", 1st International Conference on Cognitive Radio Oriented Wireless Networks and Communications, 2006.

[GRA05]   Grandblaise, D. Kloeck, C. Moessner, K. Rodriguez, V. Mohyeldin, E. Pereirasamy, M.K. Jijun Luo Martoyo, I.; "Techno - economic of collaborative based secondary spectrum usage - E2R research project outcomes overview," DySPAN 2005, 8-11 Nov. 2005, page(s): 318-327

[HAI09]   Hai Jiang; Lifeng Lai; Rongfei Fan; Poor, H.V.; , "Optimal selection of channel sensing order in cognitive radio," Wireless Communications, IEEE Transactions on , vol.8, no.1, pp.297-307, Jan. 2009

[HAM02]   Hamalainen, M.; et al.; Latva-aho, M.; "On the UWB system coexistence with GSM900, UMTS/WCDMA, and GPS", IEEE Journal on Selected Areas in Communications, Volume 20, Dec. 2002

[HAN08]   Hang Liu; Dan Yu; Xiangwei Kong; , "A New Approach to Improve Signal Classification in Low SNR Environment in Spectrum Sensing," Cognitive Radio Oriented Wireless Networks and Communications, 2008. CrownCom 2008. 3rd International Conference on , vol., no., pp.1-5, 15-17 May 2008

[HAS06]   Hassan Rezaei, et al,; "New Similarity Measure Between Two Fuzzy Sets," Journal of Advanced Computational Intelligence and Intelligent Informatics. Vol.10 Nov. 2006

[HAY05]   Haykin, S.; , "Cognitive radio: brain-empowered wireless communications," Selected Areas in Communications, IEEE Journal on , vol.23, no.2, pp. 201- 220, Feb. 2005

[HEA10]   He, A.; Kyung Kyoon Bae; Newman, T.R.; Gaeddert, J.; Kyouwoong Kim; Menon, R.; Morales-Tirado, L.; Neel, J.J.; Youping Zhao; Reed, J.H.; Tranter, W.H.; , "A Survey of Artificial Intelligence for Cognitive Radios," Vehicular Technology, IEEE Transactions on , vol.59, no.4, pp.1578-1592, May 2010

[HEI08]   Heidi Steendam, "B-VHF: a Cognitive Radio System for Aeronautical Communication", Symposium on Software Defined and Cognitive Radios, December 12, 2008

[HER08]   Herrera, M.M.; Bonastre, A.; Capella, J.V.; "Performance Study of Non-beaconed and Beacon-Enabled Modes in IEEE 802.15.4 under Bluetooth Interference", The Second International Conference on Mobile Ubiquitous Computing, Systems, Services and Technologies, 2008.

[HOV05]   Hoven, N. Sahai, A.; "Power scaling for cognitive radio," International Conference on Wireless Networks, Communications and Mobile Computing, 2005, 13-16 June 2005, Volume: 1, on page(s): 250- 255

[HOY08]   Hoyhtya, M.; Pollin, S.; Mammela, A.; , "Performance improvement with predictive channel selection for cognitive radios," Cognitive Radio and Advanced Spectrum Management, 2008. CogART 2008. First International Workshop on , vol., no., pp.1-5, 14-14 Feb. 2008

[HSU06]   Hsu, A.C.-C.; Wei, D.S.L.; Kuo, C.-C.J.; "Coexistence Mechanism Using Dynamic Fragmentation for Interference Mitigation between Wi-Fi and Bluetooth", Military Communications Conference, 2006

[HYO08]   Hyoil Kim; Shin, K.G.; , "Efficient Discovery of Spectrum Opportunities with MAC-Layer Sensing in Cognitive Radio Networks," Mobile Computing, IEEE Transactions on , vol.7, no.5, pp.533-545, May 2008

[ISU06]   Isukapalli, Y. & Rao, B. D.; "Erodicity of wireless channels and temporal prediction", Fortieth Asilomar Conference on Signals, Systems and Computers, Oct-Nov 2006, 473-477

[JEF98]   Jeff A. Bilmes; "A gentle tutorial of the EM algorithm and its application to parameter estimation for Gaussian mixture and hidden Markov models," International computer science institute and department of electrical engineering and computer science, U.C. Berkley, April 1998.

[JIN06]   Jinn-Tsong Tsai; Jyh-Horng Chou; Tung-Kuan Liu; , "Tuning the structure and parameters of a neural network by using hybrid Taguchi-genetic algorithm," Neural Networks, IEEE Transactions on , vol.17, no.1, pp.69-80, Jan. 2006

[JIN07]   Jing Zhu; Waltho, A.; Xue Yang; Xingang Guo: "Multi-Radio Coexistence: Challenges and Opportunities", 16th International Conference on Computer Communications and Networks, 2007. Volume, 13-16 Aug. 2007.

[JOL08]   Jo Lynn Tan; bin Sha'ameri, A.Z.; , "Signal Analysis and Classification of Digital Communication Signals using Adaptive Smooth-Windowed Wigner-Ville Distribution," Telecommunication Technologies 2008 and 2008 2nd Malaysia Conference on Photonics. NCTT-MCP 2008. 6th National Conference on , vol., no., pp.260-266, 26-28 Aug. 2008

[JUE08]   Jue Wang; Qing Tao; , "Machine Learning: The State of the Art," Intelligent Systems, IEEE , vol.23, no.6, pp.49-55, Nov.-Dec. 2008

[JUN09]   Jun Ma; Li, G.Y.; Biing Hwang Juang; , "Signal Processing in Cognitive Radio," Proceedings of the IEEE , vol.97, no.5, pp.805-823, May 2009

[KON06]   M. Konrad, W. Koch and J. Huschke, "Coexistence Analysis of Bluetooth and Cellular UMTS in the 2500 - 2690 MHz Band," in IEEE Wireless Communications and Networking Conference, Las Vegas, NV USA, April 2006

[KUPRI]   Kupris, Gerald, Freescale Halbleiter GmbH, "Wireless Sensor Networks - from Recent Developments to Industrial Standards", Schatzbogen 7, 81829 München, Germany

[KYO07]   Kyouwoong Kim; Akbar, I.A.; Bae, K.K.; Jung-sun Urn; Spooner, C.M.; Reed, J.H.; , "Cyclostationary Approaches to Signal Detection and Classification in Cognitive Radio," New Frontiers in Dynamic Spectrum Access Networks, 2007. DySPAN 2007. 2nd IEEE International Symposium on , vol., no., pp.212-215, 17-20 April 2007

[LAW89]   Lawrence R. Rabiner, "A tutorial on hidden Markov models and selected applications in speech recognition", Proceedings of the IEEE 77, 1989.

[LEE08]   Yun-Ho Lee; "Channel Prediction by Doppler Frequency Estimation with Simplified AR modeling", 10th International Conference on Advanced Communication Technology. Volume 1, 17-20 Feb. 2008 Page(s):3 - 8

[LEH07]   Le, H.-S.T.; Qilian Liang; "An Efficient Power Control Scheme for Cognitive Radios," IEEE Wireless Communications and Networking Conference, 2007. WCNC 2007. 11-15 March 2007 Page(s):2559 – 2563

[LLE08]   lleri, O.; Mandayam, N.B.; , "Dynamic spectrum access models: toward an engineering perspective in the spectrum debate," Communications Magazine, IEEE , vol.46, no.1, pp.153-160, January 2008

[MAC09]   MacKenzie, A.B.; Reed, J.H.; Athanas, P.; Bostian, C.W.; Buehrer, R.M.; DaSilva, L.A.; Ellingson, S.W.; Hou, Y.T.; Hsiao, M.; Jung-Min Park; Patterson, C.; Raman, S.; da Silva, C.; , "Cognitive Radio and Networking Research at Virginia Tech," Proceedings of the IEEE , vol.97, no.4, pp.660-688, April 2009

[MCH07]   McHenry, M. Livsics, E. Nguyen, T. Majumdar, N.; "XG dynamic spectrum access field test results," IEEE Communications Magazine, June 2007, Volume: 45, Issue: 6, On page(s): 51-57

[MEI07]   Meier, Uwe; Witte, Stefan; Helmig, Kai; Hoeing, Michael; Schnueckel, Markus; Krause, Hermann: "Performance Evaluation and Prediction of a Bluetooth Based Real-Time Sensor Actuator System in Harsh Industrial Environments". in: ETFA 2007, Greece

[MIT09]   Mitola, J.; , "Cognitive Radio Architecture Evolution," Proceedings of the IEEE , vol.97, no.4, pp.626-641, April 2009

[MIT99]   J. Mitola, "Cognitive radio: Model-based competence for software radios," Ph.D. dissertation, Dept. of Teleinformatics, KTH, 1999

[MUS95]   Musliner, D.J.; Hendler, J.A.; Agrawala, A.K.; Durfee, E.H.; Strosnider, J.K.; Paul, C.J.; , "The challenges of real-time AI," Computer , vol.28, no.1, pp.58-66, Jan 1995

[MW]   http://www.merriam-webster.com/dictionary

[MYR01]   Myrtveit, I.; Stensrud, E.; Olsson, U.H.; , "Analyzing data sets with missing data: an empirical evaluation of imputation methods and likelihood-based methods," Software Engineering, IEEE Transactions on , vol.27, no.11, pp.999-1013, Nov 2001

[NANOT]   http://www.nanotron.com/EN/index.php

[NGU10]   Nguyen Quoc Dinh; Sung-Wook Kim; Dong-Sung Kim; , "Performance evaluation of priority CSMA-CA mechanism on ISA100.11a wireless network," Computer Sciences and Convergence Information Technology (ICCIT), 2010 5th International Conference on , vol., no., pp.991-996, Nov. 30 2010-Dec. 2 2010

[NOL06]   Nolan, Keith E. Sutton, Paul Doyle, Linda E.; "An Encapsulation for Reasoning, Learning, Knowledge Representation, and Reconfiguration Cognitive Radio Elements," 1st International Conference on Cognitive Radio Oriented Wireless Networks and Communications, 2006. 8-10 June 2006, On page(s): 1-5

[NOL07]   Nolan, K.E.; Sutton, P.D.; Doyle, L.E.; Rondeau, T.W.; Le, B.; Bostian, C.W.; "Dynamic Spectrum Access and Coexistence Experiences Involving Two Independently Developed Cognitive Radio Testbeds", 2nd IEEE International Symposium on New Frontiers in Dynamic Spectrum Access Networks, 2007.

[NTIAC]   http://www.ntia.doc.gov/osmhome/allochrt.pdf

[OHN05]   Ohno, K.; Ikegami, T.; "Interference mitigation study for the coexistence of bi-phase UWB and multi-band OFDM", IEEE International Conference on UWB 2005.

[PAL03]   Palicot, J.; Roland, C.; , "A new concept for wireless reconfigurable receivers," Communications Magazine, IEEE , vol.41, no.7, pp. 124- 132, July 2003

[PEN05]   Pengfei He; Yinghua Lu; Hongxin Zhang; Jiangang Lu; "A pulse shaping method for UWB avoiding the frequency coexistence interference with WLAN", 2nd International Conference on Mobile Technology, Applications and Systems, 2005.

[PIN08]   Pingzhou Tu; Xiaojing Huang; Dutkiewicz, E.; "Adaptive Subband Selection in OFDM-Based Cognitive Radios for Better System Coexistence," 3rd International Conference on Cognitive Radio Oriented Wireless Networks and Communications, 2008. CrownCom 2008, 15-17 May 2008 Page(s):1 – 6

[PRA08]   Prasad, R.V.; Pawelczak, P.; Hoffmeyer, J.A.; Berger, H.S.; , "Cognitive functionality in next generation wireless networks: standardization efforts," Communications Magazine, IEEE , vol.46, no.4, pp.72-78, April 2008

[QIN07]   Qing Zhao; Lang Tong; Ananthram Swami; Yunxia Chen; , "Decentralized cognitive MAC for opportunistic spectrum access in ad hoc networks: A POMDP framework," Selected Areas in Communications, IEEE Journal on , vol.25, no.3, pp.589-600, April 2007

[QIN08]   Qinqin Chen; Ying Wang; Bostian, C.W.; , "Universal Classifier Synchronizer Demodulator," Performance, Computing and Communications Conference, 2008. IPCCC 2008. IEEE International , vol., no., pp.366-371, 7-9 Dec. 2008

[QIX06]   Qixiang Pang; Leung, V.C.M.; "Improved Channel Classification and Scheduling for Non-collaborative Bluetooth/ WLAN Coexistence," IEEE 63rd Vehicular Technology Conference, 2006. VTC 2006-Spring, Volume 3, 7-10 May 2006 Page(s):1303 - 1307

[QIX07]   Qixiang Pang; Leung, V.C.M.; "Channel Clustering and Probabilistic Channel Visiting Techniques for WLAN Interference Mitigation in Bluetooth Devices", IEEE Transactions on Electromagnetic Compatibility, 2007

[RAL00]   Ralston, E. D. Reilly, and D. Hammendinger (eds.), "Encyclopedia of Computer Science (4th ed.)," New York: Grove's Dictionaries (2000)

[RIE07]   C. J. Rieser, T. W. Rondeau, C. Bostian, W. R. Cyre, and T. M. Gallagher,; "Cognitive radio engine based on genetic algorithms in a network," U.S. Patent 7 289 972, Oct. 2007.

[ROB03]   Robert J. Berger.; "Open Spectrum: A Path to Ubiquitous Connectivity," ACM Queue 1, 3 , May 2003 , 60-68.

[SCH07]   Scheible, G.; Dacfey Dzung; Endresen, J.; Frey, J.-E.; , "Unplugged but connected [Design and implementation of a truly wireless real-time sensor/actuator interface]," Industrial Electronics Magazine, IEEE , vol.1, no.2, pp.25-34, Summer 2007

[SD105] http://standards.ieee.org/getieee802/download/802.15.1-2005.pdf

[SD117] IEEE 802.11-2007 standard.

[SD406] http://standards.ieee.org/getieee802/download/802.15.4-2006.pdf

[SED03] S. Edelkamp. Memory limitation in artificial intelligence. In J. F. Sibeyn P. Sanders, U. Meyer, editor, Memory Hierarchies, volume 2625 of Lecture Notes in Computer Science, pages 233–250. Springer, 2003.

[SHA07] Sharma, P. Chandra, K.; "Prediction of State Transitions in Rayleigh Fading Channels," IEEE Transactions on Vehicular Technology, March 2007, Volume: 56, Issue 2, page(s): 416-425

[SHR11] Shravan Rayanchu, Ashish Patro, Suman Banerjee; "Airshark: Detecting Non-WiFi RF Devices using Commodity WiFi Hardware," ACM IMC 2011, Berlin Germany.

[SHR12] Shrestha, Ganesh Man; Ahmad, Kaleem; Meier, Uwe: Statistical Analysis and Predictive Modeling of Industrial Wireless Coexisting Environments. In: WFCS 2012, Lemgo/Detmold, Germany May 2012.

[SIT10] Sithamparanathan Kandeepan, Radoslaw Piesiewicz, Tuncer C. Aysal, Abdur Rahim Biswas, and Imrich Chlamtac, "Spectrum Sensing for Cognitive Radios with Transmission Statistics: Considering Linear Frequency Sweeping," EURASIP Journal on Wireless Communications and Networking, vol. 2010, Article ID 123674, 13 pages, 2010

[SMK98] S.M. Kay, Fundamentals of Statistical Signal Processing: Detection Theory. Englewood Cliffs, NJ: Prentice-Hall, 1998.

[SOU01] M. R. Souryal and R. L. Pickholtz, "Adaptive modulation with imperfect channel information in OFDM," in IEEE Proc. of Int. Conf. on Comm., June 2001, pp. 1861–1865.

[STD18] IEEE Std 1900.1-2008, "IEEE Standard Definitions and Concepts for Dynamic Spectrum Access: Terminology Relating to Emerging Wireless Networks, System Functionality, and Spectrum Management " 2008

[STD23] "Draft Recommended Practice for Information technology Telecommunications and Information exchange between systems Local and metropolitan area networks Specific Requirements-Part 15.2: Coexistence of Wireless Personal Area Networks with Other Wireless Devices Operating in Unlicensed Frequency Bands Replaced by IEEE 802.15.2-2003," IEEE Std P802.15.2/D09 , vol., no., 2003

[STD28]   "IEEE Recommended Practice for the Analysis of In-Band and Adjacent Band Interference and Coexistence Between Radio Systems," *IEEE Std 1900.2-2008* , vol., no., pp.1-94, July 29 2008

[STE11]   Steven M. Kay, Fundamentals of Statistical Signal Processing, Volume 2: Detection Theory, 2011, Published by Pearson.

[SUA07]   Suansook, S.; Aramvith, S.; Prapinmongkolkarn, P.; "Comparative Performance Analysis of WiMAX and WLAN with WPAN Coexistence in UL Band", Intelligent Signal Processing and Communication Systems, 2007.

[SUNDA]   http://www.sundance.com/default.asp

[TEK04]   Tektronix, Inc., Fundamentals of Real-Time Spectrum Analysis, www.tektronix.com/rsa. 2004.

[THO07]   Thomas W. Rondeau, "Application of Artificial Intelligence to Wireless Communications" PhD dissertation, Virginia Polytechnic Institute and State University, September 20, 2007

[TIN03]   Ting-Yu Lin; Yu-Chee Tseng; "Collision analysis for a multi-Bluetooth picocells environment", IEEE Communications Letters, Volume 7, Issue 10, Oct. 2003

[TMM97]   T. M .Mitchell, "Machine Learning," published by McGraw Hill, 1997

[TOS08]   Toscano, E.; Lo Bello, L.; "Cross-channel interference in IEEE 802.15.4 networks", IEEE International Workshop on Factory Communication Systems, 2008.

[TSC04]   15-08-0581-02-004e-time-slotted-channel-hopping-mac

[TSCH4]   15-08-0581-02-004e-time-slotted-channel-hopping-mac

[VEN08]   R. Venkatesha Prasad, Pzemyslaw Pawelczak, James A. Hoffmeyer, H. Steven Berger, "Cognitive Functionality in Next Generation Wireless Networks: Standardization Efforts", IEEE Communications Magaznie, vol. 46, no. 4, pp. 72-78, Apr. 2008

[WAG92]   W.A. Gardner, et al., "Signal interception: Performance advantages of cyclic-feature detectors," IEEE Trans. Comm, Jan. 1992.

[WEB01]   http://grouper.ieee.org/groups/scc41/index.html

[WEB02]   http://standards.ieee.org/getieee802/download/802.11y-2008.pdf

[WEB03]   http://www.ieee802.org/16/le/

[WEB04]   http://grouper.ieee.org/groups/802/11/Reports/tgh_update.htm

[WEB05]   http://standards.ieee.org/prod-serv/80211n.html

[WEB06]   http://www.ict-aragorn.eu/index.php?id=introduction

[WEB07]   http://www.cognitiveradio.wireless.vt.edu/dokuwiki/doku.php?id=research

[WEB08]   http://www.ieee802.org/22/

[WEI07]   Wei Yuan; Xiangyu Wang; Linnartz, J.-P.M.G.; "A Coexistence Model of IEEE 802.15.4 and IEEE 802.11b/g", 14th IEEE Symposium on Communications and Vehicular Technology in the Benelux, 2007

[WEN99]   Wen Wei; Mendel, J.M.; , "A fuzzy logic method for modulation classification in nonideal environments," Fuzzy Systems, IEEE Transactions on , vol.7, no.3, pp.333-344, Jun 1999

[WSA10]   WSAN System Specification, Draft in PI Review, Version 0.9 – Date: November 2010

[WUD05]   Wu Dan; Gu Xuemai; Guo Qing; , "A new scheme of automatic modulation classification using wavelet and WSVM," Mobile Technology, Applications and Systems, 2005 2nd International Conference on , vol., no., pp.5 pp.-5, 15-17 Nov. 2005

[XIA10]   Xiao Yu Wang; Wong, A.; Pin-Han Ho; , "Extended Knowledge-Based Reasoning Approach to Spectrum Sensing for Cognitive Radio," Mobile Computing, IEEE Transactions on , vol.9, no.4, pp.465-478, April 2010

[XIE06]   Gang Xie, Ranran Zhang, Y. L.; "Simplified and Adaptive Prediction Algorithm of Time-varying Wideband Channels", International Symposium on Communications and Information Technologies, Oct 2006, 264-267

[XIZ11]   Xi Zhang; Hang Su; , "CREAM-MAC: Cognitive Radio-EnAbled Multi-Channel MAC Protocol Over Dynamic Spectrum Access Networks," Selected Topics in Signal Processing, IEEE Journal of , vol.5, no.1, pp.110-123, Feb. 2011

[YAR07]   Yarkan, S.; Arslan, H.; , "Binary Time Series Approach to Spectrum Prediction for Cognitive Radio," Vehicular Technology Conference, 2007. VTC-2007 Fall. 2007 IEEE 66th , vol., no., pp.1563-1567, Sept. 30 2007-Oct. 3 2007

[YIH07]   Yihong Gong, Wei Xu,; "Machine Learning for Multimedia Content Analysis," Springer, 2007

[YOU09]   Youping Zhao; Shiwen Mao; Neel, J.O.; Reed, J.H.; "Performance Evaluation of Cognitive Radios: Metrics, Utility Functions, and Methodology," Proceedings of the IEEE, Volume 97, Issue 4, April 2009 Page(s):642 – 659

[YUK04]   Yu-Kwong Kwok; Chek, M.C.-H.; "Design and evaluation of coexistence mechanisms for Bluetooth and IEEE 802.11b systems," 15th IEEE International Symposium on Personal, Indoor and Mobile Radio Communications, 2004. PIMRC 2004, Volume 3, 5-8 Sept. 2004 Page(s):1767 – 1771

[ZAN01]   J. Zander and S. L. Kim, Radio Resource Management for Wireless Networks. Norwood, MA: Artech House, 2001.

[ZHI08]   Zhi Quan; Shuguang Cui; Poor, H.; Sayed, A.; , "Collaborative wideband sensing for cognitive radios," Signal Processing Magazine, IEEE , vol.25, no.6, pp.60-73, November 2008

[ZHU07]   Zhu, Qiang; Wong, Wing Shing; "Multi-Group Coexistence in License-Exempt Networks without Information Exchange", Cognitive Radio Oriented Wireless Networks and Communications, 2007. CrownCom 2007.

[ZIGBE]   ZigBee Specification, Document 053474r17

8.2 Bibliography

[AIM00]   Aimin Sang; San-qi Li; , "A predictability analysis of network traffic," INFOCOM 2000. Nineteenth Annual Joint Conference of the IEEE Computer and Communications Societies. Proceedings. IEEE , vol.1, no., pp.342-351 vol.1, 2000

[ART07]   Artem Tkachenko, et al. "Cyclostationary Feature Detector Experiments using Reconfigurable BEE2". International Conference on Dynamic Spectrum Access Networks, April 2007, page(s) 216-219.

[BAL08]   Baldo, N.; Zorzi, M.; , "Fuzzy logic for cross-layer optimization in cognitive radio networks," Communications Magazine, IEEE , vol.46, no.4, pp.64-71, April 2008

[BOR05]   Bor-Sen Chen; Bore-Kuen Lee; Sheng-Kai Chen; , "Adaptive power control of cellular CDMA systems via the optimal predictive model," Wireless Communications, IEEE Transactions on , vol.4, no.4, pp. 1914- 1927, July 2005

[CAB06]   Cabric, D.; O'Donnell, I.D.; Chen, M.S.-W.; Brodersen, R.W.; , "Spectrum sharing radios," Circuits and Systems Magazine, IEEE , vol.6, no.2, pp.30-45, 2006

[CHR04]   Christian James Rieser; "Biologically Inspired Cognitive Radio Engine Model Utilizing Distributed Genetic Algorithms for Secure and Robust Wireless Communications and Networking," Ph.D. Dissertation, Virginia Polytechnic Institute and State University, 2004

[CHU08]   Chuan-Chin Pu; Wan-Young Chung; , "Mitigation of Multipath Fading Effects to Improve Indoor RSSI Performance," Sensors Journal, IEEE , vol.8, no.11, pp.1884-1886, Nov. 2008

[CHU10]   Chun-Han Ko; Hung-Yu Wei; , "Game Theoretical Resource Allocation for Inter-BS Coexistence in IEEE 802.22," Vehicular Technology, IEEE Transactions on , vol.59, no.4, pp.1729-1744, May 2010

[DEN10]   Deng-Feng Li; , "Mathematical-Programming Approach to Matrix Games With Payoffs Represented by Atanassov's Interval-Valued Intuitionistic Fuzzy Sets," Fuzzy Systems, IEEE Transactions on , vol.18, no.6, pp.1112-1128, Dec. 2010

[GAR88]   Gardner, W.A.; , "Signal interception: a unifying theoretical framework for feature detection," Communications, IEEE Transactions on , vol.36, no.8, pp.897-906, Aug 1988

[GNURD]   http://gnuradio.org/redmine/projects/gnuradio/wiki

[HAR08]   Harada, H.; , "A Feasibility Study on Software Defined Cognitive Radio Equipment," New Frontiers in Dynamic Spectrum Access Networks, 2008. DySPAN 2008. 3rd IEEE Symposium on , vol., no., pp.1-12, 14-17 Oct. 2008

[HOP03]   Hopgood, A.A.; , "Artificial intelligence: hype or reality?," Computer , vol.36, no.5, pp. 24-28, May 2003

[ITU06]   ITU Handbook, "Teletraffic Engineering, ITU-D," Study Group 2, June 2006, http://www.itu.int/.

[JAE10]   Jaeweon Kim; Andrews, J.G.; , "Sensitive White Space Detection with Spectral Covariance Sensing," Wireless Communications, IEEE Transactions on , vol.9, no.9, pp.2945-2955, September 2010

[KUB10]   Kubo, Y.; Watanabe, S.; Nakamura, A.; McDermott, E.; Kobayashi, T.; , "A Sequential Pattern Classifier Based on Hidden Markov Kernel Machine and Its Application to Phoneme Classification," Selected Topics in Signal Processing, IEEE Journal of , vol.4, no.6, pp.974-984, Dec. 2010

[LAZ99]   Lazzerini, B.; Reyneri, L.M.; Chiaberge, M.; , "A neuro-fuzzy approach to hybrid intelligent control," Industry Applications, IEEE Transactions on , vol.35, no.2, pp.413-425, Mar/Apr 1999

[LEH08]   Le, H.-S.T.; Ly, H.D.; , "Opportunistic spectrum access using Fuzzy Logic for cognitive radio networks," Communications and Electronics, 2008. ICCE 2008. Second International Conference on , vol., no., pp.240-245, 4-6 June 2008

[LIF11]   Lifeng Lai; El Gamal, H.; Hai Jiang; Poor, H.V.; , "Cognitive Medium Access: Exploration, Exploitation, and Competition," Mobile Computing, IEEE Transactions on , vol.10, no.2, pp.239-253, Feb. 2011

[MIR00]   Mirabbasi, S.; Martin, K.; , "Classical and modern receiver architectures," Communications Magazine, IEEE , vol.38, no.11, pp. 132- 139, Nov 2000

[MIT06]   J. Mitola, "Cognitive Radio Architecture," 2006 by John Wiley & Sons, Inc.

[NAM03]   Namjin Kim; Kehtarnavaz, N.; Yeary, M.B.; Thornton, S.; , "DSP-based hierarchical neural network modulation signal classification," Neural Networks, IEEE Transactions on , vol.14, no.5, pp. 1065- 1071, Sept. 2003

[NILSS]   http://ai.stanford.edu/~nilsson/MLBOOK.pdf

[NIY08]   Niyato, D.; Hossain, E.; , "Competitive spectrum sharing in cognitive radio networks: a dynamic game approach," Wireless Communications, IEEE Transactions on , vol.7, no.7, pp.2651-2660, July 2008

[PEN10]   Pengbo Si; Hong Ji; Yu, F.R.; Leung, V.C.M.; , "Optimal Cooperative Internetwork Spectrum Sharing for Cognitive Radio Systems With Spectrum Pooling," Vehicular Technology, IEEE Transactions on , vol.59, no.4, pp.1760-1768, May 2010

[RHW99]   R. H. Walden, "Analog-to-Digital Converters Survey and Analysis", IEEE Journal on Selected Areas in Communications, April 1999.

[SEN09]   Senhua Huang; Xin Liu; Zhi Ding; , "Optimal Transmission Strategies for Dynamic Spectrum Access in Cognitive Radio Networks," Mobile Computing, IEEE Transactions on , vol.8, no.12, pp.1636-1648, Dec. 2009

[SEO07]   Seok-Beom Roh; Pedrycz, W.; Sung-Kwun Oh; , "Genetic Optimization of Fuzzy Polynomial Neural Networks," Industrial Electronics, IEEE Transactions on , vol.54, no.4, pp.2219-2238, Aug. 2007

[SHA08]   Sharma, R.; Gopal, M.; , "Hybrid Game Strategy in Fuzzy Markov-Game-Based Control," Fuzzy Systems, IEEE Transactions on , vol.16, no.5, pp.1315-1327, Oct. 2008

[SHE09]   Sheng-Yuan Tu; Kwang-Cheng Chen; Prasad, R.; , "Spectrum Sensing of OFDMA Systems for Cognitive Radio Networks," Vehicular Technology, IEEE Transactions on , vol.58, no.7, pp.3410-3425, Sept. 2009

[TAN09]   Tandra, R.; Sahai, A.; Mishra, S.M.; , "What is a Spectrum Hole and What Does it Take to Recognize One?," Proceedings of the IEEE , vol.97, no.5, pp.824-848, May 2009

[TIA06]   Tian, Zhi; Giannakis, Georgios B.; , "A Wavelet Approach to Wideband Spectrum Sensing for Cognitive Radios," Cognitive Radio Oriented Wireless Networks and Communications, 2006. 1st International Conference on , vol., no., pp.1-5, 8-10 June 2006

[TUM10]   Tumuluru, V.K.; Ping Wang; Niyato, D.; , "A Neural Network Based Spectrum Prediction Scheme for Cognitive Radio," Communications (ICC), 2010 IEEE International Conference on , vol., no., pp.1-5, 23-27 May 2010

[VAP99]   Vapnik, V.N.; , "An overview of statistical learning theory," Neural Networks, IEEE Transactions on , vol.10, no.5, pp.988-999, Sep 1999

[WEB00]   http://standards.ieee.org/getieee802/download/802.15.2-2003.pdf

[WAG08]   Wagstaff, A.J.; , "Logarithmic cyclic frequency domain profile for automatic modulation recognition," Communications, IET , vol.2, no.8, pp.1009-1015, September 2008

[WAL06]   Waltz, D.L.; , "Evolution, Sociobiology, and the Future of Artificial Intelligence," Intelligent Systems, IEEE , vol.21, no.3, pp.66-69, Jan.-Feb. 2006

[YER09]   Yeary, M.B.; Nemati, S.; Tian-You Yu; Yadong Wang; Yan Zhai; , "A Support-Vector-Machine-Based Approach to RF Sensor Spectral Signature Classifications," Instrumentation and Measurement, IEEE Transactions on , vol.58, no.1, pp.221-228, Jan. 2009

[YIN09]   Yin Zhendong; , "Research of Communication Signal Modulation Scheme Recognition Based on One-Class SVM Bayesian Algorithm," Wireless Communications, Networking and Mobile Computing, 2009. WiCom '09. 5th International Conference on , vol., no., pp.1-4, 24-26 Sept. 2009

[YOU10]   Young, S.; , "Cognitive User Interfaces," Signal Processing Magazine, IEEE , vol.27, no.3, pp.128-140, May 2010

[YUC09]   Yucek, T.; Arslan, H.; , "A survey of spectrum sensing algorithms for cognitive radio applications," Communications Surveys & Tutorials, IEEE , vol.11, no.1, pp.116-130, First Quarter 2009

[ZHE10]   Zhen Fang; Zhan Zhao; Daoqu Geng; Yundong Xuan; Lidong Du; Xunxue Cui; , "RSSI variability characterization and calibration method in wireless sensor network," Information and Automation (ICIA), 2010 IEEE International Conference on , vol., no., pp.1532-1537, 20-23 June 2010

[ZHO08]   Zhou, L.; Zenebe, A.; , "Representation and Reasoning Under Uncertainty in Deception Detection: A Neuro-Fuzzy Approach," Fuzzy Systems, IEEE Transactions on , vol.16, no.2, pp.442-454, April 2008

Appendix A1

A1: Existing Radio Technologies, Coexistence and Cognitive Radio: State-of-the-art

A1.1   Problems with existing radio technologies

Immense research has been done to investigate the performance of existing radio technologies in a variety of environments. An overview on the performance investigation of existing radio technologies in coexisting environments is provided in the following:

[JIN07] discusses three major sources that caused interference among existing radio systems: transmitter noise, receiver blocking, and inter-modulation, and emphasizes that they can occur among radios even when they are operated in different bands in both collocated and close proximity environments. Regulatory standards related to coexistence are inadequate to provide interference protection in these environments.

[AHM08] investigated the coexistence properties of WPAN systems like Bluetooth IEEE 802.15.1, ZigBee IEEE 802.15.4, IEEE 802.15.4a based CSS, and narrow-band FSK, and suggests that without careful selection of communication parameters each of these technologies can suffer performance degradation in coexistence environments.

In [KON06] the authors have analyzed the coexistence of Bluetooth and UMTS FDD for collocated frequency bands (2.4 GHz ISM band / 2.5 GHz IMT-2000 extension band) with a separation of 16.5 MHz. It is shown by means of radio network simulations and a mathematical model of Bluetooth (BT) radio frequency (RF) receiver blocking that the reception of an external BT signal in an UMTS terminal with integrated BT is seriously disturbed by strong UMTS uplink signals. In a worst case scenario when a 12.2 kbit/s UMTS voice or a 64 kbit/s UMTS data service is used, a BT link failing up to 90% and 100% was observed.

In [SUA07] the impact of BT modeled as uniformly spread interference on WiMAX IEEE 802.16 is evaluated and compared with that of WLAN IEEE 802.11b. It is shown that the probability of collision of BT with WLAN IEEE 802.11b can be as high as 0.5 for 20m distance. The level of BT interference on

WiMAX 802.16 is much less than that of WLAN IEEE 802.11b and is observed to be less than 0.1 at 20m distance but can be higher for greater distances.

BT was considered as an optimal solution for industrial coexisting applications [AHM08, MEI07] because of its ability to identify 'good' and 'bad channels' with the help of adaptive algorithms. But when multiple WLANs and/or BT piconets coexist, the number of 'good' channels can be very low and the BT devices may be starved of radio resources due to their excessive courtesy [QIX07] hence even making the adaptive algorithms unsuccessful. While the packet error probability also increases [TIN03] as the traffic load or the number of piconets grows. Small packets (DH1) suffer fewer collisions than large ones (DH5) due to shorter transmission durations.

[WEI07] presents a coexistence model of IEEE 802.15.4 and IEEE 802.11b/g based on two aspects: power and timing. With IEEE 802.11b interference the throughput of the IEEE 802.15.4 node goes down to zero in a worst case scenario. The cross-channel interference in IEEE 802.15.4 networks [TOS08] can also affect its performance while the beacon enabled mode has shown better performance than the nonbeacon-enabled mode. Bluetooth interference degraded the performance of IEEE 802.15.4 in both modes [HER08].

The coexistence constraints may lead to a significant underutilization of the available UWB capacity [CAS07], and as a result the system may be 'coexistence limited' or 'interference limited' depending on whether the coexistence constraints are satisfied or not. [HAM02] shows that the system performance suffers most if the interference and the nominal center frequency of the UWB system are overlapping.

A1.2   Performance Analysis of State-of-the-Art Wireless Technologies

Atmel, Bluetooth, NanoNET, ZigBee, and WLAN and are used in these experiments. Performance of each of these technologies, except WLAN, is studied as recipient as well as an interferer. Moreover, all these experiments are done in a lab environment and the QoS is measured in terms of BER and PLR only. Each experiment includes only two technologies, one as a recipient and the other one as an interferer. The experimental setup includes one pair of nodes for each participant technology where respective nodes are placed in a cross sectional constellation with 3 m distance as shown in Fig. A.1. Except for the WLAN system, all demonstrators employ cyclic traffic. The parameters studied are transmission power, retransmission mechanism, bitrate, cycle time, packet size, bandwidth, no. of interferers, traffic load and signal-to-interference ratio (SIR). It is worth mentioning that each parameter could not be configured for each participant technology because of limitations of available devices. Therefore the aim of these experiments was to study each parameter at least for one technology either as recipient or interferer.
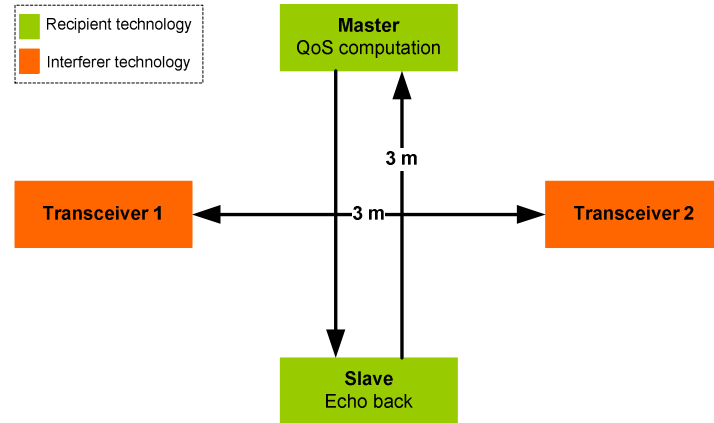
Figure A.1: *Experimental setup used for performance analysis of state-of-the-art technologies*

The following is a summary of reconfigurable parameters of the demonstrators:

- The Bluetooth based demonstrator allows only choosing a packet type. A single slot, 3-slot or 5-slot packet can be used.

- NanoNET transmission power and retransmission mechanism can be reconfigured.

- The Atmel demonstrator can choose either 72 kbps or 500 kbps bitrate.

- The ZigBee system operates with its default parameters that can't be tuned.

- The WLAN system is studied only as an interferer. Running more than one parallel WLAN networks helps to study the influence of increased occupied bandwidth particularly in case of a recipient Bluetooth system. Furthermore, download type internet based traffic is used for the WLAN system where traffic load can also be changed by changing the number of nodes connected to an access point at any time. I performed experiments with only one (best case) and two connected nodes (worst case), however increasing the number of nodes is expected to make the WLAN interference further stronger for coexisting systems.

A1.3   Reference Measurements without interferers

The QoS of selected technologies without any interference, presented in Fig. A.2, are taken as reference measurements. The Bluetooth system has no errors at all. The BER for ZigBee also remains zero while the PLR is almost 0.28 %. For the nanoNET system the PLR is zero while the BER is in the order of 1e–4. For the Atmel system the BER is 0.2 %, and the PLR is 0.76 %.
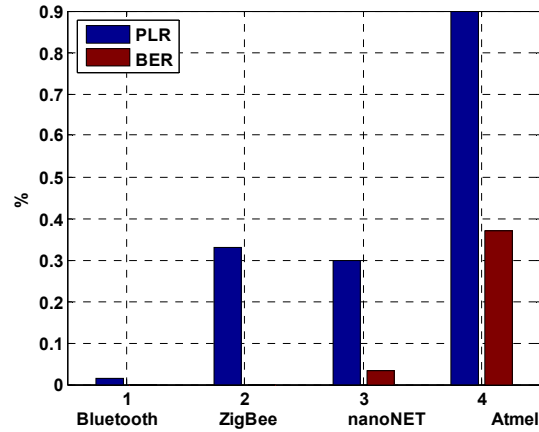
Figure A.2: *Reference measurement: PLR and BER in lab without any interference for Bluetooth(1-slot packet), nanoNET(6.90 dBm), Atmel(500 kbps), ZigBee(default).*

A1.3.1 Performance in Coexisting Environments

Only the worst case and the best case results of all experiments, shown in Fig. A.3 and Fig. A.4 respectively, are presented in this section. The combinations of parameters causing these results are mentioned in captions of these figures and are briefly discussed in the following paragraphs for each participant technology.
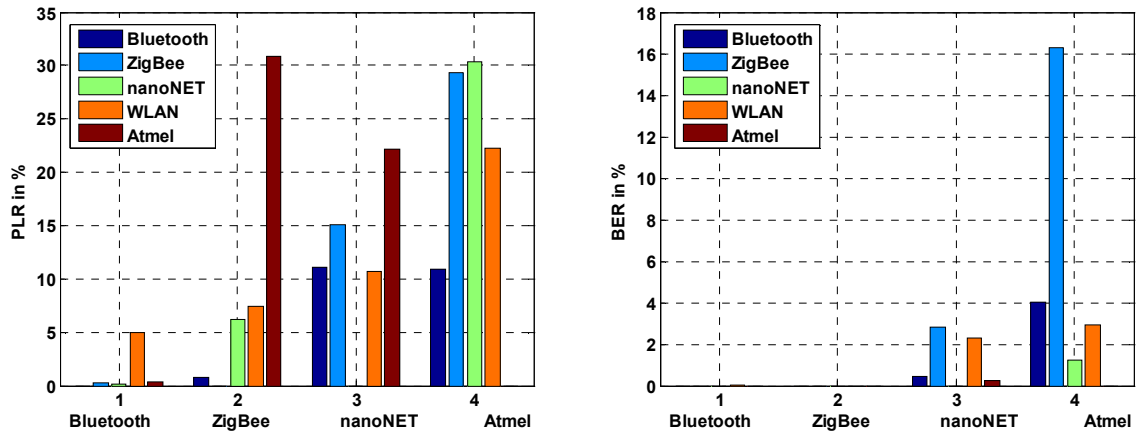

Figure A.3: *The worst case PLR and BER for tested systems in the presence of selected interferers (legend shows interferers). Bluetooth(5-slot packet), nanoNET(6.90 dBm and retransmission as interferer, -16 dBm without retransmission as recipient), Atmel(72 kbps), WLAN(two parallel networks with 2 active nodes in each network).*
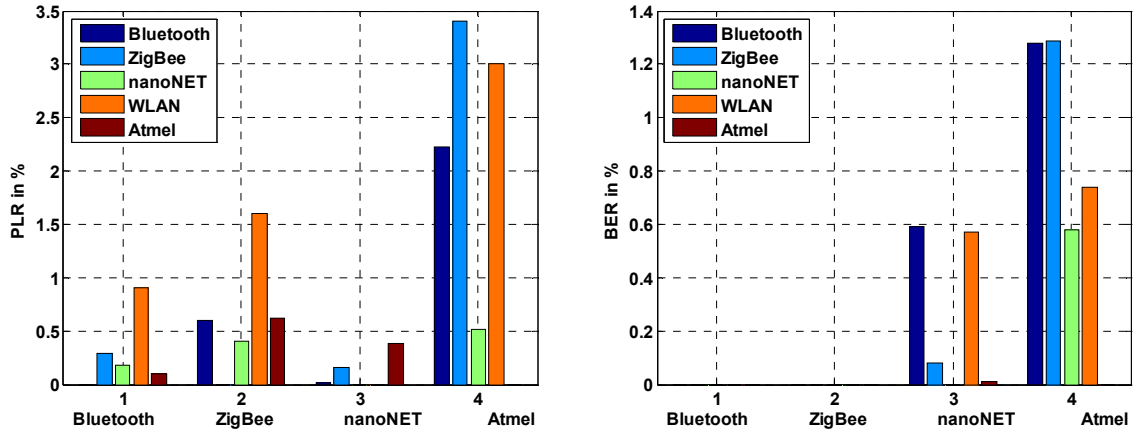
Figure A.4: *The best case PLR and BER for tested systems in the presence of selected interferers (legend shows interferers). Bluetooth(1-slot packet), nanoNET(-16 dBm, with retransmission as recipient and without retransmission as interferer), Atmel(500 kbps), WLAN(one network with single node).*

Bluetooth: Longer packet length made the Bluetooth system worse interfere and more vulnerable to interference of coexisting systems. Moreover, by increasing the occupied bandwidth the Bluetooth system starts suffering higher losses. For example, the worst case measured PLR and BER are 5.0 % and ~1e-5 when two parallel WLAN networks (working in WLAN channel 2 and WLAN channel 7), each with two nodes, are used for interference.

Table A.1: *SIR values for selected technologies (with nanoNET's minimum transmission power)*

	Bluetooth	ZigBee	nanoNET	Atmel
Bluetooth	-	-20dB	-36dB	-16dB
WLAN	0dB	-20dB	-36dB	-16dB
ZigBee	20dB	-	-16dB	4dB
nanoNET	36dB	16dB	-	20dB
Atmel	16dB	-4dB	-20dB	-

Recipient and interferer technologies are listed in row and column order respectively.

WLAN: WLAN is the worst interferer for the FHSS based Bluetooth system as it offers 0 dB SIR and covers 20 MHz of the frequency band. I.e. 20 Bluetooth channels will be skipped by the adaptive frequency hopping algorithm for a single active WLAN channel. Increasing the number of active WLAN channels and active nodes in each network worsen the interference of WLAN system.

NanoNET: Using retransmission mechanism and higher transmission power i.e. 6.90 dBm provides best combination for nanoNET system as a recipient. But, both these parameters increase the physical strength of interference of nanoNET system. However, the nanoNET system with -16 dBm transmission power is the best as interferer among all technologies because of lowest offered SIR. Consequently, though it affects three times more Bluetooth channels than a single WLAN network, but the Bluetooth system still suffers almost negligible interference. Other technologies are also least affected with -16 dBm nanoNET interference.

ZigBee: Since the ZigBee based system is using acknowledgement and retransmission mechanism it is not the hardest affected recipient. Moreover, because of error correction/detection codes it always discards packets with bit errors and consequently it never produce any bit errors in these experiments. But more discarded packets also trigger more retransmissions, eventually increasing the strength of ZigBee interference to other coexisting systems.

Atmel: It is the hardest affected recipient system because it does not employ any error correction/detection mechanisms. A low bit rate for the Atmel system increases the collision probability of its symbols with those of the interfering systems because of longer symbol durations. Eventually, the Atmel system with 72 kbps is more vulnerable to interference and worse interferer than 500 kbps variant of it.

A1.4   Existing non cognitive solutions to improve coexistence

An overview of existing non-cognitive solution to improve wireless coexistence is presented in the following. It can be observed that none of these methods is generic and each addresses the improvement of a specific DUT in the coexistence of a particular interferer.

[HSU06] presents Dynamic Fragmentation Algorithm (DFA) using dynamic fragmentation to improve the coexistence ability of Wi-Fi in the presence of Bluetooth interference. The proposed scheme tries to optimize the MAC layer packet length such that a Wi-Fi device has a better chance to avoid the interference caused by Bluetooth devices.

[JIN07] compares various coexistence techniques and relevant standardization efforts and proposes a media independent coexistence service (MICE) layer. It suggests that the performance of a multi-radio

system can be further improved if necessary support and modification is added to individual wireless technology, e.g. air interface / wireless protocols.

UWB in coexistence of different systems is studied in [OHN05-PEN05]. [OHN05] evaluates the effect of interference between pulse bi-phase IR-UWB and MB-OFDM. It proposes a multi-carrier type template waveform to mitigate the influence of interference from MB-OFDM to IR-UWB. A pulse shaping method for UWB has been proposed in [PEN05] to generate pulses whose power spectra fit to the FCC frequency mask and thus improves the coexistence of UWB with IEEE802.11a WLAN.

Relying on a blind hop timing and frequency estimation algorithm, [JIN06] proposes a collision resolution technique that resolves collided data packets without retransmission to enable coexistence of multiple Bluetooth piconets. While [YUK04] suggests an approach called ISOAFH (Interference Source Oriented adaptive frequency hopping). It proposes a customized channel classification process, thereby simplifying the time and space complexity of the mechanism.

Two coexistence strategies for a non-coherent MIR-UWB system are proposed in [DEH09]. First is a static coexistence approach, in which sub-bands of the MIR-UWB system are completely deactivated before any data transmission occurs. In contrast, a more dynamic coexistence strategy is based on system specific channel estimation in conjunction with a robust interference detection algorithm. Thereby, without any adaptation of the MIR-UWB system parameters, sub-bands are used for data transmission in accordance to an adapted two-dimensional bandplan array which considers interference-free time-frequency gaps.

Software upgrades to the medium access control of the 802.16 BS are proposed in [BER06] in order to enable its reliable operation in coexistence with 802.11. Thereby, no 802.11 frame transmissions are required by an 802.16 system. However from the perspective of 802.11a, the proposed method can be regarded as unfair as coexistence is enabled in partly blocking 802.11a out of the medium.

Two new techniques to enhance the existing Bluetooth and WLAN coexistence mechanisms are proposed in [QIX06]. The first one is channel clustering, which is used to classify the channel status more accurately. The second one is called probabilistic channel visiting, which is used to more reasonably allocate the channel resources between WLAN and BT devices.

A1.5   Cognitive radio used to improve coexistence

Cognitive radios are being researched for use in all kind of wireless applications mainly in cellular, military, emergency, industrial, and consumer areas. Some important possible applications include increase spectral usage, interference mitigation & coexistence optimization, dynamic resource

management, and multi-lingual/multi-purpose communication system. Following provides an overview of CR research only in the area of interference mitigation and coexistence optimization.

[ZHU07] discusses an access protocol that is based on setting a uniform transmission power and sensing threshold for all license-exempt band frequency channel cognitive radio based transmitters, to guarantee the coexistence in the sense that a certain minimum signal-to-interference ratio (SIR) is ensured at the receivers. In a similar research work [HOV05] local SNR of the primary signal is used as a metric for power control rule. The coexisting cognitive radio (SU) must adjust its power levels according to its potential proximity to the protected primary receiver.

A transmit power control system using Fuzzy Logic System to provide cognitive radios the ability to coexist with primary (licensed) users in the same frequency band is presented in [LEH07]. With built-in fuzzy power controller, a cognitive radio is able to opportunistically adjust its transmit power in response to the changes of the interference level to primary user (PU), the distance to PU and its received power difference at the base station (BS) while satisfying the requirement of sufficiently low interference to PU. Linguistic knowledge of transmit power control (TPC) is obtained from a group of network experts rather than a single expert.

An adaptive sub-band selection technique based on orthogonal frequency division multiplexing (OFDM) is proposed in [PIN08] to avoid interference for better system coexistence in ISM bands. Under the assumption that the interference power level and the interfered frequency bands are identified at the receiver, interference thresholds, determined over both Gaussian and multipath fading channels, are applied to adaptively select the transmission sub-bands so that interference is avoided and the system coexistence issues are relaxed.

While [NOL07] analyzes two independently developed dynamic spectrum access test beds to exploit spectrum opportunities. It explores the ability of these two different cognitive radio architectures, using different wireless communication schemes, to coexist on non-interfering and interfering bases.

A protocol Cognitive Medium Access (CMA) is proposed in [GEI07]. It aims at improving coexistence with a set of independently evolving WLAN bands. A time-slotted physical layer for the cognitive radio is considered and CMA is derived based on experimental models. The cognitive radio's hopping sequence is altered by predicting the WLAN's medium access based on a stochastic model such that it preferably hops to bands not currently used by the WLAN.

In [ZHI08] the universal software radio peripheral (USRP)/GNURadio is used to study the coexistence of more than one cognitive radio in common frequency bands. [HEI08] proposes B-VHF, which is a cognitive radio based multi carrier aeronautical radio solution intended to coexist with existing devices. It

offers double capacity than current systems with the same safety level. Ultra wide bandwidth (UWB) technology as one of the enabling transmission techniques for the implementation of CR systems is investigated in [GIO06].

Cognitive Medium Access (CMA) schemes for sharing spectrum with a set of parallel WLAN bands are proposed in [GEI08]. The derivation of the scheme is based on a measurement based interference study as well as a stochastic model which captures the WLAN's medium access. The CMA schemes proposed in this paper are classified as according to fully observable (FO-CMA) and partially observable (PO-CMA) systems. According to the results presented both schemes significantly outperform blind hopping schemes.

A1.6   Artificial intelligence (AI) and statistical methods in cognitive radios (CR)

A cognitive wrapper encapsulating a reconfigurable radio core is presented in [NOL06]. The influence of this wrapper can be varied in order to vary the 'intelligence' of the cognitive radio between the two extremes of a baseline radio, and a highly-complex and evolved system to account for scenarios where complex cognition may not be necessary. Observations, actions and conclusions developed by the cognitive radio can be stored in a variable-length memory delay-Line. A selective memory mechanism enables the relevance of aspect of this information to be varied.

In [ZHI08] an autoregressive channel prediction model for cognitive radio systems to estimate spectrum holes is presented. This model adopts a second-order autoregressive process and a KALMAN filter. A BAYES risk criterion for spectrum hole detection is presented by considering interference temperature and channel idle probability. Theoretical analysis and simulations show that CR systems based on this scheme can greatly reduce the number of collisions between licensed users and rental users.

[YAR07] proposes the use of binary time series for spectrum occupancy characterization and prediction. Derived time series models are tested in terms of raw residuals and AKAIKE information criteria (AIC). Two types of spectrum occupancy schemes, namely, deterministic and non–deterministic schemes, are considered. It is observed that this approach performs very well for deterministic occupancy schemes.

The channel predictive modeling for time-varying channels to mitigate the uncertainties in channel state information (CSI) due to fading and motion effects is also a hot topic and the research done in this area will provide us some guideline as we are also interested to predict the behavior of channel in this project.

In [LEE08] a channel prediction method using the estimation of DOPPLER spectrum is proposed and investigated to predict channel state information in time varying channels. The autoregressive model for the DOPPLER spectrum is employed in order to get reliable channel prediction coefficients. Furthermore, [SHA07] proposes an approach for selecting the channel sampling rate based on SNR and bit-error-rate (BER) constraints. A channel model using a second-order autoregressive (AR-2) process is applied at the selected sampling rate to predict the channel-state.

In mobile situations the effect of outdated channel information in the presence of quickly time-varying channels can be significant. The use of channel prediction is shown to mitigate the impact of outdated channel information and improve performance when the DOPPLER spread or mobile velocity is high [SOU01]. [FOR02] suggested a prediction algorithm for adaptive OFDM systems and presented simulation based results to show how the uncertainty in channel state information due to DOPPLER spread and limits on the reverse link bandwidth can be lessened by using this prediction algorithm.

[ISU06] studied the role of ergodicity in wireless channel prediction. Following the sinusoidal channel model, conditions under which the ergodic assumption is valid are presented. Due to the lack of ergodicity in a typical real world wireless channel, least squares prediction, an approach based on time averages, is motivated as opposed to linear minimum mean squared error channel prediction, an approach based on ensemble averaging. It also studied methods such as forward-backward and rank reduction for high quality channel prediction.

[AGU07] used heuristics to design complex predictors in WLAN scenarios. It used WLAN measurement traces for the simulative evaluation of the influence of channel prediction errors in the performance of a threshold-based adaptive modulation scheme, considering also the case of delayed channel feedback.

[XIE06] proposed a simplified minimum mean-square error channel prediction of time-varying wideband channels. Furthermore, it applied an adaptive filter algorithm into channel prediction without any channel statistic information.

Appendix A2

A2: Standardization Efforts and Notable Projects related to Coexistence and Cognitive Radios

Related standards and patents

[BUL09/VEN08/WEB01]   The 1900 WG projects form a new standards series within the IEEE, established in 2005 jointly by the IEEE Communications Society and IEEE Electromagnetic Compatibility Society. The objective of 1900 is to develop standards in the areas of dynamic spectrum access (DSA), cognitive radio (CR), interference management, coordination of wireless systems, and advanced spectrum management. Particularly IEEE 1900.2 will provide technical guidelines for analyzing the potential for coexistence or in contrast interference between radio systems operating in the same frequency band or between different frequency bands. On the other hand IEEE 1900.5 will define a policy language (or a set of policy languages or dialects) to specify interoperable, vendor-independent control of Cognitive Radio functionality and behavior for Dynamic Spectrum Access resources and services.

IEEE 802.11y [WEB02] adds new cognitive oriented concepts to 802.11-2007. One is Contention based protocol (CBP) – It is an enhancement to the carrier sensing and energy detection mechanisms of 802.11 in order to meet the FCC's definition of a contention based protocol. The other one is extended channel switch announcement (ECSA) which provides a mechanism for an access point to notify stations of its intention to change channel frequency or bandwidth. This mechanism will allow for the WLAN to continuously choose the channel that is the least noisy and the least likely to cause interference. ECSA is also used in 802.11n [WEB05], making it possible to switch between the 3.65GHz, 2.4GHz and 5GHz bands. Whereas IEEE 802.11h [WEB04], so called spectrum managed 802.11a, supports dynamic frequency selection and transmit power control for WLANs to share spectrum.

[WEB03] IEEE 802.16h-License exempt task group is aimed to specify improved mechanisms, as policies and MAC enhancements, to enable coexistence among license-exempt systems based on IEEE Standard 802.16 and to facilitate the coexistence of such systems with primary users through an adaptive channel selection mechanism.

The IEEE 802.22 working group [WEB08] on wireless regional area networks (WRAN) is working to develop a standard for a cognitive radio-based PHY/MAC air interface for use by license-exempt devices on a non-interfering basis to coexist in spectrum that is allocated to the TV broadcast service.

A multiple-objective genetic algorithm (GA) for both efficient optimizations of radio configuration and as the basis for machine learning is embodied in a CE in a project at Virginia Tech. In 2004, a patent application was filed describing this technology; this patent, titled "Cognitive Radio Engine Based on Genetic Algorithms in a Network" was issued in 2007 [RIE07]

Large scale projects and research groups involved in CR research

Many universities and organizations are involved in cognitive radio research. In some cases several universities and organizations across multiple countries are cooperating with each other. A glimpse of well known large scale projects is provided in the following.

The XG Radio program [MCH07], from Defense Advanced Research Projects Agency (DARPA) uses dynamic spectrum access technology to determine locally unused spectrum, and then operates on these channels without causing interference to existing *non-cooperative* users. Initial results from tests conducted in August 2006 showed satisfactory results for the XG Radio system. There were three major test criteria: to *cause no harm* (avoid interference), to *work* (form and maintain connected networks), and to *add value* (efficiently use spectrum).

The Adaptive Reconfigurable Access and Generic interfaces for optimization in Radio Networks (ARAGORN) project [WEB06] aims to explore key enabling technologies that facilitate the application of machine intelligence and adaptive communications technologies in the optimization of resource usage in wireless networks. Most particularly, the goal is to apply methods originating from the artificial intelligence community in order to increase the efficiency and system performance of the present day and future systems following the cognitive radios and networks paradigm.

In a big project "Cognitive wireless technology" at Virginia Tech [MAC09/WEB07] the radio is being treated as a Biological System. This means that like animals and people radio seek their own kind (other radios with which they want to communicate), avoid or outwit enemies (interfering radios), find a place to live (usable spectrum), conform to the etiquette of their society (the federal communications commission), make a living (deliver the services that their user wants), and deal with entirely new situations and learn from experience.

The End-to-End Reconfigurability (E2R) [GRA05], project aims at bringing full benefits of the valuable diversity within the Radio Eco-Space, composed of wide range of systems such as Cellular, Wireless Local Area and Broadcast. The key objective of the E2R project is to devise, develop and trial

architectural design of reconfigurable devices and supporting system functions to offer an expanded set of operational choices to the users, applications and service providers, operators, regulators in the context of heterogeneous mobile radio systems

Some other well known groups involved in large scale research on CR are at Trinity College in Dublin (Ireland), WinLab at Rutgers University (USA), Kansas University (USA), and RWTH Aachen University (Germany), and the Berkeley Wireless Research Center at the University of California Berkeley (USA).

Appendix A3

A3: Feature Analysis of State-of-the-art Wireless Technologies

The following standard wireless technologies are used in this research work and described in Table A3.1-Table A3.9 with respect to selected PHY/MAC layer parameters. Where, selected PHY/MAC parameters are channel definition (bandwidth (BW), center frequency (f_c)), pulse shape, modulation, hopping pattern, time behavior, bitrate, symbol rate and transmission power. Moreover, all these technologies operate in 2.4 GHz ISM band.

5. IEEE 802.15.1 based technologies

   a. Bluetooth

   b. Wireless Interface for Sensors and Actuators (WISA)

   c. Wireless Sensor Actuator Network for Factory Automation (WSAN)

6. IEEE 802.15.4 based technologies

   a. ZigBee/ZigBee Pro (non-hopping system)

   b. WirelessHART

   c. ISA100.11a

   d. IEEE 802.15.4a Based NanoNET

7. IEEE 802.11 based Wireless Local Area Network (WLAN)

8. Atmel's ATR2406 based proprietary transceiver

IEEE 802.15.1 Based Technologies

Table A3**.1:** *IEEE 802.15.1/Bluetooth [SD105, BTS01]*

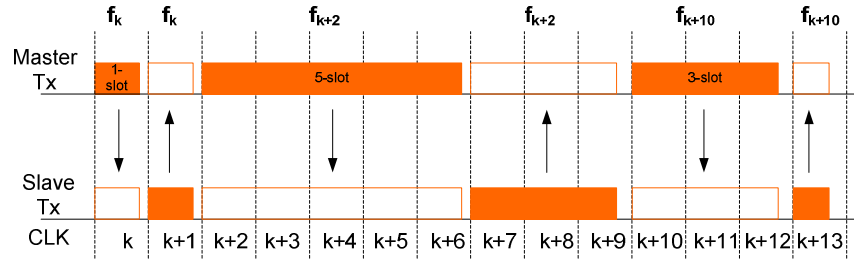| Features	Value
Channel definition:	79 channels, each with 1 MHz bandwidth are defined. The center frequencies are given by $f_c = 2402 + k$ MHz, $k = 0,…,78$.
Pulse shape	Gaussian 0.5
Modulation	Gaussian frequency shift keying (GFSK)
Hopping pattern	A pseudo-random sequence is used to compute following four types of channels: • *Basic piconet physical channels:* A basic channel hopping sequence, which has a very long period length and does not show repetitive patterns over a short time interval. It distributes the hop frequencies equally over the 79 MHz during a short time interval (see simulated signal in Fig. A3.2 right plot). • *Adapted piconet physical channels:* The slave uses the same frequency as the preceding master transmission when adaptive frequency hopping (AFH) is in effect. It is called same channel mechanism (see Fig. A3.1). AHF uses less than the full 79 frequencies that the basic piconet uses (see Fig A3.2 left plot). • *Inquiry scan physical channel:* An inquiry hopping sequence/ inquiry response hopping sequence is used with 32 wake-up frequencies distributed equally over the 79 MHz, with a period length of 32. • *Page scan physical channel:* A page hopping sequence/ page response hopping sequence is used with 32 wake-up frequencies distributed equally over the 79 MHz, with a period length of 32. (see measured page hopping sequence in Fig. A3.10)
Temporal pattern	TDD/TDMA with slot time 625 µs is used. Nodes can choose 1/3/5 slot packets as shown in Fig. A3.1.
Bitrate /Symbol rate	1 Mbps/1 Msps
Transmission power	Three device classes 1, 2 and 3 are defined with maximum transmission power 20 dBm, 4dBm and 0 dBm respectively.

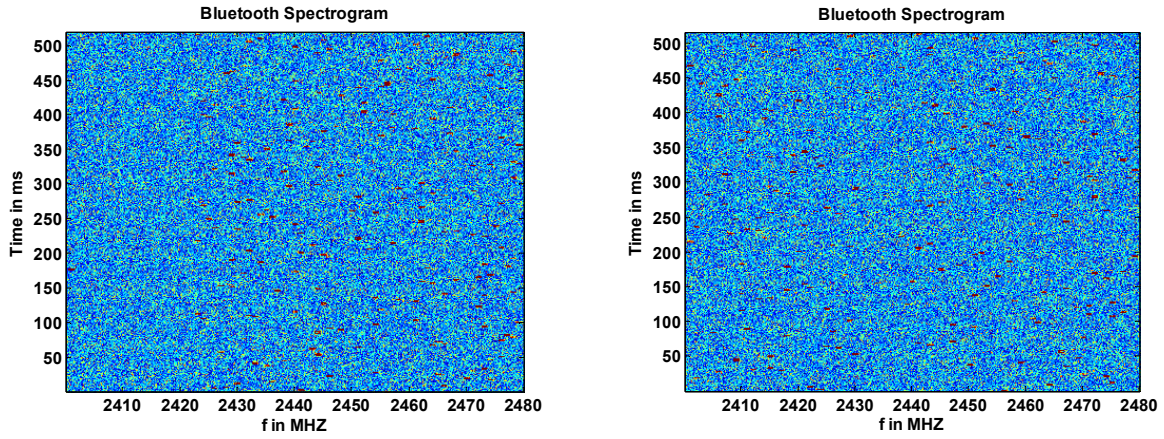**Figure A3.1:** *Same channel effect and multi-slot packets of Bluetooth.*

Figure A3.2: *Simulated Bluetooth spectrogram. 1st channel of IEEE 802.11 is blacklisted in left figure. Right spectrogram is without blacklisting. Duty cycle = 100%, Rayleigh fading with AWGN.*

Table A3.2: *WISA [SCH07]. See Fig.* A3.6 *for simulated WISA spectrogram.*

Features	Value
Channel definition:	• 77 channels, each with 1 MHz bandwidth are defined. The center frequencies are given by $f_c = 2403 + k$ MHz, $k = 0,…,76$. • These channels are further divided into 7 disjoint subbands (see Fig. A3.3), each subband containing 11 hop frequencies.
Pulse shape	Same as IEEE 802.15.1
Modulation	Same as IEEE 802.15.1
Hopping pattern	• Full duplex is enabled using FDD. 4 uplinks {UL_1, UL_2, UL3, UL_4} and 1 downlink 'DL' channel is used simultaneously (see Fig. A3.4) • Each sensor/actuator (S/A) is part of one of four uplink.

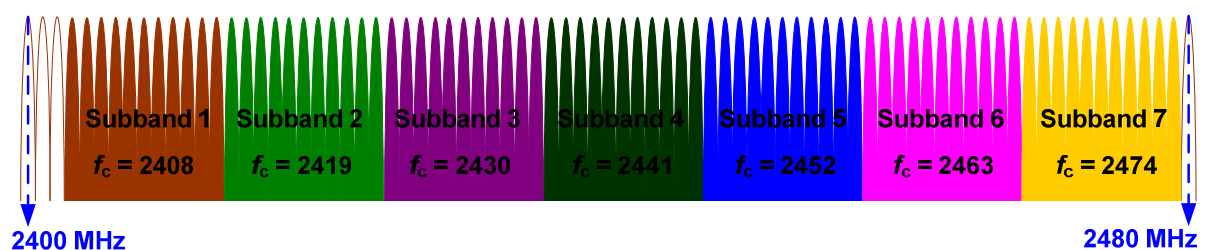|	
	• These five frequencies remains constant over one TDMA frame (defined later). Consequently, each hopping sequence has a period length of $7 \times 11 = 77$ frames. • Consecutive frames must be in different subbands. • The (duplex) spacing between downlink and uplink frequencies is at least three subbands. • The four concurrent uplinks are in the same subband and hop with a fixed spacing of at least 2 MHz.
Temporal pattern	• 120 nodes are accommodated in a single cell using FDD/TDMA (Fig. A3.4, Fig. A3.5). • The TDMA frame length, $T_{frame} = 2048$ µs. Time slot called 'SSlot' is 64 µs. A double slot is referred as 'DSlot and is 128 µs. • To support up to 120 S/As per cell, each S/A may transmit over uplink in one out of 30 'SSlots' per frame. A 'DSlot' for uplink is also allowed, which halves the total number of nodes in a single cell. • Each S/A uses 'SSlot' to transmit using uplink, hence in total 8 nodes can transmit one packet each within a single 'DSlot' of master node. • Master acknowledges, over downlink link, all 8 packets in a single 128 bit packet in third 'DSlot'. It gives a 256 µs turnaround time.
Bitrate /Symbol rate	Same as IEEE 802.15.1
Transmission power	0 dBm

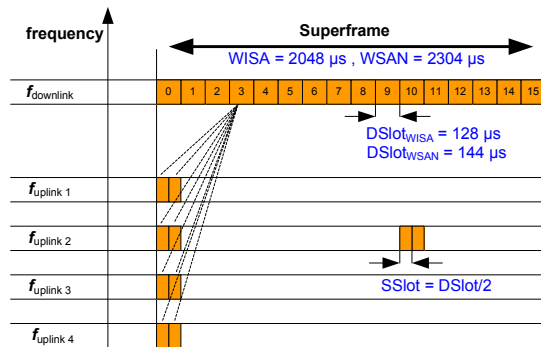**Figure A3.3:** *WISA/WSAN sub-bands*

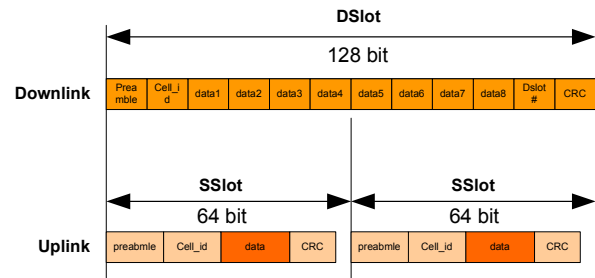**Figure A3.4:** *FDD/TDMA based structure of WISA/WSAN*

Figure A3.5: *WISA downlink and uplink slots. ACK is sent to eight nodes in a single DSlot. However, using DSlot for uplink will halve this amount.*
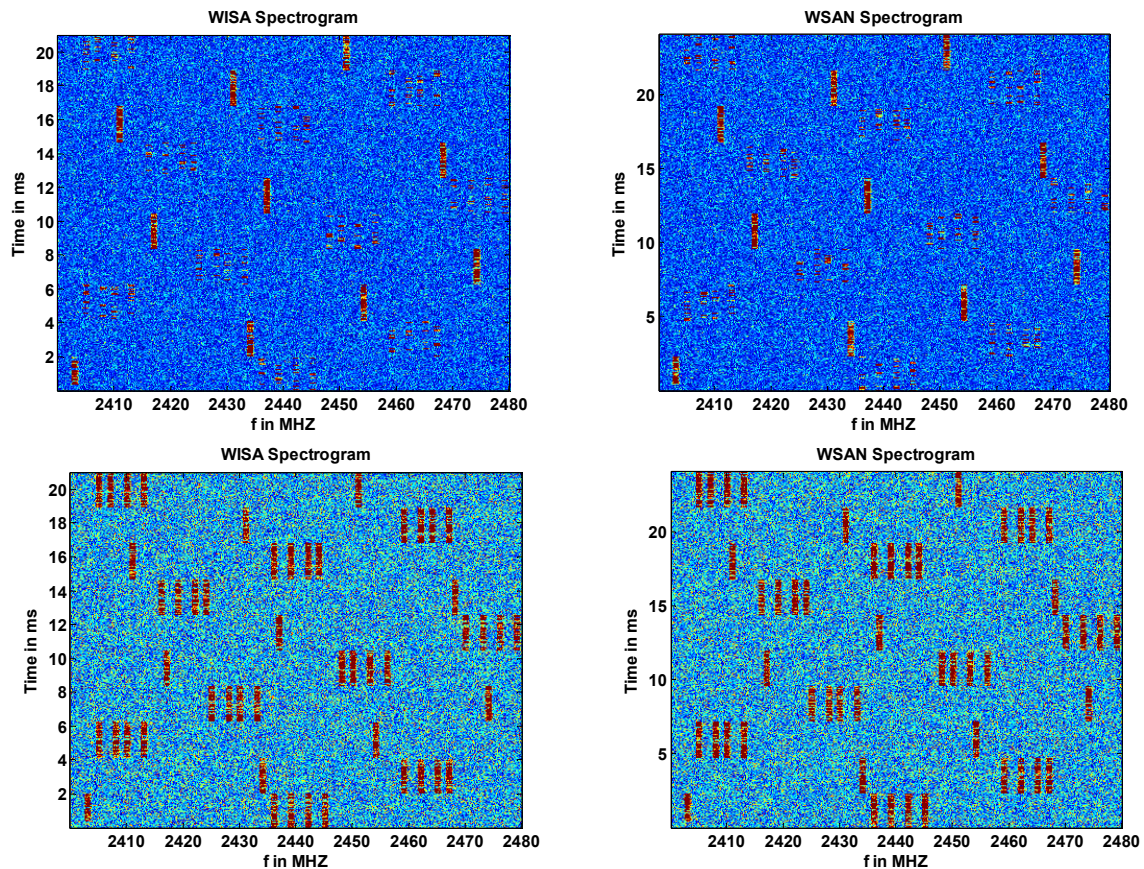

Figure A3.6: *Simulated WISA/WSAN spectrograms. Upper plots are for 25% randomly active nodes, while lower plots are for 100% active nodes. Random numbers are based on Uniform distribution. Rayleigh fading with AWGN is used.*

NOTE: Note that WISA and WSAN differ from each other only in terms of slot length.

Table A3.3: *WSAN [WSA10]. See Fig.* A3.*6 for simulated WSAN signal.*

WSAN is completely identical to WISA except for the following.

- T_{frame} = 2304 µs.

- SSlot = 72 µs, DSlot = 144 µs.

IEEE 802.15.4 based technologies

The ZigBee system uses the IEEE 802.15.4 specification without any amendments. The ZigBee PRO standard additionally supports frequency agility that consists of scanning available channels to determine the channel with the least interference, which is then selected and used by all ZigBee devices. Although the IEEE 802.15.4 standard defines PHYs in 868/915 MHz and 2.4 GHz bands but only the later one is discussed here. Other IEEE 802.15.4 based technologies included are wirelessHART and ISA100.11a both of which are hopping systems and the chirp spread spectrum (CSS) based nanoNET system.

Table A3.4: *IEEE 802.15.4/ ZigBee/ZigBee Pro [*SD406, ZIGBE*]*

Features	Value
Channel definition:	16 channels are defined each with bandwidth = 2 MHz. Center frequency can be calculated using $f_c = 2405 + 5\,(k - 11)$ MHz, for $k = 11, 12, …, 26$.
Pulse shape	Half sine
Modulation	DSSS/O-QPSK (Offset - Quadrature Phase Shift Keying)
Hopping pattern	No
Temporal pattern	CSMA-CA channel access mechanism, optional frame structure, optional guaranteed time slots, and optional acknowledgement.
Bitrate /Symbol rate	250 kbps/62.5 ksps
Transmission power	In the range –3 dBm …10 dBm, with 0 dBm being typical value.

Table A3.5: *WirelessHART [*DEJ10, TSCH4*]. See Fig.* A3.*9 for simulated spectrogram of wirelessHART.*

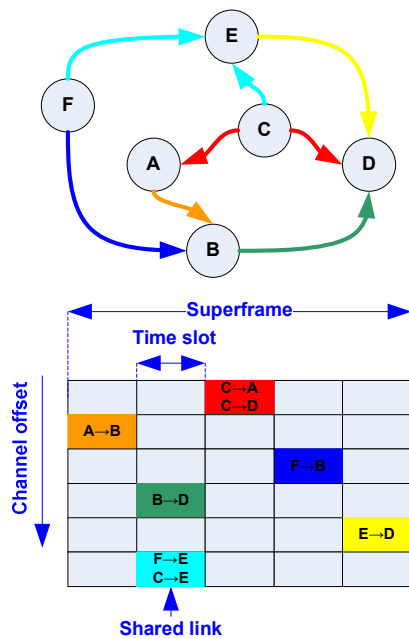| Features	Value
Channel definition:	Only first 15 channels of IEEE 802.15.4 are used, channel 26 is not supported.
Pulse shape	Same as IEEE 802.15.4
Modulation	Same as IEEE 802.15.4
Hopping pattern	- Time Slotted Channel Hopping (TSCH) is used (see Fig. A3.7) - A node transmits using a pre-assigned *link*. Where, *Link = (Timeslot , Channel Offset)* and *0 ≤ channel offset < Number_of_channels*. - Frequency hops on a per-transaction (time slot) basis and is computed on the basis of link's timeslot and channel offset as follows: *Ch # = hopping table ((SlotNo + Channel Offset) % Number_of_Channels).* Where the hopping table is a random sequence of active channels. - Channel blacklisting supported, therefore there can be less than 15 active channels at a particular time. - A link can be dedicated or shared. A link is shared using CSMA with random backoff method.
Temporal pattern	- TDMA with each time slot of 10 msec duration is used. - Device-to-device communication within a single timeslot includes transmission and reception of packet and acknowledgement. - A collection of time slots form a superframe. The size of a superframe may vary, depending on required number of slots at a particular time. The superframes are then repeated at a fixed rate throughout the network lifetime.
Bitrate /Symbol rate	Same as IEEE 802.15.4
Transmission power	+10 dBm

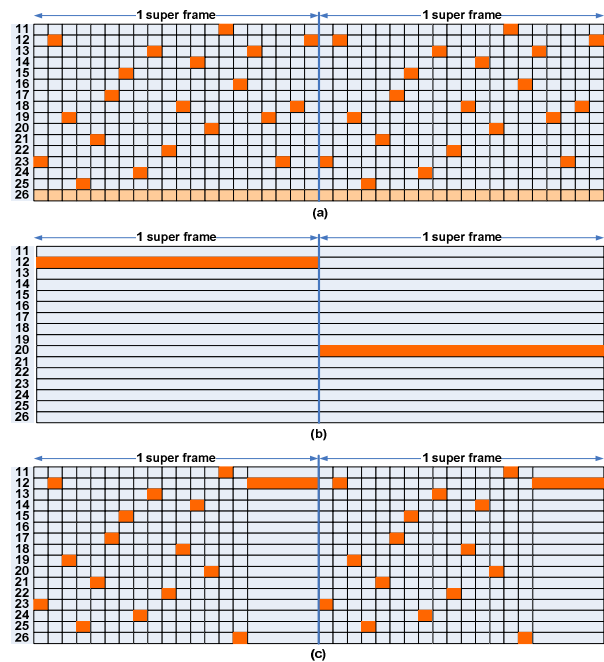**Figure A3.7:** *TSCH, supported by WirelessHART and ISA 100.11a.*

Figure A3.8: *ISA100.11a hopping patterns a) slotted hopping, b) slow hopping, c) hybrid hopping*

Table A3.6: *ISA100.11a [NGU10, KUPRI]. See Fig. A3.9 for simulated spectrogram of ISA100.11a.*

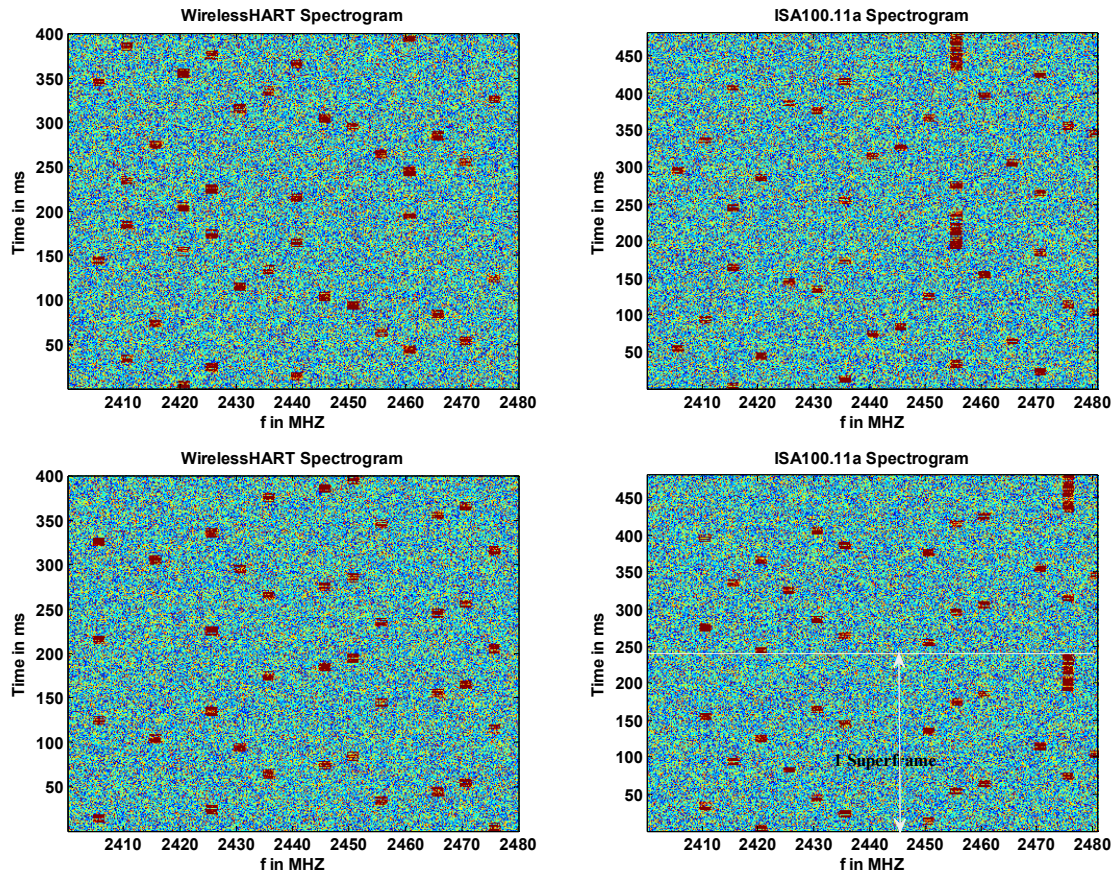| Features	Value
Channel definition:	Same as IEEE 802.15.4
Pulse shape	Same as IEEE 802.15.4
Modulation	Same as IEEE 802.15.4
Hopping pattern	In addition to TSCH, it allows slow hopping and hybrid hopping techniques. A complete superframe can be occupied by a single node in slow hopping. Whereas, some nodes use multiple slots while others single slots in hybrid hopping method as shown in Fig. A3.8.
Temporal pattern	Superframe structure, with slot time 10 ms-15 ms
Bitrate /Symbol rate	Same as IEEE 802.15.4
Transmission power	Same as wirelessHART

Figure A3.9: *WirelessHART and ISA100.11a simulated spectrograms for two superframes with 20 nodes. Upper plots are without blacklisting, while the lower ones blacklist 25% channels randomly. ISA100.11a is using hybrid frequency hopping. Note that wirelessHART doesn't use 26th channel. Rayleigh fading with AWGN is used.*

NOTE: Please note that in TSCH only difference between wirelessHART and ISA100.11a is the use of 26th channel in ISA100.11a. Slow and hybrid hopping are entirely distinct features of ISA100.11a.

Table A3.7: *IEEE 802.15.4a based NanoNET[NANOT]. See Fig.* A3.*10 for spectrogram and PSD of nanoNET signal.*

Features	Value
Channel definition:	Single channel covering the entire 2.4 GHz ISM band. However effective bandwidth is 64 MHz.
Pulse shape	Linear frequency modulated chirp pulse as shown in Fig. A3.10b.
Modulation	2-ary and 4-ary CSS modulation.
Hopping pattern	Non-hopping
Temporal pattern	Implementation dependent, however the one used in this thesis work employs periodic transmissions with ~1 ms ON time and arbitrarily selected time period or cycle time.
Bitrate /Symbol rate	500 kbps, 1 Mbps, 2 Mbps / 500 ksps, 1Msps
Transmission power	-16 dBm…+6.90 dBm

IEEE 802.11 based technologies

The IEEE 802.11 standard was first published in 1997 to implement wireless local area networks (WLAN). Since then it has received many amendments to become a family of standards. Important physical layer amendments include, 'a' in 1999, 'b' in 1999, 'g' in 2003 and 'n' in 2009. IEEE 802.11g based devices are used in this research work, therefore only this particular variant is discussed in Table A3.8.

Table A3.8: *IEEE 802.11g based WLAN [SD117].*

Features	Value
Channel definition:	13 channels with bandwidth 20 MHz are offered in most of the world. However some countries use less (11 for USA) or more (14 for Japan) channels.
Pulse shape	Window
Modulation	BPSK, QPSK, 16-QAM and 64-QAM using OFDM.

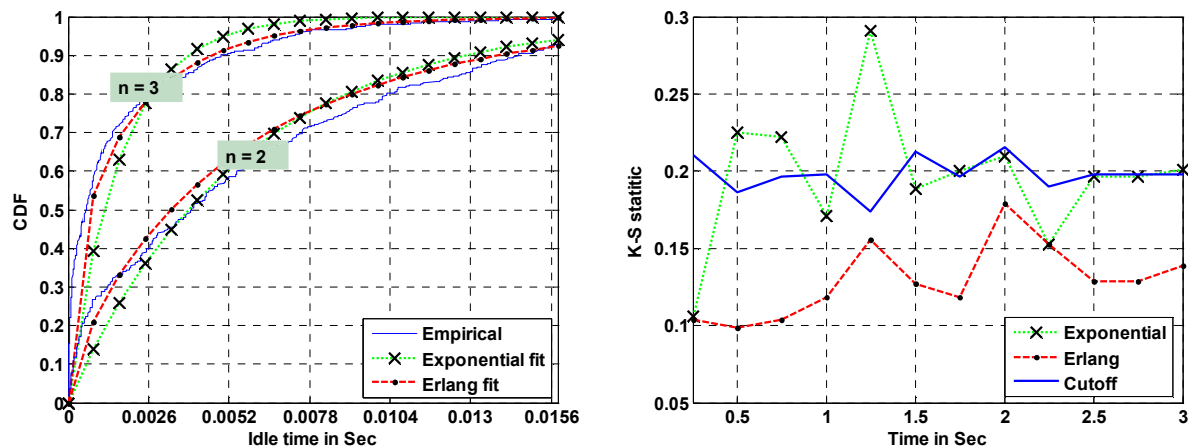| Hopping pattern	Non-hopping
Temporal pattern	Implementation dependent. But mostly it is used for internet based traffic which can be modeled as Poisson arrival process. Expected number of arrivals in a given time interval, called arrival rate, is the single parameter defining this distribution. Inter-arrival times follows Erlang or Exponential distribution as shown in Fig. A3.10 for skype based WLAN traffic with 2 and 3 active nodes.
Bitrate /Symbol rate	6 Mbps, 9 Mbps, 12 Mbps, 18 Mbps, 24 Mbps, 36 Mbps, 48 Mbps, 54 Mbps using 52 sub-carriers.
Transmission power	+20 dBm

Figure A3.10: *Left plot shows goodness-of-fit analysis for skype based WLAN traffic for 'n' number of active nodes. In right side plot, goodness-of-fit analysis using Kolmogorov-Smirnov (K-S) test with significance level α = 0.5. Erlang distribution shows better goodness of fit, while exponential distribution sometimes crosses the threshold defined by the K-S test.*

Atmel, a proprietary technology

It is a proprietary system realized using an ATR2406 transceiver from Atmel [A4779] and is used in experiments throughout in this thesis work. It will be shortly referred as 'Atmel'.

Table A3.9: *Atmel.*

| Features	Value
Channel definition	95 channels with channel bandwidth 0.864 MHz.
Pulse shape	Gaussian
Modulation	2-FSK
Hopping pattern	Non-hopping
Temporal pattern	Implementation dependent, however the one used in this thesis work employs periodic transmissions using an arbitrarily selected cycle time.
Bitrate /Symbol rate	72 kbps, 500 kbps /72 ksps, 500 ksps
Transmission power	+4 dBm

Appendix A4

A4: NFSC: Special cases

Selecting filter bandwidth: As mentioned earlier in section 4.1.3, the bandwidth of filter is controlled by the bandwidth of PU and a constant D. In order to avoid false detection of a narrower signal when a wider signal is actually present, it is necessary to filter the narrower signal wider than its actual bandwidth. I found $D_{NanoNET} = 1$, $D_{WLAN} = 2$, $D_{IEEE\ 802.15.4} = 4$ and $D_{Atmel}/D_{IEEE\ 802.15.1} = 8$ as optimal values during experiments. Figure A4.1 shows SM scores of WLAN and Atmel based signals using two different values of D. It can be seen that using the same threshold value, one set of values of D for both systems results in correct detections while the other set results in false detection for the narrower signal.
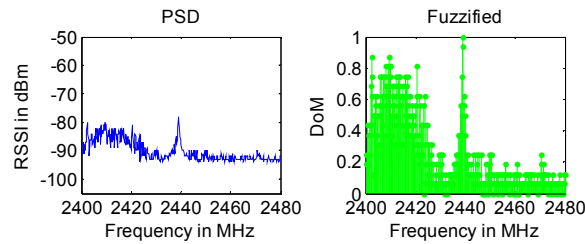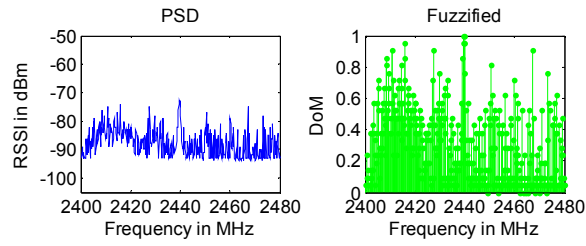

**(a)** *WLAN and Atmel PUs are operating with weak signal levels.*
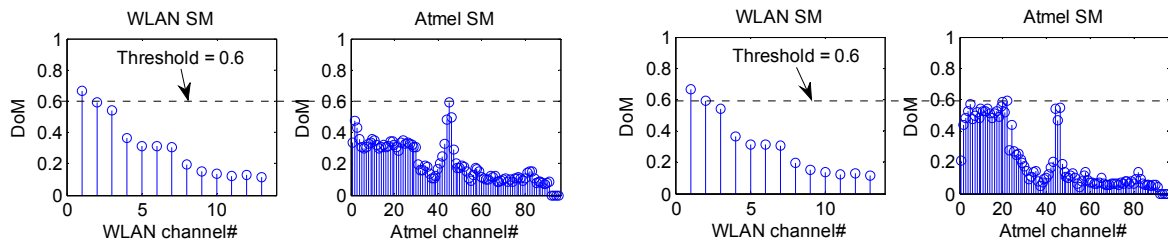
(b) *SM of signal shown in 'a', $D_{WLAN} = 2$, $D_{Atmel} = 8$. Both PU signals are correctly identified.*

(c) *SM of signal shown in 'a', $D_{WLAN} = 1$, $D_{Atmel} = 1$. The WLAN signal is incorrectly identified as an Atmel signal.*

Figure A4.1: *Narrowband data acquisition: Bandwidth of filters, controlled by constant D, significantly influences the SM score.*

Noisy signal: A very noisy signal acquired using the CC2500 based narrowband sensor is shown in Fig. A4.2a along with its FPS. Corresponding SM scores for two primary systems are plotted in A4.2b, which shows a global increase in SM scores but respective PU systems are still distinguishable using a threshold value.

(a) *Noisy signal, a WLAN and an Atmel PU are operating*
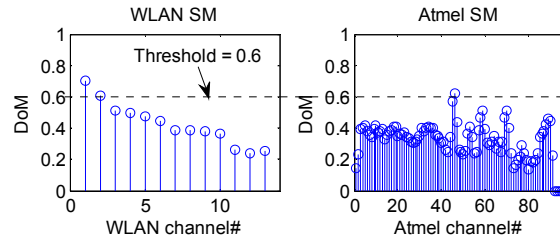
(b) *SM of signal shown in 'd', $D_{WLAN} = 2$, $D_{Atmel} = 8$. Both PU signals are correctly identified.*

Figure A4.2: *Narrowband data acquisition: processing a noisy signal.*

Appendix A5

A5: Receiver Operating Characteristics curve

Receiver Operating Characteristics (ROC) curve is used to evaluate the performance of sensing, detection, and classification. The ROC curve represents the relation of *sensitivity* and *specificity*:

- **Sensitivity** is the measure of how accurately an algorithm detects a PU when it is actually *present*. It is also called *true positive rate* (TPR).

- **Specificity** is the measure of how accurately an algorithm detects the absence of a PU when it is *not present*. It is also called *true negative rate* (TNR). Table A5.1 and Table A5.2 present formulas to calculate different statistics used for ROC curve and an example ROC curve is shown in Fig. A5.1.

Table A5.1 *Confusion matrix (positve class: PU present, negative class: PU is absent)*

		Detected Class	
		Positive (PU)	Negative (Noise)
Actual Class	Positive (PU)	**True Positive (TP)**	**False Negative (FN)**
	Negative (Noise)	**False Positive (FP)**	**True Negative (TN)**

Table A5.2 *Interpretation of some important statistics derived from the confusion matrix*

| Measure	Formula	Intuitive Meaning
Precision	TP / (TP + FP)	The percentage of positive predictions that are correct.
Recall / Sensitivity (TPR)	TP / (TP + FN)	The percentage of positive labeled instances that were predicted as positive.
Specificity (TNR)	TN / (TN + FP)	The percentage of negative labeled instances that were predicted as negative.
Accuracy	(TP + TN) / (TP + TN + FP + FN)	The percentage of predictions that are correct.
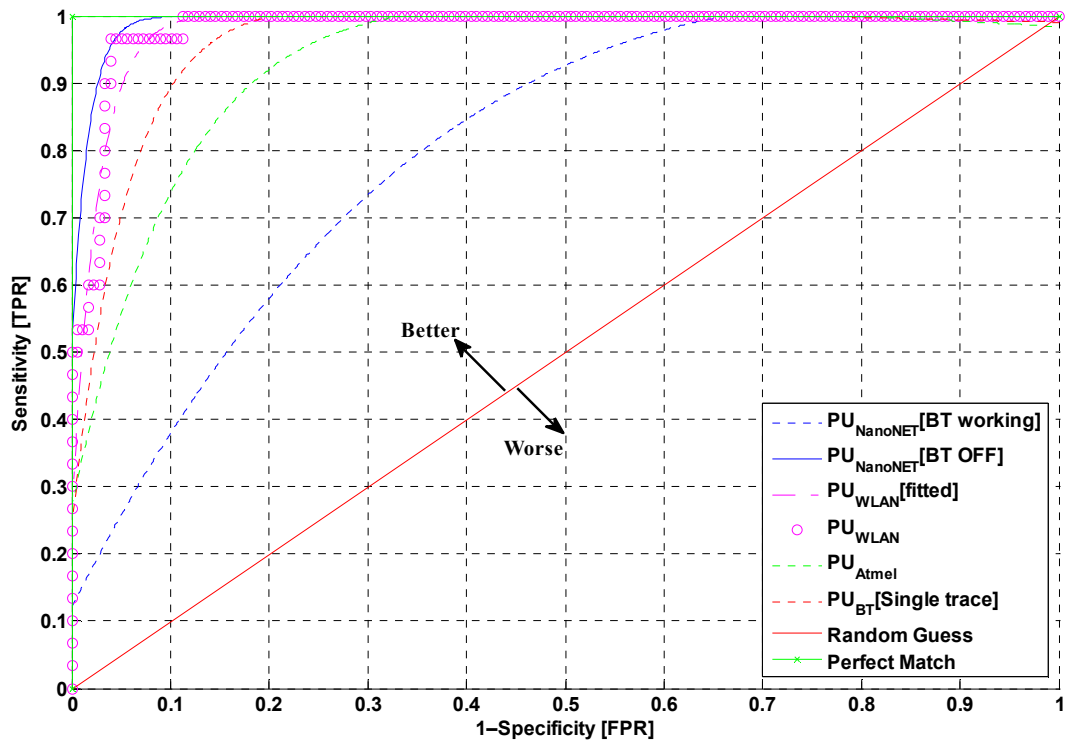
Figure A5.1: *Example ROC curves using neuro-fuzzy signal classifier (NFSC)*